Electrophysiological characterization and functional importance of midbrain dopaminergic neurons projecting to the primary motor cortex

Valentin Plateau

THÈSE PRÉSENTÉE POUR OBTENIR LE GRADE DE

Docteur de l'Université de Bordeaux

ÊCOLE DOCTORALE SCIENCES DE LA VIE ET DE LA SANTÉ

SPÉCIALITÉ NEUROSCIENCES

Par Valentin PLATEAU

Caractérisation électrophysiologique et importance fonctionnelle des neurones dopaminergiques du mésencéphale projetant au cortex moteur primaire

Soutenue le 03/02/2023 devant le jury :

M. Denis COMBES	Université de Bordeaux	Président du jury
Mme. Ingrid BUREAU	Aix-Marseille Université	Rapporteur
M. Jacques BARIK	Université Côte d'Azur	Rapporteur
Mme. Catherine LE MOINE	Université de Bordeaux	Examinateur
M. Emmanuel VALJENT	Université de Montpellier	Examinateur
Mme. Morgane LE BON-JÉGO	Université de Bordeaux	Directeur de thèse

Table of contents

List of abbreviations

3-MT: **3**-**m**ethoxy**t**riptamine

5-HT3aR: serotoninergic receptor 3a

AAV: **a**deno-**a**ssociated **v**irus

AC: **a**denylyl **c**yclase

AHP: **a**fter **h**yper**p**olarization

ALDH: **al**dehyde **de**-**h**ydrogenase

ANOVA: **an**alysis **o**f **va**riance

AP: **a**ction **p**otential

BNST: **b**ed **n**ucleus of the **s**tria **t**erminalis

CamKII: **ca**lcium/cal**m**odulin **k**inase **II**

cAMP: **c**yclic **AMP**

CCK: **c**hole**c**ysto**k**inin

ChR2: **ch**annel**r**hodopsin **2**

COMT: **c**atechol-**O**-**m**ethyl**t**ransferase

CThN: **c**ortico**th**alamic **n**euron

D1: **d**opamine receptor **1**

D2: **d**opamine receptor **2**

DβH: **d**opamine **β**-**h**ydroxylase

DA: **d**op**a**mine

DAergic: **d**op**a**min**ergic**

DAG: **d**i**a**cyl**g**lycerol

DAT: **d**op**a**mine **t**ransporter

DOPAC: 3,4-**di**hydr**o**xy**p**henyl**ac**etic acid

DOPA-DC: **DOPA de**-**c**arboxylase

DRN: **d**orsal **r**aphe **n**ucleus

dSNcM: **d**orsal tier of the **s**ubstantia **n**igra *pars* ***c****ompacta*, **m**edial part

EPSC: **e**xcitatory **p**ost**s**ynaptic **c**urrent

FG: **f**luoro**g**old™

GABA: **γ**-**a**mino**b**utyric **a**cid

GFP: **g**reen **f**luorescent **p**rotein

HVA: **h**omo**v**anillic **a**cid

IN: **i**nter**n**euron

IP_3: **i**nositol **t**ri**p**hosphate

IPSC: **i**nhibitory **p**ost**s**ynaptic **c**urrent

IT-CCN: **i**ntra**t**elencephalic **c**ortico**cor**tical **n**euron

IT-CStrN: **i**ntra**t**elencephalic **c**ortico**str**iatal **n**euron

ITN: **i**ntra**t**elencephalic **n**euron

KW: **K**ruskal-**W**allis

LDTg: **l**atero**d**orsal **t**egmentum nucleus

LHB: **l**ateral **h**a**b**enula

LHT: **l**ateral **h**ypo**t**halamus

M1: primary motor cortex

MAO-A: **m**ono**a**mine **o**xidase **A**

MAO-B: **m**ono**a**mine **o**xidase **B**

mPFC: **m**edial **p**re**f**rontal **c**ortex

MSN: **m**edium **s**piny **n**euron

nAcc**: n**ucleus **acc**umbens

PAG: **p**eri**a**queductal **g**rey

PBP: **p**ara**b**rachial **p**igmented nucleus

PD: **P**arkinson's **d**isease

PFC: **p**re**f**rontal **c**ortex

PIF: **p**ara**i**nter**f**ascicular nucleus

PiP_2: **p**hosphat**i**dylinositol 4,5-**bisp**hosphate

PKA: **p**rotein **k**inase **A**

PKC: **p**rotein **k**inase **C**

PLC: **p**hospho**l**ipase **C**

PN: **p**yramidal **n**euron

PNMT: **p**henylethanolamine **N**-**m**ethyl**t**ransferase

PNu: **p**aranigral **n**ucleus

PPTg: **p**edunculo**p**ontine **teg**mentum

PTN: **p**yramidal **t**ract **n**euron

PV: **p**ar**v**albumin

RMTg: **r**ostro**m**edial **t**e**g**mentum nucleus

SN: **s**ubstantia **n**igra

SNc: **s**ubstantia **n**igra *pars* ***c****ompacta*

SPRT: **s**ingle **p**ellet **r**eaching **t**ask

SST: **s**omato**st**atin

TH: **t**yrosine **h**ydroxylase

VGLUT2: **v**esicular **glu**tamate **t**ransporter type **2**

VIP: **v**asoactive **i**ntestinal **p**eptide

VMAT: **v**esicular **m**ono**a**mine **t**ransporter

vSNcM: **v**entral tier of the **s**ubstantia **n**igra *pars* ***c****ompacta*, **m**edial part

VTA: **v**entral **t**egmental **a**rea

VTAR: **v**entral **t**egmental **a**rea, **r**ostral part

WSR: **W**ilcoxon **s**igned **r**ank

Summary

The primary motor cortex plays a crucial role in motor processes, but also in cognitive processes such as motor skill learning, which is essential for daily life actions such as typing on a keyboard, playing a musical instrument, or even writing. Motor skill learning process in the primary motor cortex is dependent of dopamine. Dopamine release in the primary motor cortex has been shown to originate from the midbrain, especially from the ventral tegmental area and the substantia nigra *pars compacta*. Depletion of these dopaminergic terminals in the primary motor cortex leads to net impairments of motor skill acquisition, as well as depletion of midbrain dopaminergic neurons, as observed during Parkinson's disease. Nonetheless, it is still unclear how dopamine acts on the networks of the primary motor cortex, its impact on different neuronal populations and the implication of its two main receptor types. Furthermore, several studies focused on the implication of dopamine at the level of the primary motor cortex, but there is no available data in the literature regarding the electrophysiological characterization of these dopaminergic neurons of the midbrain projecting to the primary motor cortex. Thus, the objectives of this thesis were to investigate, using patch clamp recordings, the intrinsic properties of midbrain dopaminergic neurons projecting to the primary motor cortex and to monitor their activity during motor skill learning, and to assess the impact of dopamine on pyramidal neurons of the primary motor cortex.

To begin with, the location of midbrain dopaminergic neurons projecting to the primary motor cortex was revealed using retrograde tracing approaches in mice. These neurons are located in rostro ventrolateral parts of the midbrain. Then, *ex vivo* electrophysiological recordings of the retrogradely identified neurons revealed that these neurons display similar intrinsic properties as nigrostriatal neurons. Monitoring the intrinsic properties of these neurons during motor skill learning has been assessed using the single pellet reaching task in mice. *Ex vivo* patch clamp recordings were made at different times of the learning process to investigate if the intrinsic properties of dopaminergic neurons projecting to the primary motor cortex change with learning. These recordings revealed an increased activity of these neurons during the learning, but not after successful acquisition of the new motor skill.

The functional impact of dopamine at the level of the primary motor cortex has then been investigated. Firstly, *ex vivo* dopamine release in the primary motor cortex has been imaged using the recently developed genetically-encoded dopaminergic sensor $GRAB_{DA1m}$. Then, taking advantage of the transgenic mouse lines DAT-Cre-Ai32 and DAT-Cre, enabling

the expression of excitatory opsins in dopaminergic neurons only, the impact of dopamine release by dopaminergic terminals in the primary motor cortex has been further investigated. To achieve this aim, recordings of pyramidal neurons took place while dopamine release from dopaminergic terminals in the primary motor cortex was triggered by an optogenetic stimulation.

As the results obtained in this part of the thesis were not conclusive, another approach has been initiated using pharmacology. In this part, the impact of D1 receptor activation and blockade has been studied on pyramidal neurons of the layer V in D1-GFP mice, which express the green fluorescent protein only in D1-expressing cells. Firstly, the mapping of D1 receptors in the primary motor cortex has been done in young and adult mice, as differences in the level of expression of this receptor have been shown in other cortices. This was not the case in the primary motor cortex. Then, *ex vivo* electrophysiological recordings of D1-expressing pyramidal neurons of the layer V of the primary motor cortex while activating or blocking D1 receptors in young or adult mice revealed an age dependent modulation of these neurons by D1 receptors. In fact, D1 receptor activation induced an increase in the excitability of pyramidal neurons of the layer V of the primary motor cortex, either in young or adult mice, while D1 receptor blockade induced a decrease in the excitability of these neurons in young mice, and an increase in the excitability of these neurons in adult mice.

This project enabled to characterize the mesocortical pathway implicated in motor skill learning, as well as clarifying the impact of dopamine on neuronal networks of the primary motor cortex.

Résumé en Français

Le cortex moteur primaire jour un rôle crucial dans les processus moteurs, mais aussi dans les processus cognitifs, notamment l'apprentissage moteur qui est essentiel dans nos actions du quotidien telles que taper des mots sur un clavier, jouer d'un instrument de musique ou encore écrire. L'apprentissage moteur au niveau du cortex moteur primaire nécessite la libération de dopamine dans le cortex moteur primaire. Il a été démontré que cette libération de dopamine par les terminaisons dopaminergiques dans le cortex moteur primaire provient du mésencéphale, plus précisément de l'aire tegmentale ventrale et du la substance noire *pars compacta*. En effet, la déplétion des fibres dopaminergiques dans le cortex moteur primaire induit de nets déficits dans l'apprentissage de nouveaux mouvements, aussi bien que la lésion sélective des neurones dopaminergiques du mésencéphale, comme il est observé au cours de la maladie de Parkinson. Néanmoins, le mode d'action de la dopamine sur ses deux types de récepteurs ainsi que son impact sur les réseaux neuronaux du cortex moteur primaire restent à ce jour mal compris. De plus, plusieurs études ont traité de l'action de la dopamine au niveau du cortex moteur primaire, mais à ce jour, aucune donnée n'est disponible dans la littérature concernant les propriétés intrinsèques des neurones du mésencéphale projetant au cortex moteur primaire. Ainsi, les objectifs de cette thèse furent de caractériser et d'étudier les propriétés intrinsèques des neurones dopaminergiques du mésencéphale projetant au cortex moteur primaire au cours de l'apprentissage moteur, ainsi que d'étudier l'impact de la dopamine sur les propriétés électrophysiologiques des neurones du cortex moteur primaire.

Dans un premier temps, des expériences de traçage rétrograde ont mis en évidence la localisation des neurones dopaminergiques projetant au cortex moteur primaire dans le mésencéphale de souris. Ces neurones sont localisés dans les parties rostro ventrolatérales du mésencéphale. Dans un second temps, ces mêmes approches de traçage ont été utilisées en combinaison à des enregistrements électrophysiologiques *ex vivo* dans le but d'étudier les propriétés intrinsèques de ces neurones. Les enregistrements ont révélé que ces neurones possèdent une signature électrophysiologique ressemblant à celle des neurones dopaminergiques de la voie nigrostriée. Ensuite, ces mêmes approches ont été utilisées au cours de l'apprentissage d'une tâche motrice chez la souris, modélisée par le *single pellet reaching task*. Les enregistrements de ces neurones au cours de l'apprentissage moteur ont révélé une hausse de leur excitabilité au cours de l'apprentissage, qui n'est plus observable lorsque la tâche motrice est apprise.

La seconde partie de cette thèse fût dédiée à l'étude de l'impact de la dopamine au niveau du cortex moteur primaire. Premièrement, la libération de dopamine dans le cortex moteur primaire a été mise en évidence grâce à l'imagerie *ex vivo* d'un senseur dopaminergique encodé génétiquement : le $GRAB_{DA1m}$. Ensuite, les lignées de souris transgéniques DAT-Cre-Ai32 et DAT-Cre, permettant l'expression d'opsines excitatrices uniquement dans les neurones dopaminergiques, ont été utilisées. Ces souris transgéniques ont permis de disséquer l'impact de la libération de dopamine dans le cortex moteur primaire par les terminaisons dopaminergiques situées dans le cortex moteur primaire. Les enregistrements ont été effectués sur les neurones pyramidaux, tout en stimulant les terminaisons dopaminergiques du cortex moteur primaire à l'aide d'une fibre optique.

Comme les résultats de la partie précédente ne furent pas concluants, une autre approche a été utilisée par l'utilisation de la pharmacologie. Dans cette partie, l'impact du récepteur D1 dans le cortex moteur primaire a été étudié chez des souris transgéniques D1-GFP jeunes et adultes. Ces souris expriment la *green fluuorescent protein* dans les cellules exprimant le récepteur D1 uniquement. Dans un premier temps, une cartographie des récepteurs D1 dans le cortex moteur primaire a été effectuée chez des souris jeunes et adultes, car des différences ont été mises en évidences dans d'autres parties du cortex en fonction de l'âge des souris. Ce ne fût pas le cas du niveau du cortex moteur primaire, où l'expression du récepteur D1 est similaire chez les souris jeunes adultes. Ensuite, des enregistrements électrophysiologiques *ex vivo* des neurones pyramidaux exprimant le récepteur D1 du cortex moteur primaire ont été effectués, tout en bloquant ou en activant les récepteurs D1, chez les souris jeunes ou adultes. Ces enregistrements ont révélé que la modulation des neurones pyramidaux du cortex moteur primaire par les récepteurs D1 est dépendante de l'âge. En effet, l'activation des récepteurs D1 a induit une augmentation de l'excitabilité des neurones pyramidaux du cortex moteur primaire chez les souris jeunes et adultes, alors que le blocage des récepteurs D1 a induit une diminution de l'excitabilité des neurones pyramidaux du cortex moteur primaire chez les souris jeunes, mais une augmentation chez les souris adultes.

Ce projet a permis de caractériser la voie mésocorticale impliquée dans l'apprentissage moteur, ainsi que de clarifier l'impact de la dopamine sur les réseaux neuronaux du cortex moteur primaire.

Introduction

1. Dopamine

1.1. Synthesis and molecular properties

Dopamine (DA) is a monoamine, and more particularly a catecholamine, as DA is composed of a catechol core and an ethylamine side chain. DA is synthesized from the amino acid tyrosine (Fig. 1.1). The enzyme tyrosine hydroxylase (TH) catabolizes the transformation of tyrosine in L-DOPA. Then, L-DOPA is metabolized in DA by the removal of its carboxyl group through the action of the DOPA decarboxylase (DOPA-DC) enzyme. As such, DA is also the precursor of other catecholamines, as DA is metabolized in norepinephrine through the action of the dopamine β-hydroxylase (DβH) enzyme, and norepinephrine is metabolized in epinephrine through the action of the phenylethanolamine N-methyltransferase (PNMT) enzyme (Fig. 1.1, Kopin, 1968). DA is produced mainly by dopaminergic (DAergic) neurons in the midbrain, in the substantia nigra *pars compacta* (SNc) and in the ventral tegmental area (VTA), the two major DAergic nuclei (Juárez Olguín et al., 2016). However, DA can be detected not only in the brain but also in periphery, such as in the gastrointestinal tract (Eisenhofer et al., 1997) and the pancreas (Mezey et al., 1996). In fact, DA is also produced by non-neuronal cells in periphery, especially epithelial cells and lamina propria cells (Eisenhofer et al., 1997; Mezey et al., 1996). DA can also be detected in the bloodstream, as it plays a role as an intrarenal natriuretic hormone (Lee, 1993). Nonetheless, the action of DA in the periphery remains unclear (Eisenhofer et al., 2004). Besides, DA cannot cross the blood brain barrier, so peripheral DA cannot act at the level of the brain (Pahuja et al., 2015).

At the presynaptic site, newly synthesized DA is transported into vesicles by a vesicular monoamine transporter, either the type 1 (VMAT1) or the type 2 (VMAT2), though the type 2 is more widely expressed in the central nervous system (Lohoff et al., 2019). This import into the vesicles is made possible by the generation of a proton gradient by vacuolar-type ATPases (Schuldiner et al., 1995; Yaffe et al., 2018). DA is released into the synaptic cleft by full fusion or kiss-and-run exocytosis, following increased intracellular calcium concentration (Westerink, 2006). This DA release necessitates an active zone-like release site, at least in the striatum (Liu et al., 2018).

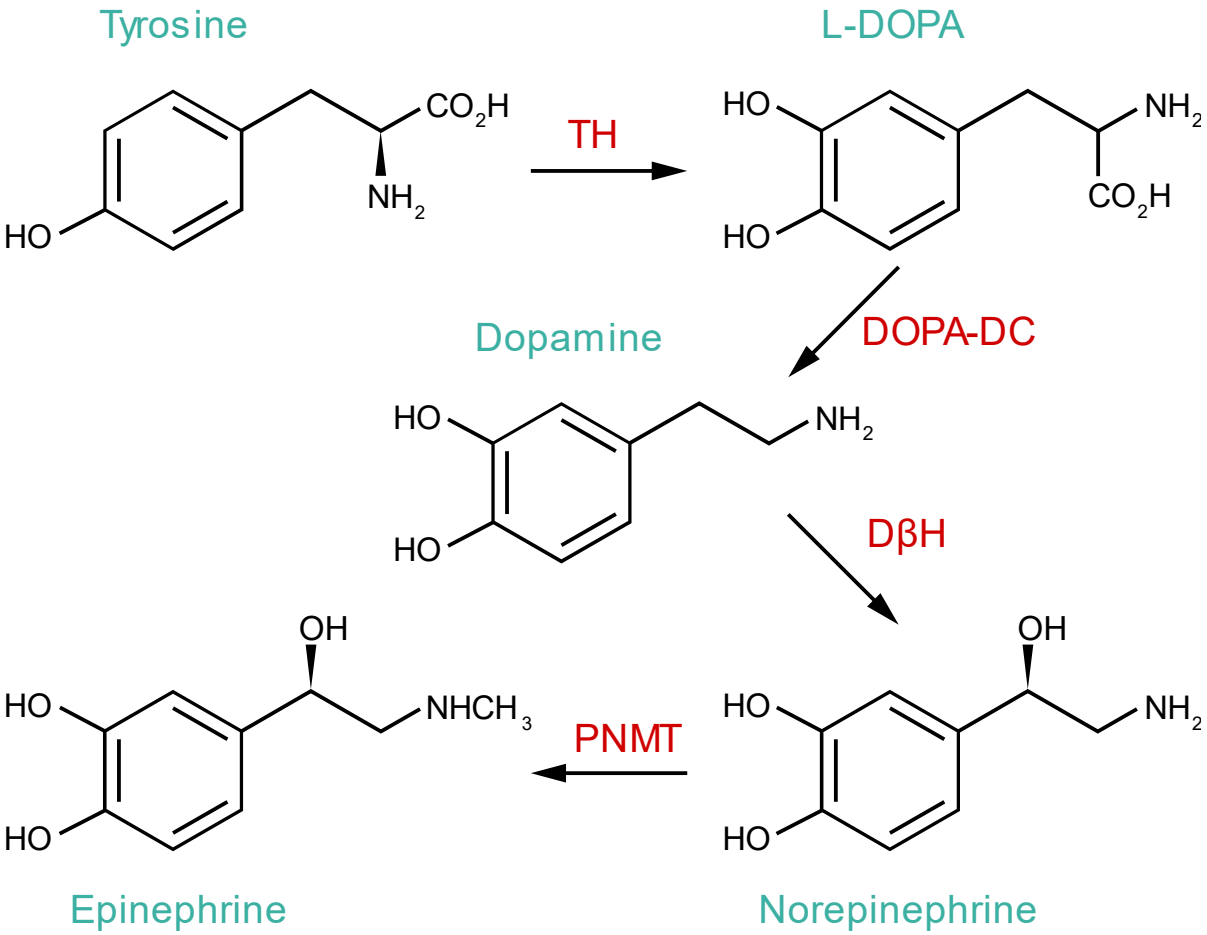

Fig. 1.1: Synthesis of catecholamines. Tyrosine is converted into L-DOPA through the action of the tyrosine hydroxylase (TH). Dopamine is synthetized from L-DOPA by the action of the DOPA-decarboxylase (DOPA-DC). Norepinephrine is produced from dopamine by the action of the Dopamine β-hydroxylase (DβH) and finally, epinephrine is produced from norepinephrine by the action of the phenylethanolamine N-methyltransferase (PNMT).

DA reuptake from the synaptic cleft is generally carried out by the DA transporter (DAT) and DA is recycled in the presynaptic neuron (Dahal et al., 2015). DA can be degraded by two enzymes: the catechol-O-methyltransferase (COMT) or the monoamine oxidase A (MAO-A) and B (MAO-B). DA is degraded into 3-methoxytyramine (3-MT) by the COMT, which can be further degraded into homovanillic acid (HVA) by the combined action of MAO-A or MAO-B and an aldehyde dehydrogenase (ALDH, Eisenhofer et al., 2004). Moreover, DA can be degraded into 3,4-dihydroxyphenylacetic acid (DOPAC) by the combined action of MAO-A or MAO-B and an ALDH, which can be further degraded into HVA by the COMT (Fig. 1.2, Eisenhofer et al., 2004). DA degradation can take place at many sites, as MAO are localized at the membrane of mitochondria (Abell and Kwan, 2000) in cell bodies as well as at the presynaptic site, in dendrites and in axons (Westlund et al., 1993), and also in glia for MAO-B (Abell and Kwan, 2000). Moreover, COMT is present in neurons such as pyramidal and

striatal medium spiny neurons (MSNs), but also abundantly in microglia and astrocytes. COMT can be found in a membrane bound form as well as in a soluble form, even if the membrane bound form is thought to be more implicated in DA metabolism (Myöhänen et al., 2010).

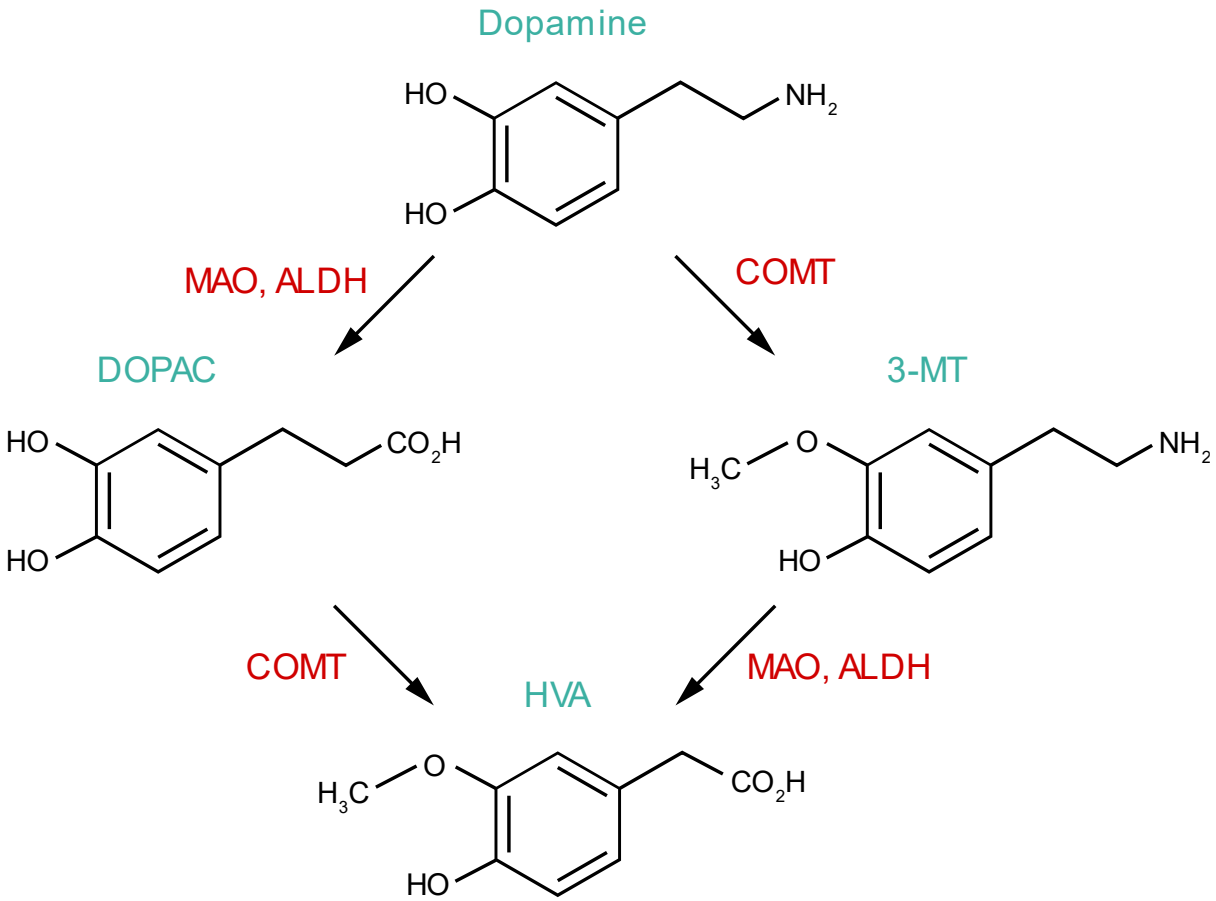

Fig. 1.2: Catabolism of dopamine. Dopamine can be degraded into 3-methoxytriptamine (3-MT) by the action of the catechol-O-methyltransferase (COMT), and then into homovanillic acid (HVA) through the combined action of the monoamine oxidase (MAO) and an aldehyde dehydrogenase (ALDH). Dopamine can also be degraded into 3,4-dihydroxyphenylacetic acid (DOPAC) through the combined action of MAO and an ALDH, and then into HVA by the action of COMT.

DA can act on two types of receptors: the D1-like receptors (D1 and D5 receptors) and the D2-like receptors (D2, D3 and D4 receptors).

1.2. D1-like receptors

1.2.1. Expression and localization of D1-like receptors in the brain

Thanks to northern blot analysis (Monsma et al., 1990; Sunahara et al., 1990; Zhou et al., 1990) and *in situ* hybridization (Anastasiades et al., 2019; Dearry et al., 1990; Monsma et al., 1990; Sunahara et al., 1990), D1 receptor mRNA has been detected in the striatum, the

nucleus accumbens (nAcc), the olfactory tubercle, the subthalamic nucleus, the cortex, especially the prefrontal cortex (PFC), and the amygdala. D1 receptors are also present in the substantia nigra (SN). In fact, binding of ^{125}I-labeled SCH23982, a specific D1 receptor ligand, has been shown in this area, but no mRNA has been detected in the SN at the time (Fremeau et al., 1991). These experiments suggested that D1 receptors are not synthesized in the SN but transported to the SN from areas projecting to the SN and synthesizing D1 receptors, presumably the striatum (Vallone et al., 2000). However, more recent studies using single cell RT-PCR revealed that most GABAergic neurons of the substantia nigra *pars reticulata* express D1 receptors (Zhou et al., 2009a).

D1-like receptors also comprises D5 receptors. First experiments investigating the distribution of D5 receptors have been made using northern blot, PCR and *in situ* hybridization (Meador-Woodruff et al., 1992; Sunahara et al., 1991; Tiberi et al., 1991; Weinshank et al., 1991). It has been shown that D5 receptor mRNA occurrence is much more restricted than the one of D1 receptors. Plus, it did not appear that D5 receptors mRNA overlap with D1 receptors mRNA. Low mRNA levels were detected in the hippocampus (Meador-Woodruff et al., 1992; Tiberi et al., 1991) and the thalamus (Tiberi et al., 1991). However, in more recent studies using immunocytochemistry, D5 receptor immunoreactivity has been detected in the cortex, the olfactory tubercle, the basal ganglia, the VTA, the SN, the raphe, the hippocampus and the brainstem (Ciliax et al., 2000). Post-synaptic D5 receptors have also been found in the subthalamic nucleus, using *in situ* hybridization (Svenningsson and Le Moine, 2002) and electron microscopy (Baufreton et al., 2003).

1.2.2. Expression of D1-like receptors during development

Most of D1-like receptors studies investigating their expression during development have been done during the 90's, thanks to autoradiographic experiments. One of these studies showed that the expression of D1-like receptors in the nAcc and the striatum increases from birth to postnatal day 28, and then decreases until adulthood (Tarazi et al., 1999). In this same study, D1-like receptors expression in other structures such as the PFC, the entorhinal cortex and the hippocampus increases from birth to a reach maximal level at adulthood (Tarazi et al., 1999). Nonetheless, previous experiments also using autoradiography showed that D1-like receptors expression in the PFC reaches a peak at 3 weeks of postnatal age and then decreases until adulthood (Leslie et al., 1991). Furthermore, D1-like receptors expression in the nAcc and the striatum was different in this study, as it increases rapidly between 1 and 2 weeks of

postnatal development and reaches a plateau afterwards (Leslie et al., 1991). These differences may come from the number of animals used in these studies (n = 3 in Leslie et al., 1991 vs n = 6 in Tarazi et al., 1999), reflecting an inter-individual differential pruning within the animals used.

1.2.3. Signaling pathways of D1-like receptors

D1-like receptors are G-protein coupled receptors, classically coupled with an activator G-protein G_s (Stoof and Kebabian, 1981). In this case, when the receptor is activated, it recruits the G_s protein, leading to the activation of the adenylyl cyclase (AC) enzyme. This enzyme produces cyclic AMP (cAMP), with ATP as a substrate. The cAMP can then activate the protein kinase A (PKA), which activates downstream signaling pathways (Fig. 1.3, Rosenbaum et al., 2009) such as CREB, which mediates the expression of genes increasing neuronal excitability (Dong et al., 2006; Lopez de Armentia et al., 2007; Viosca et al., 2009; Zhou et al., 2009b).

Nonetheless, D1-like receptors can also be coupled with a $G_{q/11}$ protein (Mannoury la Cour et al., 2007). With this coupling, the activation of D1-like receptors recruits the $G_{q/11}$ protein, which activates the phospholipase C (PLC) enzyme. This enzyme catalyzes the production of inositol triphosphate (IP_3) and diacylglycerol (DAG) from phosphatidylinositol 4,5-bisphosphate (PiP_2, Rosenbaum et al., 2009). On one hand, the DAG activates the protein kinase C (PKC). The actions of the PKC are multiple, as it can activate downstream signaling pathways, leading to the increase of expression of immediate early genes such as c-fos (Nakakuki et al., 2010), but it can also phosphorylate NMDA receptors (Lin et al., 2006; Lu et al., 1999). This phosphorylation is necessary to both increase and maintenance of the increased evoked responses of NMDA currents (Barre et al., 2016). On the other hand, IP_3 activates an IP_3 receptor at the membrane of the endoplasmic reticulum, leading to the release of calcium ions in the cytoplasm (Rosenbaum et al., 2009). These calcium ions can further activate the PKC, or increase the activity of the calcium/calmodulin kinase II (CamKII) enzyme. This enzyme phosphorylates the AMPA receptors at the surface of the neuron, leading to the increase in the average conductance of the channels (Lisman et al., 2012). The CamKII enzyme can induce the insertion of extra AMPA receptors at the synapse (Fig. 1.3, Lisman et al., 2012).

DA receptors, including D1-like receptors, activate β-Arrestin pathways (Del'Guidice, 2011), even if these pathways are more classically linked to D2-like receptors. The activation of these pathways leads to the desensitization of DA receptors by clathrin-mediated endocytosis (Del'Guidice, 2011) in order to avoid over-stimulation of the receptors (Lohse et al., 1990).

Furthermore, D1 receptors can activate β-Arrestin 2 pathway, leading to the activation of MAP kinase pathway kinases RAF, MEK and ERK (Luttrell et al., 2001), supporting the activation of ERK by β-Arrestin 2 (Ahn et al., 2004).

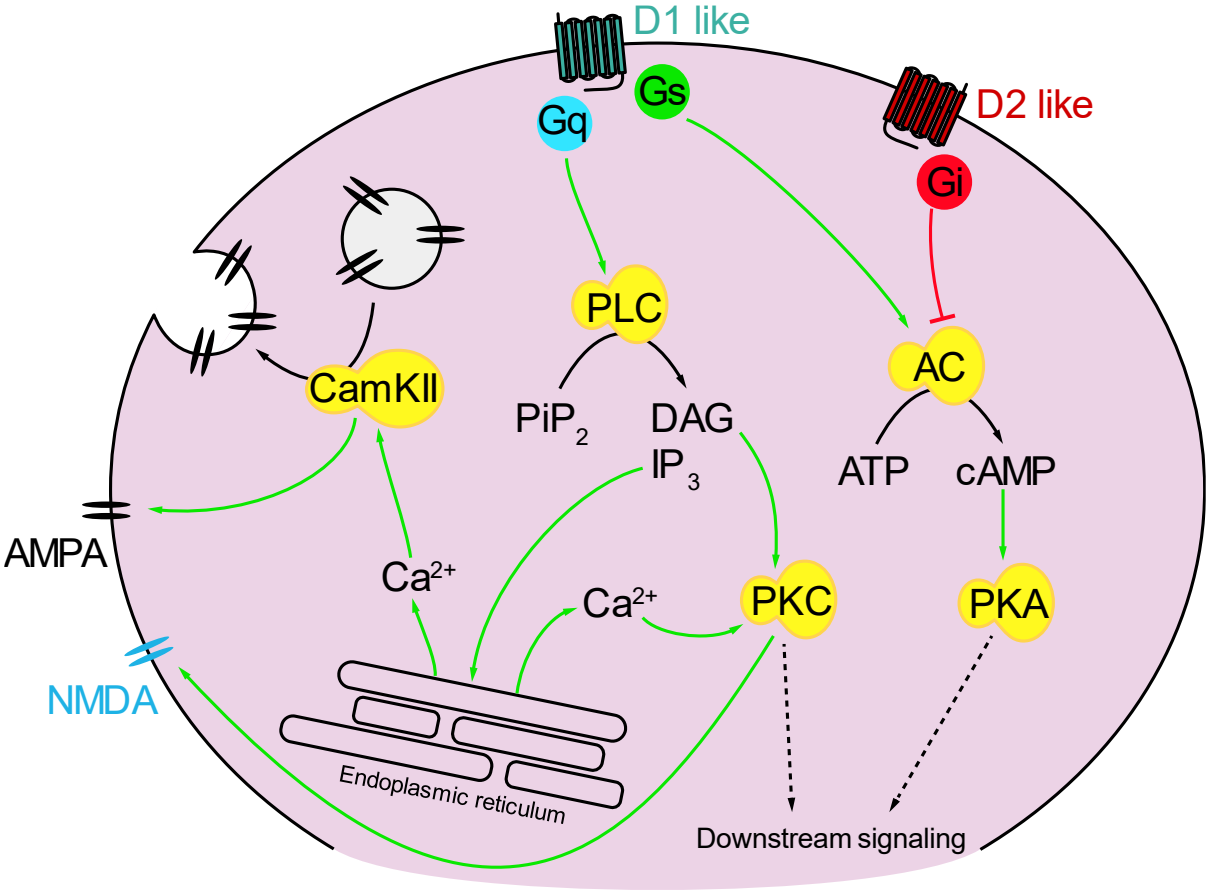

Fig. 1.3: Main signaling pathways of dopaminergic receptors. D1 receptors are coupled with G_s or G_q proteins. Activation of G_s protein leads to the activation of adenylyl cyclase (AC), which produces cAMP from ATP. The produced cAMP activates the protein kinase A (PKA), leading to downstream signaling pathways activation. Activation of G_q protein will activate the phospholipase C (PLC), which produces diacylglycerol (DAG) and inositol triphosphate (IP_3) from phosphatidylinositol bisphosphate (PiP_2). On one hand, the DAG will activate the protein kinase C (PKC), which can activate downstream signaling pathways and increase the activity of NMDA receptors. On the other hand, the IP_3 will trigger release of calcium ions (Ca^{2+}) from the endoplasmic reticulum. Ca^{2+} can activate the PKC and interact with the calmodulin kinase II (CamKII), which will increase the activity of AMPA receptors and promote the insertion of new AMPA receptors at the plasma membrane. D2 receptors are coupled with Gi proteins, which activation negatively regulates the activity of AC, and thus the levels of cAMP, leading to decreased activity of the PKA and so of its downstream signaling pathways.

1.2.4. Physiological functions

As D1 receptors are expressed in the PFC (Anastasiades et al., 2019), it is not surprising to find that they are implicated in cognitive processes. In fact, intracerebroventricular infusion of D1-agonist SKF 38393 impaired working memory performance in rats performing a radial arm maze task (Levin and Rose, 1995). Moreover, post-training injection of D1-agonist SKF

38393 in the caudate nucleus improved the performance of rats performing a similar a radial arm maze task (Packard and White, 1991). These findings highlight the importance of the regulation of D1 receptors in cognitive processes, as much as the dissociation between cortical and subcortical memory processes. It is thus not surprising to find that D1 receptors are implicated in the pathophysiology of schizophrenia, a major cognitive disorder. Negative symptoms of schizophrenia, such as anhedonia, asociality, alogia and avolition, are linked to a reduced D1 receptor activation (Shen et al., 2012).

The DAergic system is widely known for its role in reward processes, which also imply the nAcc. It has been shown that D1 receptors are implicated in these processes. Indeed, D1 agonist SKF38393 injection in the nAcc increases the cocaine self-administration in rats in a dose-dependent manner (Maldonado et al., 1993). Moreover, D1 receptor knock out in mice abolish the pre-reward excitation of nAcc neurons, which is thought to be important in the motivational phase, but not in the reward or post-reward phases *per se* (Tran et al., 2005). Thus, D1 receptor knock out results in motivation alterations due to lack of functionality in the nAcc.

It is widely known that D1-receptors are expressed in striatal MSNs. These D1-expressing MSNs project to the inhibitory output of basal ganglia structures: the substantia nigra *pars reticulata* and the globus pallidus internal part, and therefore form the so-called direct pathway (Albin et al., 1989). D1 receptor activation enhances the activity of these MSNs. As MSNs are inhibitory, the direct pathway lifts the tonic inhibition exerted by basal ganglia output structures on motor execution-related areas, thus promoting motor execution. During Parkinson's disease (PD), the lack of DA at the level of D1-expressing MSNs plays a central role in motor impairments. In fact, the lower activity of D1-expressing MSNs induced by lack of D1 receptor activation leads to the increase of the tonic inhibition exerted by the output structures of basal ganglia on motor execution-related structures, such as the thalamus and the motor cortex (Nambu et al., 2015). Furthermore, D1 receptor-mediated ERK activation has been shown to participate in DA-modulated behaviours, such as drug-mediated hyperlocomotor behaviour (Urs et al., 2011; Valjent et al., 2006).

Using a mouse model of D1 receptor conditional knock out (*i.e.*, a mouse model in which the expression of D1 receptors can be controlled by tetracycline), the D1 receptors reversible knock out impairs locomotion, as the walking speed is slowed down when D1 is downregulated by injection of tetracycline (Nakamura et al., 2020). Similar results were obtained in mice following bilateral injection of D1 receptor antagonist SCH23390 in the dorsal

striatum (Centonze et al., 2003; Nakamura et al., 2020). More recently, it has been shown that D1 receptors are implicated in motor skill learning, by mediating synaptic plasticity through PLC activation in the primary motor cortex (M1, Rioult-Pedotti et al., 2015). At the level of M1, D1 receptors are implicated in the stabilization of dendritic spines of pyramidal neurons (PNs, Guo et al., 2015).

Postsynaptic D5 receptors have been found in the subthalamic nucleus. At this level, D5 receptors shapes the neuronal firing, as they potentiate burst-firing pattern (Baufreton et al., 2003). Moreover, application of the D1/D5 agonist SKF 82958 reduces the strength of cortical inputs on subthalamic nucleus neurons (Froux et al., 2018). These mechanisms may participate in information processing throughout the basal ganglia circuitry and thus be of importance in movement initiation, control and execution.

1.3. D2-like receptors

1.3.1. Expression and localization of D2-like receptors in the brain

D2-like receptors comprises D2, D3 and D4 receptors. It has been shown thanks to autoradiographic (Camps et al., 1990) and *in situ* hybridization (Bouthenet et al., 1991) experiments that D2 receptors and D2 receptors mRNA are mainly expressed in basal ganglia structures, such as in the caudate putamen and the nAcc, but also in the olfactory tubercle. D2 expressing cells have also been reported in cortices, as hemagglutinin-immunopositive cells were observed in the M1 of Drd2-Cre:ribotag mice (Cousineau et al., 2020), and D2 receptors have been observed in the PFC using electron microscopy (Wang and Pickel, 2002). Moreover, D2 receptor mRNA has been discovered in the SNc and in the VTA, highlighting a presynaptic location of D2 receptors (Vallone et al., 2000).

In comparison to D2 receptors, D3 receptors are expressed in a more restricted manner. Autoradiographic experiments revealed that D3 receptors mRNA are mainly expressed in the ventral striatum, the bed nucleus of the stria terminalis (BNST) and the olfactory tubercle (Bouthenet et al., 1991). *In situ* hybridization experiments have also revealed high levels of D3 mRNA in the island of Calleja and in the nAcc (Le Moine and Bloch, 1996). D3 receptors are also expressed in the thalamus, but also in the SNc and the VTA (Bouthenet et al., 1991; Vallone et al., 2000), indicating a presynaptic location of D3 receptors, just like D2 receptors.

D4 receptors distribution in brain areas has been less extensively studied, but using northern blot, D4 receptor mRNA has been detected in the amygdala, the frontal cortex, the

midbrain and the medulla. Nonetheless, only low mRNA levels have been detected in the basal ganglia (Van Tol et al., 1991).

1.3.2. Expression of D2-like receptors during development

As for D1-like receptors, D2-like receptors expression during development has been studied using autoradiographic experiments. A study carried out by the same team which has done the experiments for D1-like receptors (Tarazi et al., 1999) concluded that the expression of D2-like receptors during development is similar to the expression D1-like receptors (Tarazi et al., 1998). In fact, the expression of D2-like receptors in the striatum and nAcc increases from birth to postnatal day 28, and then decreases until adulthood (Tarazi et al., 1998). Moreover, it was found in this study that the expression of D2-like receptors in the PFC, the entorhinal cortex and the hippocampus increases from birth to reach maximal level at adulthood (Tarazi et al., 1998), as they found for D1-like receptors (Tarazi et al., 1999). However, more recent RT-PCR and western blot experiments showed that D2 receptors maximal expression is reached at postnatal day 15 and then decreases until reaching adulthood, at both mRNA and protein levels (Rani and Kanungo, 2006). These differences may come from the model used (rats for Tarazi et al., 1998 vs mice for Rani and Kanungo, 2006), but also from the experimental design. Moreover, differences may exist between the different cortices, leading to an overall different expression of D2 receptors between all cortices compared to specific cortical areas. Finally, D2 receptor mRNA and protein expression have been shown to decline progressively in the cerebellum from birth to adulthood (Rani and Kanungo, 2006).

1.3.3. Signaling pathways of D2-like receptors

D2-like receptors are coupled with an inhibitory G protein $G_{i/0}$ (Rosenbaum et al., 2009). This way, when D2-like receptors are activated, they recruit the $G_{i/0}$ protein, which inhibits the activity of the AC (Fig. 1.3). Thus, the production of cAMP decreases, and the PKA is less activated, leading to a decreased activation of downstream signaling pathways including CREB (Rosenbaum et al., 2009). As CREB mediates the expression of genes increasing the excitability of neurons (Dong et al., 2006; Lopez de Armentia et al., 2007; Viosca et al., 2009; Zhou et al., 2009b), the decreased activity of CREB leads to a decreased excitability of neurons. A recent study also revealed an activation of the PLC enzyme by D2 receptors in M1, which challenges the classical view in which D2 receptors inhibit the AC and thus decreases the neuronal excitability (Rioult-Pedotti et al., 2015). Moreover, D2-like receptors can activate GIRK

channels via its G_0 coupling, leading to a decreased membrane excitability (Huang et al., 2013a).

As D1-like receptors, D2-like receptors can also activate cAMP-independent pathways such as the β-Arrestin pathway, leading to a receptor desensitization as previously described for D1 receptors (cf paragraph 1.2.3., Del'Guidice, 2011; Lohse et al., 1990).

1.3.4. Physiological functions

D2 receptors can be expressed at the presynaptic site. As such, they are called autoreceptors, and can exert a powerful negative feedback on presynaptic neurons, by decreasing their firing rate, reducing their synthesis and release of neurotransmitter (Missale et al., 1998; Sibley, 1999; Wolf and Roth, 1990). D2 autoreceptors have been shown to be implicated in the development of DAergic neurons during embryonic stages, notably by activating the ERK signaling pathway (Sung et al., 2006; Yoon et al., 2011). D2 autoreceptors activation classically leads to a decreased synthesis and release of DA by the presynaptic neuron, leading to a decreased locomotor activity, whereas D2 receptors localized at the postsynaptic site will tend to increase moderately the locomotor activity (Beaulieu and Gainetdinov, 2011). Indeed, depletion of D2-expressing MSNs in the striatum projecting forming the indirect pathway leads to locomotor activity and action initiation impairments (Augustin et al., 2020). In a similar manner, lentiviral-mediated depletion of striatal D2 receptors accelerates the onset of addiction-like behaviour in rats (Johnson and Kenny, 2010). Moreover, obese rats displays lower levels of D2-receptors compared to control rats (Huang et al., 2006; Johnson and Kenny, 2010), highlighting a role of D2 receptors in the regulation of food intake. Moreover, D2 receptors are implicated in motor skill learning, by mediating synaptic plasticity through PLC activation in M1, as D1 receptors (Rioult-Pedotti et al., 2015). At the level of M1, D2 receptors are implicated in the formation of new dendritic spines on PNs (Guo et al., 2015).

D2 receptors have been shown to play a role in cognitive processes, such as cognitive flexibility (van Holstein et al., 2011), episodic memory (Lisman et al., 2011; Nyberg et al., 2016) and associative learning (Puig and Miller, 2015). Furthermore, D2 receptors are implicated, as D1-receptors, in working memory processes (Levin and Rose, 1995; Packard and White, 1991). Thus, it is not surprising to find that D2 receptors are implicated in the pathophysiology of cognitive disorders, especially schizophrenia. In fact, the DAergic hypothesis of schizophrenia stipulates a hyperactivity of the DAergic system in the striatum,

and a decreased DAergic transmission in the cortex, both through D2 receptors. Indeed, D2 receptor basal activation is more important in the striatum of schizophrenic patients (Abi-Dargham et al., 2000). Interestingly, a biased D2-receptor ligand activating cortical D2 receptors and inhibiting striatal D2 receptors has been recently discovered. This biased ligand induces the activation of β-Arrestin 2 pathway in the cortex but not in the striatum. This activation leads to an increase in the excitability of cortical D2-expressing interneurons (INs), which is not observable in striatal D2-expressing MSNs (Urs et al., 2016). An hyperactivity of D2 receptors has also been hypothesized in Tourette's syndrome as D2 receptors antagonists improves the symptoms (Uhr et al., 1986), but it has not been reported in all patients (Wong et al., 1997). Taken together, these findings indicate that D2 receptor plays an important role in several cognitive processes, and that an imbalance of D2 receptor activity leads to severe disorders.

As D2 receptors, D3 receptors can also be autoreceptors. Thanks to pharmacological experiments (Gainetdinov et al., 1996; Zapata and Shippenberg, 2002) and studies in D3-receptor knock out mice (Joseph et al., 2002), it has been demonstrated that D3 autoreceptors complement D2 autoreceptors activity by decreasing the firing frequency of the presynaptic neurons, as well as modulating the release of DA (Joseph et al., 2002; Sibley, 1999). Post synaptic D3 receptors are implicated in locomotion, as D3 receptor mutant mice exhibit hyperlocomotor activity (Vallone et al., 2000). Apart from these mechanisms, D3 receptors physiological functions remain largely unknown, as for the functional role of D4 receptors, essentially as a lot of studies investigated the role of DA in motor execution, and D4 receptor expression in motor areas is limited. (Missale et al., 1998; Sibley, 1999). However, even if D4 receptor expression in motor-related areas is low, D4 mutant mice exhibit locomotor activity reduction (Vallone et al., 2000).

2. DAergic neurons of the midbrain

2.1. Embryonic origins

Most of DAergic neurons in the adult brain are located in the ventral midbrain, which represents 400,000 – 600,000 neurons in the human, and 20,000 – 30,000 neurons in the mouse (Hegarty et al., 2013). These neurons are generated by mesencephalic floor plate cells (Ono et al., 2007), and the induction of these cells is under the control of sonic hedgehog, LMX1A and LMX1B proteins (Blaess and Ang, 2015; Veenvliet and Smidt, 2014). The further steps after the induction of the mesencephalic floor plate cells involve the cellular proliferation of the

DAergic progenitors and neurogenesis, which relies on the combination of several transcription factor, such as Corin, MSX1, Neurog2 and Ascl1 (Blaess and Ang, 2015). These progenitors ultimately form three anatomically distinct clusters: A8, A9 and A10, which develop into the retrorubal field, the SNc and the VTA, respectively. The VTA is also divided in distinct areas: the parabrachial pigmented nucleus (PBP), the parainterfascicular nucleus (PIF), the paranigral nucleus (PNu) and the rostral part of the VTA (VTAR, Fig. 1.4). However, these groups seem to be heterogeneous, as they contain subsets of DAergic neurons implicated in specific behavioural responses (Poulin et al., 2018).

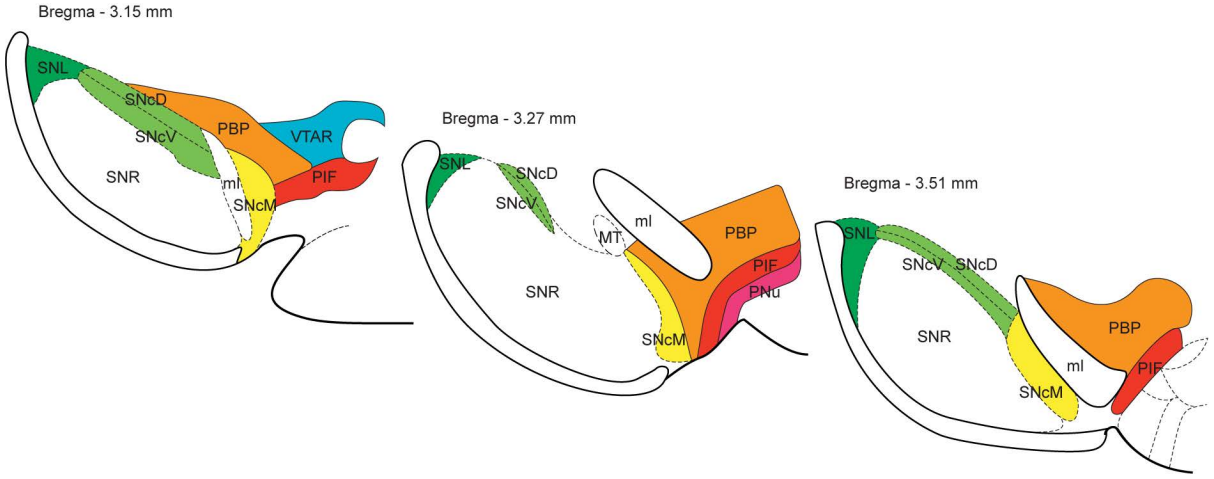

Fig. 1.4: Midbrain nuclei containing dopaminergic neurons in adult mouse brain. Schematic representation midbrain nuclei from 3 coronal slices, from the most rostral (left) to the most caudal (right). ml: medial lemniscus, MT: medial terminal nucleus of the optic tract, PBP: parabrachial pigmented nucleus, PIF: parainterfascicular nucleus, PNu: paranigral nucleus, SNcD: substantia nigra *pars compacta*, dorsal tier, SNL: substantia nigra *pars lateralis*, SNR: substantia nigra *pars reticulata*, VTAR: ventral tegmental area, rostral part. Taken from Subramaniam and Roeper, 2016.

Thanks to single cell qRT-PCR studies, midbrain DAergic neurons have been more recently classified in two categories, depending on their molecular profile: ALDH1a1-expressing and OTX2-expressing neurons (Poulin et al., 2014), even though other categories can exist depending on the expression or not of other molecular markers. These two neuronal populations are segregated in the midbrain: ALDH1a1-expressing neurons are localized in the SNc, whereas OTX2-expressing neurons are localized in medial parts of the VTA (Fig. 1.5, Poulin et al., 2014). Also, they display different gene expression profiles. In ALDH1a1-expressing neurons, PITX3 plays a crucial role in the end of the differentiation process of DAergic progenitors, as it enables the expression of ALDH1a1 in these neurons. Furthermore, PITX3 interacts with Nurr1, a nuclear receptor essential in DAergic phenotyping, as it enables the expression of TH, VMAT2 and dopamine transporter (DAT, Blaess and Ang, 2015; Saucedo-Cardenas et al., 1998). Thus, PITX3 gives the molecular identity to these DAergic

neurons, and also plays a role by itself by inducing the expression of brain derived neurotrophic factor in these neurons (Veenvliet and Smidt, 2014). In OTX2 neurons, OTX2 also controls the molecular signature of the neurons, by inhibiting KCNJ6 (GIRK2) channel, a potassium channel implicated in somatodendritic D2 receptors downstream signaling (Lammel et al., 2008). OTX2 also represses the expression of the DAT, but increases the expression of axonal guiding factors. These features may imply that OTX2-expressing neurons comprise VTA mesocortical neurons (Subramaniam and Roeper, 2016).

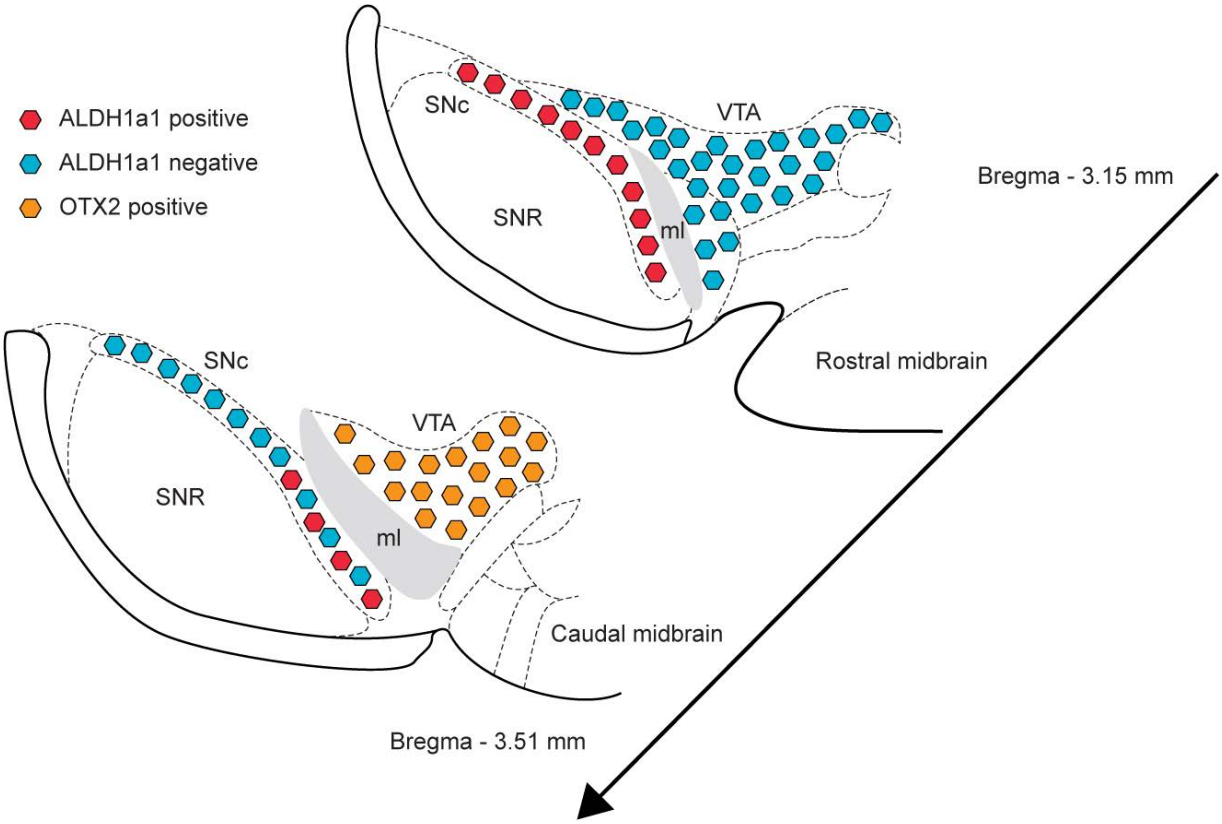

Fig. 1.5: Diversity of midbrain dopaminergic neurons in adult mouse brain. Schematic representation of midbrain nuclei from 2 coronal slices, from the most rostral (right) to the most caudal (left). ALDH1a1 positive DAergic neurons are mainly found in rostral parts of the substantia nigra *pars compacta* (SNc), and some in more caudal parts of the SNc. OTX2 positive DAergic neurons are mainly found in caudal parts of the ventral tegmental area (VTA). ml: medial lemniscus, SNr: substantia nigra *pars reticulata*. Taken from Subramaniam and Roeper, 2016.

2.2. DAergic neurons of the SNc

2.2.1. Inputs and outputs

Using retrograde tracing approaches, it has been shown that the main inputs to SNc DAergic neurons come from striatal MSNs (Fig. 1.6, Watabe-Uchida et al., 2012). Nonetheless, other basal ganglia nuclei also send projection to SNc DAergic neurons. In fact, SNc DAergic neurons receive GABAergic projections from the external part of the globus pallidus, the

striatum, the substantia nigra *pars reticulata* (Lee and Tepper, 2009; Watanabe et al., 2009). The rostromedial tegmentum nucleus (RMTg) also sends GABAergic projections to the SNc (Matsui and Williams, 2011). SNc neurons also receive excitatory glutamatergic inputs from M1, the secondary motor cortex M2, the primary somatosensory cortex, and also few of the subthalamic nucleus (Lee and Tepper, 2009; Watabe-Uchida et al., 2012).

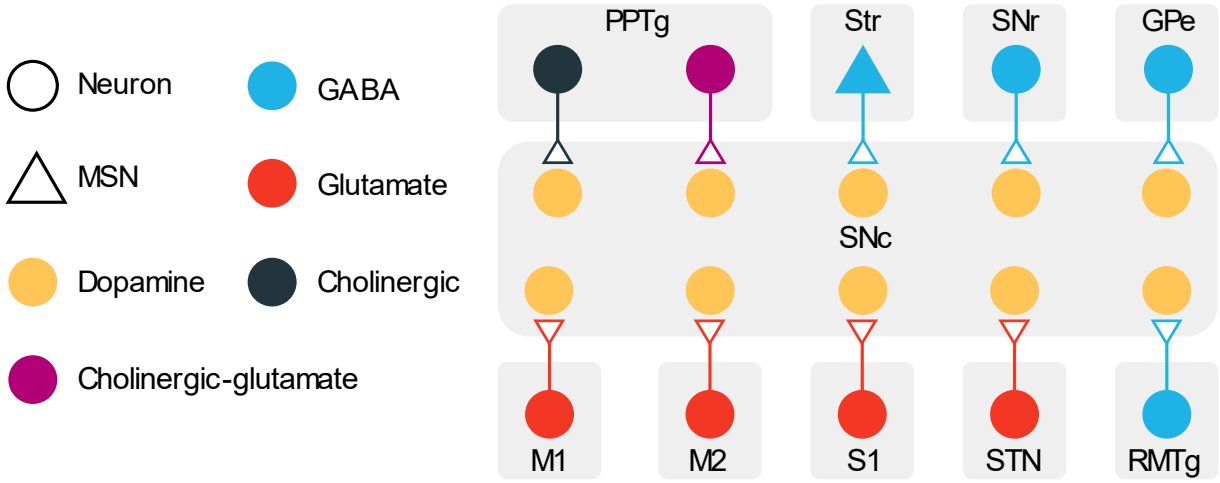

Fig. 1.6: Inputs to SNc dopaminergic neurons. DAergic neurons of the substantia nigra *pars compacta* (SNc) receive glutamatergic inputs from the primary motor cortex (M1), the secondary motor cortex (M2), the primary somatosensory cortex (S1) and the subthalamic nucleus (STN). SNc DAergic neurons also receive GABAergic inputs from the globus pallidus external part (GPe), the substantia nigra *pars reticulata* (SNr), medium spiny neurons (MSN) of the striatum (Str) and from the rostromedial tegmentum (RMTg). Both cholinergic and cholinergic-glutamate neurons of the pedunculopontine tegmentum (PPTg) send projections to SNc DAergic neurons.

SNc DAergic neurons are well known to project to striatum (Albin et al., 1989). Depending on whether they express or not the transcription factor SOX6, these neurons are not located in the same part of the SNc, and they do not project in the same area of the striatum. In fact, SOX6-positive DAergic neurons are located in the ventral SNc and project to the dorsal striatum, whereas SOX6-negative DAergic neurons are located in the dorsal part of the SNc and project to the medial, ventral and caudal striatum (Fig. 1.10, Pereira Luppi et al., 2021). In addition, SNc neurons have been shown to project to M1 (Hosp et al., 2011, 2015), nAcc, olfactory tubercle and amygdala (Poulin et al., 2018). These neuronal populations are quite distinct from each other. In fact, nAcc projecting SNc neurons express the cholecystokinin (CCK), as well as those which project to the olfactory tubercle, whereas amygdala-projecting SNc neurons express the vesicular glutamate transporter type 2 (VGLUT2, Fig. 1.10, Poulin et al., 2018).

2.2.2. Electrophysiological properties

The electrophysiological signature of SNc DAergic neurons has been well characterized thanks to *ex vivo* patch clamp recordings (Fig. 1.7, Lammel et al., 2008; Liss et al., 2005). One of the most typical properties of SNc DAergic neurons is their spontaneous spiking activity at ~3 Hz in a pacemaker mode, with slow and broad action potentials (APs). This spontaneous spiking activity is generated by slow oscillation of intracellular calcium concentration. This process is mediated by the slow and broad APs, which maximize the entry of calcium in the cell by activating efficiently L-type calcium channels at the plasma membrane, and also the intracellular release of calcium ions by the endoplasmic reticulum (Surmeier, 2018). This spontaneous electrical activity is downregulated by the neurons themselves, as they do express D2 autoreceptors linked to inwardly rectifying potassium channels GIRK2 (Beckstead et al., 2004; Liss and Roeper, 2008), whose activation leads to a membrane hyperpolarization. The expression of D2 receptors by SNc DAergic neurons is a hallmark of these neurons, as all midbrain DAergic neurons do not express D2 receptors.

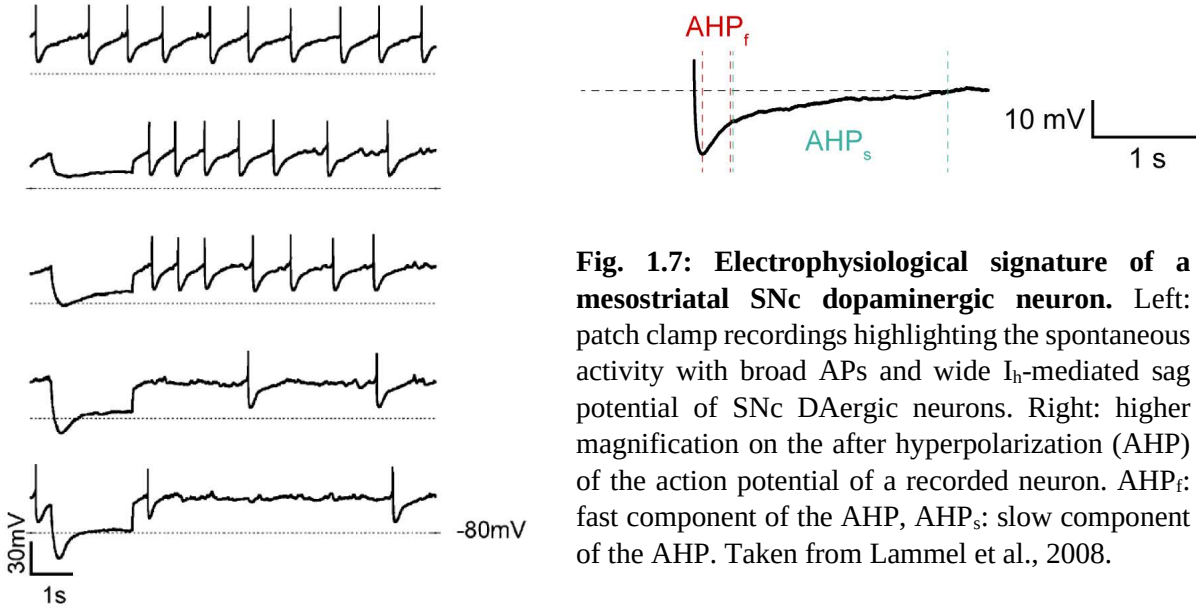

Fig. 1.7: Electrophysiological signature of a mesostriatal SNc dopaminergic neuron. Left: patch clamp recordings highlighting the spontaneous activity with broad APs and wide I_h-mediated sag potential of SNc DAergic neurons. Right: higher magnification on the after hyperpolarization (AHP) of the action potential of a recorded neuron. AHP_f: fast component of the AHP, AHP_s: slow component of the AHP. Taken from Lammel et al., 2008.

One other feature is the large I_h-mediated sag potential displayed by SNc DAergic neurons, which is induced by HCN channels activation (Lammel et al., 2008). These channels are activated by subthreshold hyperpolarizing currents, and they are permeable to sodium and potassium ions, leading to a fast repolarization of the neuron's membrane potential (Benarroch, 2013).

The after hyperpolarization (AHP) of SNc DAergic neurons' APs is quite complex, and can be divided in fast component and a slow one (Fig. 1.7, Nedergaard, 2004). The fast component is dependent on SK-type potassium channels, which are activated by calcium ions

influx through low threshold T-type calcium gated channels, while the fast component is calcium-independent. The slow component can last for several seconds depending on the duration of the neuronal excitation, and is likely to depend on ERG potassium channels, which are quickly deactivated when membrane potential is repolarized (Nedergaard, 2004).

2.2.3. Physiological roles and implication in brain diseases

SNc neurons have a modulatory role on MSNs of the striatum, which then exert a powerful influence on the basal ganglia circuitry (Fig. 1.8, Albin et al., 1989). On one hand, DA release by SNc neurons activates D1-expressing MSNs of the direct pathway. These MSNs inhibit the structures of the basal ganglia loop: the substantia nigra *pars reticulata* and the globus pallidus internal part, which exert a tonic inhibition on brain areas in charge of motor execution, such as the motor thalamus and the motor cortex. Thus, the activation of the D1 receptors of D1-expressing MSNs by SNc DAergic neurons is thought to promote motor execution. On the other hand, DA release by SNc neurons inhibits D2-expressing MSNs of the indirect pathway. These MSNs normally inhibit the globus pallidus external part, which inhibits the subthalamic nucleus, the only excitatory nucleus of the basal ganglia. The subthalamic nucleus normally activates the inhibitory output structures of basal ganglia, thus promoting movement inhibition. As the inhibition on the subthalamic nucleus is diminished due to the inhibition of external part globus pallidus neurons' by D2-expressing MSNs, the tonic inhibition exerted by output structures on brain areas in charge of motor execution is therefore exacerbated by subthalamic nucleus excitatory inputs. Thus, the action of DA at the level of the basal ganglia loop is bimodal. The excitation of the direct pathway MSNs is thought to promote movement execution, and the inhibition of indirect pathway MSNs is thought to inhibit unnecessary movements. The consequences of the loss of SNc nigrostriatal neurons are best illustrated by PD, during which the loss of DA tone in the striatum leads to a decrease in the activity of the direct pathway MSNs and to an increase in the activity of indirect pathway MSNs (Fig. 1.8, Albin et al., 1989; de la Crompe et al., 2020). This imbalance in the activation of these two pathways is responsible of PD symptoms, such as akinesia, bradykinesia, and rigidity (Nambu et al., 2015). Moreover, loss of DA tone during PD leads to an abnormal level of oscillatory spike synchrony at β frequencies (12 - 30 Hz) in the basal ganglia loop and in motor-related areas (de la Crompe et al., 2020; Mallet et al., 2008). This pathological oscillations are thought to participate in the pathophysiology of PD by decreasing the level of information processed in basal ganglia circuits (Brown, 2007).

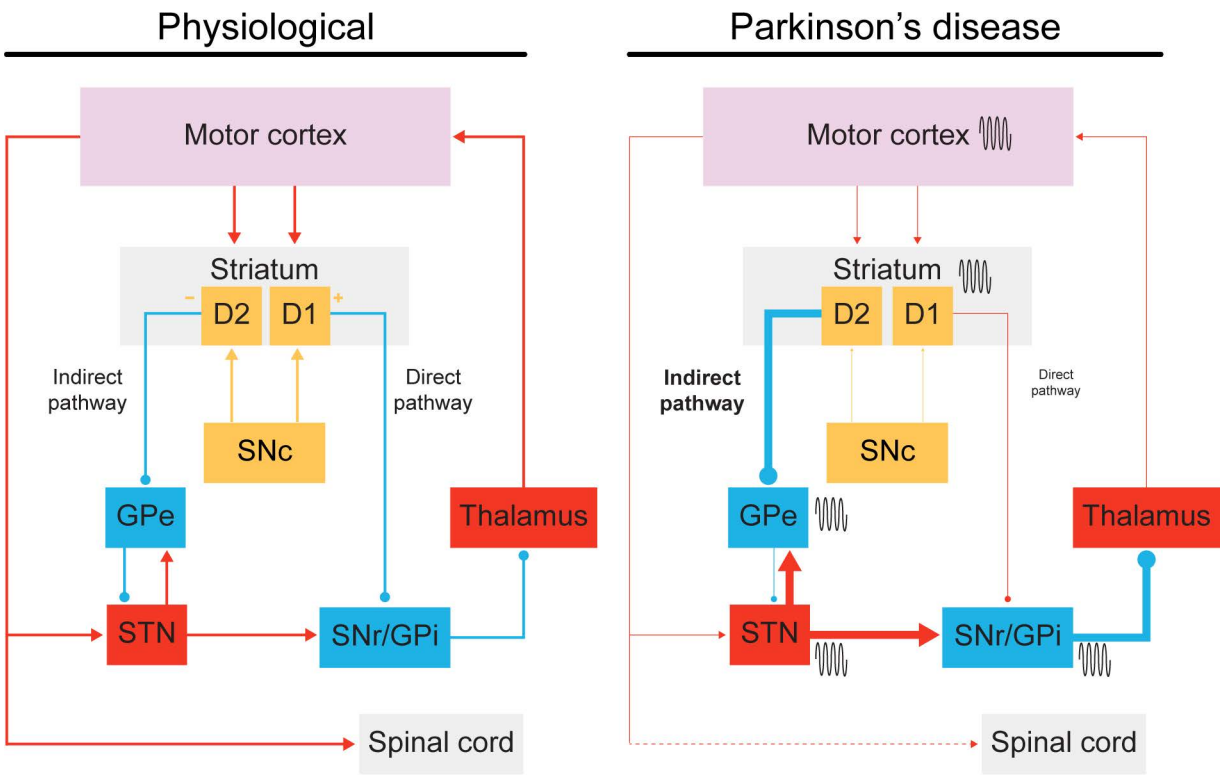

Fig. 1.8: Simplified scheme of basal ganglia circuitry in physiological and Parkinsonian conditions. The degeneration of the substantia nigra *pars compacta* during Parkinson's disease (right) leads to firing rate changes in basal ganglia nuclei (indicated by the thickness of the arrows), which induces an overactivation of the indirect pathway and an underactivation of the direct pathway. These firing rate changes are associated with an abnormal level of synchronization of the activity of basal ganglia and motor related structures (indicated by the waves). Red arrows represent excitatory projections, and blue arrows represent inhibitory projections. GPe: globus pallidus external part, GPi: globus pallidus internal part, SNc: substantia nigra *pars reticulata*, SNr: substantia nigra *pars compacta*, STN: subthalamic nucleus.

As the role of SNc DAergic neurons has been principally studied for their implication in PD and motor function, the role of their projections in limbic structure such as the nAcc and the amygdala remains unclear. Such is the case of the role of these neurons in olfactory processes.

2.3. DAergic neurons of the VTA

The VTA is a heterogeneous structure comprising several types of neurons. In fact, the VTA comprises DAergic neurons, but also GABAergic and glutamatergic neurons (Fields et al., 2007; Hnasko et al., 2012; Yamaguchi et al., 2007). As this work focuses on DAergic neurons of the midbrain (and so, not only of the VTA), only VTA DAergic neurons will be described here.

2.3.1. Inputs and outputs

Recent tracing studies helped to dissect the direct monosynaptic inputs on VTA DAergic neurons (Fig. 1.9, Beier et al., 2015; Omelchenko and Sesack, 2009). These approaches revealed that the main GABAergic inputs on VTA DAergic neurons come from neurons located in the dorsal raphe nucleus (DRN), the periaqueductal grey (PAG). *Ex vivo* patch clamp recordings also revealed that VTA DAergic neurons receive inhibitory inputs from the lateral hypothalamus (LHT, Nieh et al., 2015). Other retrograde approaches using cholera toxin B revealed that VTA also receives GABAergic inputs from the RMTg (Matsui and Williams, 2011). Furthermore, glutamatergic inputs on VTA DAergic neurons have also been found, notably from the lateral habenula (LHB), the BNST, the medial PFC (mPFC, Carr and Sesack, 2000), the pedunculopontine tegmentum (PPTg) and the laterodorsal tegmentum nucleus (LDTg). The PAG and the DRN, which send GABAergic inputs onto VTA DAergic neurons, also send glutamatergic inputs on these neurons (Beier et al., 2015; Watabe-Uchida et al., 2012). Even if nAcc projections have been found using the same techniques, *in vivo* recordings showed that most of these projections are onto non DAergic neurons, especially GABAergic neurons (Xia et al., 2011). *In vivo* electrophysiological recordings revealed a local connectivity between glutamatergic neurons and DAergic neurons inside the VTA, as exciting glutamatergic VTA neurons induces AP firing in VTA DAergic neurons (Wang et al., 2015). Local connectivity also involves VTA GABAergic projections onto VTA DAergic neurons (van Zessen et al., 2012).

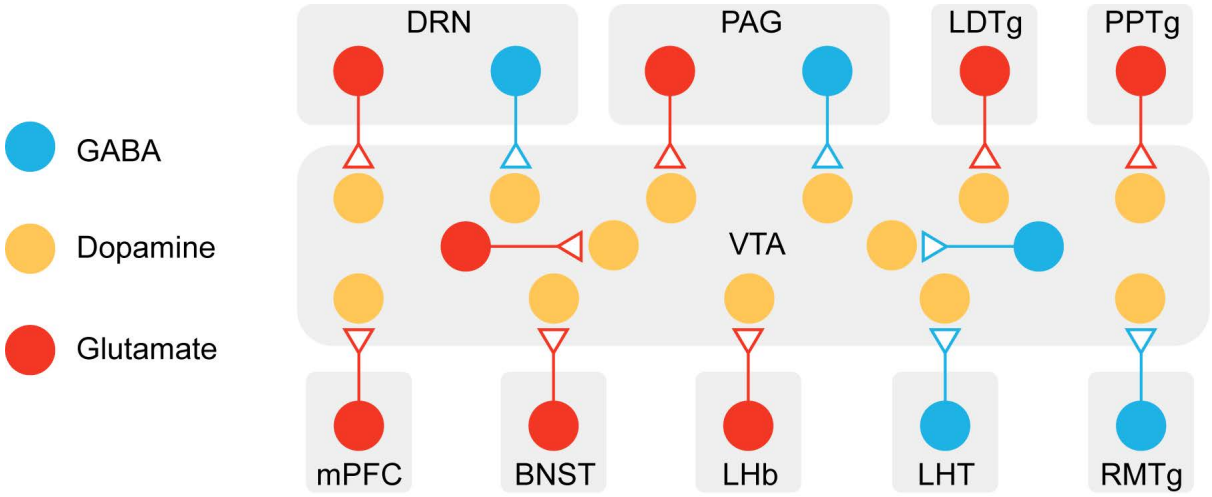

Fig. 1.9: Inputs to VTA dopaminergic neurons. DAergic neurons of the ventral tegmental area (VTA) receive glutamatergic inputs from the dorsal raphe nucleus (DRN), the periaqueductal grey (PAG), the laterodorsal tegmentum nucleus (LDTg), the pedunculopontine tegmentum (PPTg), the medial prefrontal cortex (mPFC), the bed nucleus of the stria terminalis (BNST) and the lateral habenula (LHb). DAergic neurons of the VTA also receive GABAergic inputs from the DRN, the PAG, the lateral hypothalamus (LHT) and the rostromedial tegmentum nucleus (RMTg). Adapted from Morales and Margolis, 2017.

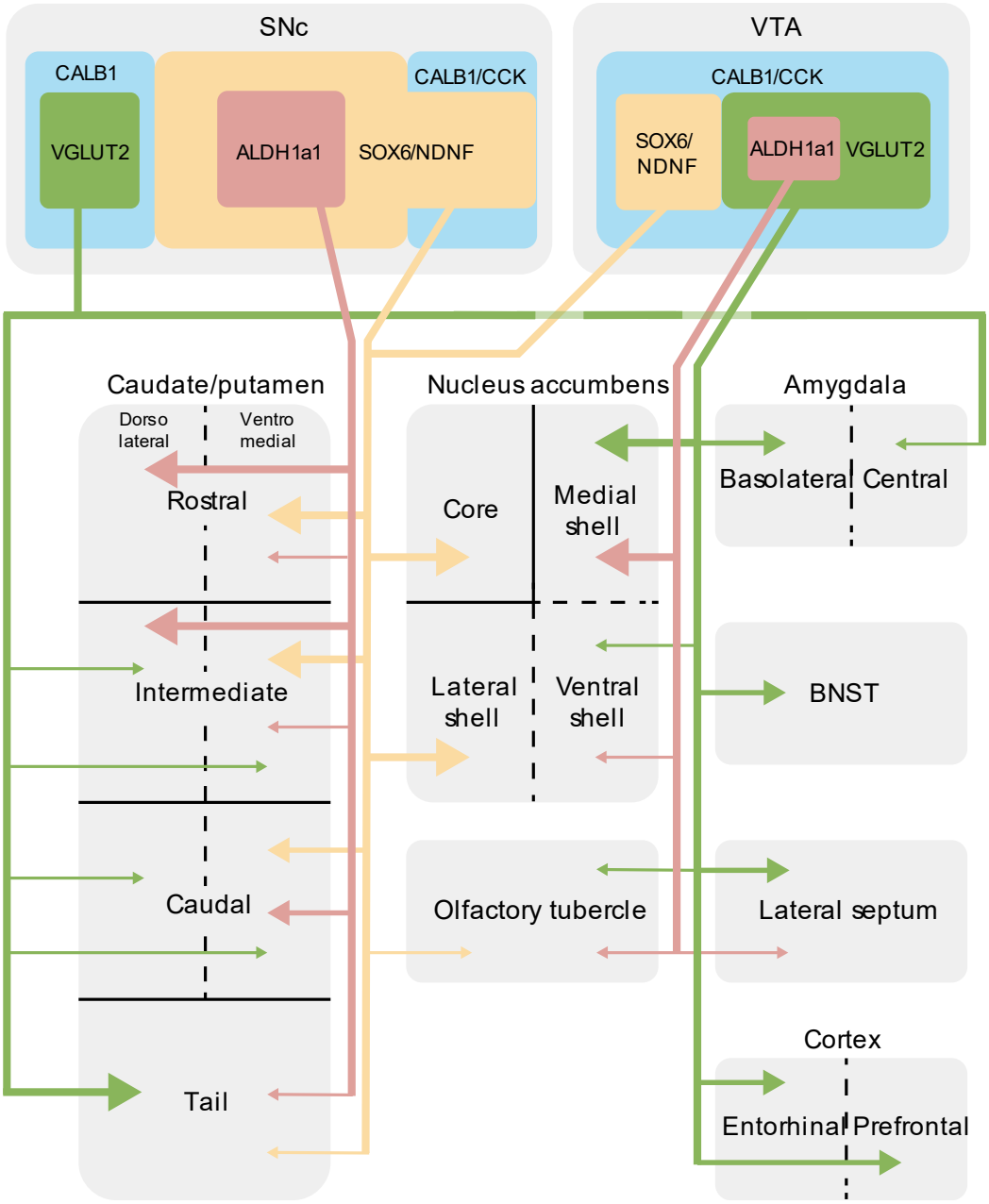

Fig. 1.10: Targets of the different genetically-defined midbrain dopaminergic neurons. CALB1/VGLUT2-expressing DAergic neurons of the substantia nigra *pars compacta* (SNc) project to the central amygdala, to the tail of the striatum and to dorsolateral and ventromedial parts of intermediate and caudal caudate/putamen. ALDH1a1/SOX6/NDNF-expressing DAergic neurons of the SNc send projections to dorsolateral and ventromedial parts of the rostral and intermediate caudate/putamen, to ventral medial part of the caudal caudate putamen and to the tail of the caudate/putamen. CALB1/CCK/SOX6/NDNF-expressing DAergic neurons of the SNc and the ventral tegmental area (VTA) project to the core and shell of the nucleus accumbens, the olfactory tubercle, the caudal and tail of the caudate/putamen and to ventromedial parts of the rostral and intermediate caudate/putamen. CALB1/CCK//VGLUT2/ALDH1a1-expressing DAergic neurons of the VTA project to the medial and ventral shell of the nucleus accumbens, to the olfactory tubercle and the lateral septum. Finally, CALB1/CCK/VGLUT2-expressing neurons of the VTA project to prefrontal and entorhinal cortices, the lateral septum, the olfactory tubercle, the bed nucleus of the stria terminalis (BNST), the basolateral amygdala and to medial and ventral shell nucleus accumbens. The thickness of the arrows indicates the structural strength of the projections. Adapted from Poulin et al., 2018.

The VTA is mostly known for its connections with the limbic system. Extensive work has been done thanks to single-cell gene expression profiling to determine the genetic profile of VTA DAergic neurons, and to sort them depending on their targets (Poulin et al., 2014, 2018). These studies revealed that genetically distinct VTA DAergic neurons project preferentially to distinct areas. More specifically, SOX6-expressing neurons in the dorsolateral VTA principally project to core and lateral shell parts of the nAcc (Fig. 1.10, Poulin et al., 2018). VTA DAergic neurons expressing ALDH1a1 project to the medial part of the shell nAcc, and to a lesser extent, to the ventral part of the shell nAcc and the lateral septum. ALDH1a1-expressing neurons which also express VGLUT2 project to the medial part of the shell nAcc, but not only. In fact, a major part of them project to the amygdala, the BNST, the prefrontal and entorhinal cortices, and a minor part of them projects to the olfactory tubercle (Poulin et al., 2018). As for SNc DAergic neurons, VTA DAergic neurons projecting to the nAcc express CCK.

2.3.2. Electrophysiological properties

Unlike in the SNc, there is a diversity of DAergic neurons in the VTA, as all VTA DAergic neurons do not display the same electrophysiological profiles. As such, not all VTA DAergic neurons display an I_h current, typical of SNc DAergic neurons, nor they always express SK-type potassium channels, crucial for the spontaneous activity of SNc DAergic neurons (Juarez and Han, 2016; Lammel et al., 2008). Thus, determining where VTA DAergic neurons project cannot be assessed only on the base of their electrophysiological signatures.

Using retrograde tracing combined with *ex vivo* electrophysiological recordings, the intrinsic properties of several types of VTA DAergic neurons depending on their targets have been investigated (Chaudhury et al., 2013; Ford et al., 2006; Lammel et al., 2008). These studies revealed that VTA DAergic neurons projecting to the mPFC, the amygdala, the nAcc core and medial shell display little or no I_h current (Ford et al., 2006; Juarez and Han, 2016), indicating little or no expression of HCN channels in these neurons. In addition, these neurons display higher sustained firing rates and increased membrane excitability in comparison to the classical view of a mesostriatal DAergic neuron (Fig. 1.11, Chaudhury et al., 2013; Lammel et al., 2008). More specifically, mPFC-projecting VTA DAergic neurons exhibit unique properties. In fact, these neurons do not display the autoinhibition mediated by D2 receptors coupled with GIRK2 channels, and their expression of D2 receptors and GIRK2 mRNA is lower compared to other mesostriatal DAergic neurons (Lammel et al., 2008), as their level of DAT expression (Juarez

and Han, 2016; Lewis et al., 2001). Thus, the release of DA by these neurons in the mPFC lasts longer that the release of DA by other VTA DAergic neurons. Conversely, VTA DAergic neurons projecting to the lateral shell of the nAcc display similar intrinsic properties as mesostriatal neurons: lower firing frequency in a pacemaker manner, with broad APs and a two-parted AHP (Lammel et al., 2008). Consistently, these lateral shell-projecting VTA DAergic neurons display the autoinhibition mediated by D2 receptors coupled with GIRK2 channels (Lammel et al., 2008).

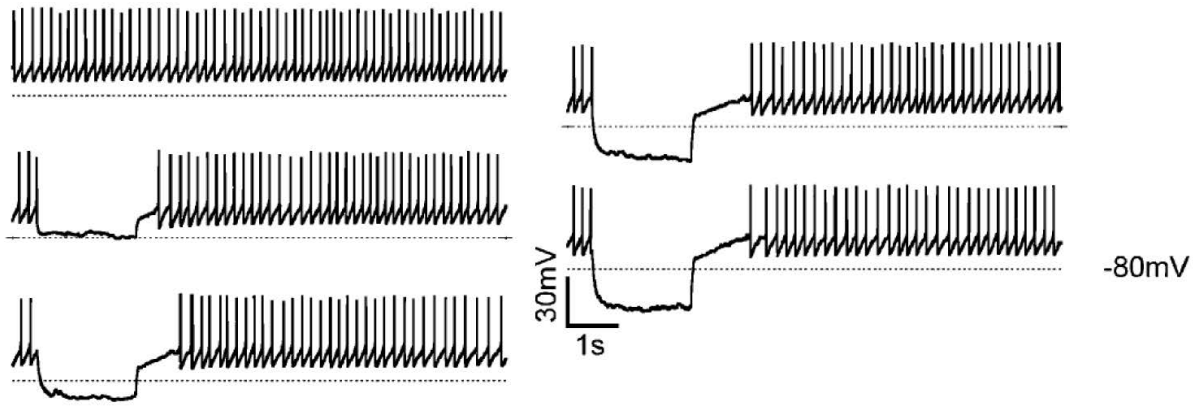

Fig. 1.11: Electrophysiological properties of a mesocortical VTA dopaminergic neuron. Patch clamp recordings of a single VTA DAergic neuron presenting the spontaneous activity and the response to negative currents increasing in intensity. Note the absence of I_h-mediated sag potential. Taken from Lammel et al., 2008.

2.3.3. Physiological roles and implication in brain diseases

The mesoaccumbens pathway, constituted of VTA DAergic neurons projecting to the nAcc, has been extensively investigated for its implication in motivational processes (Bromberg-Martin et al., 2010). As VTA DAergic neurons have distinct targets, they modulate motivational behaviour in several ways. In fact, it has been shown that VTA DAergic neurons projecting to different structures also receive inputs from other different structures, forming different sub-circuits implicated in different behaviours. As such, the LHB mainly sends projections to mPFC-projecting VTA DAergic neurons, whereas the LDTg mainly projects to VTA DAergic neurons projecting to the lateral shell of the nAcc (Lammel et al., 2012). These two subcircuits have a bimodal impact on motivational processes. In fact, the optogenetic activation of LHB neurons projecting to mPFC-projecting VTA DAergic neurons induces a conditioned place aversion. Inversely, the optogenetic activation of LDTg neurons projecting to lateral shell nAcc-projecting VTA DAergic neurons induces a conditioned place preference (Fig. 1.12, Lammel et al., 2012). Mesoaccumbens VTA DAergic neurons also receive

monosynaptic inputs from VGLUT3-expressing DRN neurons (Geisler et al., 2007; Qi et al., 2014). The selective activation of the terminals of these glutamatergic neurons in the VTA elicits APs in VTA DAergic neurons, leading to DA release in the nAcc. This DA release promotes D1 receptors activation, inducing a conditioned place preference, reversed by the application of D1 receptor antagonist, but not D2 receptor antagonist (Fig. 1.12, Qi et al., 2014). Reward feeling is also mediated by anterior cortex projections to mesoaccumbens VTA DAergic neurons. Indeed, mice repeatedly self-activated by optogenetics the anterior cortex projections' to VTA during a self-administration task, which was abolished by the infusion of a non-selective DA antagonist (Beier et al., 2015).

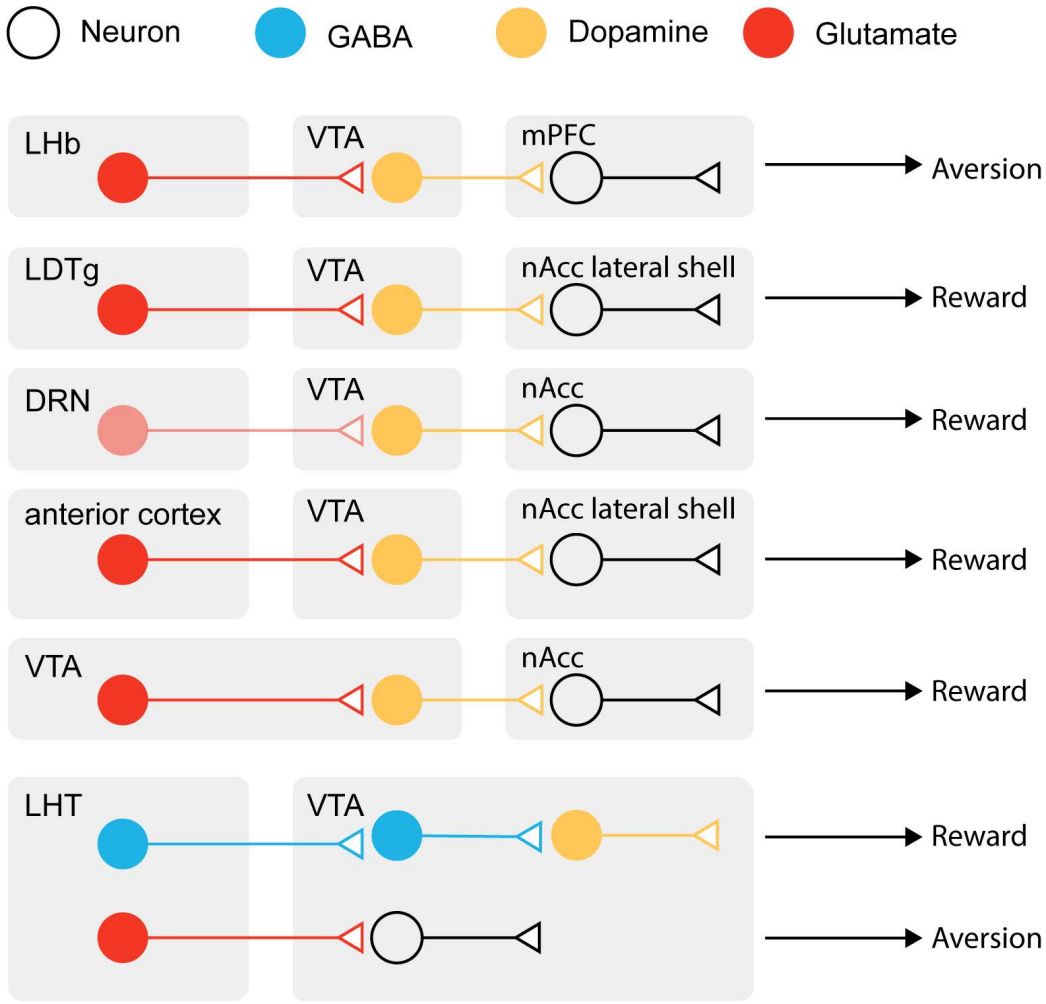

Fig. 1.12: VTA dopaminergic neurons' pathways involved in reward and aversion processes. Glutamatergic inputs to the ventral tegmental area (VTA) DAergic neurons from the laterodorsal tegmentum nucleus (LDTg), the dorsal raphe nucleus (DRN) and the anterior cortex are implicated in reward processes. Glutamatergic inputs to the VTA originating from the lateral habenula (LHb) and the lateral hypothalamus (LHT) are implicated in aversion processes. Local VTA glutamatergic neurons synapsing to VTA DAergic neurons are implicated in reword processes, and silencing of local VTA GABAergic neurons by LHT GABAergic neurons is implicated in reward processes too. Taken from Morales and Margolis, 2017.

Local connections within the VTA have also been reported to play a role in mediating reward processes. In fact, combined retrograde tracing and electron microscopy experiments revealed that VGLUT2 expressing neurons in the VTA make excitatory synapses on mesoaccumbens VTA DAergic neurons. The selective activation of VGLUT2 positive neurons in the VTA induces place preference, which is abolished by the infusion of glutamatergic antagonists into the VTA (Fig. 1.12, Wang et al., 2015). Moreover, GABAergic VTA neurons also modulate reward processing through local connectivity. In fact, the inhibition of VTA GABAergic neurons induced by the activation of GABAergic inputs from the LHT induces a release of DA in the nAcc and a place preference. Conversely, the activation of VTA GABAergic neurons induced by the activation of glutamatergic inputs from the LHT induces a decrease of DA release in the nAcc and a place aversion (Fig. 1.12, Nieh et al., 2016).

As VTA DAergic neurons play an important role in mediating reward processes, it is not surprising to find that their dysfunctions are the core of several reward disorders, such as drug abuse or alcoholism. Indeed, *in vivo* recordings have shown that alcohol intake induces an increase in VTA DAergic neurons' firing rate (Gessa et al., 1985), as well as an increase in the levels of DA in the nAcc (Di Chiara and Imperato, 1985). Moreover, *ex vivo* electrophysiological recordings in acutely dissociated VTA DAergic neurons revealed that ethanol is able to modulate them directly (Brodie et al., 1999). *In vivo* electrophysiological recordings showed a decrease in the activity of VTA DAergic neurons during alcohol withdrawal (Diana et al., 1993), which correlates with decreased DA levels in the nAcc (Weiss et al., 1996). Apart from alcohol, several drugs of abuse also act on VTA DAergic neurons' transmission, such is the case of cocaine. Cocaine inhibits the reuptake of DA from the synaptic cleft by inhibiting presynaptic DAT (Giros et al., 1996), leading to a prolonged DA tone. Nonetheless, this also induces a prolonged activation of D2 autoreceptors on VTA DAergic neurons, which results in a decrease of DA synthesis, storage into vesicles and release, and this mechanism is further reinforced by the chronic administration of cocaine (Juarez and Han, 2016).

One particular type of VTA DAergic neurons projecting to the mPFC has been identified, and displays low levels of DAT expression (Lammel et al., 2008). In fact, the mPFC maintains extracellular DA levels for a longer time in comparison to the striatum. This suggests that the lower level of DAT expression in mPFC-projecting VTA DAergic neurons may have relevant implication in mPFC processes, such as working memory and executive functions (Juarez and Han, 2016). Thus, abnormalities in the mesocortical pathway are thought to

contribute to the pathophysiology of cognitive disorders, such as schizophrenia. More specifically, a lower release of DA by VTA DAergic neurons in the PFC is thought to contribute to negative symptoms and cognitive impairments in schizophrenia (Patel et al., 2014), which include alogia, impairments in working memory and attentional processes, anhedonia and asociality (Shen et al., 2012).

In rats, some VTA DAergic neurons send projections to M1 (Hosp et al., 2015), a key structure for motor learning (Molina-Luna et al., 2009). The DA released by these neurons are instrumental for M1-mediated motor skill learning (Hosp et al., 2011). In fact, 6-OHDA injection in the VTA resulted in the loss of motor skill learning ability in a reaching task, without impairing the already acquired movements. Moreover, this DA depletion in the VTA also induced a diminution of DAergic terminals within M1. Furthermore, L-DOPA injection in M1 restores motor skill learning abilities. These results support the hypothesis that the DA necessary for M1-mediated motor skill learning is released by midbrain DAergic neurons (Hosp et al., 2011).

2.4. Midbrain DAergic neurons that corelease other neurotransmitters

Midbrain DAergic neurons can release DA only, but some of them can also co-release GABA or glutamate. SNc and VTA DAergic neurons projecting monosynaptically onto striatal MSNs can corelease DA and GABA (Tritsch et al., 2012). However, the enzymes responsible for the synthesis of GABA or the proteins implicated in the vesiculation of GABA have been detected in a very small fraction of midbrain DAergic neurons (Hédou et al., 2000; Poulin et al., 2014; Tritsch et al., 2012). In fact, all midbrain DAergic neurons do not synthetize GABA *de novo* and release it onto striatal MSNs, but uptake GABA from the synaptic cleft through GABA transporter 1. The GABA is then stored into vesicles through VMAT2 and can therefore be released by DAergic terminals (Melani and Tritsch, 2022; Tritsch et al., 2014). In addition to this mechanism, some DAergic neurons can also synthetize GABA through ALDH1a1 enzyme, as the selective inhibition of this enzyme decreases GABA release in the dorsal striatum (Kim et al., 2015).

DA and glutamate corelease by VTA DAergic neurons has also been identified. In fact, DA-glutamate co-transmission has been described for the first time *in vitro* using immunostainings and electrophysiological recordings in cultured rat DAergic neurons (Sulzer et al., 1998). These neurons possess the ability to synthetize DA as they also express DOPA-DC (Li et al., 2013). Some of these neurons express DAT and VMAT2, and thanks to *ex vivo*

electrophysiological recordings and voltammetry experiments, it has been shown that these neurons can release DA (Zhang et al., 2015) and glutamate (Hnasko et al., 2010; Stuber et al., 2010). However, some of these neurons do not express DAT nor VMAT2, indicating an inability of these neurons to reuptake DA and store it into vesicles (Li et al., 2013). Using electron microscopy, it has been shown that VGLUT2 and VMAT2 expression can be segregated into distinct adjacent axons of DAergic neurons projecting to the nAcc (Zhang et al., 2015). Nonetheless, VGLUT2 and VMAT2 expression can also be found segregated into different micro domains of the same axon, with VGLUT2 expression localized in the axon terminal and VMAT2 expression localized in the axonal segment close to the axon terminal (Zhang et al., 2015). These terminals are functional, as it has been shown that these neurons can release both DA and glutamate using optogenetics (Zhang et al., 2015). Overall, these results suggest that vesicles containing DA or glutamate in DAergic-glutamatergic neurons are released from segregated micro domains.

3. The primary motor cortex (M1)

3.1. Role in motor execution

M1 is a large cortical area playing a crucial role in motor execution and planning (Cousineau et al., 2022; Ebbesen and Brecht, 2017; Whishaw et al., 1986). The involvement of M1 in the execution of motor functions was first demonstrated in 1870 by Fritsch and Hitzig, as they shown that an electrical stimulation in M1 induced discrete movements in contralateral muscle groups of awake dogs (translated to English and republished: Fritsch and Hitzig, 2009). Descriptive studies of M1 have then been carried out using electrical stimulations in M1 in anesthetized humans, to try to attribute motor function of specific body parts to sub parts of M1. These studies highlighted the existence of a somatotopy in M1, which can be defined by the presence of a map of body parts in M1, firstly described as the homunculus (Penfield and Boldrey, 1937). The size of the representation of a body part within M1 is function of the complexity of the movements performed by the body part of interest, as body parts which can achieve complex movements have larger representation in M1, and vice versa (Cousineau et al., 2022). Consequently, lesion experiments in M1 showed that the larger the lesion, the bigger the motor impairments (Touvykine et al., 2016; Whishaw, 2000). Moreover, as body parts in charge of fine movement execution have a bigger representation within M1, larger lesions induce long lasting deficits in the execution of fine dexterous movements and digits control (Cousineau et al., 2022). Nonetheless, lesion studies in rodents also showed that the execution

of non-dexterous movements does not imply M1, whereas M1 is always needed for the learning of new motor skills (Kawai et al., 2015). Rodents are also able to recover their motor functions after M1 lesions, and the time needed to recover depends on the severity of the lesions. This recovery may indicate the existence of compensatory mechanisms mediated by subcortical areas to ensure motor execution even in the absence of a fully functional M1, as it has been postulated for primates (Darling et al., 2011; Leyton and Sherrington, 1917; Zaaimi et al., 2012).

3.2. Organization of M1

As other cortices, M1 is composed of ~80% of glutamatergic PNs and ~20% of GABAergic INs (Callaway et al., 2021; Shipp, 2007). However, unlike other cortices, the existence of the layer IV in M1 is debated (Barbas and García-Cabezas, 2015; Donoghue and Wise, 1982). However, recent functional studies revealed a synaptic organization reminiscent of somatosensory layer IV in M1, suggesting the existence of circuit comparable to the layer IV in M1 (Yamawaki et al., 2014; Yao et al., 2021).

3.3. Cellular populations of M1 and electrophysiological features

3.3.1. Pyramidal neurons

PNs are the most represented cellular type in M1, and they are so called due to the triangle shape of their soma reminiscent of pyramids. PNs are the main excitatory neurons of the cortex, and they are present in all layers of the cortex, except for layer I (Gerfen et al., 2018). PNs can be classified in different categories depending on their downstream targets, their molecular profile and their electrophysiological properties: intratelencephalic neurons (ITNs), corticothalamic neurons (CThNs) and pyramidal tract neurons (PTNs, Fig. 1.13, Harris and Shepherd, 2015). ITNs can be further divided in two big categories: intratelencephalic corticocortical neurons (IT-CCNs) and intratelencephalic corticostriatal neurons (IT-CStrNs).

IT-CCNs constitute the first main type of ITNs. They are found in layers II-III of M1 and they project inside the telencephalon, more specifically inside the neocortex (Fig. 1.13, Harris and Shepherd, 2015). They project to both ipsilateral and contralateral cortices, and inside the ipsilateral neocortex in which they make synapses onto other IT-CCNs as well as PTNs and IT-CStrNs (Morishima, 2006; Shepherd, 2013). The main molecular marker used to recognize IT-CCNs is the DNA-binding protein SATB2, even if it is not specific of IT-CCNs as it is expressed by ITNs neurons in general (Greig et al., 2013). Concerning their electrical

properties, IT-CCNs display a low I_h current (Fig. 1.14), meaning they express low levels of HCN channels. The shape of their APs is quite large compared to other PNs and repetitive firing results in adaptation (Fig.1. 14, Hattox and Nelson, 2007; Morishima, 2006; Sheets et al., 2011). IT-CCNs are mainly thought to contribute to motor control, notably by promoting inhibition in motor areas, which would be important for the relevant selection of PNs implicated in a given motor task (Battaglia-Mayer and Caminiti, 2019).

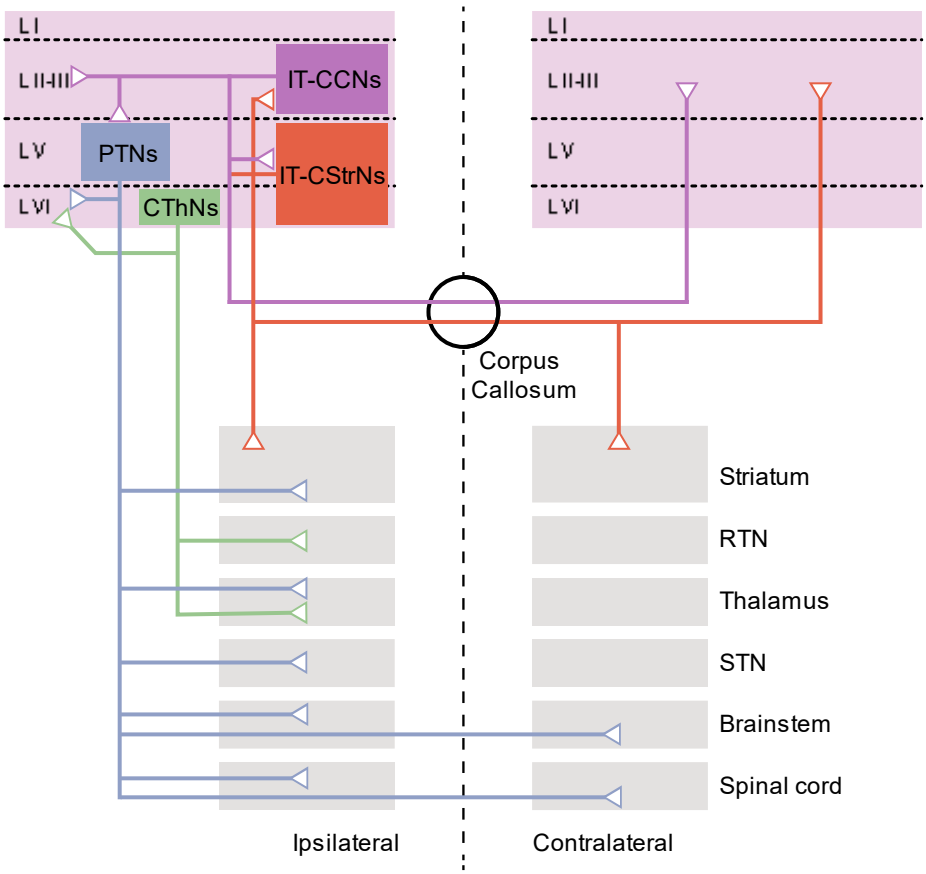

Fig. 1.13: Classification of pyramidal neurons based on their projection sites. Intratelencephalic corticocortical neurons (IT-CCNs) project to ipsilateral pyramidal tract neurons (PTNs) and intratelencephalic corticostriatal neurons (IT-CStrNs) as well as neurons in layers II-III. IT-CCNs project also to contralateral cortices through the corpus callosum. IT-CStrNs project to ipsilateral IT-CCNs and striatum, as well as contralateral striatum and cortices through the corpus callosum. PTNs send projection to ipsilateral layer VI neurons, striatum, thalamus and subthalamic nucleus (STN). They also send projection to ipsilateral and contralateral brainstem and spinal cord, but not through the corpus callosum. Corticothalamic neurons (CThNs) Send projections to layer VI neurons and to ipsilateral striatum and reticular thalamic nucleus (RTN). Taken from Shepherd, 2013.

IT-CStrNs constitute the second main type of ITNs neurons. The distinction between IT-CCNs and IT-CStrNs is not always easy to make, as the distinction between both classes is not always made in the literature. In fact, as IT-CCNs, IT-CStrNs send projection to ipsilateral and contralateral cortices, as they make synapses onto IT-CCNs. Nonetheless, they also send

projections to the ipsilateral and contralateral striatum, and unlike IT-CCNs, IT-CStrNs are mainly represented in layers V-VI (Fig. 1.13, Shepherd, 2013). Thus, ITNs neurons can be found in layers II to VI (Cousineau et al., 2022; Shepherd, 2013). As for ITNs neurons in general, they are recognized by their expression of the molecular marker SATB2. The electrophysiological properties of IT-CStrNs are quite similar to those of IT-CCNs, as their APs are wide and they fire APs in a phasic, adaptative manner, with low I_h current (Fig. 1.14, Hattox and Nelson, 2007; Morishima, 2006; Sheets et al., 2011). IT-CStrNs represent the main glutamatergic input in the basal ganglia loop. They are thought to preferentially innervate direct pathway MSNs, thus promoting movement execution (Lei, 2004). However, *in vivo* electrophysiological recordings challenged this view, by showing a similar amount of innervation of direct pathway MSNs and indirect pathway MSNs by IT-CStrNs (Ballion et al., 2008). Thus, clear roles of IT-CStrNs regarding motor execution promotion or selection need to be clarified, even if their implication in motor processes is not questioned.

Another category of PNs represented in M1 is PTNs. These neurons are found in layer V and send few projections to ipsilateral cortices, and other projections to several subcortical structures such as the striatum, the subthalamic nucleus and to a lesser extent the thalamus (Donoghue and Kitai, 1981; Kita and Kita, 2012; Parent and Parent, 2006). They project to these structures only ipsilaterally as they do not send projections through the corpus callosum or other commissures (Shepherd, 2013). They send projections to both ipsilateral and contralateral brainstem and spinal cord (Shepherd, 2013). Unlike ITNs neurons, they do not express the DNA binding protein SATB2, but instead they express the transcription factors CTIP2 (also known as BCL11b) and FEZF2 which are used to identify them in the neocortex, including in M1 (Greig et al., 2013; Shepherd, 2013). However, this segregation between ITNs neurons expression SATB2 and PTNs expression CTIP2 has been more recently called into question, as neurons expressing both CTIP2 and SATB2 have been discovered in the cortex and the hippocampus (Digilio et al., 2015; Harb et al., 2016; Lickiss et al., 2012; Nielsen et al., 2014). They also display different intrinsic properties compared to ITNs neurons. In fact, they exhibit a higher I_h current than ITNs neurons, indicating a higher expression or functionality of HCN channels (Fig. 1.14). Moreover, they do not fire APs in an adaptative manner, but in a tonic, even accelerating way, as their frequency tend to increase with the time of firing (Fig. 1.14). In M1, this property arises from the expression of D-type potassium channels (Miller et al., 2008), which are activated by subthreshold voltage and are permissive for potassium entry in the neuron, leading to a faster repolarization (Bekkers and Delaney, 2001). In M1, the main

role of PTNs is to enable motor execution of contralateral limb, as their projections to the spinal cord decussate at the level of the medulla (*i.e.*, just before the spinal cord, Baker et al., 2018). In fact, the activity of PTNs is correlated with motor execution, as they form a topographical ensemble in which successive activation of PTNs leads to muscle contraction, and thus to movement execution (Wang et al., 2017).

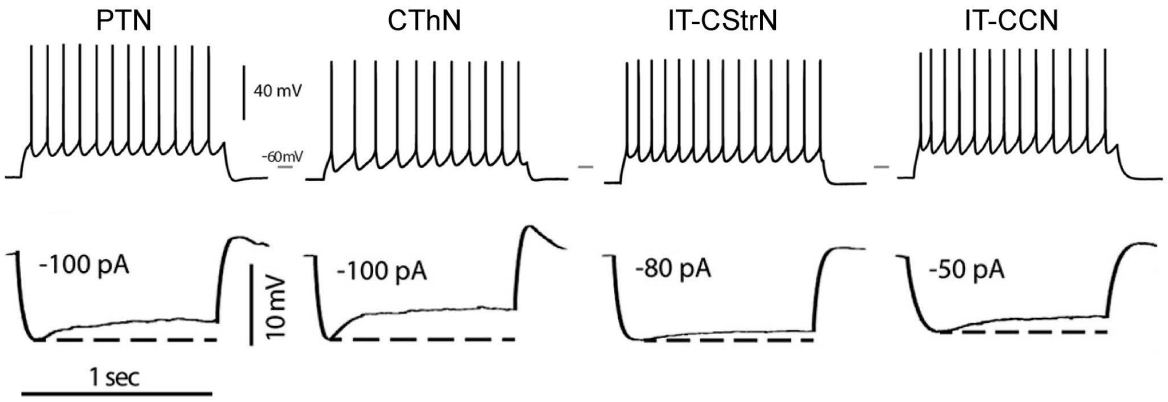

Fig. 1.14: Classification of M1 Layer V pyramidal neurons based on their electrophysiological signature. Top: Representative firing pattern of a pyramidal tract neuron (PTN), a corticothalamic neuron (CThN), an intratelencephalic corticostriatal neuron (IT-CStrN) and an intratelencephalic corticocortical neuron (IT-CCN) after a depolarizing current. Bottom: Responses to a hyperpolarizing current of a PTN, a CThN, an IT-CStrN and an IT-CCN. Taken from Oswald et al., 2013.

The last main category of PNs present in M1 are the CThNs. These neurons are found in deep layers of the cortex (*i.e.*, layer VI) and project only to the thalamus and the thalamic reticular nucleus, even if few branches in the ipsilateral cortices (Shepherd, 2013). As PTNs also send projections to the thalamus, the main difference between CThNs and PTNs is that PTNs also send projections to the brainstem and subcerebral structures. CThNs can be identified by their expression of the transcription factor TBR1 (McKenna et al., 2011). They fire APs in a regular manner (Harris and Shepherd, 2015), are mostly silent in *in* vivo recordings (Beloozerova et al., 2003; Sirota, 2005) and display a prominent I_h current, indicating a higher expression or functionality of HCN channels in CThNs compared to ITNs (Fig. 1.14, Oswald et al., 2013). Their implications in physiological processes remain largely unknown. They are thought to reinforce motor control by projecting to inhibitory neurons in the thalamus, which in turn inhibit PNs in M1 in order to select neurons relevant to the ongoing motor task (Shepherd and Yamawaki, 2021).

3.3.2. Interneurons

In the neocortex, INs neocortex represent ~20% of the total cells (Markram et al., 2004). They are divided in three big categories, which are themselves divided in sub-categories: The parvalbumin-expressing (PV) INs, the somatostatin-expressing (SST) INs and INs expressing the serotoninergic receptor 3a (5-HT3aR, Fig. 1.15, Lim et al., 2018).

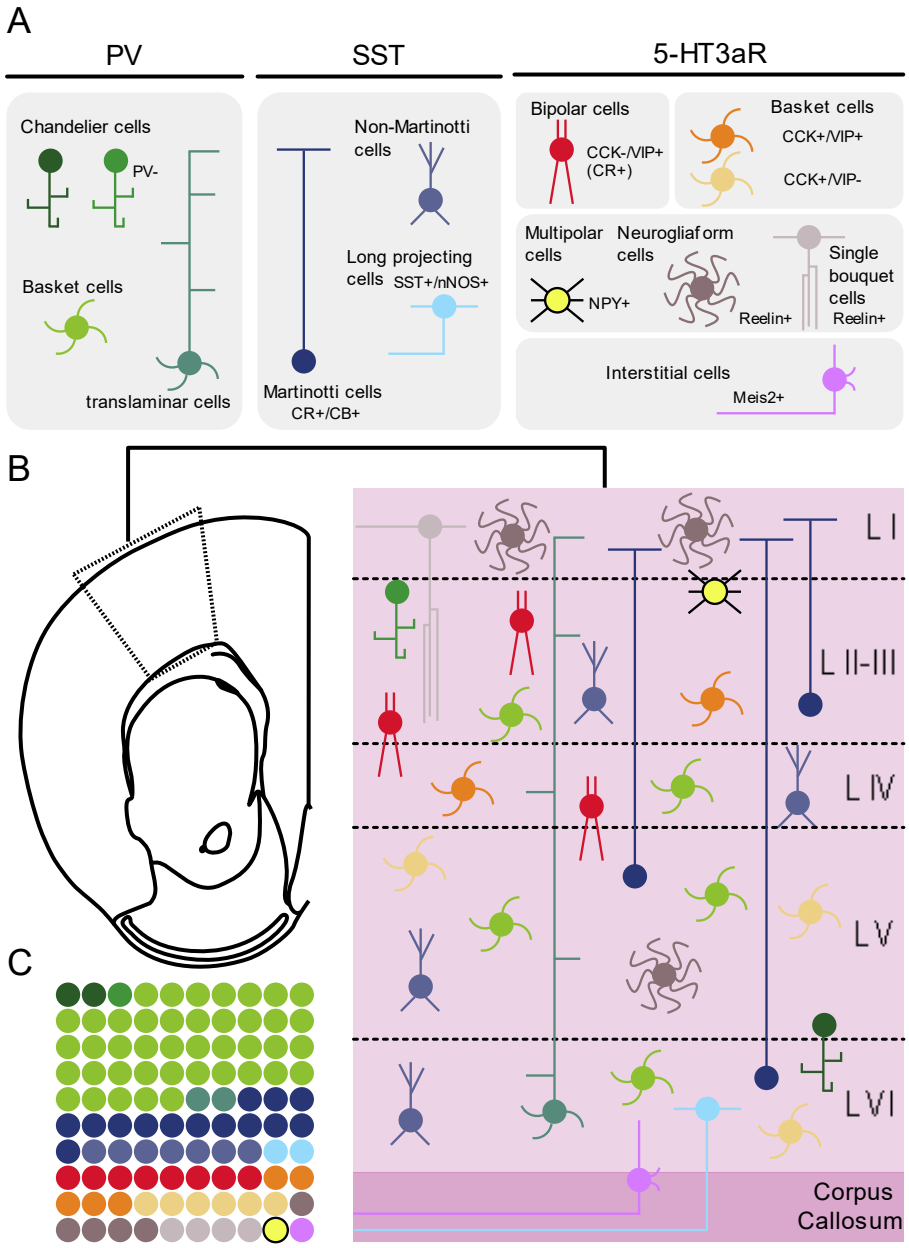

Fig. 1.15: The different types of interneurons in the neocortex. A. The three major classes of INs and their subtypes. **B.** Schematic representation of the laminar distribution of INs. Some INs are represented in most layers of the cortex, such as PV+ basket cells, while others are rarely found, such as Meis2+ INs. **C.** Approximative distribution of INs in the neocortex, color coded as in A. Taken from Lim et al., 2018.

PV INs are the most abundant category of INs inside the neocortex, as they represent 40% of the INs (Rudy et al., 2011). They are divided in three subclasses: the basket cells, the

chandelier cells and the translaminar cells (Lim et al., 2018). Basket cells are represented in all cortical layers, except layer I, and are the most represented type of IN in the neocortex across all categories (Fig. 1.15). They specialize in the targeting of proximal dendrites of PNs and are the main supplier of perisomatic inhibition of PNs, making them powerful regulators of cortical activity (Kisvárday et al., 1993; Markram et al., 2004; Wang, 2002). Basket cells are also interconnected by reciprocal inhibitory synapses (Isaacson and Scanziani, 2011). PV-expressing chandelier cells are abundant at the limit between layers V and VI (Fig. 1.15, Lim et al., 2018; Taniguchi et al., 2013). They innervate the axon initial segment of PNs (DeFelipe, 1997; Isaacson and Scanziani, 2011; Rudy et al., 2011), enabling them to outweigh the dendritic integration of excitatory postsynaptic currents (EPSCs) and thus to control PNs firing rate (Kawaguchi, 1997; Markram et al., 2004). Finally, translaminar cells are the third type of PV INs. They are less common than the two previous types of INs, and are mostly located in layer VI (Fig. 1.15, Lim et al., 2018). They send axons in all cortical layers and target PNs (Bortone et al., 2014). Most of PV INs are fast-spiking INs, (Fig. 1.16, Hu et al., 2014; Lee et al., 2014; Markram et al., 2004; Rudy et al., 2011), firing APs often at more than 1 KHz (Rudy and McBain, 2001). They are recognizable by their small input resistance, high amplitude rapid after-hyperpolarization, and low resting membrane potential close to -80 mV (Cousineau et al., 2020; Ferguson and Gao, 2018). Some PV INs in M1 also project to the striatum on both D1- and D1-expressing MSNs, even though they target preferentially the D1-expressing ones. They also contact striatal cholinergic interneurons (Melzer et al., 2017).

SST INs are the second type of INs represented in M1. They are classically divided in two groups: Martinotti cells and non-Martinotti cells, even if a third class exists: long-projecting cells (Fig. 1.15, Lim et al., 2018). Martinotti cells are present in layer II-III, V and VI, and they represent 60% of SST INs in these layers (Nigro et al., 2018). They are characterized by a long axon which branches in layer I (Wang et al., 2004). Most of Martinotti cells fire APs in an adaptating manner (Fig. 1.16) with a bursty onset, even if some of them fire in an irregular manner (Wang et al., 2004). These cells are implicated in disynaptic inhibition between PNs (Silberberg and Markram, 2007). Non-Martinotti cells are represented in all cortical layers, except for layer I, and do not have a long axon branching in layer I as Martinotti cells (Fig. 1.15, Lim et al., 2018). They generally exhibit lower input resistance compared to Martinotti cells, and rapid spiking rate with a stuttering pattern of discharge, but not as fast as fast spiking INs (Fig. 1.16, Nigro et al., 2018). In the neocortex, SST non Martinotti cells primarily target PV INs in layer IV, inducing the disinhibition of L4 PNs (Nigro et al., 2018). Finally, few SST

INs send long projections into the corpus callosum to other cortices. They are located in deep layers, especially layer VI (Fig. 1.15, Lim et al., 2018). Not much is known about these neurons. They often express the neuronal nitric oxide synthase and display irregular or adaptating firing patterns (Fig. 1.16, Lim et al., 2018), and are implicated in sleep regulation (Dittrich et al., 2012). As well as PV INs, some SST INs in M1 also project to the striatum on both D1- and D1-expressing MSNs, without a preferential target between these two cell types. They also contact striatal cholinergic interneurons (Melzer et al., 2017).

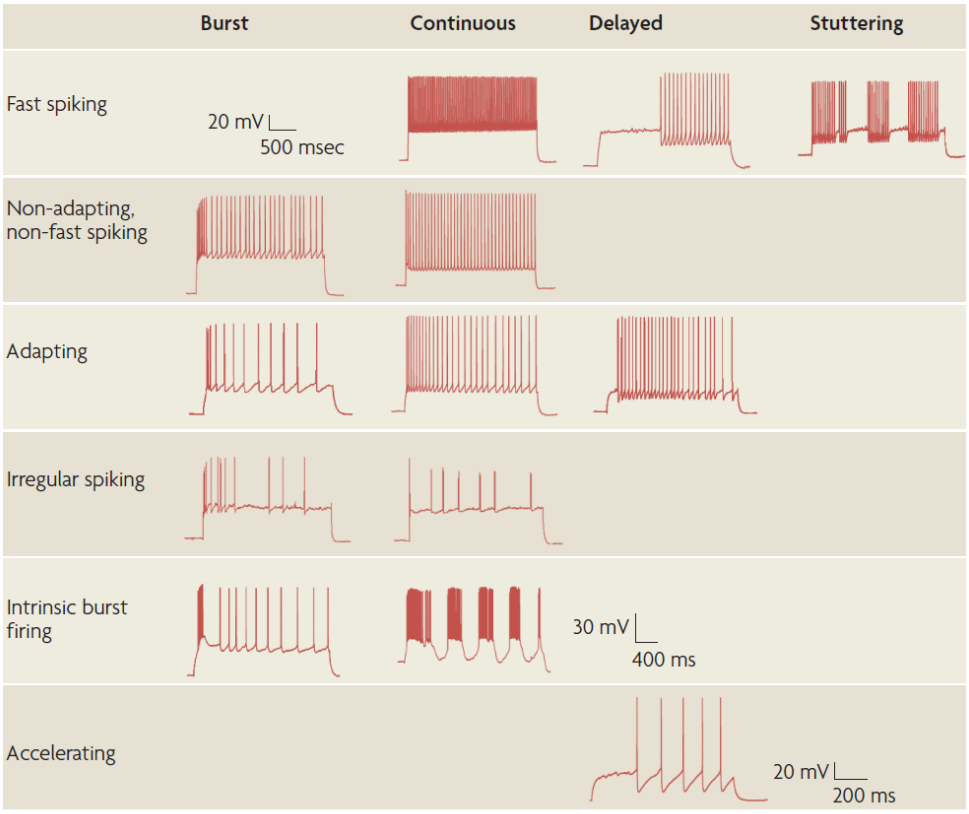

Fig. 1.16: The different types of interneurons based on their electrophysiological signature. Fast-spiking interneurons (INs) can fire APs in bursty, continuous, delayed or stuttering patterns. Non-adapting, non-fast spiking INs can fire APs in bursty and continuous patterns. Adaptating INs can fire APs in bursty, continuous or delayed patterns. Irregular spiking can fire APs in bursty or continuous patterns. Intrinsic burst firing INs can fire APs in bursty or continuous patterns. Finally, accelerating INs fire APs in delayed patterns. Taken from Bouzas et al., 2008.

The last type of INs represented in M1 are the 5-HT3aR expressing INs. This group is heterogeneous and composed of many cells. Among this group, bipolar cells expressing the vasoactive intestinal peptide (VIP) are the most common type (Fig. 1.15). They are present in layers II-III mostly, even if some are present in layer IV (Prönneke et al., 2015). They can fire APs in a continuous adaptating or irregular spiking pattern (Fig. 1.16, Prönneke et al., 2015), and send projection to SST and PV INs, making them disinhibitory INs (Jiang et al., 2015).

Other cells express VIP but are basket cells instead of bipolar cells (Fig. 1.15). The VIP basket cells co-express CCK, and are present in superficial layers of the neocortex (*i.e.*, layer II-III and IV, mainly, Fig. 1.15, Lim et al., 2018). Nonetheless, not all 5-HT3aR basket cells INs express VIP. These non-VIP basket cells also express CCK, but are represented in deep layers of the neocortex (mainly layers V and VI, Fig. 1.15, Lim et al., 2018). These two types of 5-HT3aR basket cells make perisomatic synapses on PNs and other INs, and fire APs in a regular or bursty pattern (Fig. 1.16, Kawaguchi and Kubota, 1998). Two subclasses of 5-HT3aR-expressing INs express reelin: neurogliaform cells and single bouquet cells. Neurogliaform cells are the most represented INs in layer I, but are also present in layer V (Fig. 1.15). They have dense axonal arborization and they display delayed spiking patterns (Fig. 1.16, Lim et al., 2018). They elicit GABA responses through $GABA_A$ and $GABA_B$ receptors on PNs, and they make electrical synapses on other INs (Oláh, 2007). Single bouquet cells are similar to neurogliaform cells and are also present in layer I, but they do not possess the same axonal arborization. Instead, they send axons which ramifies to deeper layers of the cortex (Fig. 1.15, Jiang et al., 2015). Furthermore, some of these single bouquet cells do not express reelin but VIP, and those display a bursty firing pattern (Fig. 1.16), in addition to lower input resistance and maximal frequency compared to neurogliaform cells (Miyoshi et al., 2010). The last two sub-classes of 5-HT3aR are sparse in the neocortex. One of them is called multipolar cells, they express VIP, they are found at the limit between layers I and II (Fig. 1.15) and they display irregular firing pattern (Miyoshi et al., 2010). The other one are the interstitial cells, they express meis2, are found in the white matter and send projections to deep layers of the cortex and to the striatum (Fig. 1.15, Lim et al., 2018). They seem to fire APs in a continuous non adaptating, non-fast-spiking pattern (Fig. 1.16, Frazer et al., 2017).

3.4. DAergic innervation of M1

First discovery of DAergic terminals in M1 dates back from the 1985 thanks to TH immunocytochemistry. These terminals were described as DAergic terminals and not as norepinephrine terminals as the experiments were made in norepinephrine terminals-depleted animals (Berger et al., 1985). It has firstly been described that DAergic innervation of M1 is restricted to deep layers in rodents and widespread in primates (Berger et al., 1991; Descarries et al., 1987; Lewis et al., 1987). More specifically, immunohistochemistry against the DAT in rats revealed a high density of DAergic terminals in the part of M1 responsible for forelimb movements, particularly in layer V (Fig. 1.17, Hosp et al., 2015; Vitrac et al., 2014). Nonetheless, more recent studies shown that in addition to M1 deep layers, more superficial

layers also receives a non-negligible amount of DAergic terminals (Raghanti et al., 2008). Using retrograde tracing approaches in rats, it has been shown that the DAergic terminals in M1 come from neurons located in the midbrain, specifically from the VTA and the SNc (Hosp et al., 2009, 2011), in a similar fashion as in the frontal cortex (Ott and Nieder, 2019). The functional impact of DA in the motor cortex is mediated by both D1-like and D2-like receptors, as they are both expressed in M1 (Camps et al., 1990; Gaspar et al., 1995; Huntley et al., 1992; Mansour et al., 1990).

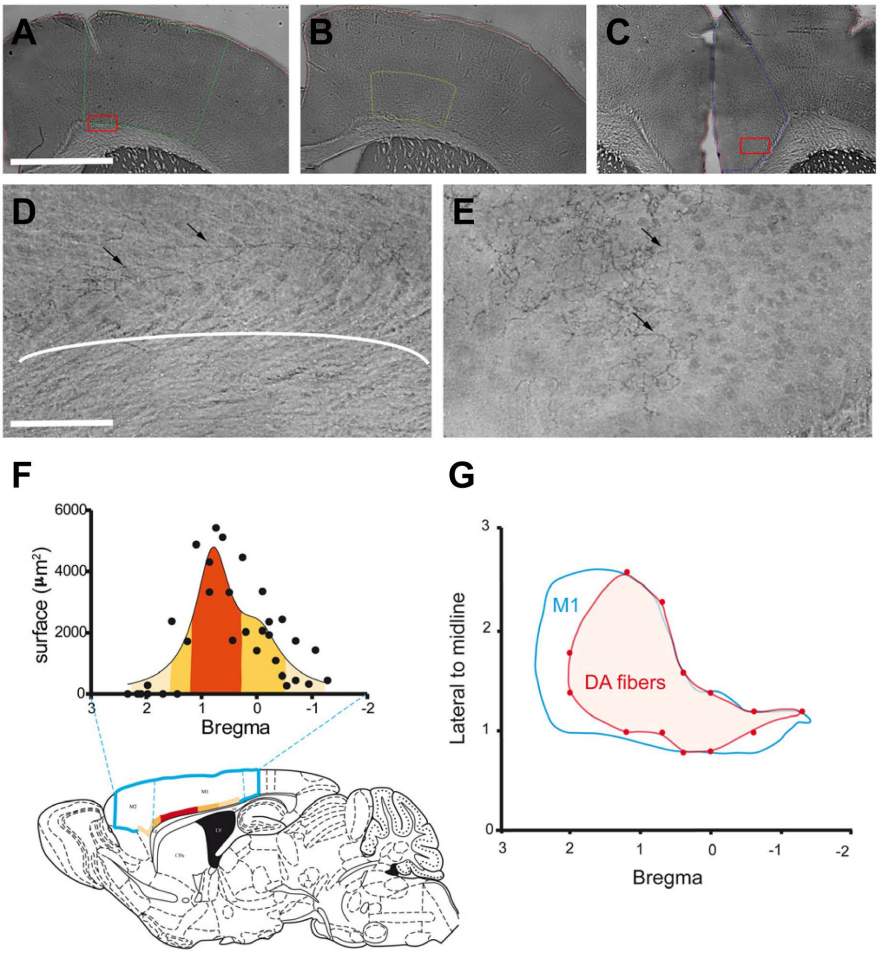

Fig. 1.17: Topography of the DAergic innervation of M1 in mice. **A-C.** Example images of DAT immunostaining in M1 (**A**), M1 deep layers (**B**) and cingular cortex (**C**). **D-E.** Higher magnification of the DAT immunostaining in M1 deepest layers (**D**) and in the cingular cortex (**E**). **F.** Sagittal view of the mouse brain with the rostrocaudal topographic distribution of DAT positive cells. **G.** Area of M1 containing DAT positive cells, view from above. Scale bars represent 100 µm (**A-C**) and 12.5 µm (**D-E**). Taken from Vitrac et al., 2014.

3.5. Roles of DAergic receptors on M1 neuronal subpopulations

3.5.1. Pyramidal neurons

PNs have been shown to express both D1-like and D2-like receptors (Awenowicz and Porter, 2002). Few studies investigated the role of D1-like receptors on M1 PNs. It has been reported that D1 receptor activation leads to the stabilization of newly formed spines in M1 during motor learning (Guo et al., 2015). Furthermore, *ex vivo* patch clamp recordings have shown that the blockade of D1 receptors in adult mice induces an increase in the excitability of M1, and a decrease of the maximal frequency of M1 PNs located in layer II-III (*i.e.*, mainly IT-CCNs), with differential effects depending on the blockade of fast synaptic transmission, suggesting an impact of D1 receptors on the entire M1 cortical microcircuit (Swanson et al., 2021). Nonetheless, recorded cells have not been identified as D1-expressing neurons prior nor after recordings. At this date, no studies have investigated the impact of the activation of D1-like receptors on the intrinsic properties of M1 PNs, more specifically concerning the activation of D1 receptors (Cousineau et al., 2022).

Concerning the role of D2-like receptors, it has been reported that D2 receptors promote new spine formation on M1 PNs during motor skill learning. Thus, the spine turnover on M1 PNs is controlled by both D1 and D2 receptors (Guo et al., 2015). The effect of D2 receptor activation on M1 PNs has given contradictory results. In fact, some *ex vivo* studies report no effect of D2 receptors activation on M1 PNs (Cousineau et al., 2020), while other *in vivo* studies reported an increase in the firing frequency of M1 PNs (Vitrac et al., 2014). Moreover, D2 receptor blockade has been shown to decrease the firing frequency of PNs *in vivo* (Parr-Brownlie, 2005), while *ex vivo* recordings reported an increase of PNs' excitability following D2 receptors blockade (Swanson et al., 2021). *In vivo* recordings have been made without blocking fast-synaptic transmission, indicating a potential role of the network on the inhibition of M1 PNs. Nonetheless, the overall lack of homogeneous experimental design creates confusion regarding the net impact of DA receptors on M1 PNs' activity.

3.5.2. Interneurons

To this date, there are no data in the literature concerning the expression of D1 receptors by INs in M1. However, D1 receptors have been shown to be expressed by INs in the PFC of rodents. In fact, VIP-expressing INs of layers II-III express D1 receptors in the PFC, but minimal expression of D1 receptor was found in PV and SST INs (Anastasiades et al., 2019), even if in the PFC of macaques, D1 receptor expression has been identified in PV INs (Chris Muly et al., 1998). *In situ* hybridization in rats also revealed that D1 mRNA is present in numerous INs expressing PV, and also in some INs expressing calbindin, in the prefrontal, the

infralimbic, the prelimbic, the anterior cingulate and the agranular cortices (Le Moine and Gaspar, 1998). In the PFC of rodents, D1 receptor activation leads to an increased excitability of VIP-expressing INs (Anastasiades et al., 2019). As for PNs, the role of D1 receptors has been less extensively studied compared to the role of D2 receptors, as no data are available concerning the blockade of D1 receptors on the activity of D1-expressing INs, even in the PFC.

The role of D2 receptors has been more widely studied in M1 INs. Particularly, they are expressed by PV INs in rodents' M1 (Cousineau et al., 2020). *Ex vivo* patch clamp recordings revealed that the activation of D2 receptors increases the excitability of PV INs isolated from the network by fast synaptic blockers. Moreover, this increased excitability can be observed at the synapses from PV INs to PNs, as D2 receptor activation on PV INs also increases the GABAergic transmission to PNs (Cousineau et al., 2020). Nonetheless, no other data are available concerning the impact of D2 receptors activation on PV INs, nor related experiments on other types of INs in M1.

3.6. Role in motor skill learning and paradigms used in rodents

Learning new motor skill requires repetition to improve the successful execution of the motor skill and to increase its speed and its accuracy over time. Once learned, the motor skill can then be retrieved and executed in a repetitive manner. Even if M1 has been known for a long time for its implication in motor execution (cf paragraph 3.1), it has been demonstrated that M1 is also a major actor of motor skill learning (Hosp et al., 2011; Kawai et al., 2015). In fact, the inhibition of the activity of M1 by blocking the protein synthesis in M1 leads to the alteration of the learning of a motor task (Ohbayashi, 2020). Moreover, rodents with M1 lesions prior to the training to a new motor sequence are unable to learn it, while M1 lesions after the learning did not impair the retrieval of the learned motor sequence (Kawai et al., 2015). However, in this particular case, the motor skill to be acquired was a lever press which did not imply dexterity and fine movements of the digits, suggesting that M1 might be more essential for execution of dexterous movements and learning of motor sequences, rather than essential for the execution of simpler motor tasks. The learning of a new motor skill is associated with a rearrangement of M1 motor map, with an increase in the size of the representation of the body part involved in the new movement in M1 (Monfils et al., 2005).

The implication of M1 in motor learning has been investigated using motor tasks, especially forelimb lever press or prehensive tasks in rodents (Guo et al., 2015; Hosp et al., 2011; Kawai et al., 2015). One of the most commonly used is the single pellet reaching task

(SPRT, Chen et al., 2014). This operant task consists of a box with a slit on one of its sides and a food plate placed in front of the slit which dispends a rewarding food, such as sucrose pellets. In order to get the pellet, rodents have to make a prehensive movement threw the slit, grab the pellet with their digits and take back the pellet to their mouth to eat it. These different sequences are interesting because they are similar to movements done by humans, making results easily transposable to humans (Klein et al., 2012). M1 cells' activity can be monitored during these tasks thanks to *in vivo* electrophysiological recording (Li et al., 2017), or imaging techniques coupled with optogenetics (Levy et al., 2020). Thanks to these different approaches, it has been shown that M1 layer V PNs (*i.e.*, PTNs and IT-CStrNs mainly) are activated during movement execution, as well as fast-spiking INs (Isomura et al., 2009; Levy et al., 2020; Li et al., 2017), whereas M1 layer II-III PNs' activity (*i.e.*, IT-CCNs' activity principally) was essentially outcome-related (Levy et al., 2020). Hence, these data suggest a segregated organization between motor function and monitoring, at the cellular and layer levels in M1.

The motor skill learning processes in M1 are dependent of DA (Hosp et al., 2011). Lesion (Hosp et al., 2011) and retrograde tracing studies (Hosp et al., 2011, 2015), showed that this DA is released in M1 by DAergic terminals whose cell bodies are located in the midbrain, essentially in the VTA and the SNc. In fact, depleting VTA DAergic neurons in the rat resulted in a drastically decreased number of DAergic terminals in M1, and in an impaired motor learning without impacting already learned movements. Moreover, the motor learning is reestablished by intracortical injections of L-DOPA (Hosp et al., 2011; Molina-Luna et al., 2009). In addition, the *in vivo* blockade of D1 or D2 receptors in rodents by cannula injections in M1 decreases the synaptic plasticity in M1 and is sufficient to impair motor skill acquisition, in a reversible manner (Molina-Luna et al., 2009). These DA-mediated plasticity mechanisms are thought to be linked with PLC downstream signaling by both D1 and D2 receptors (Rioult-Pedotti et al., 2015). The blockade of D2 receptors in M1 has also been shown to decrease the activity of M1 neurons, leading to increased movement times (*i.e.*, bradykinesia) during a reaching task in rats (Parr-Brownlie, 2005). Furthermore, the spine turnover of M1 neurons is dependent of DA: while D1 receptor is associated with spine selection, D2 receptor activation increases the spine formation (Guo et al., 2015). These data emphasize that the prominent role of M1 in motor skill acquisition is dependent on DAergic transmission from midbrain DAergic neurons.

Hypothesis and objectives

The DAergic innervation in M1 has been shown to be important for M1 computations during motor skill learning, as the blocking of the DAergic transmission in M1 is sufficient to disrupt motor acquisition. Although the architecture of the DAergic system within M1 has been well characterized anatomically in mice, the level of understanding of DA origin and effect in M1 is not completely understood. The cell bodies of these DAergic terminals have been identified in the midbrain of rats, especially in the VTA and in the SNc. However, these DAergic neurons have not been yet identified in other models, such as in mice. Besides, the electrophysiological properties of these neurons have not been investigated in any animal models, neither prior nor during or after motor skill learning, even if they have been shown to be necessary for these processes. Moreover, few data are available in the literature regarding the impact of DA on M1 neuronal populations. Especially, the impact of D1 receptors in layer V on M1 neuronal populations has been less studied that the one of D2 receptors. Furthermore, a mapping of D1 receptors has been made in other cortical structures such as the PFC of young and adult mice, but there are no data in the literature on an age-dependent expression of D1 receptors in M1 PNs. Likewise, no data are available concerning the impact of D1 receptor activation and inhibition on the intrinsic properties of PNs at young and adult states. These lacks of data in the literature highlight the gap in our knowledge of the electrophysiological characterization and functional importance of these midbrain DAergic neurons projecting to M1. **Hence, the global aim of this study was to characterize anatomically and functionally the mesocortical DAergic pathway from the midbrain to M1.** The objectives of this thesis were, on one hand, to identify and characterize the intrinsic properties of midbrain DAergic neurons projecting to M1, and then to study their activity during motor learning; and on the other hand, to study the functional importance of this DAergic innervation at the level of M1 neurons, especially through D1 receptors. As DA in M1 is necessary for acquisition but not for maintenance nor execution of motor skills, the hypothesis was that the pattern of activity of M1-projecting midbrain DAergic neurons is of importance to modulate the activity of M1 cortical microcircuits, especially the activity of PNs to enable motor skill learning processes. Concerning the role of D1 receptors, as it has been shown that they are positively coupled to the PLC in M1, the hypothesis was that their activation would increase the excitability of the M1 layer V PNs of adult mice. The comparison between young and adult mice was purely data-driven.

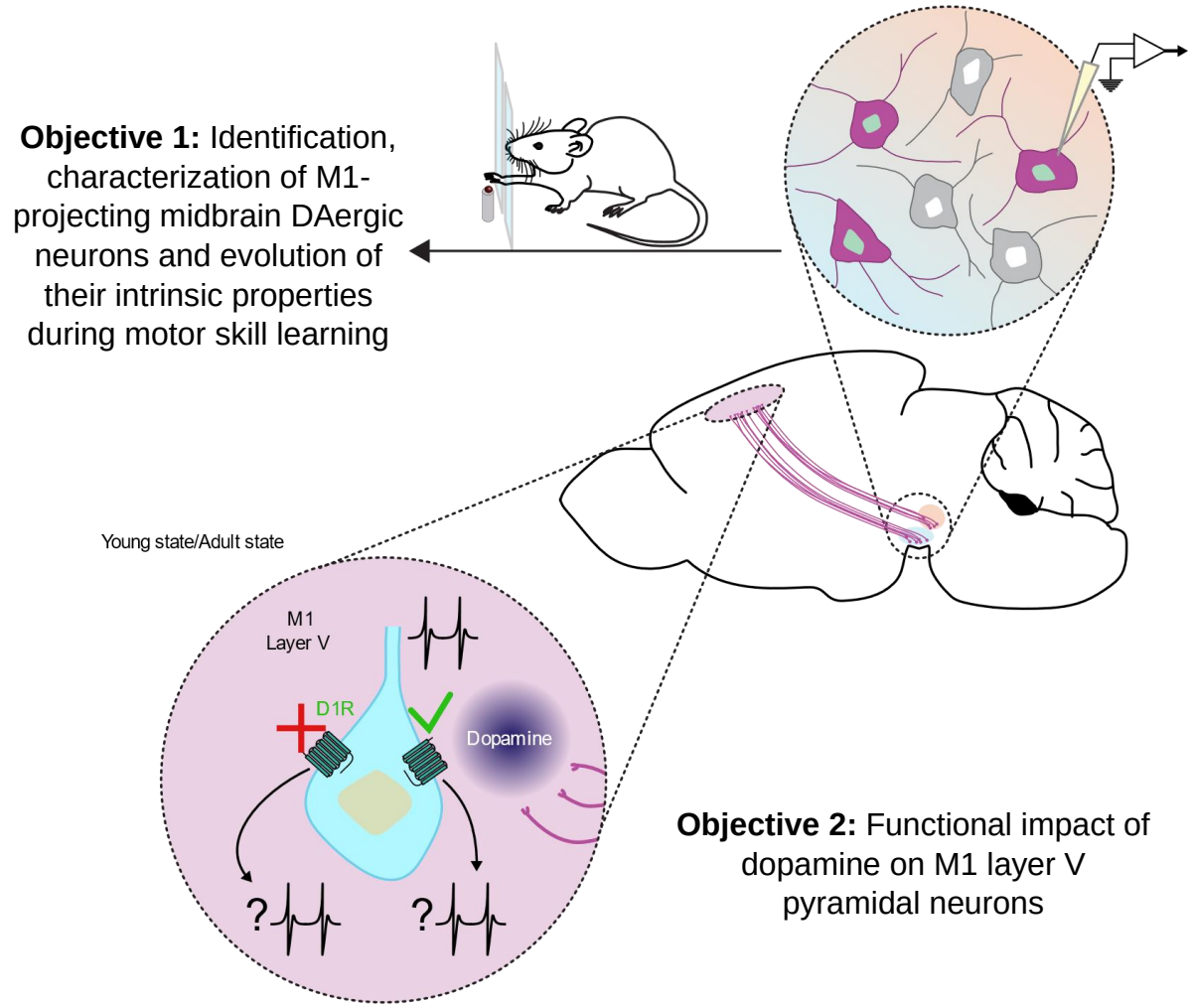

Fig. 2.1: Main objectives of the thesis. Objective 1: identification, electrophysiological characterization of M1-projecting midbrain DAergic neurons and evolution of their intrinsic properties during a skill reaching task. **Objective 2:** functional impact of DA on M1 layer V PNs.

The specific objectives of the present study were (Fig. 2.1):

I- To identify and characterize the DAergic neurons projecting to M1 in mice, and to monitor their activity during motor skill learning (Fig. 2.1).

Firstly, retrograde tracing experiments using the retrograde tracer fluorogold (FG) were performed to map midbrain DAergic neurons projecting to M1. Then, the neurons labelled with FG were recorded using *ex vivo* patch clamp recording in acute brain slices, and verified for TH expression with post-hoc immunohistochemical labeling.

Secondly, the activity and the intrinsic properties of these identified M1-projecting midbrain DAergic neurons were monitored during motor skill learning. To this aim, retrograde tracing approaches were used in mice as described before. These mice were then trained to an

operant task enabling the study of motor skill learning: the SPRT. Then, *ex vivo* electrophysiological recordings of the retrogradely labelled neurons were performed at different times of the motor learning, to investigate how the intrinsic properties of these neurons change during motor skill learning.

II- To investigate the effect of DA release from M1-projecting midbrain DAergic neurons on M1 layer V PNs (Fig. 2.1).

In a first time, the endogenous DA release in M1 has been demonstrated *ex vivo* in acute brain slices using a newly developed genetically encoded DAergic sensor: the $GRAB_{DA1m}$. The release of DA was induced by an electrical stimulation, and control experiments were carried out in the striatum to first test if the DAergic sensor was working properly, as the striatum is known to receive massive DAergic inputs. These experiments could be used to further characterize *in vivo* the time course of DA release in M1 during motor skill learning.

In a second time, the transgenic mouse lines DAT-Cre-Ai32 and DAT-Cre were used to enable the expression of excitatory opsins in DAergic neurons to manipulate them. The impact of DA release by DAergic terminals on M1 layer V PNs was studied *ex vivo* on acute brain slices, using optogenetics to induce the activation of the DAergic terminals in M1, and thus DA release.

Finally, the impact of D1 receptor activation and blockade on M1 layer V PNs has been investigated. The transgenic mouse line D1-GFP was used in this part, enabling the identification of D1-expressing cells in M1 by their expression of the green fluorescent protein (GFP). Young and adult mice were used in this part, to further investigate a potential differential regulation of M1 layer V PNs over time. Firstly, a mapping of D1 receptors has been made in M1, using immunohistochemical labeling for molecular markers which are thought to be specific of PTNs and ITNs: CTIP2 and SATB2, respectively. Then, *ex vivo* electrophysiological recordings of M1 layer V PNs were performed in young and adult mice, in control conditions or with the bath application of D1 receptor agonist or antagonist. PNs were identified by the shape of their soma and their electrophysiological properties.

Material & methods

1. Animals

All experiments were performed in accordance with the guidelines of the French Agriculture and Forestry Ministry for handling animals (APAFIS #26 770 and #14 255) and the official European guidelines (Directive 2010/63/UE). Male and female mice were housed separately under artificial conditions of light (12/12 h light/dark cycle, light on at 7:00 a.m.), with water access *ad libitum*. Food access was restricted only for mice undergoing behavioural experiments, as the task implied them to be motivated enough to eat. The weight of these mice was set at 90% of their initial weight, and mice below 80% of their initial weight were immediately removed from experiments and given access to food. These same mice were housed separately during the week of behavioural experiments to control the food intake of each mouse.

Different mouse lines were used during this thesis. DAT-Cre mice (Slc6a3$^{tm1(cre)Xz}$/J) were used for behavioural experiments mainly and were aged between 6 to 10 weeks at the beginning of the experiments. These mice express the gene of the Cre-recombinase enzyme under the promoter of the DAT, enabling Cre-dependent expression of gene of interests in DAergic neurons only. DAT-Cre mice were also used to enable channelrhodopsin 2 (ChR2) expression in DAT-expressing midbrain neurons only, to stimulate midbrain DAergic terminals in M1 during *ex vivo* electrophysiological recordings of M1 PNs. Another mouse line used in this thesis was the DAT-Cre-Ai32 mouse line. These mice are obtained by crossing DAT-Cre mice with B6;129S-Gt(ROSA)26Sor$^{tm32(CAG-COP4*H134R/EYFP)Hze}$/J (Ai32) mice (mice expressing the excitatory opsin ChR2, whose expression is conditioned by the expression of the Cre-recombinase enzyme in the neurons). As DAT-Cre mice express the Cre recombinase only in DAT-expressing neurons, the excitatory opsin ChR2 is only expressed by DAT-expressing neurons in DAT-Cre-Ai32 mice. These DAT-Cre-Ai32 mice were used to stimulate midbrain DAergic terminals in M1 during *ex vivo* electrophysiological recordings of M1 PNs. Finally, D1-GFP mice (Tg(Drd1-EGFP)X60Gsat), aged between 6 to 10 weeks for adult mice and between P16 and P25 for young mice were used for investigation on the impact of D1 receptor activation and inhibition of M1 layer V PNs.

2. Behaviour

To assess motor skill learning, the SPRT was used (Chen et al., 2014). The mice were placed in a box (Fig. 3.1A, B, Imetronic, France) and had to grab a sucrose pellet (Bio-serv, USA) through a slit. To this aim, the mice were handled 3 days for them to be acquainted with the experimenter and to avoid stress. Then, they were food restricted to 90% of their body weight and isolated to monitor the food consumption of each animal. The mice were then habituated to the experimental setup for two days: they were placed 10 minutes in the operant box with pellets inside the box at the level of the slit, to enable the mice to know where they can get the food. After the habituation phase, the shaping process began, which consisted in determining the preferred paw of the mice. To this end, the mice were placed in the operant box and the session was stopped after 20 attempts to catch a pellet outside the slit with their paws, or after a maximum of 20 minutes. A mouse was considered "right-handed" or "left-handed" when it did at least 70% trials with one paw. After the shaping process, stereotaxic injections (cf paragraph **3.**) were performed.

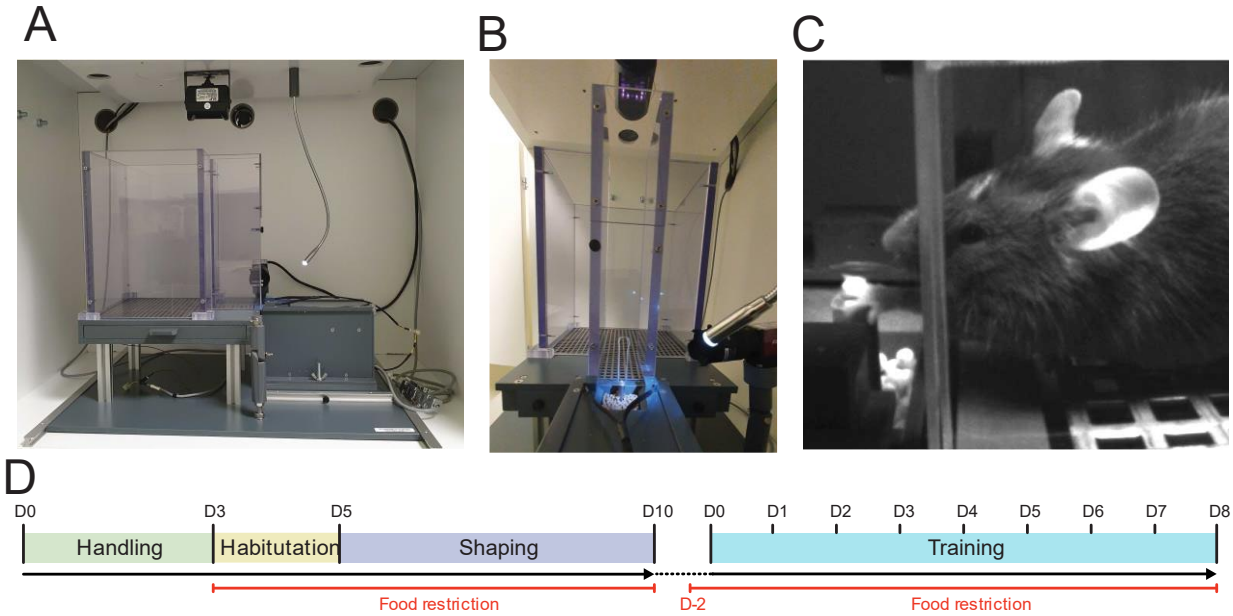

Fig. 3.1: The single pellet reaching task operant box. A. Sideview of the box. **B.** Frontview of the box. **C.** Picture of a mouse performing the task. **D.** Timeline of the experimental protocol.

After a week of recovery time, the mice began the task. The slit was positioned a bit to the right for "right-handed" mice, and a bit to the left for "left-handed" mice, and a high acquisition frequency and high definition CCTV camera (Manta, Allied Vision, Germany) is positioned on the side of the preferred paw of the animal to record the paw and the finger trajectories during the reaching movements of the mice (Fig. 3.1C). The mice underwent the

SPRT for 8 consecutive days in which they stayed 20 minutes inside the box or the time they needed to do 50 trials with their preferred paw (Fig. 3.1D). Trials were classified in 4 categories: "fail" when the mice failed to target and at least touch the pellet, "touch" when the mice touched the pellet without grasping it, "drop" when the mice grabbed the pellet but dropped it before the end of the movement (*i.e.*, before grabbing the pellet to their mouth), and "success" when the mice successfully grabbed the pellet to their mouth. Mice were considered "learner" if their success rate increased over the training sessions to reach ~50-60%, and if the trajectories of their movement became reproducible over the training sessions. The other mice were considered as "non-learner".

3. Stereotaxic injections

3.1. Retrograde tracing

The mice were deeply anesthetized using 4.5% isofluorane. They were administered buprenorphine (buprecare, i.p., 0.120 mg/kg), carprofen (rimadyl, i.p., 4.8 mg/kg) and lidocaine (lurocaine, local scalp s.c., 24 mg/kg). The scalp was then shaved with a trimmer, and mice were placed in a stereotaxic frame (RWD, USA) equipped with a heating pad set at 37.8°C. Isofluorane was lowered at 1.5% for all other steps of the surgery. The eyes of the mice were protected from the light by application of an ophthalmic gel (ocrygel, TVM lab, France). After checking the disappearance of all arousal reflexes, scalp incision was practiced with a scalpel, and the skull was leveled to be flat by taking coordinates at the bregma and lambda reference points. A difference of ± 0.05 mm was considered acceptable. Then, a hole was drilled in the skull with a microdrill (78001, RWD, USA) and 90 nL of 2% 2-Hydroxystilbene-4,4′-dicarboxamidine bis(methanesulfonate) (Fluorogold™ (FG), Sigma-Aldrich, France) was injected with a picopump PV820-A (World Precision Instruments, USA) at each of the following coordinates (in mm from bregma): AP: -0.5, ML: ±1.08, DV: -0.7/-0.35; AP: 0.5, ML: ±1.08, DV: -0.7/-0.35; AP: 0.5, ML: ±1.32, DV: -0.7/-0.35; AP: 1.5, ML: ±1.32, DV: -0.7/-0.35 in order to target all M1. After the injections, the scalp was sutured and the mice were placed in a cage with a hot plate for a better waking up. The mice were followed 3 days after surgery to ensure the welfare of the animals and to detect any signs of discomfort. Before any further experiments, two weeks were necessary to let FG migrate.

3.2. Injection of the DAergic sensor $GRAB_{DA1m}$

To assess the DA release in M1, the following adeno-associated virus (AAV) containing the D2-modified receptor genetically encoded fluorescent sensor $GRAB_{DA1m}$ (Sun et al., 2018) under the human synapsin (hSyn) promoter was injected in M1, and in the striatum as a control: AAV9-hSyn-$GRAB_{DA1m}$.WPRE.hGH ($1{,}68x10^{13}$ gpc/mL, IMN Vector Core). The hSyn promoter is pan-neuronal, enabling the expression of the sensor in all neurons. The procedure was the same as previously described, with the same coordinates for M1 injection. 100 nL of AAV9-hSyn-$GRAB_{DA1m}$.WPRE.hGH was injected at each coordinate. Striatum injection coordinates were the following (in mm from bregma): AP: 0.5, ML: ±1.08, DV: -2.75/-2.25; AP: 0.5, ML: ±1.32, DV: -2.75/-2.25. Six weeks of expression were waited after injection to ensure proper expression of the sensor.

3.3. Injection of the channelrhodopsin 2

To stimulate midbrain DAergic neurons during patch clamp experiments, the following AAV containing the excitatory opsin ChR2 was injected in the SNc and the VTA prior to the experiments: AAV2.5-EF1a-DIO-hChR2(H134R)-EYFP.WPRE.hGH ($6{,}72x10^{12}$ gcp/mL, UNC Vector Core). The double-floxed inverse open reading frame (DIO) enables the expression of the ChR2 only in the presence of the Cre-recombinase enzyme. Thus, as the viruses were injected in DAT-Cre mice, the opsin were expressed only in DAT-expressing neurons (*i.e.*, DAergic neurons in a vast majority). The procedure was the same as previously described, 45 nL of AAV2.5-EF1a-DIO-hChR2(H134R)-EYFP.WPRE.hGH was injected at each coordinate. The SNc coordinates were the following ones (in mm from bregma): AP: -3.16, ML: ±1.25, DV: -4.25; AP: -3.30, ML: ±1.25, DV: -4.25. The VTA coordinates were the following ones (in mm from bregma): AP: -3.16, ML: ±0.5, DV: -4.5; AP: -3.30, ML: ±0.5, DV: -4.5. After the injections, the injection pipette was set in place for 3 minutes to avoid leak in upper structures. Five weeks of expression were waited after the injections to ensure proper expression of the opsin. After slice preparations (cf paragraph **4.**), a LED-light source (473 nm, 100 mW; Prizmatix Ltd., Israël) connected to an optic fiber (Ø: 500 µm; numeric aperture: 0.63) was placed at the region of interest to either stimulate the terminals of infected neurons in areas of interest (*i.e.*, M1 or striatum), or stimulate putative infected neurons at the injection site (*i.e.*, midbrain).

4. Slice preparation

Mice were deeply anesthetized using ketamine with xylazine (100 and 20mg/ kg, i.p., respectively). After the disappearance of all arousal reflexes, a thoracotomy was done to enable

the transcardial perfusion with an ice-cooled and oxygenated with carbogen (95% O_2/5% CO_2) cutting solution containing 250 mM sucrose, 2.5 mM KCl, 1.25 mM NaH2PO4·H2O, 0.5 mM CaCl2·H2O, 10 mM MgSO4·7H2O, 10 mM D-glucose and 26mM NaHCO3. The brains were then quickly removed and glued to the stage of a vibratome (VT1200S; Leica Microsystems, Germany) and placed into a cutting chamber filled with the cutting solution and oxygenated with carbogen. The brains were then cut in 300µm thick sections, which were then incubated for 1 hour into a 37°C warmed ACSF containing 126 mM NaCl, 2.5 mM KCl, 1.25 mM NaH2PO4·H2O, 2 mM CaCl2·H2O, 2 mM MgSO4·7H2O, 26 mM NaHCO3, and 10 mM D-glucose, 1 mM sodium pyruvate and 4.9 µM L-gluthathione reduced and oxygenated with carbogen. Slices were then placed at room temperature for 30 minutes before any recording was made.

5. Drugs

Drugs were prepared in double-distilled water as concentrated stock solutions, then aliquoted and stored at -20°C. Drugs were diluted daily at the experimental concentrations and perfused in the recording chamber. In experiments using them, glutamatergic AMPA/kainate and NMDA receptors were blocked with 20 µM 6,7-dinitroquinoxaline-2,3-dione (DNQX, Tocris, UK) and 50 µM D-(-)-2-amino-5-phosphonopentanoic acid (AP V, Tocris, UK) respectively, and $GABA_A$ receptors were blocked using 10 µM 6-Imino-3-(4-methoxyphenyl)-1(6*H*)-pyridazinebutanoic acid hydrobromide (GABAzine, Tocris, UK). To block D1 receptors, 1 µM D1 receptor antagonist (*R*)-(+)-7-Chloro-8-hydroxy-3-methyl-1-phenyl-2,3,4,5-tetrahydro-1*H*-3-benzazepine hydrochloride (SCH 23390, Sigma, France) was used, and to activate D1 receptors, 2.5 µM D1 receptor agonist (±)-6-Chloro-2,3,4,5-tetrahydro-1-phenyl-1*H*-3-benzazepine hydrobromide (SKF 81297, Tocris, UK) was used. To block D2 receptor, 2 µm of (*S*)-(-)-5-Aminosulfonyl-*N*-[(1-ethyl-2-pyrrolidinyl)methyl]-2-methoxybenzamide (sulpiride, Tocris, UK) was used. Sulpiride was the only drug dissolved in DMSO. Electrophysiological recordings or imaging experiments were made 20 minutes after drug application.

6. *Ex vivo* electrophysiological recordings

Single slices were placed in a recording chamber continuously perfused with a recording solution containing 126 mM NaCl, 3 mM KCl, 1.25 mM NaH2PO4·H2O, 1.6 mM CaCl2·H2O, 2 mM MgSO4·7H2O, 10 mM D-glucose and 26 mM NaHCO3, oxygenated with carbogen and heated at 32°C. Slices were visualized under IR-DIC and fluorescence microscopy using an

axio examiner Z.1 microscope (Zeiss, Germany) equipped with a 63X water-immersion objective (W Plan-Apochromat 63X/1.0 VIS-IR, Zeiss) and an Axiocam MRm camera (Zeiss, Germany). Recordings of neurons were made using patch pipettes of impedance between 4-9 MΩ. These pipettes were made from glass capillaries (GC150F10; Warner Instruments, USA) pulled with a horizontal pipette puller (P-97; Sutter Instruments, USA). Recordings made in whole cell configuration were done using an internal pipette solution containing 135 mM K-gluconate, 3.8 mM NaCl, 1 mM MgCl2·6H2O, 10 mM HEPES, 0.1 mM Na4EGTA, 0.4 mM Na2GTP, 2 mM MgATP and 5.4 mM biocytin (pH = 7.2, ~292 mOsm). Recordings made in cell attached configuration were done with the same internal pipette solution, and some of them were made with the same medium containing also QX-314 (2 mM) to inhibit voltage-gated sodium channels. This enabled to record only the currents and not the resulting APs to clearly see the amplitude of the recorded currents. Recordings were corrected for a junction potential of -13 mV. Experiments were done with a Multiclamp 700B amplifier and digidata 1550B digitizer controlled by clampex 11.0 (Molecular Devices LLC, USA). Recordings were acquired at 20 kHz and low-pass filtered at 4 kHz. Series resistance was monitored throughout the experiment by voltage steps of -5 mV, and data were discarded when the series resistance changed by > 20%. After recordings, slices were fixed for 24 hours at 4°C in a solution of PBS 0.01 M containing 4% of paraformaldehyde (Thermofisher, USA), then washed and stored in PBS 0.01 M containing 0.03% of azide (Sigma, France) until further histological processing.

7. Live imaging

For live imaging experiments, slices were prepared as described for *ex vivo* electrophysiological recordings experiments, and the same solutions were used. Slice were observed under IR-DIC on an epifluorescence microscope NiE (Nikon instruments, Japan) equipped with a 4x objective CFI E plan apochromat 4X/0.10 (Nikon, Japon), a 60x immersion objective CFI APO NIR 60X/1.0 (Nikon instruments, Japan) and a camera Zyla sCMOS (Andor technology, Ireland). A bipolar electrical probe was applied at the $GRAB_{DA1m}$ injection sites to stimulate putative DAergic terminals in this area, elicit DA release in this area. The software NIS-Elements BR (Nikon instruments, Japan) was used for imaging and the frequency of acquisition was set at 20 fps.

8. Histology

Transcardial perfusion were made on the mice following the same procedure as described for slice preparation, except the ACSF used did not contain sodium pyruvate and

glutathione reduced. The brains were then post-fixed at 4°C in a solution of PBS 0.01 M containing 4% paraformaldehyde for 24 hours, washed and cut in 50 µm thick slices with a vibratome (VT1000S; Leica Microsystems, Germany). Slices were then processed for immunohistochemical labeling. For that aim, slices were put in a blocking buffer for 2 hours, and then placed 48 hours in a solution of PBS 0.01M/Triton X-100 0.3% (Sigma, France) containing the primary antibodies at indicated concentration (Table 1). After the incubation time, slices were washed 3 times in PBS 0.01 M (Sigma, France), then incubated with the secondary antibodies for 2 hours, washed 3 times again with PBS 0.01 M and then mounted onto slides in DAPI fluoromount medium or fluoromount medium (SouthernBiotech, UK). Biocytin revelation was made with streptavidin (1:500, life technologies, S32357) during secondary antibody incubation. Images were taken with a confocal microscope (Leica TCS SP8) head mounted on an upright stand DM6 FS (Leica Microsystems, Germany) with a HC PL APO 20x/0.75 IMM CORR CS2 objective for counting images or with a HC Plan Apo CS2 63X oil NA 1.40 for patched neurons images. The microscope is equipped with four laser lines (405 nm, 488 nm, 552 nm and 638 nm) in order to image quadruple immunohistochemistry.

Table 1: List of the primary antibodies used

Antigen	**Host**	**Dilution**	**Supplier**	**# Catalog**	**# Lot**
CTIP2	Rat	1:500	Abcam	ab18465	GR3272266-4
GFP	Chicken	1:1000	Aves lab	GFP-1010	GFP3717982
GFP	Chicken	1:1000	Abcam	ab13970	GR3190550-21
SATB2	Mouse	1:300	Abcam	ab51502	GR273053-6
TH	Rabbit	1:1000	Abcam	ab6211	GR199969-4
TH	Mouse	1:1000	Millipore	MAB318	3596692

9. Analysis

For behavioural analysis, success percentages were obtained as the percentage of successful trials over the total number of attempts. Learning curves were then generated as the success percentages as a function of the days of training. Kinematic analyses were done manually using the Kinovea software. The coordinates of the position of the paw across the videos were then exported and plotted in Prism to reconstitute the whole trajectories of the different movements.

Electrophysiological data were analyzed using clampfit 10.7 (Molecular Devices, USA). Input-output (F-I) curves were generated by injecting increasing depolarizing currents of 1 s each, and by counting the number of APs for each step. Currents of 50 pA increments ranging from -150 pA to 150 pA were used in experiments concerning midbrain DAergic neurons, whereas currents of 25 pA increments ranging from -150 pA to 225 pA were used in experiments concerning D1 receptors. Input resistance was calculated using Ohm's law: $R\ (M\Omega) = \left(\frac{\Delta U\ (V)}{I\ (A)}\right)/1 \times 10^6$, with I a -50 pA injected current in current clamp mode and ΔU the difference between the baseline and the voltage recorded during the injection of the current. The rheobase was obtained by injecting increasing depolarizing currents of 500 ms each (10 pA increments), and when an AP was triggered, increasing depolarizing currents of 1 pA increments starting at 10 pA below the current value for which an AP was triggered were applied until an AP was triggered. The current value for which a single AP was triggered was considered as the rheobase of the neuron. AP half width and peak amplitude were obtained with threshold search in clampfit 10.7. AP threshold was measured in clampfit as the beginning of the rising slope of the phase plots of the neurons. These phase plots were made at rheobase using clampfit 10.7. Electrophysiological traces were further processed using Origin 7 (OriginLab, USA).

For live imaging, video recordings were opened in Fiji and traces were obtained by plotting the z axis profile in areas of interest. Values were exported, and $\Delta F/F_0$ was calculated, with F_0 as the mean of the five first baseline values.

For cell counting, confocal images were opened in Fiji and either all neurons were counted in the area of interest (for retrograde tracing experiments) with the ROI manager, or stereology was used (for D1-expressing neurons in M1). For stereology counting, a 150 µm thick rectangle was placed in the center of M1. Neurons at the top and right edges were

discarded from counting, while neurons at the down and left edges were kept. Layers were delimitated using SATB2 staining for layers I and II-III, and CTIP2 labeling to position the layer V.

10. Statistics

Statistical analyses were performed using Prism 9.3.1 (GraphPad Software Inc, USA). Concerning patch clamp analysis, in experiments concerning D1 receptors, Wilcoxon signed rank (WSR) test was used to compare paired data. In this case, for graphs associated to experiments concerning D1 receptors, the black dotted line represents the mean ± standard error to the mean (SEM) of all neurons, and the transparent-colored lines represent individual neurons. In motor learning experiments, to compare intrinsic properties of neurons in more than two groups, Kruskal-Wallis (KW) test followed by Dunn's multiple comparison test were used. In all patch clamp experiments, firing frequency comparisons were made with two-way multiple comparisons analysis of variance (ANOVA) followed by Bonferroni post hoc. In all tests, the level of significance was set at $p < 0.05$. Data are represented as mean ± SEM.

Results

1. Retrograde tracing of midbrain DAergic neurons from M1

The first thing done in this thesis was to map M1-projecting DAergic neurons in midbrain nuclei. To achieve this, the retrograde tracer FG has been injected in the M1 of 3 mice (Fig. 4.1A, B). After two weeks of expression, mice were sacrificed, their brains extracted and cut into 50µm thick sagittal slices, which were processed for TH immunostaining in order to identify DAergic neurons. Pictures were then taken under a confocal microscope, and counting was done on 6 sections containing the midbrain for each brain (*i.e.*, 18 sections in total), from 0.70 mm lateral to bregma to 0.40 mm lateral to bregma. On all the counted neurons, 6.58 ± 0.46% of them were labeled with FG (FG+), and 80 ± 5.92% of the FG+ neurons also expressed TH (FG+/TH+, Fig. 4.1C).

FG+ neurons were mainly found in the VTA, as 44.04 ± 6.70% of them were localized in the VTAR and 23.85 ± 3.86% in the PBP. Nonetheless, 16.54 ± 3.88% and 12.84 ± 5.54% of them were found in the dorsal part of the medial SNc (dSNcM) and the ventral part of the medial SNc (vSNcM), respectively. Few FG+ neurons were found in the PIF and the PNu (Fig. 4.1D). They were equally distributed across the midbrain sections, with a little more of them present at 0.65 mm lateral from bregma (Fig. 4.1E).

FG+/TH+ neurons were principally located in the SNc, especially in the vSNcM as 50.34 ± 2.17% of them were reported in this area, and 8.80 ± 4.54% of them were located in the dSNcM. The VTA also contains a non-negligible amount of FG+/TH+ neurons, as 22.80 ± 3.72% were located in the VTAR and 11.51 ± 1.07% in the PBP. Few of these neurons were found in the PIF and the PNu (Fig. 4.1D). FG+/TH+ neurons seemed to be localized in more lateral parts of the midbrain, as 40% of them are localized at 0.70 mm lateral from bregma, and their number decreases while getting closer to the interhemispheric sulcus (Fig. 4.1E, 4.2A). At 0.70 mm lateral from bregma, an average of 62 FG+/TH+ neurons were counted, with a vast majority of 85.23 ± 5.99% of them located in the vSNcM (Fig. 4.2A, B), 9.27 ± 5.91% in the dSNcM and 5.5 ± 1.26% in the VTAR (Fig. 4.2B). At 0.65 mm lateral from bregma, 32 FG+TH+ neurons were counted on average, with 66.58 ± 8.40% of them located in the vSNcM, 20.55 ± 7.90% in the dSNcM and 12.87 ± 2.02% in the VTAR (Fig. 4.2B). At 0.60 mm lateral from bregma, 16 FG+/TH+ neurons were counted on average, with 97.62 ± 2.38% of them located in the VTAR, while the 2.38 ± 2.38% remaining were found in the vSNcM (Fig. 4.2B).

At 0.50 mm lateral from bregma, an average of 17 FG+TH+ neurons were counted. Most of them (53.28 ± 6.19%) were localized in the VTAR. The remaining neurons were found in the PBP and the PNu, 26.35 ± 1.48% and 20.37 ± 7.50%, respectively (Fig. 4.2B). At 0.45 mm lateral from bregma, only 9 neurons were counted on average, with 71.43 ± 1.48% of them located in the PBP, 14.88 ± 11.50% of them located in the PNu, 11.31 ± 6.21% of them located in the VTAR and finally, 2.38 ± 2.38% of them located in the PIF (Fig. 4.2B). At 0.40 mm lateral from bregma, 12 FG+/TH+ neurons were counted on average, and were located in the PBP (62 ± 6.57%) or the PIF (38 ± 6.57%, Fig. 4.2B).

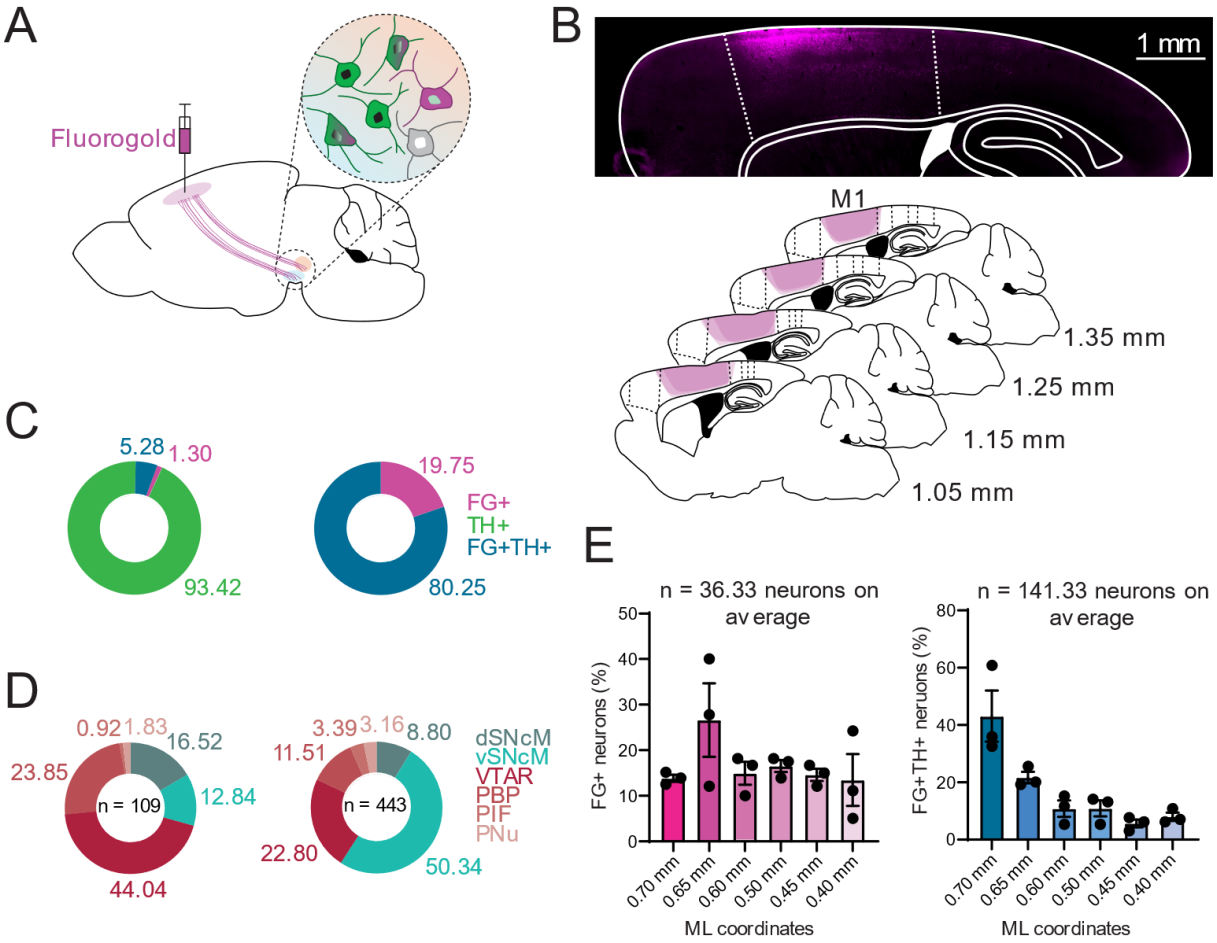

Fig. 4.1: Location of M1-projecting midbrain neurons. A. Experimental design. **B.** Top: picture of a sagittal slice with an injection site at 1.35 mm from bregma, with M1 delineated by dotted lines. Bottom: sagittal slices representing the superimposed fluorogold injections sites of the 3 mice used for this experiment, from 1.05 mm from bregma to 1.35 mm from bregma. **C.** Left: total repartition of counted neurons, *i.e.*, FG+ neurons (magenta), TH+ neurons (green) and FG+TH+ neurons (blue). Right: Repartition of FG+ neurons depending on their expression of TH (*i.e.*, FG+TH- in magenta, FG+TH+ in blue). **D.** Total distribution of FG+ (left) and FG+/TH+ (right) neurons among the different midbrain nuclei. **E.** Repartition of FG+ (left) and FG+/TH+ neurons (right) though the medio-lateral (ML) axis. All data are shown in percentage. dSNcM: dorsal part of the medial SNc, PBP: parabrachial pigmented nucleus, PIF: parainterfascicular nucleus, PNu: paranigral nucleus, vSNcM: ventral part of the medial SNc

Taken together, these results highlight a ventrolateral location of M1-projecting DAergic neurons in mouse midbrain.

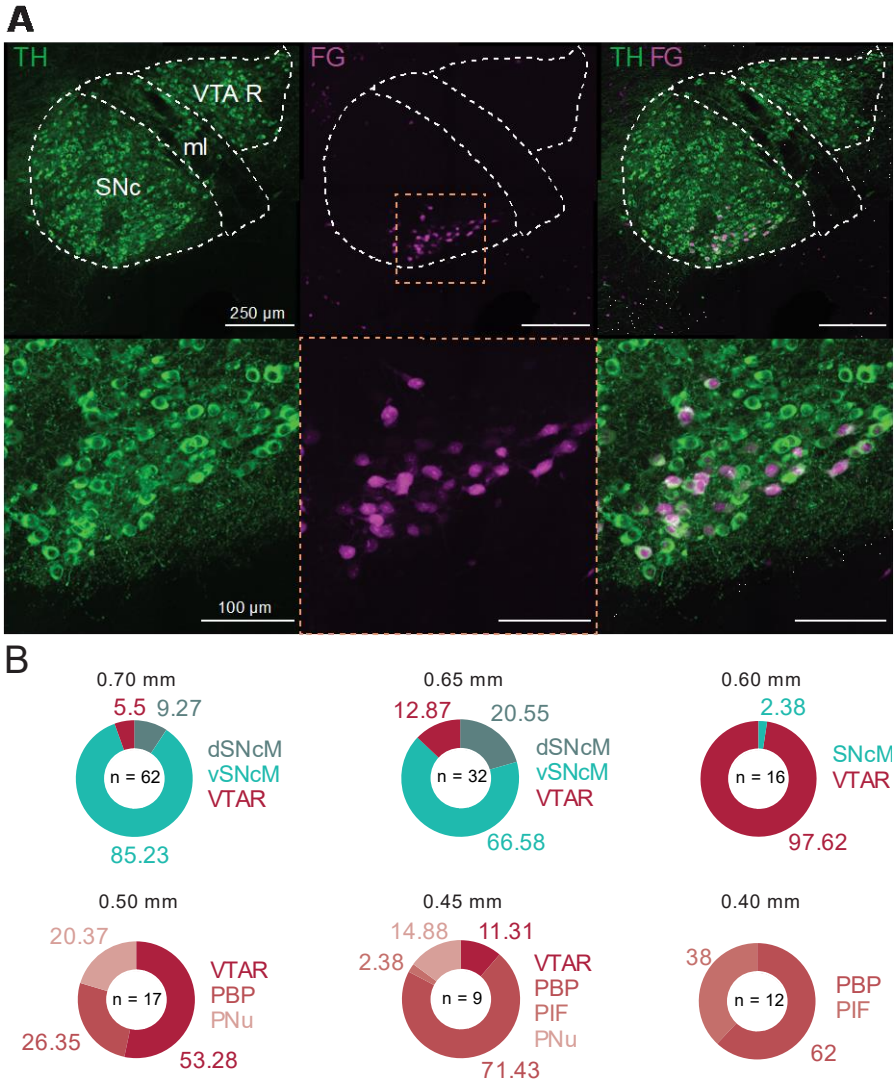

Fig. 4.2: Location of M1-projecting midbrain dopaminergic neurons in subnuclei of the midbrain. A. Maximal projection of confocal images of 50 µm thick sagittal slices at 0.70 mm lateral from bregma. Upper panel images show the different midbrain structures, with FG labeling in magenta and TH immunostaining in green. Lower panel images show a higher magnification of the upper panel images, at the level of the dashed square. **B.** Distribution of FG+/TH+ neurons among the different midbrain nuclei depending on the medio lateral axis. First rows show the distribution from 0.70 to mm 0.60 mm lateral from bregma, and the second rows show the distribution from 0.50 mm to 0.40 mm lateral from bregma. The n is an average over the neurons counted in all the mice used (N = 3). All data are shown in percentage. dSNcM: dorsal part of the medial SNc, PBP: parabrachial pigmented nucleus, PIF: parainterfascicular nucleus, PNu: paranigral nucleus, vSNcM: ventral part of the medial SNc

2. *Ex vivo* electrophysiological characterization of M1-projecting midbrain DAergic neurons

After having identified and localized M1-projecting midbrain DAergic neurons, the next step was to characterize the electrophysiological features of these neurons. To this aim, the

same retrograde tracing approach has been used to label and target these neurons. Mice were then sacrificed, their brains extracted and cut into 300µm acute brain slices. *Ex vivo* whole cell patch clamp recordings have then been performed on these neurons (Fig. 4.3A). Recording pipettes were filled with biocytin to retrieve post-hoc the recorded neurons and to verify the DAergic nature of the neurons with TH immunostaining. All recorded neurons (n = 23) expressed TH (Fig. 4.3B).

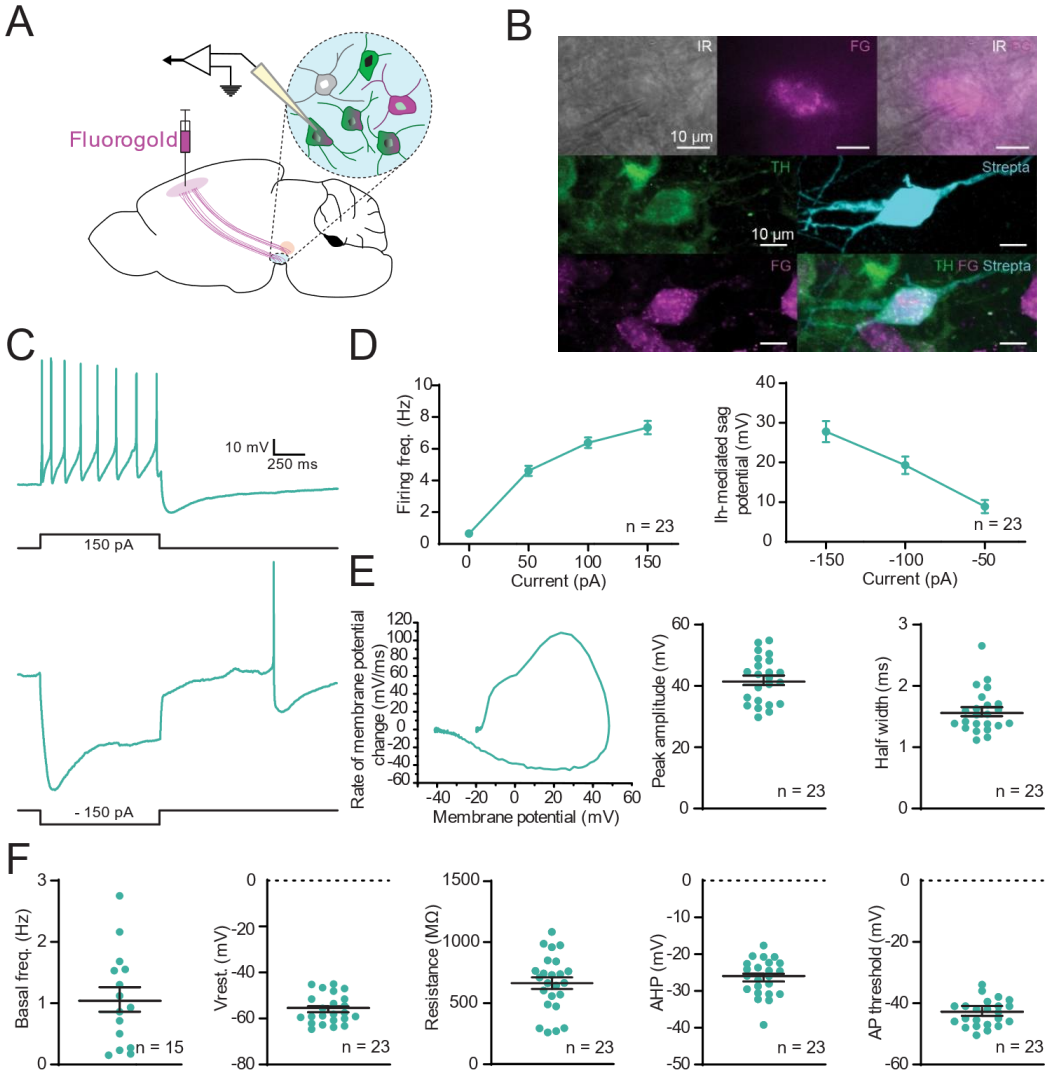

Fig. 4.3: Ex vivo electrophysiological characterization of M1-projecting dopaminergic neurons. A. Experimental design (color code for neurons: magenta = FG+, green = TH+, pink/green = FG+TH+, grey = FG-TH-). **B.** Example of a patched neuron under IR-DIC (upper panel) and colocalization of TH, FG and streptavidin (lower panel) in the recorded neuron. **C.** Example of recordings of a neuron, in response to 150 pA (upper panel) and to -150 pA (lower panel) current injection. Note the broad AP with a two-phased AHP following the inhibitory injected current. **D.** Input/Output curve (left) and Ih-mediated sag potential amplitude (right). **E.** Parameters of the APs of the neurons: phase plot of a typical recorded neuron (left), AP peak amplitude (middle) and AP half width of recorded neurons (right). **F.** Cellular parameters of recorded neurons, *i.e.*, basal frequency (Basal freq.), resting membrane potential (Vrest.), input resistance, after hyperpolarization amplitude (AHP) and AP threshold. n = 23 neurons, N = 6 mice.

The intrinsic properties of these neurons were investigated. Recorded DAergic neurons displayed a high amplitude I_h-mediated sag potential following the injection of inhibitory currents of -150, -100 and -50 pA (Fig. 4.3C, D). These neurons were not able to fire APs when the intensity of stimulations was superior to 150 pA. Indeed, for these stimulations, depolarization blocks were observed, and no more than 8 APs were evoked by the maximal intensity stimulation (Fig. 4.3C, D). The APs of these neurons have a peak amplitude of ~40 mV and a half width of ~1.5 ms (Fig. 4.3E). The AP threshold in these neurons was about 42 mV, and the APs were followed by a large AHP of 25 mV in average composed of a first fast component and followed by a second slow one (Fig. 4.3F, the two-phased AHP is observable on Fig. 4.3C). All recorded neurons displayed spontaneous activity ranging from 0.1 Hz to 3 Hz (Fig. 4.3F). Recorded neurons displayed a resting potential of 55 mV in average, and an input resistance of around 650 MΩ (Fig. 4.3F).

These results enabled to characterize in mice the intrinsic properties of M1-projecting midbrain DAergic neurons, which are reminiscent of those of in mesostriatal neurons, as described in the literature.

3. Evolution of the intrinsic properties of M1-projecting midbrain DAergic neurons during motor learning

Because DA in M1 is instrumental for motor skill learning, the hypothesis of this part was that the intrinsic properties of the midbrain DAergic neurons projecting to M1 may change during motor skill learning. To assess the changes in excitability underwent by M1-projecting midbrain DAergic neurons, *ex vivo* electrophysiological recordings of these neurons were made at different times in the learning process (Fig. 4.4A). The mice were trained for 8 consecutive days to the SPRT (Fig.4.4A). Learning curves were made for each mouse, enabling the segregation of two groups of mice: the successful acquisition group and the unsuccessful acquisition group (Fig. 4.4C). Kinematic analyses were made on learner mice to observe the refinement of their movement after the training (Fig. 4.4D). *Ex vivo* electrophysiological recordings took place at different times of the learning (2, 5 or 8 days of training) to investigate the evolution of electrophysiological properties of M1-projecting midbrain DAergic neurons during the learning processes, in learner mice only (Fig. 4.4C, 4.5A). Again, recording pipettes were filled with biocytin to enable post-hoc labeling of recorded neurons and verify their expression of TH.

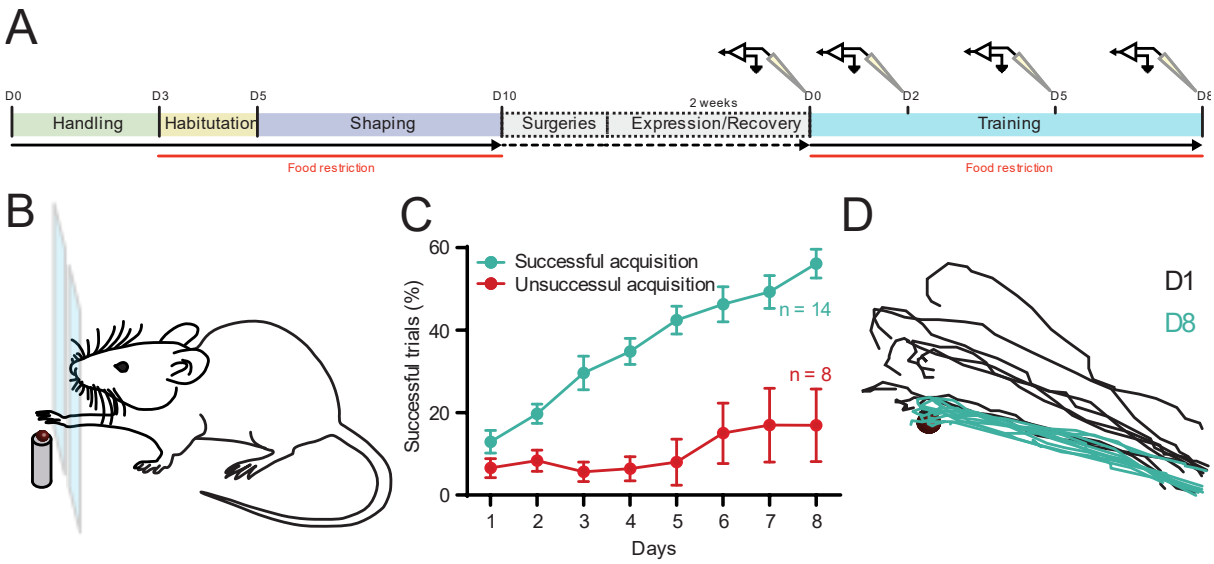

Fig. 4.4: Modelization of motor skill learning in mice. A. Timeline of the experiment **B.** Schematic representation of the single pellet reaching task. **C.** Learning curves representing the success rate over days of training. The green curve represents mice successfully learning the task, the red curve represents mice unable to efficiently learn the task. **D.** Superimposed kinematics of 8 movement trajectories of the paw of a learner mouse after 1 day (black) and 8 days (green) of training.

Recorded neurons presented the same features as the ones described before in untrained and unshaped mice: broad APs, I_h-mediated sag potentials and two-phased AHP (Fig. 4.3). The intrinsic properties of these neurons were compared across the different times of learning (*i.e.*, day 0 vs. day 2 vs. day 5 vs. day 8, Fig. 4.5B). Recorded neurons fired more APs after 5 days of training compared to after 8 days of training, in response to 100 pA (Fig. 4.5B, two-way repeated measures ANOVA, $F_{(3,30)} = 312.4$, $p < 0.05$, n = 11) and 150 pA stimulations (Fig. 4.5B, C, two-way repeated measures ANOVA, $F_{(3,30)} = 312.4$, $p < 0.0001$, n = 11). Moreover, FG-labeled neurons fired more APs after 5 days of training compared to after 2 days of training, in response to a 150 pA stimulation (Fig 4.5B, C, two-way repeated measures ANOVA, $F_{(3,30)} = 312.4$, $p < 0.01$, n = 10). No significant differences were found concerning the other intrinsic properties, *i.e.*, the AP threshold, the basal frequency (Fig. 4.5D), the resting membrane potential (Vrest.), the input resistance, the I_h-mediated sag potential (Fig. 4.5E), the AHP, the AP peak amplitude and half width (Fig. 4.5F, D, KW, $p > 0.05$).

Overall, these results suggest that the excitability of M1-projecting midbrain DAergic neurons in mice is increased during motor skill learning, but not anymore after successful acquisition of the motor task.

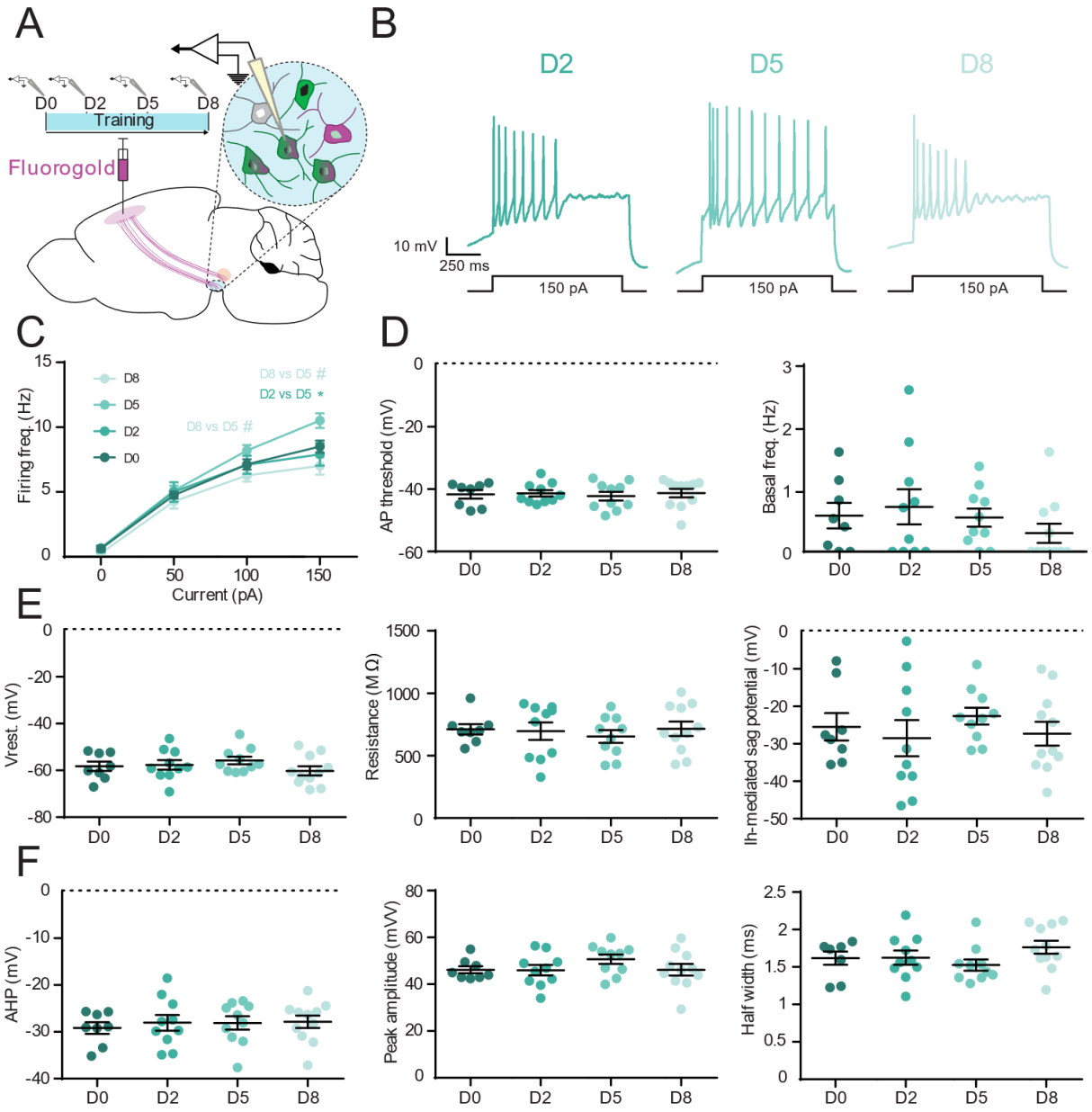

Fig. 4.5: Evolution of the activity of M1-projecting dopaminergic neurons during motor skill learning. A. Experimental design. **B.** Example of recordings of neurons in response to 150 pA current injection, after 2 days (left), 5 days (middle) and 8 days (right) of training. **C.** Input/output curve at different times of motor learning, *# $p < 0.05$ (two-way repeated measures ANOVA). **D.** AP threshold (left) and basal frequency (basal freq.) measurements at different times of motor learning (Kruskal-Wallis test (KW)). **E.** From left to right: Resting membrane potential (Vrest.), input resistance and Ih-mediated sag potential evolutions at different times of motor skill learning. The sag potentials were elicited by a -150 pA current. **F.** From left to right: after hyperpolarization (AHP), peak amplitude and halfwidth evolutions of the APs at different times of motor learning (KW).

Release of DA in M1

After having identified and characterized the M1-projecting DAergic neurons, the next step was to highlight and describe the endogenous release of DA in M1. To visualize the release

of DA in M1, the novel genetically encoded fluorescent sensor $GRAB_{DA1m}$ was used (Fig.4.6A). This sensor is a modified D2 receptor in which the circular permutated enhanced GFP has been inserted in its third intracellular loop (Fig. 4.6A). When DA binds to this sensor, it induces a conformational change of the proteins M13 and calmodulin linked to the circular permutated enhanced GFP, leading to a fluorescence intensity increase (Fig. 4.6A).

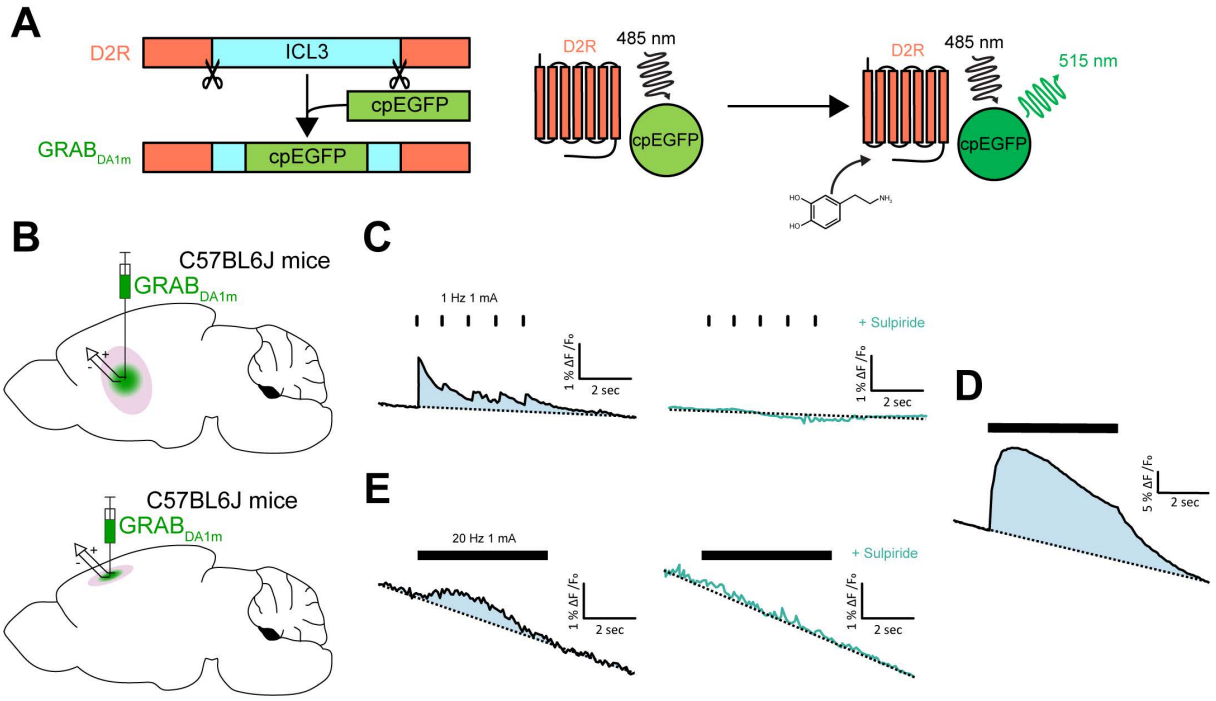

Fig. 4.6: Imaging dopamine release in M1 *ex vivo* using epifluorescence. A. Design of the GRAB sensor used. Left: schematic diagram of the insertion of the circular permutated enhanced GFP in the 3rd intracellular loop of D2 receptor. Right: operating mode of the DAergic sensor. The binding of dopamine to the D2 receptor induces a conformational change of the proteins linked to the circular permutated enhanced GFP, leading to the emission of green light at 515 nm following the excitation at 485 nm. **B.** Experimental design for striatum (top) and M1 (bottom) experiments. **C.** Variation of fluorescence in the striatum following an electrical stimulation in the striatum at 1 Hz frequency and 1 mA intensity in control condition (right) or with dopamine D2 receptor antagonist sulpiride (left). n = 2. **D.** Variation of fluorescence in the striatum following an electrical stimulation in the striatum at 20 Hz frequency and 1 mA intensity. **E.** Variation of fluorescence in M1 following an electrical stimulation in M1 at 20 Hz frequency and 1 mA intensity in control condition (right) or with dopamine D2 receptor antagonist sulpiride (left). n = 6. N = 2 mice.

Firstly, the efficacy of $GRAB_{DA1m}$ was tested *ex vivo*. To achieve this, injections of the sensor were carried out in the striatum, a structure largely innervated by DAergic fibers. After a minimum of 6 weeks of expression, the mice were sacrificed, their brains extracted and cut into acute brain 300 µm thick slices to make *ex vivo* imaging experiments using an epifluorescence microscope. An electrical stimulation in the striatum was used to elicit the release of neurotransmitters in this area, including DA (Fig. 4.6B). In the striatum, the electrical stimulation elicited a high increase of the fluorescence, at 1 mA intensity, 1 Hz frequency with

1 ms stimulation duration of each pulse (Fig. 4.6C, n = 2), as well as at 1mA intensity, 20 Hz frequency with 1 ms stimulation duration of each pulse (Fig. 4.6D, n = 2, N = 2 mice). This effect was not observable anymore with the bath application of the D2 receptor DAergic antagonist sulpiride (Fig. 4.6C, n = 2, N = 2 mice). All stimulations lasted 5 seconds.

After validating the functionality of $GRAB_{DA1m}$ in *ex vivo* imaging experiments, imaging in M1 took place, while stimulating electrically the terminals in M1 (Fig. 4.6E). An electrical stimulation of 1mA intensity, 20 Hz frequency with 1 ms stimulation duration of each pulse lasting for 5 seconds elicited a slight fluorescent increase of 0.5% $\Delta F/F_0$, which was not observable anymore with the bath application of D2 DA antagonist sulpiride (Fig. 4.6E, n = 6, N = 2 mice).

These experiments demonstrated that there is a slight release of DA in M1.

4. Recording of the activity of M1 layer V PNs following the stimulation of DAergic terminals in M1

4.1. In DAT-Cre-Ai32 mice

After studying DA release in M1, the next step was to investigate the impact of the release of DA on the intrinsic properties of M1 neurons. For this aim, PNs were recorded as they can express both D1 and D2 receptors (Cousineau et al., 2020; Swanson et al., 2020; Vitrac

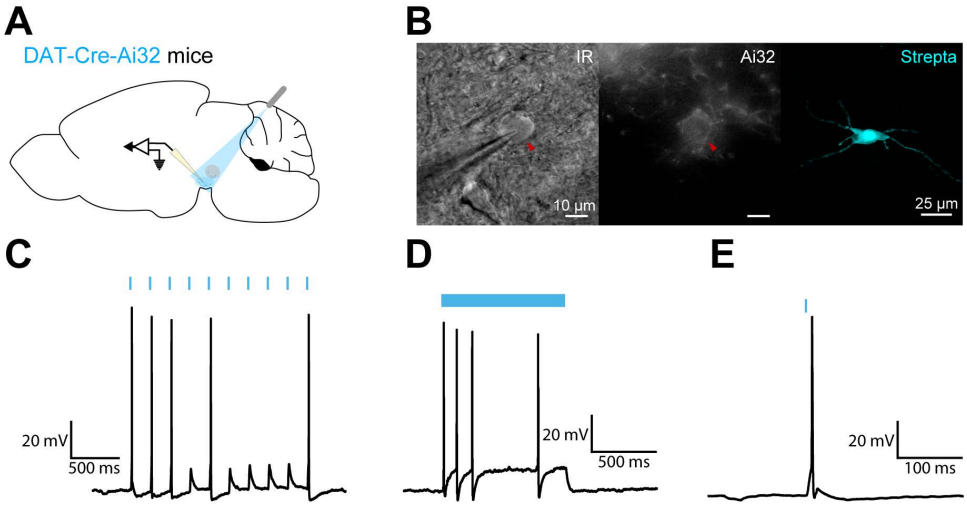

Fig. 4.7: Manipulation of the activity of dopaminergic neurons in the midbrain following a light stimulation in DAT-Cre-Ai32 mice. A. Experimental design. **B.** Example of a patched neuron under IR-DIC (left) with the opsin expression in green (middle) and revealed post hoc with streptavidin (right). **C.** Light reliability induced APs in a recorded neuron following a 5 Hz train stimulation of 1 ms duration each. **D.** APs elicited by a flash of light of 1 s. **E.** AP recorded following a single flash of 1 ms. n = 14 neurons, N = 4 mice. λ = 491 nm.

et al., 2014). PNs were recorded in the layer V as it is the layer displaying most of DAergic terminals in M1. DAT-Cre-Ai32 mice were used as they already express an excitatory opsin in DAergic neurons, thus enabling the activation of DAergic terminals in M1 with an optical fiber.

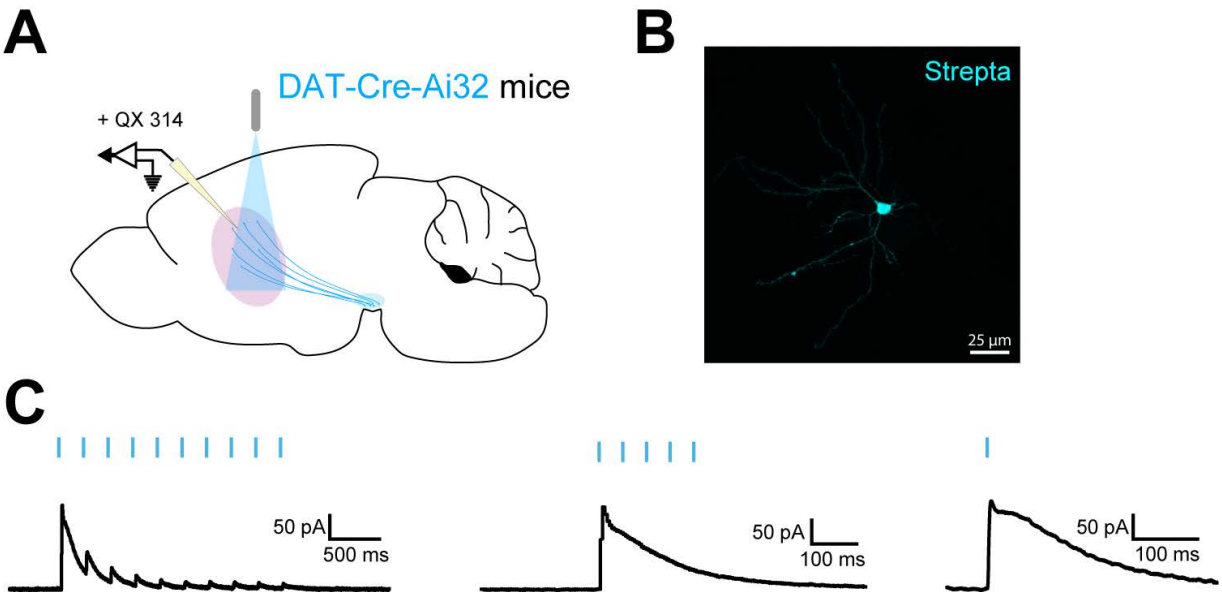

Fig. 4.8: Currents elicited by the light stimulation of dopaminergic terminals in a striatal medium spiny neuron in DAT-Cre-Ai32 mouse. A. Experimental design. **B.** The recorded neuron revealed post hoc with streptavidin. **C.** From left to right: evoked currents recorded following a 5 Hz train light stimulation of 1 ms duration each, a 20 Hz train stimulation of 1 ms duration each and a single photostimulation of 1ms. All recordings were made with a membrane potential clamped at -13 mV. n = 1. λ = 491 nm.

The first thing done was to test the validity of the DAT-Cre-Ai32 model. For this, two experiments were done. The first one was to record *ex vivo* DAergic neurons in the midbrain and to stimulate them with an optic fiber to see if light can elicit APs in these neurons (Fig. 4.7A, B). A continuous light stimulation induced a long-lasting depolarization of recorded neurons typical of channelrhodopsin currents (Fig. 4.7D, n = 14). Furthermore, a single light stimulation of 1 ms duration was sufficient to trigger an AP (Fig. 4.7E), and a train stimulation of 5 Hz with 1 ms duration each stimulation triggered several APs (Fig. 4.7C).

The second experiment was to verify that manipulating these DAergic neurons can elicit synaptic responses in the striatum, which is richly innervated by DAergic fibers. For this, the optic fiber was placed above the striatum (Fig. 4.8A), and a MSN was intracellularly recorded (Fig. 4.8B) in voltage clamp configuration in presence of QX-314 in the recording pipette to block voltage-gated sodium channels, and therefore AP generation. In the first recorded neuron, light stimulations induced a large inhibitory current, either after a single stimulation of 1 ms or

trains of stimulation at 5 Hz or 20 Hz frequency with 1 ms duration of each pulse (Fig. 4.8C, n = 1), confirming the inhibition of striatal MSNs by γ-aminobutyric acid (GABA) release by DAergic terminals (Tritsch et al., 2012).

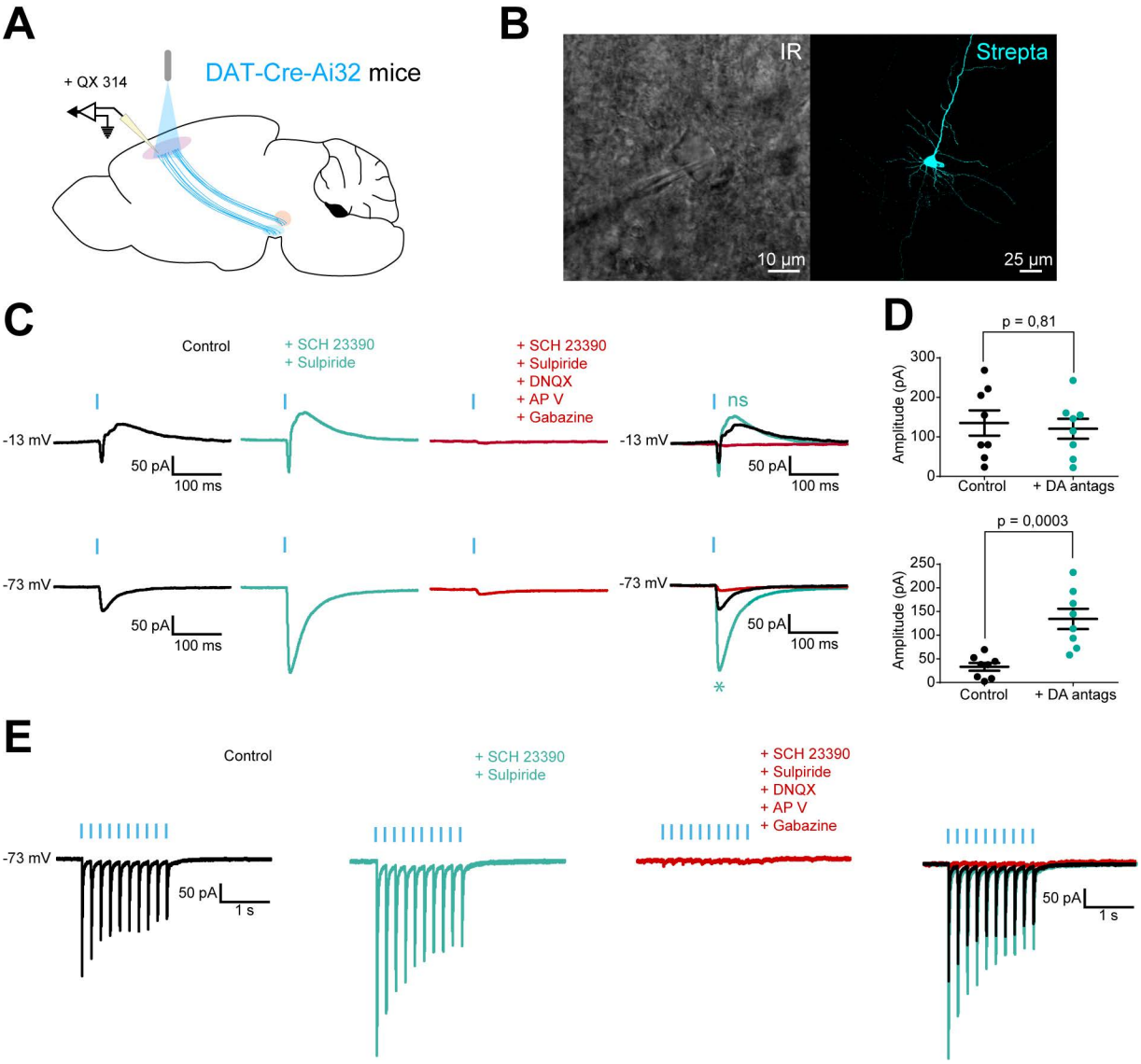

Fig. 4.9: Currents elicited by the light stimulation of dopaminergic terminals in M1 pyramidal neurons in DAT-Cre-Ai32 mice. A. Experimental design. **B.** Example of a patched neuron under IR-DIC (left) and revealed post hoc with streptavidin (right). **C.** Upper panel, from left to right: evoked currents recorded at -13 mV following a single photostimulation of 1 ms in control conditions, with D1 and D2 receptors antagonists SCH 23390 and sulpiride, with dopamine D1 and D2 receptors antagonists and fast synaptic glutamatergic and GABAergic blockers DNQX, AP V and gabazine, superimposition of all conditions. Lower panel: same as upper panel, but with the membrane potential clamped at -73 mV. **D.** Quantification of the amplitude of the currents recorded at -13 mV (top) and -73 mV (bottom), in control conditions or with DA antagonists. **E.** From left to right: evoked currents recorded at -73 mV following a 5 Hz train stimulation of 1 ms duration each in control conditions, with D1 and D2 receptors antagonists and fast synaptic transmission blockers DNQX, AP V and gabazine, trace superimposition of all conditions. n = 8 neurons, N = 3 mice. * $p < 0.05$, ns = non-significant (WSR). $\lambda = 491$ nm.

After the DAT-Cre-Ai32 model was validated, recordings in M1 took place while stimulating DAergic terminals in M1 (Fig. 4.9A). Recordings were made on M1 layer V PNs (Fig. 4.9B), also with QX-314 to block voltage-gated sodium channels, to record only the currents evoked by the light stimulation and not AP-related currents. When the membrane potential was clamped at -73 mV, a light flash of 1 ms evoked an EPSC in PNs (Fig. 4.9C, n = 8). When the membrane potential was clamped at -13 mV, the recordings revealed also an inhibitory postsynaptic current (IPSC) induced by the 1 ms light stimulation (Fig. 4.9C, n = 8). The amplitude of the EPSCs was exacerbated by the bath application of DAergic antagonists (Fig. 4.9D, WSR, $p < 0.05$, n = 8), but not the amplitude of IPSCs (WSR, $p > 0.05$, n = 8). These responses were abolished when fast synaptic transmission blockers were bath applied (Fig. 4.9C, n = 8). Similar results were obtained following a light train stimulation at 5 Hz with 1 ms duration for each stimulation (Fig. 4.9E, n = 8). It should be noted that these results were obtained in only 3 mice from the same litter.

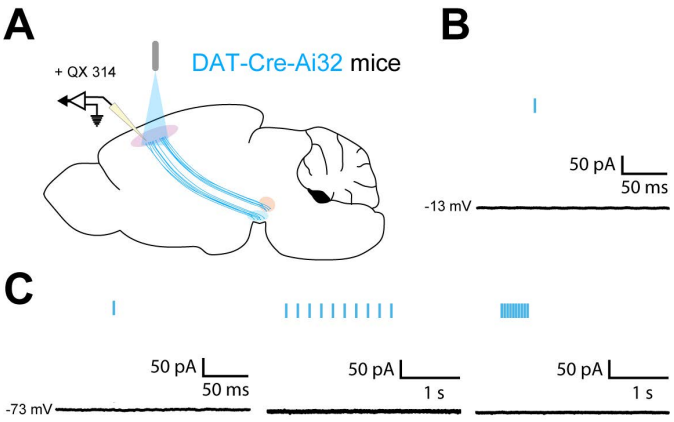

Fig. 4.10: Currents elicited by the light stimulation of dopaminergic terminals in M1 pyramidal neurons in the majority of DAT-Cre-Ai32 mice. A. Experimental design. **B.** Evoked current recorded in a M1 PN clamped at -13 mV following a 1 ms photostimulation **C.** From left to right: recording of a PN following a single stimulation of 1 ms, a 5 Hz train stimulation of 1 ms duration each, a 20 Hz train stimulation of 1 ms duration each with the membrane potential clamped at -73 mV. n = 55 neurons, N = 15 mice. λ = 491 nm.

In 15 mice from another different litters, no currents were elicited following light stimulations (Fig. 4.10A), neither inhibitory currents (Fig. 4.10B, n = 55) nor excitatory currents (Fig. 4.10C, n = 55). Single pulses of 1 ms and 10 ms were tested, as well as 5Hz and 20 Hz train stimulations of 1 ms duration each pulse.

4.2. In DAT-Cre mice

Next step was to clear up the results obtained with the DAT-Cre-Ai32 mice. As experiments were conclusive for only few mice of the same litter, the validity of the model was tackled. For this aim, DAT-Cre mice were used, in which an AAV containing a DIO-ChR2 was

injected in the SNc and the in VTA. The DIO enabled the selective expression of the opsin in Cre-expressing neurons only, *i.e.*, DAT-expressing neurons in this case.

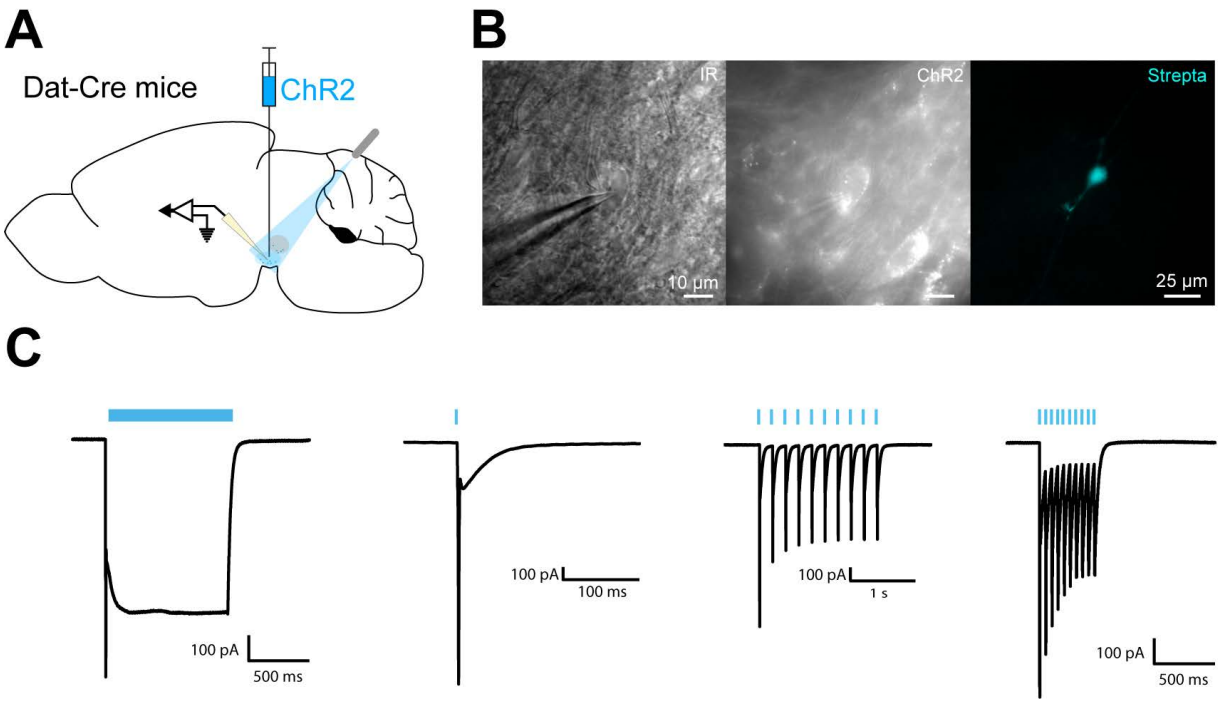

Fig. 4.11: Currents elicited by the light stimulation in the midbrain of DAT-Cre mice. A. Experimental design, injection of the following construct containing the ChR2 in M1: AAV2.5-EF1a-DIO-hChR2(H134R)-EYFP.WPRE.hGH. **B**. Example of a patched neuron under IR-DIC (left), with the opsin fluorescence (middle) and revealed post hoc with streptavidin (right). **C.** From left to right: currents elicited by a continuous blue light stimulation of 1 s duration, by a single light stimulation of 1 ms, by a train stimulation at 5 Hz of 1 ms duration each pulse, or by a train stimulation at 20 Hz of 1 ms duration each pulse. All recordings were made with a membrane potential clamped at -73 mV. n = 5 neurons, N = 4 mice. λ = 491 nm.

To validate this new model and to be sure that the conditions were the same with this model and with the DAT-Cre-Ai32 model, the same control experiments as previously described were done in this new model. First, the good expression of the opsin was verified, and midbrain neurons were recorded while applying the light stimulation (Fig. 4.11A, B). An inward current (typical of a ChR2 current) was elicited by a light stimulation of 1 ms duration, with one single pulse of 1 ms or trains of stimulation at 5 Hz or 20 Hz with 1 ms duration for each pulse (Fig. 4.11C). The second experiment was to make a control recording in the striatum while stimulating DAergic terminals in this area (Fig. 4.12A). In the first neuron recorded (Fig. 4.12B), a single light stimulation of 1 ms elicited IPSCs (Fig. 4.12C, n = 1) as well as light train stimulation at 5 Hz or 20 Hz for 1 ms duration of each stimulation (Fig. 4.12C, n = 1), as it has been previously reported (Tritsch et al., 2012).

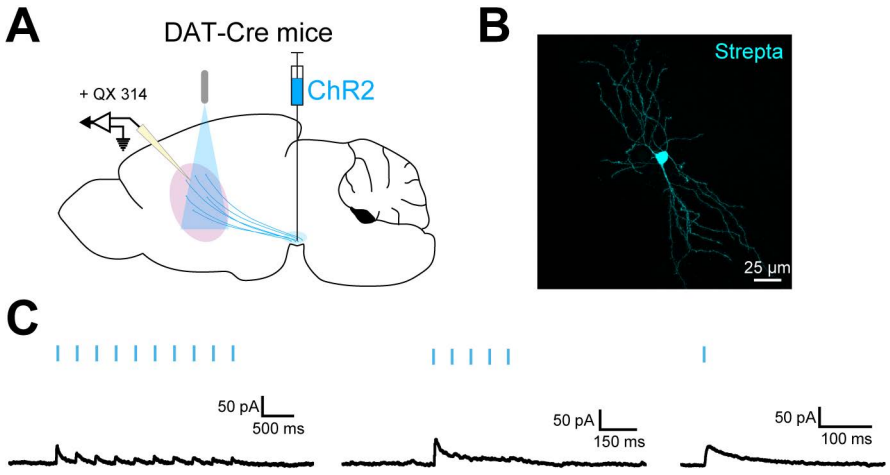

Fig. 4.12: Currents elicited by the light stimulation of dopaminergic terminals in a striatal medium spiny neuron in DAT-Cre mouse. A. Experimental design. **B.** The recorded neuron revealed post-hoc with streptavidin. **C.** Evoked current recorded following a 5 Hz train stimulation of 1 ms duration each (left), a 20 Hz train stimulation of 1 ms duration each (middle) and a single stimulation of 1ms (right). All recordings were made with a membrane potential clamped at -13 mV. n = 1. λ = 491 nm.

After the control experiments, it was clear that the conditions between DAT-Cre-Ai32 and ChR2-injected DAT-Cre mice were similar, concerning the opsin expression and the functional connectivity to the striatum. Hence, recordings in M1 took place (Fig. 4.13A). Recordings were made on M1 layer V PNs (Fig. 4.13B) with QX-314 to block voltage-gated sodium channels, to avoid the recording of APs-related currents. Light stimulations did not elicit any EPSCs (Fig. 4.13C) nor IPSCs (Fig. 4.13D) in M1 PNs. As for DAT-Cre-Ai32 mice, single pulses of 1 ms and 10 ms were tested, as well as 5Hz and 20 Hz train stimulations of 1 ms duration each pulse.

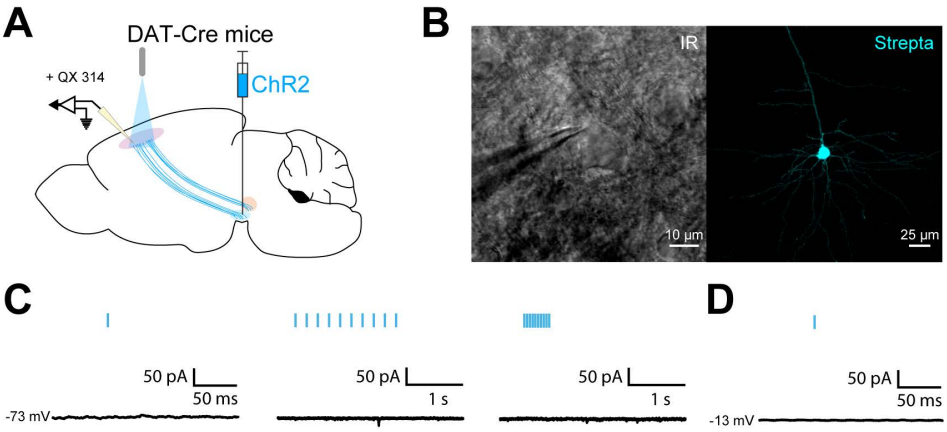

Fig. 4.13: Currents evoked by the light stimulation of dopaminergic terminals in M1 pyramidal neurons in DAT-Cre mice. A. Experimental design. **B.** Example of a recorded neuron under IR-DIC (left) and revealed post hoc using streptavidin (right). **C.** Evoked current recorded in a PN following a single stimulation of 1 ms (left), a 5 Hz train stimulation of 1 ms duration each (middle) and a 20 Hz train stimulation of 1 ms duration each (right), with the membrane potential clamped at -73 mV. **D.** Evoked current recorded in a PN following a 1 ms flash with the membrane potential clamped at -13 mV. n = 15 neurons, N = 3 mice. λ = 491 nm.

5. Mapping of D1 receptors in M1

As previous optogenetic experiments were not conclusive, a new experimental design was used to investigate the functional impact of DA on M1 neurons. As D1 receptors have been less characterized than D2 receptor in M1, the location and impact of D1 receptors were investigated in M1, using immunohistological labeling and pharmacological experiments during patch clamp recordings in D1-GFP mice, respectively. The first thing done in this part of the thesis was to map D1 receptor cells in M1. As differences in the density of D1 expressing cells between young (3 weeks old) and adult (6 weeks old) mice have been reported in the PFC (Leslie et al., 1991), counting has been done in the M1 of young and adult mice. The number of D1-expressing cells was quite similar at young and adult states, as an average of 119 and 109 cells were counted in the M1 of young and adult mice, respectively (n = 3 slices/mouse, N = 3 mice). The location of these D1-expressing cells was also similar in the M1 of young and adult mice. Nonetheless a few more D1-expressing cells were found in the layer II-III compared to other layers in young mice, whereas D1-expressing cells were more equally distributed between layers II-III, V and VI in adult mice. In the M1 of young mice, 26.08 ± 1.62% of D1 receptor-expressing cells were localized in layer VI, 28.89 ± 2.28% in layer V, 44.23 ± 2.22% in layer II/III and less than 1% in layer I (Fig. 4.14A). In adult mice, 29.81 ± 1.32% of cells expressing the D1 receptor were localized in layer VI, 33.81 ± 1.38% in layer V, 35.63 ± 0.99% in layer II/III and less than 1% in layer I (Fig. 4.14B).

As there is a wide diversity of PNs within M1 (cf introduction paragraph 3.3.1, for review, see Callaway et al., 2021), the expression of D1 receptors in different types of PNs was tackled. To achieve this aim, CTIP2 and SATB2 transcription factors were used as molecular markers for subcerebral (PTNs) and callosal (ITNs) projection-neurons in young and adult mice. D1 receptor-expressing neurons were divided in four categories: neurons expressing only D1 receptor, neurons expressing D1 receptor and only CTIP2, neurons expressing D1 receptor and only SATB2 and neurons expressing D1 receptor and both CTIP2 and SATB2 (Fig. 4.15A, B).

Neurons expressing only D1 receptor were mostly localized in layer II-III, either in young and adult mice (Fig. 4.15C, D). In young mice, 17 cells were counted on average (n = 3 slices/mouse, N = 3 mice) and were distributed as following: 17.50 ± 3% in layer VI, 17.85 ± 3.44% in layer V, 58.01 ± 3.57% in layer II-III and 6.64 ± 1.83% in layer I (Fig. 4.15C). In adult mice, 20 cells were counted in average (n = 3 slices/mouse, N = 3 mice) and were

distributed as following: 23.05 ± 5.61% in layer VI, 20.75 ± 3.60% in layer V, 52.09 ± 5.09% in layer II-III and 4.11 ± 1.07% in layer I (Fig. 4.15D).

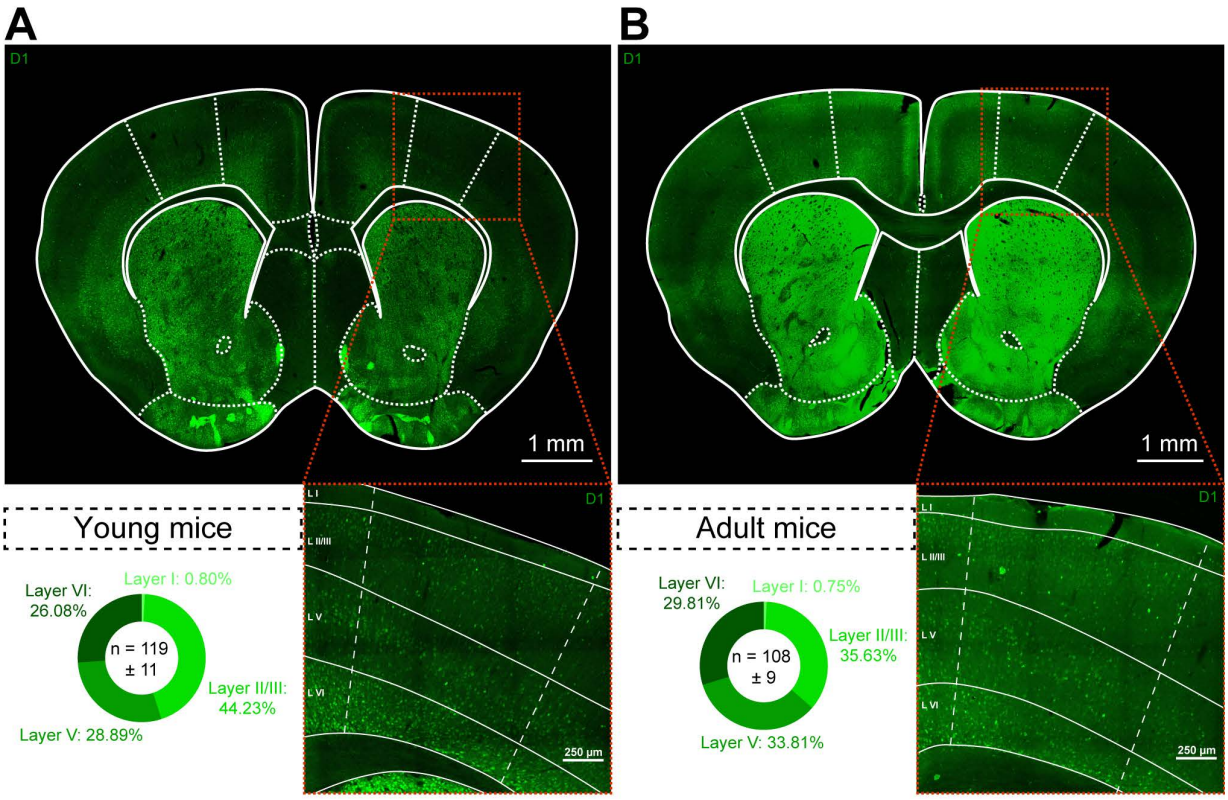

Fig. 4.14: Mapping of D1 receptor-expressing neurons in M1 layers. A. Top: whole slice image of D1-expressing cells in young mouse. Bottom left: repartition of D1 positive cells in M1 layers of young mice. The given n is the average number of counted neurons. For each category, the darker the color, the deeper the layer. Bottom right: example of the labeling obtained for D1 in the M1 of young mice. **B.** Same as A. for adult mice. n = 3 slices/mouse, N = 3 mice.

Few neurons expressing D1 receptor and only CTIP2 were counted, and they were mostly localized in layer VI, either in young or adult mice (Fig. 4.15C, D). An average of 4 cells were counted in young mice (n = 3 slices/mouse, N = 3 mice), and 2 cells in adult mice (n = 3 slices/mouse, N = 3 mice). The repartition of D1 and CTIP2 expressing cells was as follow. In young mice, 13.89 ± 7.38% of D1 and CTIP2 expressing cells were found in layer II-III, 23.51 ± 7.68% in layer V and 62.60 ± 11.73% in layer VI. In adult mice, 14.82 ± 11.26% of D1 and CTIP2 expressing cells were found in layer II-III, 24.07 ± 12.76% in layer V and 61.11 ± 16.20% in layer VI (Fig. 4.15C, D).

Most of the D1 receptor expressing cells coexpressed SATB2, both in young and adult mice. An average of 66 cells were counted in young mice (n = 3 slices/mouse, N = 3 mice), and 50 cells in adult mice (n = 3 slices/mouse, N = 3 mice). These cells were mainly localized in layer II-III, either in young (63.46 ± 3.05%) and adult (58.38 ± 3.95%) mice (Fig. 4.15C, D).

25.03 ± 2.46% and 32.63 ± 2.68% of these cells were found in the layer V of young and adult mice respectively. Finally, 11.51 ± 2.20% and 8.99 ± 3.16% of these D1 and SATB2 expressing cells were found in the layer VI of young and adult mice, respectively (Fig. 4.15C, D).

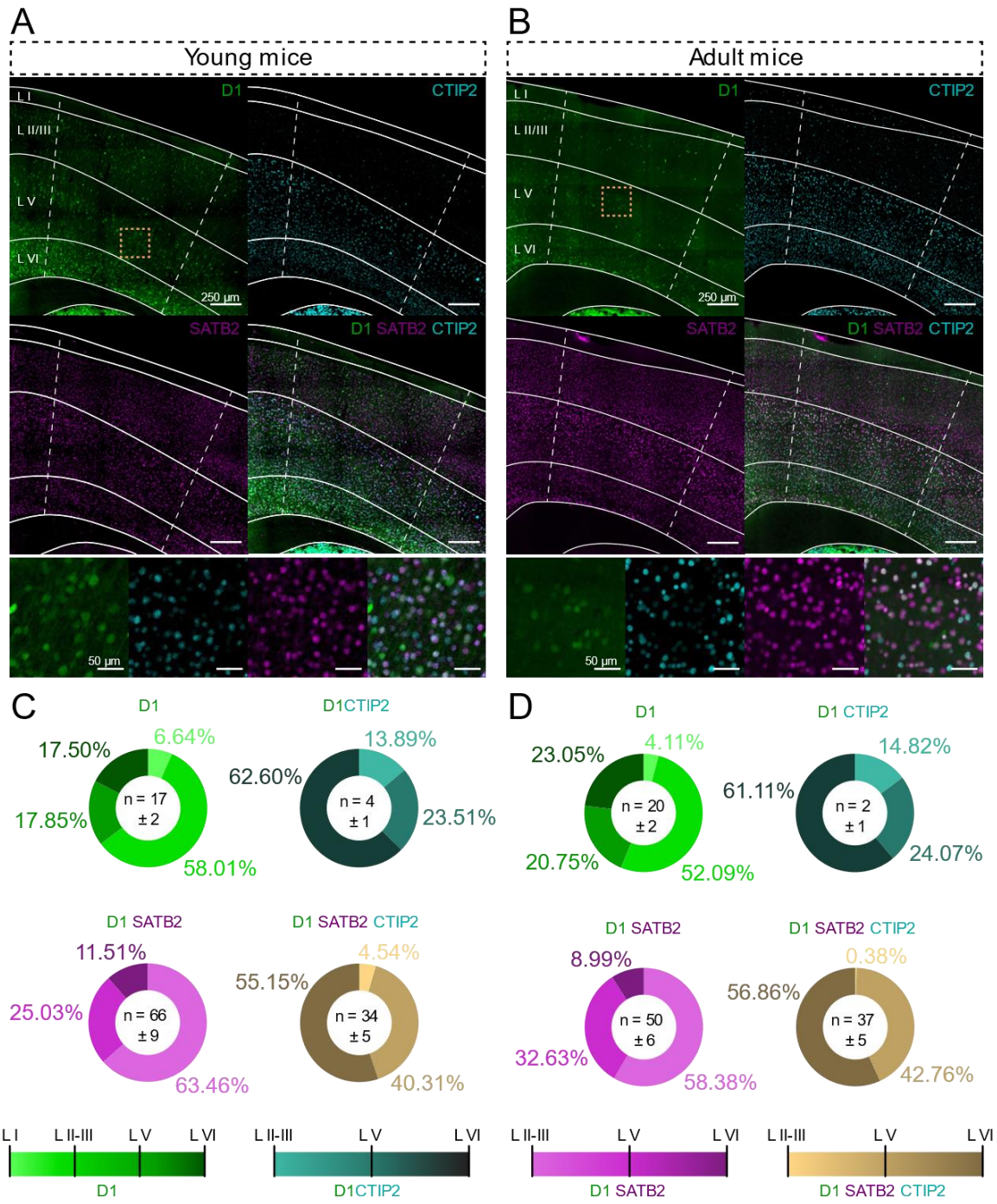

Fig. 4.15: Expression of pyramidal neurons' markers SATB2 and CTIP2 by D1 positive neurons in M1. A. Top: Example of the labeling obtained for D1 (green), CTIP2 (cyan) and SATB2 (magenta) in the M1 of a young mouse. Down: higher magnification of the pictures in the layer V at the level of the dotted square in D1 picture. **B.** Same as A. for adult mice. **C.** Repartition of neurons expressing only D1 (green), neurons expressing only D1 and CTIP2 (blue), neurons expressing only D1 and SATB2 (magenta) and neurons expressing D1 and both CTIP2 and SATB2 (brown) in M1 layers of young mice. The given n are an average of the counted neurons. For each category, the darker the color, the deeper the layer (scales are given at the bottom). **D.** Same as C. for adult mice. n = 3 slices/mouse, N = 3 mice.

At last, neurons expressing D1 and also both CTIP2 and SATB2 have also been reported and counted in this study. They were mainly found in the layer VI of young (55.15 ± 3.66%) and adult (56.86 ± 3.08%) mice (Fig. 4.15C, D, n = 3 slices/mouse, N = 3 mice either young or adult). Few of them were counted in layer II-III, with only 4.54 ± 1.43% and 0.38 ± 0.38% of them reported in the layer II-III of young and adult mice, respectively. The remaining of these cells were found in layer V, with 40.31 ± 3.40% of them in the layer V of young mice and 42.76 ± 3.08% of them in the layer V of adult mice (Fig. 4.15C, D).

Taken together, these results suggest that the location of D1 receptors in the mouse brain is similar at young and adult states.

6. Impact of activation and blockade of D1 receptors on D1-expressing M1 layer V PNs' intrinsic properties

The mapping of D1 receptors in M1 done, the next step was to characterize the effect of D1 receptors on M1 PNs. Layer V is classically considered as an output layer involved in the top-down control of other brain areas. One of its features is the diversity of PNs that

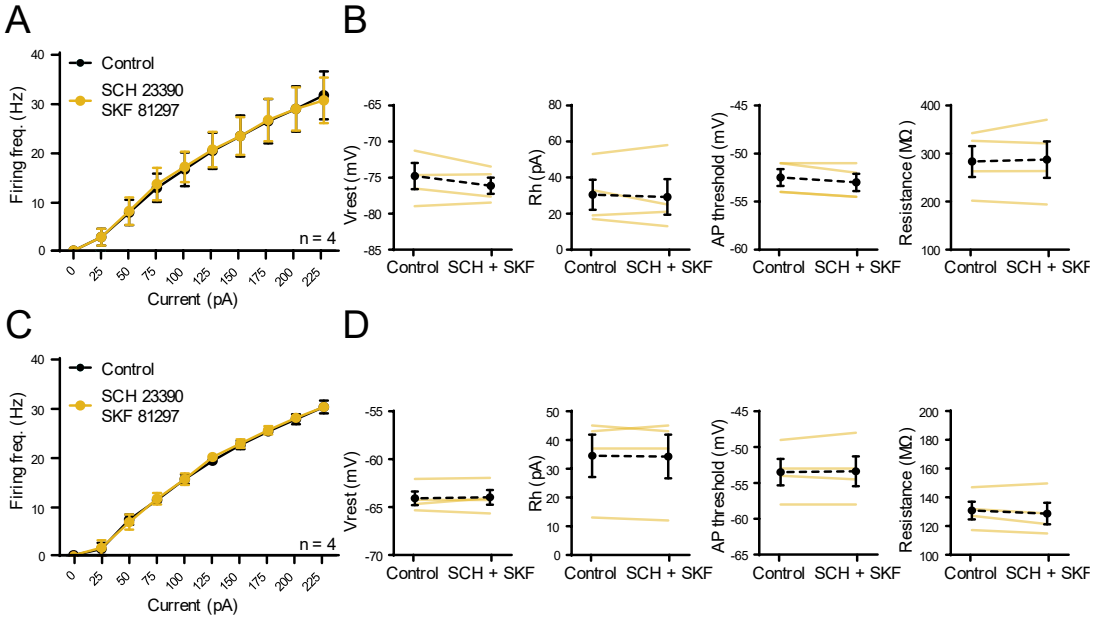

Fig. 4.16: Effect of the co-application of D1 agonist SKF 81297 and D1 antagonist SCH 23390 on M1 pyramidal cells' excitability. A. Input/output curve in young mice, n = 4. **B.** Cell parameters in young mice, from left to right: resting membrane potential, rheobase, AP threshold and input resistance. n = 4. **C.** Input/output curve in adult mice, n = 4. **D.** Cell parameters in adult mice, from left to right: resting membrane potential, rheobase, AP threshold and input resistance. n = 4.

composes this layer, which send information to other cortical and sub-cortical structures (Harris and Shepherd, 2015). As DAergic fibers largely innervate this layer (Vitrac et al., 2014), the

modulation exerted by D1 receptors was specifically studied in this layer V in young and adult mice. D1-GFP mice were also used in this part, enabling the identification and the targeting of D1-expressing neurons. These mice were sacrificed, their brains extracted and cut into acute brain 300µm thick slices. *Ex vivo* patch clamp recordings of the intrinsic properties of PNs were made in presence of the synaptic blockers DNQX (50 µM), AP V (20 µM) and GABAzine (10 µM), to be sure that the effects observed were not due to a network effect (*i.e.*, a di- or polysynaptic effect).

6.1. <u>D1 receptor inhibition</u>

First, the effect of D1 receptor blockade on PNs intrinsic properties in M1 layer V has been assessed in young mice. D1 receptors were blocked by perfusing 1 µM of D1 receptor antagonist SCH 23390 in the recording chamber 20 minutes prior to recordings (Fig. 4.17A).

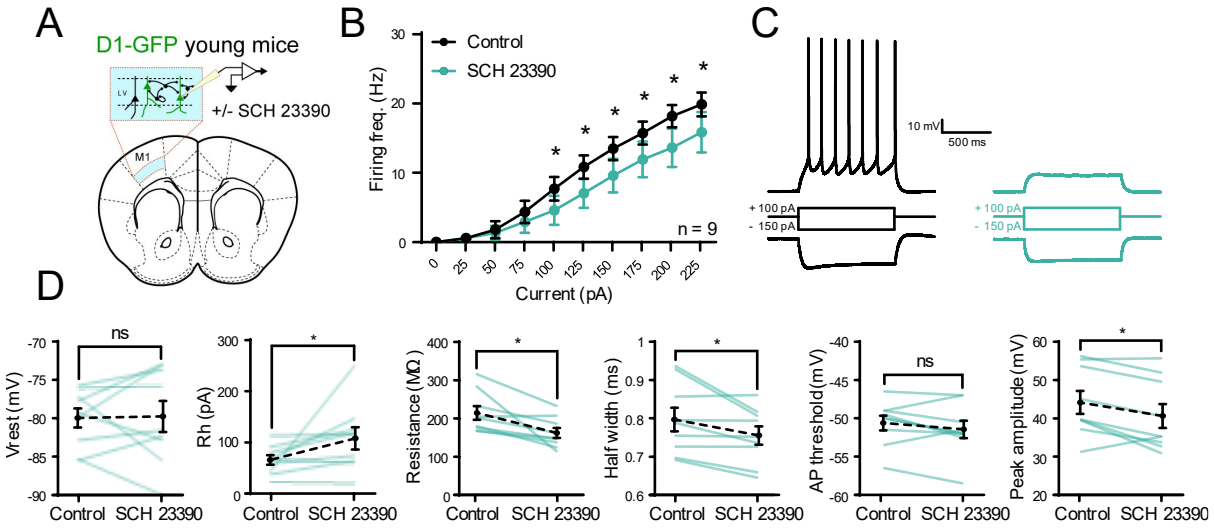

Fig. 4.17: Effect of D1 receptor antagonist SCH 23390 on M1 pyramidal cells' properties in young mice. A. Experimental design. **B.** Input/output curve. n = 9. * $p < 0.05$ (two-way repeated measures ANOVA). **C.** Example traces of a recorded neuron in control condition (right) and with SCH 23390 (left). **D.** Cell parameters, from left to right: resting membrane potential, rheobase, input resistance, AP half width, AP threshold and AP peak amplitude. n = 9. * $p < 0.05$, ns = non-significant (WSR).

In young mice, bath application the D1 antagonist changed the intrinsic properties of the PNs recorded. Many parameters were measured. From a stimulation intensity of 100 pA, PNs fired less APs in response to somatic injection of depolarizing currents in presence of SCH 23390 compared to control conditions (Fig. 4.17B, two-way repeated measures ANOVA, $F_{(9, 72)} = 48.58$, $p < 0.0001$, n = 9), as illustrated by the recorded traces and by the frequency/current input-output curve (Fig. 4.17C). Furthermore, the rheobase of these neurons was significantly higher with SCH 23390 compared to control conditions (WSR, $p < 0.05$, n = 9), and the input

resistance, the AP half width and peak amplitude were significantly lower with SCH 23390 compared to control conditions (Fig. 4.17D, WSR, $p < 0.05$, n = 9). No significant differences were observed concerning the resting membrane potential and the AP threshold between SCH 23390 and control conditions (Fig. 4.17D, WSR, $p > 0.05$, n = 9). The significant effects observed were due to the blocking of D1 receptors as the recordings obtained when D1 receptors agonist SKF 81297 and antagonist SCH 23390 were simultaneously perfused in the bath were similar to the control condition in young mice (Fig. 4.16 A, n = 4).

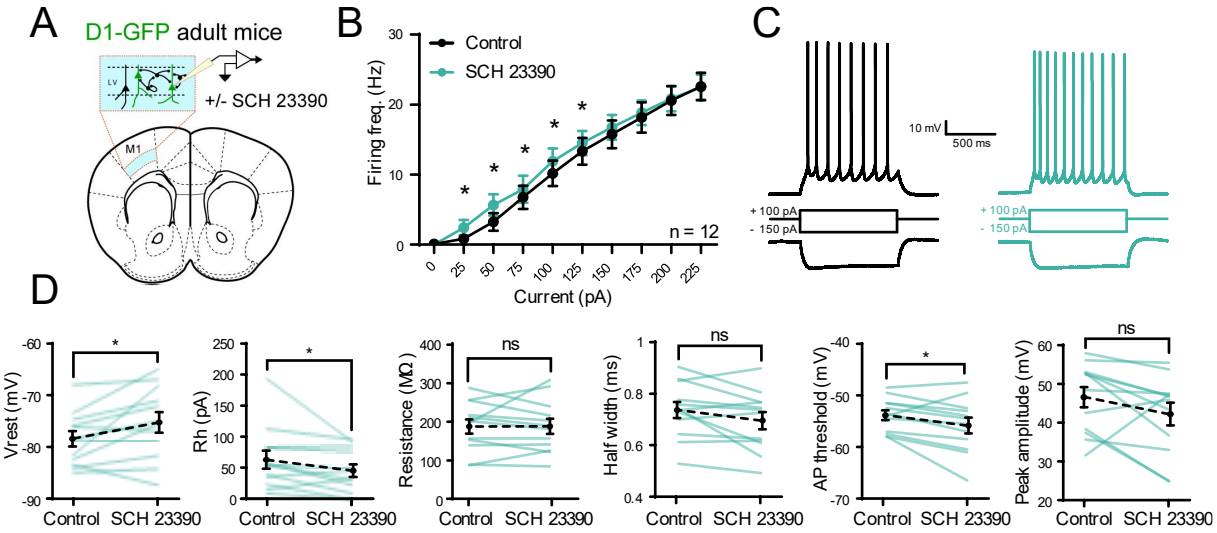

Fig. 4.18: Effect of D1 receptor antagonist SCH 23390 on M1 pyramidal cells' properties in adult mice. A. Experimental design. **B.** Input/output curve. n = 12. * $p < 0.05$ (two-way repeated measures ANOVA). **C.** Example traces of a recorded neuron in control condition (right) and with SCH 23390 (left). **D.** Cell parameters, from left to right: resting membrane potential, rheobase, input resistance, AP half width, AP threshold and AP peak amplitude. n = 12. * $p < 0.05$, ns = non-significant (WSR).

Then, the same experiments were performed in adult mice (Fig. 4.18A). Interestingly, M1 layer V PNs fired more APs following low intensity stimulation ranging from 25 pA to 125 pA with 1 µM SCH 23390 than in control conditions (Fig. 4.18B, C, two-way repeated measures ANOVA, $F_{(9, 99)} = 124.4$, $p < 0.0001$, n = 12). Similarly, the resting membrane potential of these neurons was higher in presence of D1 receptor antagonist SCH 23390 compared to control conditions (Fig. 4.18D, WSR, $p < 0.05$, n = 12). Furthermore, the rheobase and the AP threshold of layer V M1 PNs were lowered by the bath application of SCH 23390 (Fig. 4.18D, WSR, $p < 0.05$, n = 12). No significant effects were observed concerning the input resistance, the AP half width and peak amplitude (Fig. 4.18D, WSR, $p > 0.05$, n = 12). The significant effects observed were also due to the blocking of D1 receptors, as same control recordings with bath application of both D1 receptors agonist SKF 81297 and antagonist SCH 23390 were similar to the control condition in adult mice (Fig. 4.16 B, n = 4).

6.2. D1 receptor activation

After D1 receptor blockade experiments, the effect of D1 receptor activation on layer V M1 PNs was assessed. The effect of D1 receptor activation on M1 layer V PNs' excitability was first investigated in young mice, by bath applying the typical D1 receptors agonist SKF 81297 (2.5 mM, Fig. 4.19A). Firstly, PNs fired more APs in response to 25 pA to 175 pA stimulation (Fig. 4.19B, two-way repeated measures ANOVA, $F_{(9, 72)} = 138.5$, $p < 0.0001$, n = 9), as shown in the example traces of a recorded neuron without (left) and with (right) D1 receptor agonist SKF 81297 (Fig. 4.19C). Furthermore, the rheobase, AP threshold, half width and peak amplitude were significantly lower with the application of D1 receptor agonist SKF 81297 compared to control conditions (Fig. 4.19D, WSR, $p < 0.05$, n = 9). No significant effect was observed concerning the resting membrane potential and the input resistance (Fig. 4.19D, WSR, $p > 0.05$, n = 9).

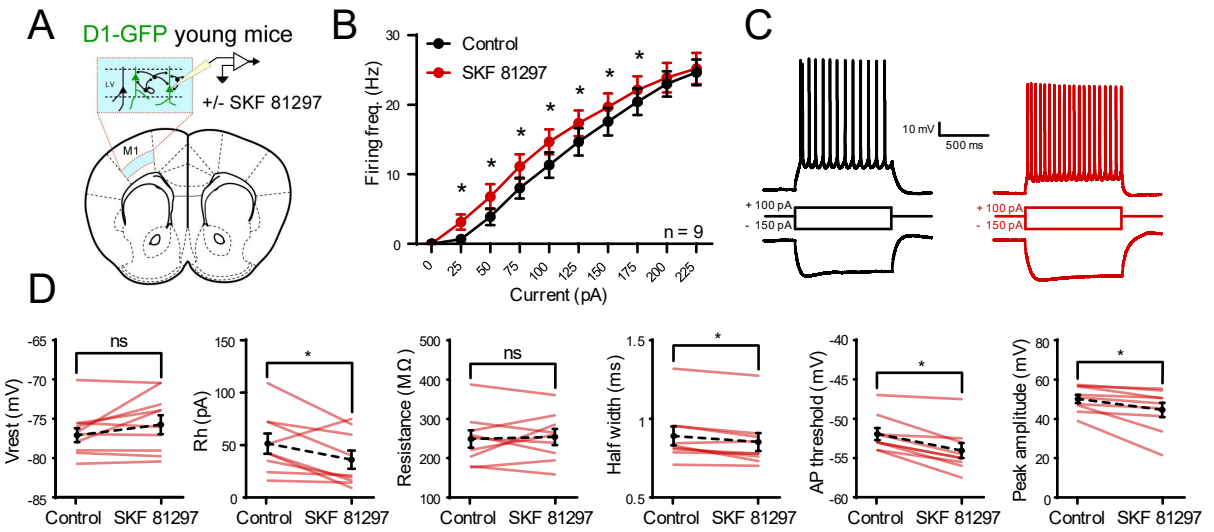

Fig. 4.19: Effect of D1 receptor agonist SKF 81297 on M1 pyramidal cells' properties in young mice. A. Experimental design. **B.** Input/output curve. n = 9. * $p < 0.05$ (two-way repeated measures ANOVA). **C.** Example traces of a recorded neuron in control condition (right) and with SKF 81297 (left). **D.** Cell parameters, from left to right: resting membrane potential, rheobase, input resistance, AP half width, AP threshold and AP peak amplitude. n = 9. * $p < 0.05$, ns = non-significant (WSR).

The effect of D1 receptor activation on layer V M1 PNs was then assessed in adult mice (Fig. 4.20A). As for young mice, from 50 pA to 175 pA intensity stimulation, PNs fired more APs in presence of SKF 81297 compared to control conditions (Fig. 4.20B, two-way repeated measures ANOVA, $F_{(9, 144)} = 306.2$, $p < 0.0001$, n = 17). This is illustrated by traces of a neuron in response to a 100 pA stimulation in presence or absence of the D1 receptor agonist (Fig. 4.20C). Moreover, the input resistance and the AP half width and threshold were significantly lower in presence of SKF 81297 compared to control condition (Fig. 4.20D, WSR, $p < 0.05$, n

= 17). No significant effect was observed concerning the resting membrane potential, the rheobase and the AP peak amplitude (Fig. 4.20D, WSR, p > 0.05, n = 17).

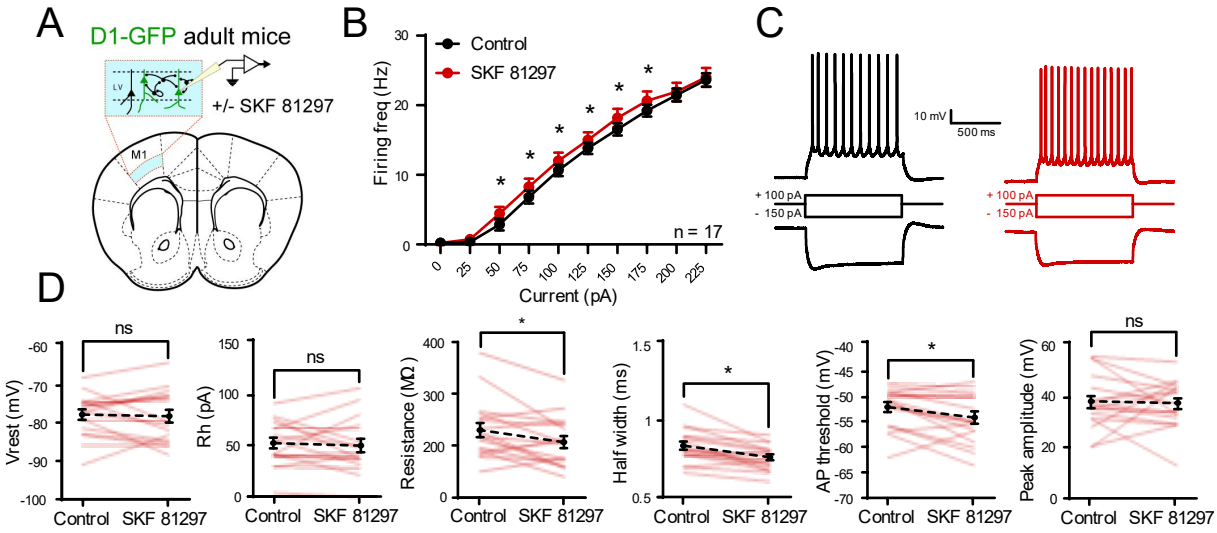

Fig. 4.20: Effect of D1 receptor agonist SKF 81297 on M1 pyramidal cells' properties in adult mice. A. Experimental design. **B.** Input/output curve. n = 17. * p < 0.05 (two-way repeated measures ANOVA). **C.** Example traces of a recorded neuron in control condition (right) and with SKF 81297 (left). **D.** Cell parameters, from left to right: resting membrane potential, rheobase, input resistance, AP half width, AP threshold and AP peak amplitude. n = 17. * p < 0.05, ns = non-significant (WSR).

Taken together, these results indicate that the modulation exerted by D1 receptors on M1 layer V PNs is function of the age of the mice.

Discussion

This thesis had two main objectives. The first one aimed to characterize the intrinsic properties of midbrain DAergic neurons projecting to M1, and to investigate how these intrinsic properties evolve during motor skill learning in mice. The second one aimed at deciphering the impact of DA on M1 layer V PNs' intrinsic properties. Using retrograde tracing approaches, the mapping of M1-projecting midbrain DAergic neurons showed that these neurons are mainly located in ventrolateral parts of the midbrain of the mice, especially in the ventral part of the medial SNc and in the rostral part of the VTA. *Ex vivo* electrophysiological recordings revealed that the intrinsic properties of these neurons are reminiscent of those of mesostriatal neurons, as they displayed low-frequency spontaneous activity with broad APs, broad I_h current and a two-phased AHP. The excitability of these neurons was increased after five days of training to a skilled motor task compared to after two days and eight days of training. Next, the functional connectivity of M1-projecting midbrain DAergic neurons on M1 layer V PNs was assessed, using *ex vivo* electrophysiological recordings on M1 layer V PNs coupled with optogenetic-induced release of DA by DAergic terminals in M1. These experiments did not enable to highlight a DAergic modulation of M1 layer V PNs, nor a corelease of GABA and/or glutamate as it has been shown in other structures. Using pharmacology, other experiments were carried out to better understand the impact of DAergic transmission by D1 receptors on M1 layer V PNs. These experiments aimed at unravelling the implication of D1 receptor on M1 layer V PNs, and at beginning to decipher contradictory results obtained in the literature. The data obtained in these experiments showed an age dependant modulation of M1 layer V PNs by D1 receptors, as their excitability was diminished or increased while blocking or activating D1 receptors in young mice, respectively, whereas their excitability was increased by both blockade or activation of D1 receptors in adult mice.

1. Retrograde tracing of midbrain DAergic neurons from M1

Although the architecture of the DAergic system within M1 has been well characterized anatomically in mice (Vitrac et al., 2014), data on the localization, the properties and the function of this specific subpopulation of DAergic neurons projecting to M1 were lacking in mice. The data obtained in this thesis showed that about 5% of midbrain DAergic neurons project to M1, and these neurons represent 80% of midbrain neurons projecting to M1. The 20% non-DAergic neurons projecting to M1 might be either glutamatergic or GABAergic neurons, as it has been shown in other cortices such as the PFC (Bouarab et al., 2019; Hur and

Zaborszky, 2005). Further histological experiments could be done to further characterize the midbrain neuronal populations projecting to M1, such as immunohistochemical labeling for GABAergic and glutamatergic neurons on brain slices of FG-injected mice.

Mapping analyses revealed that M1-projecting midbrain DAergic neurons are mainly located in rostral ventrolateral parts of the midbrain, especially in the ventral part of the medial SNc and in the rostral part of the VTA, forming a *continuum* between these two areas. This kind of *continuum* has also been reported in primates, but at a more dorsal location (Williams, 1998). Due to their location in the midbrain, these neurons are susceptible to express ALDH1a1, as ALDH1a1 DAergic neurons are located in the rostral midbrain of mice (Poulin et al., 2014), and also SOX6, as they are ventrally located in the midbrain (Pereira Luppi et al., 2021). Thus, it may be possible that in mice, SNc DAergic neurons projecting to the dorsal striatum also sends projection to M1, as SOX6-prositive neurons project in this area (Pereira Luppi et al., 2021). This would not be surprising, as nigrostriatal neurons also send collaterals to somatosensory cortex (Björklund and Dunnett, 2007). Few neurons have been counted in more caudal parts of the midbrain, especially the subnuclei of the VTA PBP, PIF and PNu. This location is in agreement with previous studies, as most of caudal DAergic neurons of the VTA in rats project to the nAcc or the PFC and are clearly distinguished from M1-projecting DAergic neurons which are located in more rostral parts in rats (Hosp et al., 2015). Nonetheless, the ventral location of these neurons in mice was quite unexpected, as they are more dorsally located in the midbrain of rats (Hosp et al., 2015). Generally, phylogenetically younger DAergic neurons are appended to dorsal parts of the midbrain compared to phylogenetically older DAergic neurons (Björklund and Dunnett, 2007; Hosp et al., 2015). This way, M1-projecting DAergic neurons phylogeny in mice might be different of the one of rats, with M1-projecting DAergic neurons developed earlier in mice phylogeny than those in rats. Taken together, these results highlight a differential location of M1-projecting DAergic neurons of the midbrain in mice compared to rats, with some characteristics more reminiscent of what has been observed in primates. Furthermore, there might be potential differences in the timing at which these neurons are developed in mice compared to rats.

2. *Ex vivo* electrophysiological characterization of M1-projecting midbrain DAergic neurons

Even if the location of M1-projecting midbrain DAergic neurons has already been described in rats, the electrophysiological features of these midbrain DAergic neurons

projecting to M1 remains poorly understood, especially since the location of these neurons is a little bit different in mice compared to rats. Thus, the intrinsic properties of M1-projecting midbrain DAergic neurons have been investigated using *ex vivo* patch clamp recordings. These recordings showed that M1-projecting midbrain DAergic neurons display typical characteristics of nigrostriatal neurons: low-frequency spontaneous activity, broad APs, wide two-phased I_h currents and large AHP (Lammel et al., 2008; Liss et al., 2005). As reported in the literature, the I_h current displayed by these neurons may imply the expression of HCN channels by these neurons (Lammel et al., 2008), which are activated by subthreshold potentials and lead to fast repolarization by enabling the entry of sodium and potassium ions (Benarroch, 2013). The two-phased AHP might be due to the dual activity of potassium channels: SK-type potassium channels in a first time, and to ERG channels in the second time (Nedergaard, 2004). Finally, the spontaneous activity displayed by these neurons may depend on the slow oscillation of intracellular calcium concentration downregulated by GIRK2-linked D2 autoreceptors (Beckstead et al., 2004; Liss and Roeper, 2008; Surmeier, 2018).

More importantly, these intrinsic properties rise the hypothesis that some nigrostriatal neurons might send collaterals to M1 in mice. In fact, DAergic neurons of the SNc projecting to the dorsal striatum are located in the same area of the recorded neurons in this study, *i.e.*, in ventral parts of the midbrain (Pereira Luppi et al., 2021). This would not be the first time that nigrostriatal neurons send collaterals in the cortex, as it has already been shown that these neurons sends collaterals in the somatosensory cortex (Björklund and Dunnett, 2007). In this case, it would be possible that nigrostriatal neurons send collaterals to M1 to modulate M1 IT-CStrNs in order to adjust M1 inputs onto MSNs. This way, M1 could activate more or less direct or indirect pathways of the basal ganglia to adjust the ongoing movement. The plasticity induced by the DA release on these IT-CStrNs may induce plasticity mechanisms which would, *in fine*, lead to the increased excitability of IT-CStrNs activating relevant MSNs in the striatum and thus contribute to the better execution of motor tasks and to refine them other time.

3. Evolution of the intrinsic properties of M1-projecting midbrain DAergic neurons during motor learning

DAergic projections from the midbrain to M1 have been shown to be crucial in mediating motor skill learning (Hosp et al., 2011; Molina-Luna et al., 2009). At the level of M1, it has been shown that DA is required for synaptic plasticity (Molina-Luna et al., 2009) and regulates spine turnover (Guo et al., 2015), which are both necessary mechanisms for motor

skill learning. Nonetheless, the evolution of the intrinsic properties of M1-projecting midbrain DAergic neurons has never been monitored during the learning process. Thus, the SPRT was used to study motor skill learning, and electrophysiological patch clamp recordings performed at different times of the motor skill learning process enabled to investigate the intrinsic properties of M1-projecting midbrain DAergic neurons over time. The plate delivering food was automatized: when a mouse grabbed a food pellet, the food deliverer went down for 3 seconds and then went back up with a pellet on it. This enabled the mice to be autonomous during the sessions and to not be disturbed by the experimenter. Secondly, this automatized food deliverer enabled more reproductible trials, as the food pellets were always placed at the same position.

The data obtained in this thesis indicate an enhanced excitability of M1-projecting midbrain DAergic neurons after 5 days of training, compared to after 2 or 8 days of training. These results are in agreement with a previous study which already reported in rats an increase in the expression of c-fos, indicating an increased activity, of M1-projecting midbrain DAergic neurons during motor skill acquisition, which is not observable anymore once the task is learned (Leemburg et al., 2018). As plateau acquisition is considered to be reach after 7-8 days of training (Guo et al., 2015; Leemburg et al., 2018), M1-projecting midbrain DAergic neurons displayed an increased activity during learning (5 days of training) compared to plateau acquisition (8 days of training). Moreover, these neurons displayed a higher excitability in response to current injections after 5 days of training compared to after 2 days of training. As most of the increase in the success percentage of mice during the SPRT occurs between the second and the fifth day of training, these results might indicate a correlation between the increase in the excitability of these neurons and the highest learning efficiency of a new fine motor task. The higher excitability of these neurons could induce a higher DA release in M1 throughout learning, thus enhancing motor skill learning. This increase in DA release would be implicated in plastic changes such as spine selection, formation and stabilization (Guo et al., 2015) as well as synaptic plasticity (Molina-Luna et al., 2009), further reinforcing the activity and the recurrent connectivity of PNs relevant of the motor task (Biane et al., 2019). As DA release is positively correlated with learning efficiency, the DA-induced plastic changes on PNs would refine the activity PNs relevant of the motor task until reaching optimal level for successful motor completion. This DA release might also act on M1 INs as well, as it has been reported that PV INs are positively modulated by DA acting on D2 receptors (Cousineau et al., 2020), possibly by a positive coupling of D2 receptors with PLC as it has been previously

shown (Rioult-Pedotti et al., 2015). Moreover, non-fast spiking INs of the PFC are also modulated by DA, as D1 and D2 receptor agonists increases the excitability of these neurons in the PFC (Tseng and O'Donnell, 2006). Thus, it would be possible that the increased DA release in M1 during motor skill learning enhances the excitability of M1 INs, whether they are fast spiking or non-fast spiking. This would therefore increase the inhibition in M1 leading to the selection of PNs relevant of the motor task. As DA release is positively correlated with learning efficiency, the selection of PNs relevant of the motor task would be more efficient during learning time course till reaching optimal level after learning completion. As the activity of midbrain DAergic neurons projecting to M1 has been assessed *ex vivo*, it could be interesting to use miniatured microscopes or fiber photometry to study the activity of these neurons *in vivo* while mice are performing the behavioural task.

4. Release of DA in M1

Even if DAergic terminals in M1 have been discovered quite a long time ago (Descarries et al., 1987) and that DA role in M1 processes is not to be questioned (Cousineau et al., 2022; Guo et al., 2015; Hosp et al., 2011; Molina-Luna et al., 2009; Rioult-Pedotti et al., 2015), the release of DA in M1 has never been characterized *ex vivo* using modern live imaging techniques. In fact, studying the kinetics of DA release and reuptake *ex vivo* would be of use to further manipulate DA release *in vivo* during a behavioural task, in a more physiological manner. Imaging data obtained in this part of the thesis showed a slight release of DA in M1 evoked by an electrical stimulation. This increase is very discrete in comparison to the release of DA in the striatum induced by the same stimulation protocols. However, this was not a surprising fact, as the DAergic innervation of M1 is also very discrete in comparison to structures receiving massive DAergic inputs such as the striatum (Descarries et al., 1987). Besides, the DAergic sensor $GRAB_{DA1m}$ is not as sensitive to DA as other DAergic sensors such as $GRAB_{DA1h}$ (Sun et al., 2018) or dLight (Patriarchi et al., 2018), indicating that other DAergic sensors might be more suitable to detect more efficiently slight DA transients. Nonetheless, $GRAB_{DA1m}$ is very specific of DA, as the application of several neurotransmitters does not elicit detectable $GRAB_{DA1m}$ fluorescent changes, at the exception of norepinephrine (Sun et al., 2018). Still, $GRAB_{DA1m}$ is more specific of DA compared to other DAergic sensors such as $GRAB_{DA1h}$, as norepinephrine induces a lower fluorescent change in $GRAB_{DA1m}$ compared to $GRAB_{DA1h}$ (Sun et al., 2018). Thus, the increase in fluorescence is likely to be only due to DA release. As DAergic terminals in M1 mainly come from the midbrain (Hosp et al., 2011, 2015), these results suggest a slight but functional release of DA in M1 by M1-

projecting midbrain DAergic neurons. Nonetheless, the use of an electrical stimulation cannot guarantee that the increase of fluorescence is specific of DA release by midbrain DAergic terminals. Moreover, the imaging experiments were done using an epifluorescence microscope, which might not be the best option to study the fast kinetics of DA release and reuptake with high resolution. 2-photon or confocal microscopy would be more suitable options to push further these experiments, as it has been for several pioneer studies (Patriarchi et al., 2018; Sun et al., 2018), but they are expensive.

5. Recording of the activity of M1 layer V PNs following the stimulation of DAergic terminals in M1

The impact of DA on M1 neurons have been the subject of several studies, whether *in vivo* (Parr-Brownlie, 2005) or *ex vivo* (Cousineau et al., 2020; Swanson et al., 2020), on PNs (Cousineau et al., 2022; Parr-Brownlie, 2005; Swanson et al., 2020; Vitrac et al., 2014) or INs (Cousineau et al., 2020), or through D1 (Swanson et al., 2020) or D2 receptors (Cousineau et al., 2020; Parr-Brownlie, 2005; Vitrac et al., 2014). Some studies also investigated the impact of DA depletion in the midbrain on M1 neurons' (Chen et al., 2019, 2021; Li et al., 2021; Swanson et al., 2020). Nevertheless, the impact of endogenous DA release in M1 has yet never been assessed.

The first *ex vivo* electrophysiological recordings made in part showed that the excitation of DAergic terminals in M1 induced presumably DA, glutamate and GABA release on M1 PNs, in DAT-Cre-Ai32 mice. Thus, DAergic neurons projecting to M1 would co-release glutamate or GABA, as it has already shown a corelease of DA and glutamate in the mPFC (Lavin et al., 2005) and the nAcc (Tecuapetla et al., 2010), as well as corelease of DA and GABA in the nAcc (Berrios et al., 2016) and the striatum (Tritsch et al., 2012). It has been shown in the midbrain that GABA production by DAergic neurons implies a non-canonical pathway dependent of ALDH1a1 enzyme (Kim et al., 2015), further emphasizing the identity of M1-projecting midbrain DAergic neurons as ALDH1a1 expressing-neurons. Furthermore, the amplitude of the glutamatergic EPSCs recorded in PNs was negatively modulated by DA, as DA transmission blockade with D1 and D2 antagonists increased the amplitude of the EPSCs. However, these results were obtained only in 3 mice of the same litter, while results from 15 other mice of different litters failed to replicate these results, as experiments done in ChR2-injected DAT-Cre mice. The most plausible explanation to these results would be a problem with the particular litter on which experiments were conclusive. An ectopic expression of the

opsin could have happened, leading to increased glutamatergic and GABAergic transmissions onto M1 layer V PNs. Also, an exacerbation of the DAergic projections from the midbrain to M1 could have been at the base of the increased transmission. As the DAergic innervation of M1 is discrete, it would be surprising to see such strong effects on M1 PNs, and most importantly on all recorded neurons as it was the case in the 3 mice of the same litter. Further investigations on this subject have not been done, as troubleshooting the DAT-Cre-Ai32 mice model was beyond the scope of this thesis.

Even if co-release of GABA and/or glutamate has not been reproductible in DAT-Cre-Ai32 mice of other litters nor in ChR2-injected DAT-Cre mice, it does not mean that DA does not impact M1 PNs' activity. In fact, studying the modulation exerted by DA on neurons is difficult, as DA does not act on ionotropic channels and does not induce post-synaptic currents *per se*, so an online readout is generally not possible. However, as DA is a neuromodulator, it would be of interest to investigate the modulation exerted by DA on a smaller scale, especially to analyze the spontaneous activity of PNs following DAergic terminal stimulations. Mini EPSCs and IPSCs analysis of voltage-clamp recordings without synaptic transmission blockers could provide information of a potential modulation of the excitability and synaptic transmission of M1 PNs by DA, as it has been shown for M1 PV INs (Cousineau et al., 2020). Furthermore, glutamate corelease with DA has been discovered in other cortical areas, such as the PFC (Kabanova et al., 2015; Zhong et al., 2020). Plus, as GABA corelease with DA has been described in the striatum by GABA reuptake through the GABA transporter 1 (Melani and Tritsch, 2022; Tritsch et al., 2012), the same mechanism would be possible in cortical areas, if cortical DAergic terminal express the GABA transporter 1. Thus, it would be possible that the corelease of GABA and/or glutamate with DA observed in some experiments of this study is present in the other experiments which failed to highlight it, but in too few neurons. This would support the hypothesis that the corelease observed in some experiments was due to an ectopic expression of the opsin, leading to a bigger release of neurotransmitters at the level of M1.

6. Mapping of D1 receptors in M1

D1 receptor mapping has been done in the PFC, and showed a differential level of expression of D1 receptors depending on the age of mice, with a 3 fold higher expression in 3 weeks old mice compared to 6 weeks old mice (Leslie et al., 1991). Conversely, other studies showed that the expression of D1 receptors continuously increases from birth to reach its maximal level at adulthood in rats (Tarazi et al., 1999). This discrepancy in the PFC rose the

question of how D1 receptors are localized in M1 as a function of the age of the mice. Thus, a part of this thesis was dedicated to the investigation of the level of expression of D1 receptors in the M1 of young and adult mice. Most D1-expressing neurons are located in deep layers of M1 (i.e., layers V and VI), regardless of the age of the mice, which is not surprising as the majority of DAergic fibers are localized in M1 deeper layers in mice (Descarries et al., 1987), even if more superficial layers are also innervated, especially in human and primates (Raghanti et al., 2008). However, a significant amount of D1-expressing neurons is localized in layer II/III too, which also makes sense as upper layers of the cortex also receive a fair amount of DAergic terminal (Berger et al., 1985; Raghanti et al., 2008). The results obtained in this thesis suggest that the distribution of D1 expressing cells is quite conserved during growth, with similar number of D1-expressing neurons in M1. A main difference between the repartition of D1-expressing neurons in M1 between young and adult mice resides in a higher expression of D1 receptors in layer II-III compared to the other layers in young mice, while the repartition is quite equal between layers in adult mice (excluding the layer I in which there are few cell bodies). This tendency to the decrease of D1-expressing cells in layer II-III during growth could be due to a synaptic pruning, as it has been shown in the PFC (Andersen et al., 2000). In contrast, the increase of the expression of D1-expressing cells in deeper layers during growth could be due to the ontogeny of PNs whose number increases until adulthood, and which is correlated with the development of new DAergic projections in M1 (Tarazi et al., 1999).

As there is a wide diversity of PNs in M1 (Callaway et al., 2021), one aim of this thesis was to classify D1-expressing neurons in different categories of PNs depending on their projection sites. Thus, two transcription factor were used: CTIP2 and SATB2, as they are described in the literature as being specific of PTNs and ITNs, respectively (Alcamo et al., 2008; Arlotta et al., 2005; Britanova et al., 2008; Digilio et al., 2015; Molnár and Cheung, 2006). The number of D1-expressing neurons coexpressing CTIP2 and/or SATB2 transcription factors counted in this thesis was similar between young and adult mice, as well as the repartition of these cells across M1 layers. Most of D1-expressing cells also express SATB2, in young as well as in adult mice. This finding was not surprising as SATB2 is widely expressed in all layers of the cortex (Huang et al., 2013b). Based on the fact that SATB2 is thought to be a transcription factor specific of ITNs (Alcamo et al., 2008; Britanova et al., 2008; Molnár and Cheung, 2006), these results suggest that most of D1-expressing neurons of M1 are ITNs. Moreover, most of counted D1/SATB2-expressing neurons were localized in layer II-III. As layer II-III is composed mainly of IT-CCNs (Shepherd, 2013), D1-expressing neurons in M1

might be composed of a majority of IT-CCNs. Nonetheless, a non-negligeable part of D1/SATB2-expressing neurons are located in deeper layers of M1, indicating that these neurons could be IT-CstrNs as they are located in deeper layers compared to IT-CCNs (Shepherd, 2013). However a non-negligible number of D1-expressing PNs coexpress SATB2 and CTIP2 in layer V and VI, even if these two molecular markers are thought to be specific of subcortical- and subcerebral-projection neurons, respectively (Alcamo et al., 2008; Arlotta et al., 2005; Britanova et al., 2008; Digilio et al., 2015; Molnár and Cheung, 2006). However, it is not the first time that the colocalization of these two markers is observed, as it has been reported in the cortex and the hippocampus (Digilio et al., 2015; Harb et al., 2016; Lickiss et al., 2012; Nielsen et al., 2014). Indeed, it has been demonstrated that colocalization of CTIP2 and SATB2 is possible in cells expressing the transcriptional adaptor LMO4, which competes with SATB2 to bind to CTIP2, thus preventing its downregulation (Harb et al., 2016). This cell population coexpressing CTIP2 and SATB2 has been shown to be divided into two subclasses, projecting either to the brainstem or to the contralateral cortex (Harb et al., 2016). Hence, CTIP2 and SATB2 may not be as specific of two different neuronal populations in M1 deeper layers, and caution must be exercised when identifying a neuronal population with only one molecular marker. This colocalization of CTIP2 and SATB2 could also be due to the threshold used for counting, as a dual pattern of CTIP2 expression was observed in counted slices: some cells display a high intensity labeling and some others a low intensity labeling. Such differences in the level of expression of CTIP2 has already been reported in mice motor and sensory cortices (McKenna et al., 2011). Thus, the colocalization of CTIP2 and SATB2 could be possible in neurons expressing a low level of CTIP2, as SATB2 is thought to negatively regulate the level of CTIP2 in neurons (Alcamo et al., 2008; Britanova et al., 2008). This colocalization could have been encountered due to a threshold not high enough to exclude the counting of neurons expressing low levels of CTIP2. This colocalization could also explain the low number of D1/CTIP2-expressing neurons counted in both young (n = 4 on average) and adult (n = 2 on average) mice, suggesting a negligible amount of PTNs expressing D1 receptors in M1, which would be in line with previous studies (Gaspar et al., 1995).

7. Impact of activation and blockade of D1 receptors on D1-expressing M1 layer V PNs' intrinsic properties

There is no consensus in the literature concerning the effect of DA receptor activation and inhibition on M1 PNs, as studies using different experimental design led to contradictory results (for review, see Cousineau et al., 2022). Moreover, there is no data available in the

literature about a potential change of D1 receptors' modulation of PNs intrinsic properties during growth. Thus, a part of this thesis was dedicated to deciphering the effect of D1 receptors on M1 PNs. *Ex vivo* electrophysiological recordings were used to record the intrinsic properties of M1 PNs while applying an agonist or an antagonist of D1 receptors. These recordings were made on D1-GFP mice to ensure recorded PNs expressed D1 receptors. Recordings took place in layer V as it is a layer in rodents which receives most of DAergic terminals (Descarries et al., 1987) and which is implicated in long range subcortical and subcerebral communications directly implicated in motor processes (Shepherd, 2013).

In this work, electrophysiological recordings of M1 layer V PNs while activating or blocking D1 receptors revealed a distinct effect in young mice and adult mice. In fact, while D1 receptor blockade decreased the excitability of M1 layer V PNs, D1 receptor activation induced an increase of the excitability of PNs in young mice. However, in adult mice, pharmacologically blocking or activating D1 receptors induced an increase in the excitability of PNs in both young and adult mice, and the effects observed in adult were not as strong as the ones observed in young animal. The results obtained in this study by recording PNs expressing D1 receptor in adult mice are in accordance with previous studies, as D1 receptor induces an increase in the excitability of M1 layer V PNs, noticeable by a higher firing frequency, and also a depolarized resting membrane potential as observed in parkinsonian conditions (Degos et al., 2013). Furthermore, D1 receptor blockade in adult mice lowered M1 layer V PNs' rheobase and AP threshold, as observed in a previous *ex vivo* study (Swanson et al., 2020). However, *in vivo* electrophysiological recordings in rodents have shown that D1 receptor blockade induces a decrease in PNs activity (Awenowicz and Porter, 2002), highlighting important differences of D1 receptor modulation of M1 layer V PNs depending on the experimental design (*in vivo* vs. *ex vivo*, and maybe anesthetized vs awake animals), with a possible effect of the network on PNs activity. In fact, it has been shown that DA also acts on GABAergic neurons in M1, notably though D2 receptors (Cousineau et al., 2020). It could be possible that the decrease of PNs activity observed *in vivo* would be due to an effect of D1 receptor blockade at the level of GABAergic neurons, which would not be noticeable *ex vivo* due to the presence of fast synaptic transmission blockers. Furthermore, as drugs are bath applied, this does not reproduce the fine physiological conditions of D1 receptors activation and blockade.

Interestingly, D1 receptor blockade in young mice induced the opposite effect to the one observed in adult mice, as it decreased the excitability of M1 layer V PNs. It is well acknowledged that D1 receptors are classically coupled with G_s protein, upregulating cAMP

intracellular levels (Stoof and Kebabian, 1981). Nonetheless, it has been shown that D1 receptors can also activate the PLC (Rioult-Pedotti et al., 2015), suggesting a coupling of D1 receptors with $G_{q/11}$ proteins. Furthermore, D1 receptors can be coupled with the $G_{i/0}$ protein (Sidhu et al., 1991) and more importantly, they can be coupled with several G proteins (Sidhu, 1998). Thus, it could be possible that during mouse development, the G protein recruited by D1 receptors following DA binding changes from a G_s or $G_{q/11}$ inducing an intracellular cascade leading to an increase in the excitability of M1 layer V PNs, to another one inducing the opposite effect, as $G_{i/0}$. A switching mechanism in G protein coupling has already been shown in other receptors, such as the corticotropin-release factor receptor in the piriform cortex (Narla et al., 2016) and the β_2-adrenergic receptor *in vitro* (Daaka et al., 1997).

For the first time, this study investigated the impact of D1 receptor activation on M1 layer V PNs' excitability and intrinsic properties. In young mice, D1 receptor activation induced an increase in M1 layer V PNs excitability, which is in accordance with the fact that a decrease of the excitability of M1 layer V PNs in young mice is observed following D1 receptor blockade. This supports that at younger stages, D1 receptors recruit an excitatory G protein. Surprisingly, the effect of D1 receptor activation in adult mice was similar as the one induced by D1 receptor blockade, as it increased the firing frequency of M1 layer V PNs following stimulation and as it lowered the AP threshold of these neurons. Furthermore, this effect is similar as the one induced by D1 receptor activation in young mice. These contradictory results might arise from the wide variety of PNs in the M1 of adult mice, which could not be representative of the results that would be obtained by recording specific types of D1-expressing PNs, as challenging as it would be. Furthermore, the agonist and antagonist of D1 receptors were bath applied, which does not reproduce the physiological release of DA in a mouse brain, highlighting the need to better understand the timescale of DA release in M1. Also, as recordings were made *ex vivo*, the extracellular levels of DA in the slices are not known, meaning that the basal level of activation of D1 receptors in control conditions is unknown. This way, the effects observed in D1-receptor blockade experiments could indirectly be due to an imbalance between D1 and D2 receptors activities.

8. Conclusion and perspectives

This thesis unraveled the location and intrinsic properties of M1-projecting midbrain DAergic neurons in mice, as well as the evolution of their properties during motor skill learning

(Fig. 6.1). Furthermore, this thesis gives insights regarding the functional importance of DA receptors on M1 PNs, especially through D1 receptors (Fig. 6.1).

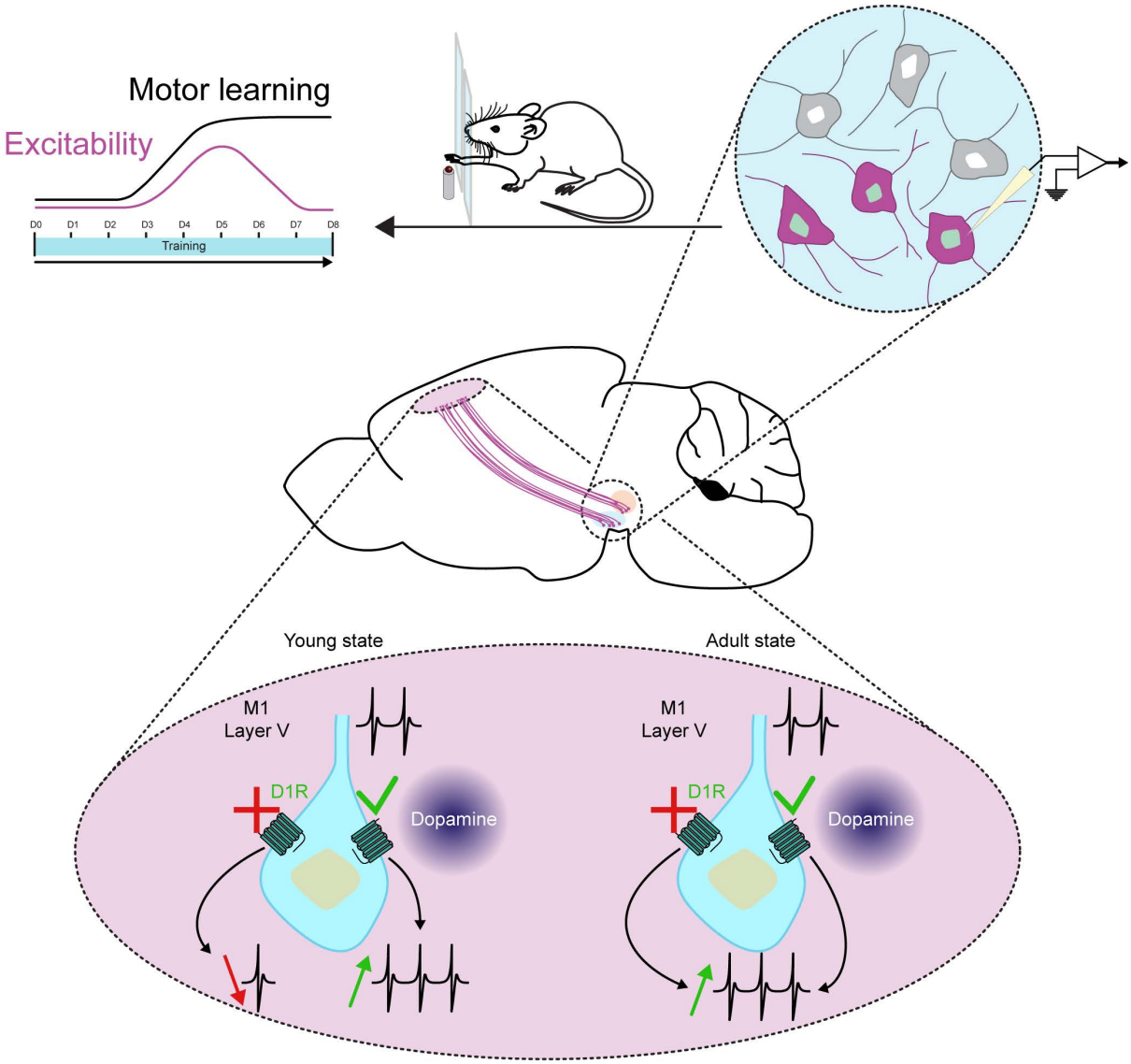

Fig. 6.1: Summary of the results obtained during this thesis. Part 1) Retrograde tracing experiments demonstrated in mice a rostro ventrolateral localization of midbrain dopaminergic neurons projecting to M1 and *ex vivo* electrophysiological recordings enabled to define their electrophysiological signature and demonstrated that their excitability increases during the learning of a new fine motor task (single pellet reaching task). **Part 2)** At the level of M1, *ex vivo* electrophysiological recordings showed that D1 receptor activation induces an increase in the excitability of pyramidal neurons in young and adult mice, whereas D1 receptor blockade induces a decrease in the excitability of these neurons in young mice, but an increase in adult mice.

Several additional experiments could be done to further characterize the midbrain to M1 pathway. As the intrinsic properties of retrogradely labeled midbrain neurons is reminiscent of that of nigrostriatal neurons, double retrograde tracing experiments could be done in a similar fashion, with the other retrograde tracer injected into the dorsal striatum as DAergic

nigrostriatal neurons project massively in this area. This experiment could indicate if the nigrostriatal neurons send collaterals in M1. Moreover, paired-pulse ratio experiments could be performed on these neurons at different times of motor skill learning to investigate the vesicle release probability from these neurons, which would give more precise information concerning the DA release at the level of M1.

Studies of the impact of D2 receptors on M1 PNs using the same experimental design as the one used in this thesis concerning D1 receptors could be conducted to try to set up a reference of DA's impact on M1 PNs' intrinsic properties *ex vivo*, to clear up the discrepancy observed in the literature on this subject. Furthermore, the impact of D1 receptors on INs activity could also be assessed *ex vivo* in a similar fashion, especially PV INs as the impact of D2 receptors activation and blockade on these INs has already been investigated in the lab.

The functional impact of DA release in M1 by DAergic terminals coming from the midbrain could be assessed deeper, notably by recording and analyzing mini EPSCs and IPSCs. These experiments could fill the gap in our knowledge concerning the controversial results obtained during this thesis regarding specific DA release from midbrain terminals in M1. As DA's action on M1 neurons' has been shown to be mediated through PLC activation (Rioult-Pedotti et al., 2015), an increase of mini EPSCs frequency and/or amplitude could be expected.

Further experiments using $GRAB_{DA1m}$ imaging could be of use to decipher the time course of DA release in M1 during motor skill learning. Using miniatured microscopes implanted in the brains of mice, it could be possible to record *in vivo* when DA is released in M1 in $GRABD_{A1m}$-injected mice performing the SPRT. The same experiments could be done in a similar fashion using an axonal GCamP whose expression is conditioned by the expression of the Cre recombinase injected directly in the midbrain of DAT-Cre mice. This would enable the imaging of midbrain DAergic fibers in the M1 of mice performing the SPRT using the same miniscopes. One limitation would be the resolution of these miniscopes which could not be high enough to image fibers, as these miniscopes basically are miniatured epifluorescence microscopes. Nonetheless, recent advances in miniatured microscopes could enable to overcome this limitation, as miniatured 2-photon microscopes are beginning to be developed (Zong et al., 2022).

The identification of the timing and of the pattern of release of DA release during motor skill learning could also enable the selective manipulation of DAergic terminals in M1. Taken advantage of the millisecond resolution of optogenetics, it could be possible to excite or inhibit

DAergic terminals in M1 when DA is normally released and thus to investigate the impact these manipulations have on motor skill learning. Also, newly developed miniscopes can record videos in two different channels (*i.e.*, in the green and the red for example). Using these miniscopes, it would be interesting to record the release of DA in one channel using the $GRAB_{DA1m}$, and to record the activity of PNs and/or INs in the other channel using calcium imaging. This kind of experiments would help to better understand the effect of DA on different neuronal populations of M1 during motor skill learning. This way, it could be possible to further investigate the evolution of the activity of M1 neuronal populations during motor skill learning, and to reproduce these activity changes using optogenetics, for example in DA-depleted mice, to try to compensate the DA depletion-induced motor skill learning impairments. These experiments could help to identify new targets for treatment of people displaying motor skill learning impairments, as observed during PD.

This project has led to a better understanding and knowledge of the origins and implications of DA in M1, at the cellular and behavioural levels.

References

Abell, C.W., and Kwan, S.-W. (2000). Molecular characterization of monoamine oxidases A and B. In Progress in Nucleic Acid Research and Molecular Biology, pp. 129–132.

Abi-Dargham, A., Rodenhiser, J., Printz, D., Zea-Ponce, Y., Gil, R., Kegeles, L.S., Weiss, R., Cooper, T.B., Mann, J.J., Van Heertum, R.L., et al. (2000). Increased baseline occupancy of D 2 receptors by dopamine in schizophrenia. Proc. Natl. Acad. Sci. *97*, 8104–8109.

Ahn, S., Shenoy, S.K., Wei, H., and Lefkowitz, R.J. (2004). Differential Kinetic and Spatial Patterns of β-Arrestin and G Protein-mediated ERK Activation by the Angiotensin II Receptor. J. Biol. Chem. *279*, 35518–35525.

Albin, R.L., Young, A.B., and Penney, J.B. (1989). The functional anatomy of basal ganglia disorders. Trends Neurosci. *12*, 366–375.

Alcamo, E.A., Chirivella, L., Dautzenberg, M., Dobreva, G., Fariñas, I., Grosschedl, R., and McConnell, S.K. (2008). Satb2 Regulates Callosal Projection Neuron Identity in the Developing Cerebral Cortex. Neuron *57*, 364–377.

Anastasiades, P.G., Boada, C., and Carter, A.G. (2019). Cell-Type-Specific D1 Dopamine Receptor Modulation of Projection Neurons and Interneurons in the Prefrontal Cortex. Cereb. Cortex *29*, 3224–3242.

Andersen, S.L., Thompson, A.T., Rutstein, M., Hostetter, J.C., and Teicher, M.H. (2000). Dopamine receptor pruning in prefrontal cortex during the periadolescent period in rats. Synapse *37*, 167–169.

Arlotta, P., Molyneaux, B.J., Chen, J., Inoue, J., Kominami, R., and Macklis, J.D. (2005). Neuronal Subtype-Specific Genes that Control Corticospinal Motor Neuron Development In Vivo. Neuron *45*, 207–221.

Augustin, S.M., Loewinger, G.C., O'Neal, T.J., Kravitz, A. V, and Lovinger, D.M. (2020). Dopamine D2 receptor signaling on iMSNs is required for initiation and vigor of learned actions. Neuropsychopharmacology *45*, 2087–2097.

Awenowicz, P.W., and Porter, L.L. (2002). Local application of dopamine inhibits pyramidal tract neuron activity in the rodent motor cortex. J. Neurophysiol. *88*, 3439–3451.

Baker, A., Kalmbach, B., Morishima, M., Kim, J., Juavinett, A., Li, N., and Dembrow, N. (2018). Specialized Subpopulations of Deep-Layer Pyramidal Neurons in the Neocortex: Bridging Cellular Properties to Functional Consequences. J. Neurosci. *38*, 5441–5455.

Ballion, B., Mallet, N., Bézard, E., Lanciego, J.L., and Gonon, F. (2008). Intratelencephalic corticostriatal neurons equally excite striatonigral and striatopallidal neurons and their discharge activity is selectively reduced in experimental parkinsonism. Eur. J. Neurosci. *27*, 2313–2321.

Barbas, H., and García-Cabezas, M. (2015). Motor cortex layer 4: Less is more. Trends Neurosci. *38*, 259–261.

Barre, A., Berthoux, C., De Bundel, D., Valjent, E., Bockaert, J., Marin, P., and Bécamel, C. (2016). Presynaptic serotonin 2A receptors modulate thalamocortical plasticity and associative learning. Proc. Natl. Acad. Sci. *113*, E1382–E1391.

Battaglia-Mayer, A., and Caminiti, R. (2019). Corticocortical Systems Underlying High-Order Motor Control. J. Neurosci. *39*, 4404–4421.

Baufreton, J., Garret, M., Rivera, A., de la Calle, A., Gonon, F., Dufy, B., Bioulac, B., and Taupignon, A. (2003). D5 (Not D1) Dopamine Receptors Potentiate Burst-Firing in Neurons of the Subthalamic Nucleus by Modulating an L-Type Calcium Conductance. J. Neurosci. *23*, 816–825.

Beaulieu, J., and Gainetdinov, R.R. (2011). The Physiology , Signaling , and Pharmacology of Dopamine Receptors. *63*, 182–217.

Beckstead, M.J., Grandy, D.K., Wickman, K., and Williams, J.T. (2004). Vesicular Dopamine Release Elicits an Inhibitory Postsynaptic Current in Midbrain Dopamine Neurons. Neuron *42*, 939–946.

Beier, K.T., Steinberg, E.E., DeLoach, K.E., Xie, S., Miyamichi, K., Schwarz, L., Gao, X.J., Kremer, E.J., Malenka, R.C., and Luo, L. (2015). Circuit Architecture of VTA Dopamine Neurons Revealed by Systematic Input-Output Mapping. Cell *162*, 622–634.

Bekkers, J.M., and Delaney, A.J. (2001). Modulation of Excitability by α-Dendrotoxin-Sensitive Potassium Channels in Neocortical Pyramidal Neurons. J. Neurosci. *21*, 6553–6560.

Beloozerova, I.N., Sirota, M.G., Swadlow, H.A., Orlovsky, G.N., Popova, L.B., and Deliagina, T.G. (2003). Activity of Different Classes of Neurons of the Motor Cortex during Postural Corrections. J. Neurosci. *23*, 7844–7853.

Benarroch, E.E. (2013). HCN channels: Function and clinical implications. Neurology *80*, 304–310.

Berger, B., Verney, C., Alvarez, C., Vigny, A., and Helle, K.B. (1985). New dopaminergic terminal fields in the motor, visual (area 18b) and retrosplenial cortex in the young and adult rat. Immunocytochemical and catecholamine histochemical analyses. Neuroscience *15*, 983–998.

Berger, B., Gaspar, P., and Verney, C. (1991). Dopaminergic innervation of the cerebral cortex: unexpected differences between rodents and primates. Trends Neurosci. *14*, 21–27.

Berrios, J., Stamatakis, A.M., Kantak, P.A., McElligott, Z.A., Judson, M.C., Aita, M., Rougie, M., Stuber, G.D., and Philpot, B.D. (2016). Loss of UBE3A from TH-expressing neurons suppresses GABA co-release and enhances VTA-NAc optical self-stimulation. Nat. Commun. *7*, 10702.

Biane, J.S., Takashima, Y., Scanziani, M., Conner, J.M., and Tuszynski, M.H. (2019). Reorganization of Recurrent Layer 5 Corticospinal Networks Following Adult Motor Training. J. Neurosci. *39*, 4684–4693.

Björklund, A., and Dunnett, S.B. (2007). Dopamine neuron systems in the brain: an update. Trends Neurosci. *30*, 194–202.

Blaess, S., and Ang, S.-L. (2015). Genetic control of midbrain dopaminergic neuron development. Wiley Interdiscip. Rev. Dev. Biol. *4*, 113–134.

Bortone, D.S., Olsen, S.R., and Scanziani, M. (2014). Translaminar inhibitory cells recruited by layer 6 corticothalamic neurons suppress visual cortex. Neuron *82*, 474–485.

Bouarab, C., Thompson, B., and Polter, A.M. (2019). VTA GABA Neurons at the Interface of Stress and Reward. Front. Neural Circuits *13*, 1–12.

Bouthenet, M.L., Souil, E., Martres, M.P., Sokoloff, P., Giros, B., and Schwartz, J.C. (1991). Localization of dopamine D3 receptor mRNA in the rat brain using in situ hybridization histochemistry: comparison with dopamine D2 receptor mRNA. Brain Res. *564*, 203–219.

Bouzas, E.A., Karadimas, P., Alexandrou, A., and Panagopoulos, I. (2008). Petilla terminology: nomenclature of features of GABAergic interneurons of the cerebral cortex. Nat. Rev. Neurosci. *9*, 557–568.

Britanova, O., de Juan Romero, C., Cheung, A., Kwan, K.Y., Schwark, M., Gyorgy, A., Vogel, T., Akopov, S., Mitkovski, M., Agoston, D., et al. (2008). Satb2 Is a Postmitotic Determinant for Upper-Layer Neuron Specification in the Neocortex. Neuron *57*, 378–392.

Brodie, M.S., Pesold, C., and Appel, S.B. (1999). Ethanol Directly Excites Dopaminergic Ventral Tegmental Area Reward Neurons. Alcohol. Clin. Exp. Res. *23*, 1848–1852.

Bromberg-Martin, E.S., Matsumoto, M., and Hikosaka, O. (2010). Dopamine in Motivational Control: Rewarding, Aversive, and Alerting. Neuron *68*, 815–834.

Brown, P. (2007). Abnormal oscillatory synchronisation in the motor system leads to impaired movement. Curr. Opin. Neurobiol. *17*, 656–664.

Callaway, E.M., Dong, H.-W., Ecker, J.R., Hawrylycz, M.J., Huang, Z.J., Lein, E.S., Ngai, J., Osten, P., Ren, B., Tolias, A.S., et al. (2021). A multimodal cell census and atlas of the mammalian primary motor cortex. Nature *598*, 86–102.

Camps, M., Kelly, P.H., and Palacios, J.M. (1990). Autoradiographic localization of dopamine D1 and D2 receptors in the brain of several mammalian species. J. Neural Transm. *80*, 105–127.

Carr, D.B., and Sesack, S.R. (2000). Projections from the Rat Prefrontal Cortex to the Ventral Tegmental Area: Target Specificity in the Synaptic Associations with Mesoaccumbens and Mesocortical Neurons. J. Neurosci. *20*, 3864–3873.

Centonze, D., Grande, C., Saulle, E., Martín, A.B., Gubellini, P., Pavón, N., Pisani, A., Bernardi, G., Moratalla, R., and Calabresi, P. (2003). Distinct Roles of D 1 and D 5 Dopamine Receptors in Motor Activity and Striatal Synaptic Plasticity. J. Neurosci. *23*, 8506–8512.

Chaudhury, D., Walsh, J.J., Friedman, A.K., Juarez, B., Ku, S.M., Koo, J.W., Ferguson, D., Tsai, H.-C., Pomeranz, L., Christoffel, D.J., et al. (2013). Rapid regulation of depression-related behaviours by control of midbrain dopamine neurons. Nature *493*, 532–536.

Chen, C., Gilmore, A., and Zuo, Y. (2014). Study Motor Skill Learning by Single-pellet Reaching Tasks in Mice. J. Vis. Exp. 1–7.

Chen, K., Yang, G., So, K.-F., and Zhang, L. (2019). Activation of Cortical Somatostatin Interneurons Rescues Synapse Loss and Motor Deficits after Acute MPTP Infusion. IScience *17*, 230–241.

Chen, L., Daniels, S., Kim, Y., and Chu, H.-Y. (2021). Cell Type-Specific Decrease of the Intrinsic Excitability of Motor Cortical Pyramidal Neurons in Parkinsonism. J. Neurosci. *41*, 5553–5565.

Di Chiara, G., and Imperato, A. (1985). Ethanol preferentially stimulates dopamine release in the nucleus accumbens of freely moving rats. Eur. J. Pharmacol. *115*, 131–132.

Chris Muly, E., Szigeti, K., and Goldman-Rakic, P.S. (1998). D1 receptor in interneurons of macaque prefrontal cortex: Distribution and subcellular localization. J. Neurosci. *18*, 10553–

10565.

Ciliax, B.J., Nash, N., Heilman, C., Sunahara, R., Hartney, A., Tiberi, M., Rye, D.B., Caron, M.G., Niznik, H.B., and Levey, A.I. (2000). Dopamine D5 receptor immunolocalization in rat and monkey brain. Synapse *37*, 125–145.

Cousineau, J., Lescouzères, L., Taupignon, A., Delgado-Zabalza, L., Valjent, E., Baufreton, J., and Le Bon-Jégo, M. (2020). Dopamine D2-Like Receptors Modulate Intrinsic Properties and Synaptic Transmission of Parvalbumin Interneurons in the Mouse Primary Motor Cortex. Eneuro *7*, ENEURO.0081-20.2020.

Cousineau, J., Plateau, V., Baufreton, J., and Le Bon-Jégo, M. (2022). Dopaminergic modulation of primary motor cortex: From cellular and synaptic mechanisms underlying motor learning to cognitive symptoms in Parkinson's disease. Neurobiol. Dis. *167*, 105674.

Daaka, Y., Luttrell, L.M., and Lefkowitz, R.J. (1997). Switching of the coupling of the β2-adrenergic receptor to different G proteins by protein kinase A. Nature *390*, 88–91.

Dahal, S., Chitti, S.V.P., Nair, M.P.N., and Saxena, S.K. (2015). Interactive effects of cocaine on HIV infection: implication in HIV-associated neurocognitive disorder and neuroAIDS. Front. Microbiol. *6*, 1–7.

Darling, W.G., Pizzimenti, M.A., and Morecraft, R.J. (2011). Functional recovery following motor cortex lesions in non-human primates : experimental implications for human stroke patients. J. Integr. Neurosci. *10*, 353–384.

Dearry, A., Gingrich, J.A., Falardeau, P., Fremeau, R.T., Bates, M.D., and Caron, M.G. (1990). Molecular cloning and expression of the gene for a human D1 dopamine receptor. Nature *347*, 72–76.

DeFelipe, J. (1997). Types of neurons synaptic connections and chemical characteristics of cells. J. Chem. Neuroanat. *14*, 1–19.

Degos, B., Deniau, J.-M., Chavez, M., and Maurice, N. (2013). Subthalamic Nucleus High-Frequency Stimulation Restores Altered Electrophysiological Properties of Cortical Neurons in Parkinsonian Rat. PLoS One *8*, e83608.

Del'Guidice, T. (2011). Role of beta-arrestin 2 downstream of dopamine receptors in the basal ganglia. Front. Neuroanat. *5*, 1–11.

Descarries, L., Lemay, B., Doucet, G., and Berger, B. (1987). Regional and laminar density of the dopamine innervation in adult rat cerebral cortex. Neuroscience *21*, 807–824.

Diana, M., Pistis, M., Carboni, S., Gessa, G.L., and Rossetti, Z.L. (1993). Profound decrement of mesolimbic dopaminergic neuronal activity during ethanol withdrawal syndrome in rats: electrophysiological and biochemical evidence. Proc. Natl. Acad. Sci. *90*, 7966–7969.

Digilio, L., Yap, C.C., and Winckler, B. (2015). Ctip2-, Satb2-, Prox1-, and GAD65-Expressing Neurons in Rat Cultures: Preponderance of Single- and Double-Positive Cells, and Cell Type-Specific Expression of Neuron-Specific Gene Family Members, Nsg-1 (NEEP21) and Nsg-2 (P19). PLoS One *10*, e0140010.

Dittrich, L., Heiss, J.E., Warrier, D.R., Perez, X.A., Quik, M., and Kilduff, T.S. (2012). Cortical nNOS neurons co-express the NK1 receptor and are depolarized by Substance P in multiple mammalian species. Front. Neural Circuits *6*, 1–11.

Dong, Y., Green, T., Saal, D., Marie, H., Neve, R., Nestler, E.J., and Malenka, R.C. (2006).

CREB modulates excitability of nucleus accumbens neurons. Nat. Neurosci. *9*, 475–477.

Donoghue, J.P., and Kitai, S.T. (1981). A collateral pathway to the neostriatum from corticofugal neurons of the rat sensory-motor cortex: An intracellular HRP study. J. Comp. Neurol. *201*, 1–13.

Donoghue, J.P., and Wise, S.P. (1982). The motor cortex of the rat: Cytoarchitecture and microstimulation mapping. J. Comp. Neurol. *212*, 76–88.

Ebbesen, C.L., and Brecht, M. (2017). Motor cortex — to act or not to act? Nat. Rev. Neurosci. *18*, 694–705.

Eisenhofer, G., Åneman, A., Friberg, P., Hooper, D., Fåndriks, L., Lonroth, H., Hunyady, B., and Mezey, E. (1997). Substantial Production of Dopamine in the Human Gastrointestinal Tract. J. Clin. Endocrinol. Metab. *82*, 3864–3871.

Eisenhofer, G., Kopin, I.J., and Goldstein, D.S. (2004). Catecholamine Metabolism: A Contemporary View with Implications for Physiology and Medicine. Pharmacol. Rev. *56*, 331–349.

Ferguson, B.R., and Gao, W.-J. (2018). PV Interneurons: Critical Regulators of E/I Balance for Prefrontal Cortex-Dependent Behavior and Psychiatric Disorders. Front. Neural Circuits *12*, 1–13.

Fields, H.L., Hjelmstad, G.O., Margolis, E.B., and Nicola, S.M. (2007). Ventral Tegmental Area Neurons in Learned Appetitive Behavior and Positive Reinforcement. Annu. Rev. Neurosci. *30*, 289–316.

Ford, C.P., Mark, G.P., and Williams, J.T. (2006). Properties and Opioid Inhibition of Mesolimbic Dopamine Neurons Vary according to Target Location. J. Neurosci. *26*, 2788–2797.

Frazer, S., Prados, J., Niquille, M., Cadilhac, C., Markopoulos, F., Gomez, L., Tomasello, U., Telley, L., Holtmaat, A., Jabaudon, D., et al. (2017). Transcriptomic and anatomic parcellation of 5-HT3AR expressing cortical interneuron subtypes revealed by single-cell RNA sequencing. Nat. Commun. *8*, 14219.

Fremeau, R.T., Duncan, G.E., Fornaretto, M.G., Dearry, A., Gingrich, J.A., Breese, G.R., and Caron, M.G. (1991). Localization of D1 dopamine receptor mRNA in brain supports a role in cognitive, affective, and neuroendocrine aspects of dopaminergic neurotransmission. Proc. Natl. Acad. Sci. *88*, 3772–3776.

Fritsch, G., and Hitzig, E. (2009). Electric excitability of the cerebrum (Über die elektrische Erregbarkeit des Grosshirns). Epilepsy Behav. *15*, 123–130.

Froux, L., Le Bon-Jego, M., Miguelez, C., Normand, E., Morin, S., Fioramonti, S., Barresi, M., Frick, A., Baufreton, J., and Taupignon, A. (2018). D5 dopamine receptors control glutamatergic AMPA transmission between the motor cortex and subthalamic nucleus. Sci. Rep. *8*, 8858.

Gainetdinov, R.R., Sotnikova, T.D., Grekhova, T. V., and Rayevsky, K.S. (1996). In vivo evidence for preferential role of dopamine D3 receptor in the presynaptic regulation of dopamine release but not synthesis. Eur. J. Pharmacol. *308*, 261–269.

Gaspar, P., Bloch, B., and Moine, C. (1995). D1 and D2 Receptor Gene Expression in the Rat Frontal Cortex: Cellular Localization in Different Classes of Efferent Neurons. Eur. J. Neurosci.

7, 1050–1063.

Geisler, S., Derst, C., Veh, R.W., and Zahm, D.S. (2007). Glutamatergic Afferents of the Ventral Tegmental Area in the Rat. J. Neurosci. *27*, 5730–5743.

Gerfen, C.R., Economo, M.N., and Chandrashekar, J. (2018). Long distance projections of cortical pyramidal neurons. J. Neurosci. Res. *96*, 1467–1475.

Gessa, G.L., Muntoni, F., Collu, M., Vargiu, L., and Mereu, G. (1985). Low doses of ethanol activate dopaminergic neurons in the ventral tegmental area. Brain Res. *348*, 201–203.

Giros, B., Jaber, M., Jones, S.R., Wightman, R.M., and Caron, M.G. (1996). Hyperlocomotion and indifference to cocaine and amphetamine in mice lacking the dopamine transporter. Nature *379*, 606–612.

Greig, L.C., Woodworth, M.B., Galazo, M.J., Padmanabhan, H., and Macklis, J.D. (2013). Molecular logic of neocortical projection neuron specification, development and diversity. Nat. Rev. Neurosci. *14*, 755–769.

Guo, L., Xiong, H., Kim, J.-I., Wu, Y.-W., Lalchandani, R.R., Cui, Y., Shu, Y., Xu, T., and Ding, J.B. (2015). Dynamic rewiring of neural circuits in the motor cortex in mouse models of Parkinson's disease. Nat. Neurosci. *18*, 1299–1309.

Harb, K., Magrinelli, E., Nicolas, C.S., Lukianets, N., Frangeul, L., Pietri, M., Sun, T., Sandoz, G., Grammont, F., Jabaudon, D., et al. (2016). Area-specific development of distinct projection neuron subclasses is regulated by postnatal epigenetic modifications. Elife *5*, 1–25.

Harris, K.D., and Shepherd, G.M.G. (2015). The neocortical circuit: themes and variations. Nat. Neurosci. *18*, 170–181.

Hattox, A.M., and Nelson, S.B. (2007). Layer V Neurons in Mouse Cortex Projecting to Different Targets Have Distinct Physiological Properties. J. Neurophysiol. *98*, 3330–3340.

Hédou, G., Chasserot-Golaz, S., Kemmel, V., Gobaille, S., Roussel, G., Artault, J.-C., Andriamampandry, C., Aunis, D., and Maitre, M. (2000). Immunohistochemical studies of the localization of neurons containing the enzyme that synthesizes dopamine, GABA, or ?-hydroxybutyrate in the rat substantia nigra and striatum. J. Comp. Neurol. *426*, 549–560.

Hegarty, S. V., Sullivan, A.M., and O'Keeffe, G.W. (2013). Midbrain dopaminergic neurons: A review of the molecular circuitry that regulates their development. Dev. Biol. *379*, 123–138.

Hnasko, T.S., Chuhma, N., Zhang, H., Goh, G.Y., Sulzer, D., Palmiter, R.D., Rayport, S., and Edwards, R.H. (2010). Vesicular Glutamate Transport Promotes Dopamine Storage and Glutamate Corelease In Vivo. Neuron *65*, 643–656.

Hnasko, T.S., Hjelmstad, G.O., Fields, H.L., and Edwards, R.H. (2012). Ventral Tegmental Area Glutamate Neurons: Electrophysiological Properties and Projections. J. Neurosci. *32*, 15076–15085.

van Holstein, M., Aarts, E., van der Schaaf, M.E., Geurts, D.E.M., Verkes, R.J., Franke, B., van Schouwenburg, M.R., and Cools, R. (2011). Human cognitive flexibility depends on dopamine D2 receptor signaling. Psychopharmacology (Berl). *218*, 567–578.

Hosp, J.A., Molina-Luna, K., Hertler, B., Atiemo, C.O., and Luft, A.R. (2009). Dopaminergic Modulation of Motor Maps in Rat Motor Cortex: An In Vivo Study. Neuroscience *159*, 692–700.

Hosp, J.A., Pekanovic, A., Rioult-Pedotti, M.S., and Luft, A.R. (2011). Dopaminergic Projections from Midbrain to Primary Motor Cortex Mediate Motor Skill Learning. J. Neurosci. *31*, 2481–2487.

Hosp, J.A., Nolan, H.E., and Luft, A.R. (2015). Topography and collateralization of dopaminergic projections to primary motor cortex in rats. Exp. Brain Res. *233*, 1365–1375.

Hu, H., Gan, J., and Jonas, P. (2014). Fast-spiking, parvalbumin+ GABAergic interneurons: From cellular design to microcircuit function. Science (80-.). *345*, 1255263–1255263.

Huang, R., Griffin, S.A., Taylor, M., Vangveravong, S., Mach, R.H., Dillon, G.H., and Luedtke, R.R. (2013a). The Effect of SV 293, a D2 Dopamine Receptor-Selective Antagonist, on D2 Receptor-Mediated GIRK Channel Activation and Adenylyl Cyclase Inhibition. Pharmacology *92*, 84–89.

Huang, X.-F., Zavitsanou, K., Huang, X., Yu, Y., Wang, H., Chen, F., Lawrence, A.J., and Deng, C. (2006). Dopamine transporter and D2 receptor binding densities in mice prone or resistant to chronic high fat diet-induced obesity. Behav. Brain Res. *175*, 415–419.

Huang, Y., Song, N.-N., Lan, W., Hu, L., Su, C.-J., Ding, Y.-Q., and Zhang, L. (2013b). Expression of Transcription Factor Satb2 in Adult Mouse Brain. Anat. Rec. *296*, 452–461.

Huntley, G.W., Morrison, J.H., Prikhozhan, A., and Sealfon, S.C. (1992). Localization of multiple dopamine receptor subtype mRNAs in human and monkey motor cortex and striatum. Mol. Brain Res. *15*, 181–188.

Hur, E.E., and Zaborszky, L. (2005). Vglut2 afferents to the medial prefrontal and primary somatosensory cortices: A combined retrograde tracing in situ hybridization. J. Comp. Neurol. *483*, 351–373.

Isaacson, J.S., and Scanziani, M. (2011). How Inhibition Shapes Cortical Activity. Neuron *72*, 231–243.

Isomura, Y., Harukuni, R., Takekawa, T., Aizawa, H., and Fukai, T. (2009). Microcircuitry coordination of cortical motor information in self-initiation of voluntary movements. Nat. Neurosci. *12*, 1586–1593.

Jiang, X., Shen, S., Cadwell, C.R., Berens, P., Sinz, F., Ecker, A.S., Patel, S., and Tolias, A.S. (2015). Principles of connectivity among morphologically defined cell types in adult neocortex. Science (80-.). *350*.

Johnson, P.M., and Kenny, P.J. (2010). Dopamine D2 receptors in addiction-like reward dysfunction and compulsive eating in obese rats. Nat. Neurosci. *13*, 635–641.

Joseph, J.., Wang, Y.-M., Miles, P.., Budygin, E.., Picetti, R., Gainetdinov, R.., Caron, M.., and Wightman, R.. (2002). Dopamine autoreceptor regulation of release and uptake in mouse brain slices in the absence of D3 receptors. Neuroscience *112*, 39–49.

Juarez, B., and Han, M.-H. (2016). Diversity of Dopaminergic Neural Circuits in Response to Drug Exposure. Neuropsychopharmacology *41*, 2424–2446.

Juárez Olguín, H., Calderón Guzmán, D., Hernández García, E., and Barragán Mejía, G. (2016). The Role of Dopamine and Its Dysfunction as a Consequence of Oxidative Stress. Oxid. Med. Cell. Longev. *2016*, 1–13.

Kabanova, A., Pabst, M., Lorkowski, M., Braganza, O., Boehlen, A., Nikbakht, N., Pothmann, L., Vaswani, A.R., Musgrove, R., Di Monte, D.A., et al. (2015). Function and developmental

origin of a mesocortical inhibitory circuit. Nat. Neurosci. *18*, 872–882.

Kawaguchi, Y. (1997). GABAergic cell subtypes and their synaptic connections in rat frontal cortex. Cereb. Cortex *7*, 476–486.

Kawaguchi, Y., and Kubota, Y. (1998). Neurochemical features and synaptic connections of large physiologically-identified GABAergic cells in the rat frontal cortex. Neuroscience *85*, 677–701.

Kawai, R., Markman, T., Poddar, R., Ko, R., Fantana, A.L., Dhawale, A.K., Kampff, A.R., and Ölveczky, B.P. (2015). Motor Cortex Is Required for Learning but Not for Executing a Motor Skill. Neuron *86*, 800–812.

Kim, J.-I., Ganesan, S., Luo, S.X., Wu, Y.-W., Park, E., Huang, E.J., Chen, L., and Ding, J.B. (2015). Aldehyde dehydrogenase 1a1 mediates a GABA synthesis pathway in midbrain dopaminergic neurons. Science (80-.). *350*, 102–106.

Kisvárday, Z.F., Beaulieu, C., and Eysel, U.T. (1993). Network of GABAergic large basket cells in cat visual cortex (area 18): Implication for lateral disinhibition. J. Comp. Neurol. *327*, 398–415.

Kita, T., and Kita, H. (2012). The subthalamic nucleus is one of multiple innervation sites for long-range corticofugal axons: A single-axon tracing study in the rat. J. Neurosci. *32*, 5990–5999.

Klein, A., Sacrey, L.-A.R., Whishaw, I.Q., and Dunnett, S.B. (2012). The use of rodent skilled reaching as a translational model for investigating brain damage and disease. Neurosci. Biobehav. Rev. *36*, 1030–1042.

Kopin, I.J. (1968). Biosynthesis and Metabolism of Catecholamines. Anesthesiology *29*, 654–660.

de la Crompe, B. de la, Aristieta, A., Leblois, A., Elsherbiny, S., Boraud, T., and Mallet, N.P. (2020). The globus pallidus orchestrates abnormal network dynamics in a model of Parkinsonism. Nat. Commun. *11*, 1570.

Lammel, S., Hetzel, A., Häckel, O., Jones, I., Liss, B., and Roeper, J. (2008). Unique Properties of Mesoprefrontal Neurons within a Dual Mesocorticolimbic Dopamine System. Neuron *57*, 760–773.

Lammel, S., Lim, B.K., Ran, C., Huang, K.W., Betley, M.J., Tye, K.M., Deisseroth, K., and Malenka, R.C. (2012). Input-specific control of reward and aversion in the ventral tegmental area. Nature *491*, 212–217.

Lavin, A., Nogueira, L., Lapish, C.C., Wightman, R.M., Phillips, P.E.M., and Seamans, J.K. (2005). Mesocortical dopamine neurons operate in distinct temporal domains using multimodal signaling. J. Neurosci. *25*, 5013–5023.

Lee, M.R. (1993). Dopamine and the Kidney: Ten Years on. Clin. Sci. *84*, 357–375.

Lee, C.R., and Tepper, J.M. (2009). Basal Ganglia Control of Substantia Nigra Dopaminergic Neurons. In Birth, Life and Death of Dopaminergic Neurons in the Substantia Nigra, G. Giovanni, V. Di Matteo, and E. Esposito, eds. (Vienna: Springer Vienna), pp. 71–90.

Lee, S.-H., Marchionni, I., Bezaire, M., Varga, C., Danielson, N., Lovett-Barron, M., Losonczy, A., and Soltesz, I. (2014). Parvalbumin-Positive Basket Cells Differentiate among Hippocampal Pyramidal Cells. Neuron *82*, 1129–1144.

Leemburg, S., Canonica, T., and Luft, A. (2018). Motor skill learning and reward consumption differentially affect VTA activation. Sci. Rep. *8*, 687.

Lei, W. (2004). Evidence for Differential Cortical Input to Direct Pathway versus Indirect Pathway Striatal Projection Neurons in Rats. J. Neurosci. *24*, 8289–8299.

Leslie, C.A., Robertson, M.W., Cutler, A.J., and Bennett, J.P. (1991). Postnatal development of D 1 dopamine receptors in the medial prefrontal cortex, striatum and nucleus accumbens of normal and neonatal 6-hydroxydopamine treated rats: a quantitative autoradiographic analysis. Dev. Brain Res. *62*, 109–114.

Levin, E.D., and Rose, J.E. (1995). Acute and Chronic Nicotinic Interactions with Dopamine Systems and Working Memory Performancea. Ann. N. Y. Acad. Sci. *757*, 245–252.

Levy, S., Lavzin, M., Benisty, H., Ghanayim, A., Dubin, U., Achvat, S., Brosh, Z., Aeed, F., Mensh, B.D., Schiller, Y., et al. (2020). Cell-Type-Specific Outcome Representation in the Primary Motor Cortex. Neuron *107*, 954-971.e9.

Lewis, D., Campbell, M., Foote, S., Goldstein, M., and Morrison, J. (1987). The distribution of tyrosine hydroxylase-immunoreactive fibers in primate neocortex is widespread but regionally specific. J. Neurosci. *7*, 279–290.

Lewis, D.A., Melchitzky, D.S., Sesack, S.R., Whitehead, R.E., Sungyoung Auh, and Sampson, A. (2001). Dopamine transporter immunoreactivity in monkey cerebral cortex: Regional, laminar, and ultrastructural localization. J. Comp. Neurol. *432*, 119–136.

Leyton, A.S.F., and Sherrington, C.S. (1917). Observations on the excitable cortex of the chimpanzee, orang-utan, and gorilla. Q. J. Exp. Physiol. *11*, 135–222.

Li, M., Wang, X., Yao, X., Wang, X., Chen, F., Zhang, X., Sun, S., He, F., Jia, Q., Guo, M., et al. (2021). Roles of Motor Cortex Neuron Classes in Reach-Related Modulation for Hemiparkinsonian Rats. Front. Neurosci. *15*, 1–23.

Li, Q., Ko, H., Qian, Z.-M., Yan, L.Y.C., Chan, D.C.W., Arbuthnott, G., Ke, Y., and Yung, W.-H. (2017). Refinement of learned skilled movement representation in motor cortex deep output layer. Nat. Commun. *8*, 15834.

Li, X., Qi, J., Yamaguchi, T., Wang, H.-L., and Morales, M. (2013). Heterogeneous composition of dopamine neurons of the rat A10 region: molecular evidence for diverse signaling properties. Brain Struct. Funct. *218*, 1159–1176.

Lickiss, T., Cheung, A.F.P., Hutchinson, C.E., Taylor, J.S.H., and Molnár, Z. (2012). Examining the relationship between early axon growth and transcription factor expression in the developing cerebral cortex. J. Anat. *220*, 201–211.

Lim, L., Mi, D., Llorca, A., and Marín, O. (2018). Development and Functional Diversification of Cortical Interneurons. Neuron *100*, 294–313.

Lin, Y., Jover-Mengual, T., Wong, J., Bennett, M.V.L., and Zukin, R.S. (2006). PSD-95 and PKC converge in regulating NMDA receptor trafficking and gating. Proc. Natl. Acad. Sci. *103*, 19902–19907.

Lisman, J., Grace, A.A., and Duzel, E. (2011). A neoHebbian framework for episodic memory; role of dopamine-dependent late LTP. Trends Neurosci. *34*, 536–547.

Lisman, J., Yasuda, R., and Raghavachari, S. (2012). Mechanisms of CaMKII action in long-term potentiation. Nat. Rev. Neurosci. *13*, 169–182.

Liss, B., and Roeper, J. (2008). Individual dopamine midbrain neurons: Functional diversity and flexibility in health and disease. Brain Res. Rev. *58*, 314–321.

Liss, B., Haeckel, O., Wildmann, J., Miki, T., Seino, S., and Roeper, J. (2005). K-ATP channels promote the differential degeneration of dopaminergic midbrain neurons. Nat. Neurosci. *8*, 1742–1751.

Liu, C., Kershberg, L., Wang, J., Schneeberger, S., and Kaeser, P.S. (2018). Dopamine Secretion Is Mediated by Sparse Active Zone-like Release Sites. Cell *172*, 706-718.e15.

Lohoff, F.W., Carr, G. V., Brookshire, B., Ferraro, T.N., and Lucki, I. (2019). Deletion of the vesicular monoamine transporter 1 (vmat1/slc18a1) gene affects dopamine signaling. Brain Res. *1712*, 151–157.

Lohse, M.J., Benovic, J.L., Caron, M.G., and Lefkowitz, R.J. (1990). Multiple pathways of rapid beta 2-adrenergic receptor desensitization. Delineation with specific inhibitors. J. Biol. Chem. *265*, 3202-3209b.

Lopez de Armentia, M., Jancic, D., Olivares, R., Alarcon, J.M., Kandel, E.R., and Barco, A. (2007). cAMP Response Element-Binding Protein-Mediated Gene Expression Increases the Intrinsic Excitability of CA1 Pyramidal Neurons. J. Neurosci. *27*, 13909–13918.

Lu, W.-Y., Xiong, Z.-G., Lei, S., Orser, B.A., Dudek, E., Browning, M.D., and MacDonald, J.F. (1999). G-protein-coupled receptors act via protein kinase C and Src to regulate NMDA receptors. Nat. Neurosci. *2*, 331–338.

Luttrell, L.M., Roudabush, F.L., Choy, E.W., Miller, W.E., Field, M.E., Pierce, K.L., and Lefkowitz, R.J. (2001). Activation and targeting of extracellular signal-regulated kinases by β-arrestin scaffolds. Proc. Natl. Acad. Sci. *98*, 2449–2454.

Maldonado, R., Robledo, P., Chover, A.J., Caine, S.B., and Koob, G.F. (1993). D1 dopamine receptors in the nucleus accumbens modulate cocaine self-administration in the rat. Pharmacol. Biochem. Behav. *45*, 239–242.

Mallet, N., Pogosyan, A., Sharott, A., Csicsvari, J., Bolam, J.P., Brown, P., and Magill, P.J. (2008). Disrupted Dopamine Transmission and the Emergence of Exaggerated Beta Oscillations in Subthalamic Nucleus and Cerebral Cortex. J. Neurosci. *28*, 4795–4806.

Mannoury la Cour, C., Vidal, S., Pasteau, V., Cussac, D., and Millan, M.J. (2007). Dopamine D1 receptor coupling to Gs/olf and Gq in rat striatum and cortex: A scintillation proximity assay (SPA)/antibody-capture characterization of benzazepine agonists. Neuropharmacology *52*, 1003–1014.

Mansour, A., Meador-Woodruff, J., Bunzow, J., Civelli, O., Akil, H., and Watson, S. (1990). Localization of dopamine D2 receptor mRNA and D1 and D2 receptor binding in the rat brain and pituitary: an in situ hybridization- receptor autoradiographic analysis. J. Neurosci. *10*, 2587–2600.

Markram, H., Toledo-Rodriguez, M., Wang, Y., Gupta, A., Silberberg, G., and Wu, C. (2004). Interneurons of the neocortical inhibitory system. Nat. Rev. Neurosci. *5*, 793–807.

Matsui, A., and Williams, J.T. (2011). Opioid-Sensitive GABA Inputs from Rostromedial Tegmental Nucleus Synapse onto Midbrain Dopamine Neurons. J. Neurosci. *31*, 17729–17735.

McKenna, W.L., Betancourt, J., Larkin, K.A., Abrams, B., Guo, C., Rubenstein, J.L.R., and Chen, B. (2011). Tbr1 and Fezf2 Regulate Alternate Corticofugal Neuronal Identities during

Neocortical Development. J. Neurosci. *31*, 549–564.

Meador-Woodruff, J.H., Mansour, A., Grandy, D.K., Damask, S.P., Civelli, O., and Watson, S.J. (1992). Distribution of D5 dopamine receptor mRNA in rat brain. Neurosci. Lett. *145*, 209–212.

Melani, R., and Tritsch, N.X. (2022). Inhibitory co-transmission from midbrain dopamine neurons relies on presynaptic GABA uptake. Cell Rep. *39*, 110716.

Melzer, S., Gil, M., Koser, D.E., Michael, M., Huang, K.W., and Monyer, H. (2017). Distinct Corticostriatal GABAergic Neurons Modulate Striatal Output Neurons and Motor Activity. Cell Rep. *19*, 1045–1055.

Mezey, E., Eisenhofer, G., Harta, G., Hansson, S., Gould, L., Hunyady, B., and Hoffman, B.J. (1996). A novel nonneuronal catecholaminergic system: exocrine pancreas synthesizes and releases dopamine. Proc. Natl. Acad. Sci. *93*, 10377–10382.

Miller, M.N., Okaty, B.W., and Nelson, S.B. (2008). Region-Specific Spike-Frequency Acceleration in Layer 5 Pyramidal Neurons Mediated by Kv1 Subunits. J. Neurosci. *28*, 13716–13726.

Missale, C., Nash, S.R., Robinson, S.W., Jaber, M., and Caron, M.G. (1998). Dopamine Receptors: From Structure to Function. Physiol. Rev. *78*, 189–225.

Miyoshi, G., Hjerling-Leffler, J., Karayannis, T., Sousa, V.H., Butt, S.J.B., Battiste, J., Johnson, J.E., Machold, R.P., and Fishell, G. (2010). Genetic Fate Mapping Reveals That the Caudal Ganglionic Eminence Produces a Large and Diverse Population of Superficial Cortical Interneurons. J. Neurosci. *30*, 1582–1594.

Le Moine, C., and Bloch, B. (1996). Expression of the d3 dopamine receptor in peptidergic neurons of the nucleus accumbens: Comparison with the D1 and D2 dopamine receptors. Neuroscience *73*, 131–143.

Le Moine, C., and Gaspar, P. (1998). Subpopulations of cortical GABAergic interneurons differ by their expression of D1 and D2 dopamine receptor subtypes. Mol. Brain Res. *58*, 231–236.

Molina-Luna, K., Pekanovic, A., Röhrich, S., Hertler, B., Schubring-Giese, M., Rioult-Pedotti, M.-S., and Luft, A.R. (2009). Dopamine in Motor Cortex Is Necessary for Skill Learning and Synaptic Plasticity. PLoS One *4*, e7082.

Molnár, Z., and Cheung, A.F.P. (2006). Towards the classification of subpopulations of layer V pyramidal projection neurons. Neurosci. Res. *55*, 105–115.

Monfils, M.H., Plautz, E.J., and Kleim, J.A. (2005). In Search of the Motor Engram: Motor Map Plasticity as a Mechanism for Encoding Motor Experience. Neurosci. *11*, 471–483.

Monsma, F.J., Mahan, L.C., McVittie, L.D., Gerfen, C.R., and Sibley, D.R. (1990). Molecular cloning and expression of a D1 dopamine receptor linked to adenylyl cyclase activation. Proc. Natl. Acad. Sci. *87*, 6723–6727.

Morales, M., and Margolis, E.B. (2017). Ventral tegmental area: cellular heterogeneity, connectivity and behaviour. Nat. Rev. Neurosci. *18*, 73–85.

Morishima, M. (2006). Recurrent Connection Patterns of Corticostriatal Pyramidal Cells in Frontal Cortex. J. Neurosci. *26*, 4394–4405.

Myöhänen, T.T., Schendzielorz, N., and Männistö, P.T. (2010). Distribution of catechol-O-

methyltransferase (COMT) proteins and enzymatic activities in wild-type and soluble COMT deficient mice. J. Neurochem. *113*, no-no.

Nakakuki, T., Birtwistle, M.R., Saeki, Y., Yumoto, N., Ide, K., Nagashima, T., Brusch, L., Ogunnaike, B.A., Okada-Hatakeyama, M., and Kholodenko, B.N. (2010). Ligand-Specific c-Fos Expression Emerges from the Spatiotemporal Control of ErbB Network Dynamics. Cell *141*, 884–896.

Nakamura, T., Rios, L.C., Yagi, T., Sasaoka, T., and Kitsukawa, T. (2020). Dopamine D1 and muscarinic acetylcholine receptors in dorsal striatum are required for high speed running. Neurosci. Res. *156*, 50–57.

Nambu, A., Tachibana, Y., and Chiken, S. (2015). Cause of parkinsonian symptoms: Firing rate, firing pattern or dynamic activity changes? Basal Ganglia *5*, 1–6.

Narla, C., Scidmore, T., Jeong, J., Everest, M., Chidiac, P., and Poulter, M.O. (2016). A switch in G protein coupling for type 1 corticotropin-releasing factor receptors promotes excitability in epileptic brains. Sci. Signal. *9*, 1–10.

Nedergaard, S. (2004). A Ca2+-independent slow afterhyperpolarization in substantia nigra compacta neurons. Neuroscience *125*, 841–852.

Nieh, E.H., Matthews, G.A., Allsop, S.A., Presbrey, K.N., Leppla, C.A., Wichmann, R., Neve, R., Wildes, C.P., and Tye, K.M. (2015). Decoding neural circuits that control compulsive sucrose seeking. Cell *160*, 528–541.

Nieh, E.H., Vander Weele, C.M., Matthews, G.A., Presbrey, K.N., Wichmann, R., Leppla, C.A., Izadmehr, E.M., and Tye, K.M. (2016). Inhibitory Input from the Lateral Hypothalamus to the Ventral Tegmental Area Disinhibits Dopamine Neurons and Promotes Behavioral Activation. Neuron *90*, 1286–1298.

Nielsen, J. V., Thomassen, M., Møllgård, K., Noraberg, J., and Jensen, N.A. (2014). Zbtb20 Defines a Hippocampal Neuronal Identity Through Direct Repression of Genes That Control Projection Neuron Development in the Isocortex. Cereb. Cortex *24*, 1216–1229.

Nigro, M.J., Hashikawa-Yamasaki, Y., and Rudy, B. (2018). Diversity and Connectivity of Layer 5 Somatostatin-Expressing Interneurons in the Mouse Barrel Cortex. J. Neurosci. *38*, 1622–1633.

Nyberg, L., Karalija, N., Salami, A., Andersson, M., Wåhlin, A., Kaboovand, N., Köhncke, Y., Axelsson, J., Rieckmann, A., Papenberg, G., et al. (2016). Dopamine D2 receptor availability is linked to hippocampal–caudate functional connectivity and episodic memory. Proc. Natl. Acad. Sci. *113*, 7918–7923.

Ohbayashi, M. (2020). Inhibition of protein synthesis in M1 of monkeys disrupts performance of sequential movements guided by memory. Elife *9*, 1–20.

Oláh, S. (2007). Output of neurogliaform cells to various neuron types in the human and rat cerebral cortex. Front. Neural Circuits *1*, 1–7.

Omelchenko, N., and Sesack, S.R. (2009). Periaqueductal gray afferents synapse onto dopamine and GABA neurons in the rat ventral tegmental area. J. Neurosci. Res. *88*, NA-NA.

Ono, Y., Nakatani, T., Sakamoto, Y., Mizuhara, E., Minaki, Y., Kumai, M., Hamaguchi, A., Nishimura, M., Inoue, Y., Hayashi, H., et al. (2007). Differences in neurogenic potential in floor plate cells along an anteroposterior location: midbrain dopaminergic neurons originate

from mesencephalic floor plate cells. Development *134*, 3213–3225.

Oswald, M.J., Tantirigama, M.L.S., Sonntag, I., Hughes, S.M., and Empson, R.M. (2013). Diversity of layer 5 projection neurons in the mouse motor cortex. Front. Cell. Neurosci. *7*, 1–18.

Ott, T., and Nieder, A. (2019). Dopamine and Cognitive Control in Prefrontal Cortex. Trends Cogn. Sci. *23*, 213–234.

Packard, M.G., and White, N.M. (1991). Dissociation of hippocampus and caudate nucleus memory systems by posttraining intracerebral injection of dopamine agonists. Behav. Neurosci. *105*, 295–306.

Pahuja, R., Seth, K., Shukla, A., Shukla, R.K., Bhatnagar, P., Chauhan, L.K.S., Saxena, P.N., Arun, J., Chaudhari, B.P., Patel, D.K., et al. (2015). Trans-Blood Brain Barrier Delivery of Dopamine-Loaded Nanoparticles Reverses Functional Deficits in Parkinsonian Rats. ACS Nano *9*, 4850–4871.

Parent, M., and Parent, A. (2006). Single-axon tracing study of corticostriatal projections arising from primary motor cortex in primates. J. Comp. Neurol. *496*, 202–213.

Parr-Brownlie, L.C. (2005). Bradykinesia Induced by Dopamine D2 Receptor Blockade Is Associated with Reduced Motor Cortex Activity in the Rat. J. Neurosci. *25*, 5700–5709.

Patel, K.R., Cherian, J., Gohil, K., and Atkinson, D. (2014). Schizophrenia: overview and treatment options. P T *39*, 638–645.

Patriarchi, T., Cho, J.R., Merten, K., Howe, M.W., Marley, A., Xiong, W.-H., Folk, R.W., Broussard, G.J., Liang, R., Jang, M.J., et al. (2018). Ultrafast neuronal imaging of dopamine dynamics with designed genetically encoded sensors. Science (80-.). *360*, eaat4422.

Penfield, W., and Boldrey, E. (1937). Somatic motor and sensory representation in the cerebral cortex of man as studied by electrical stimulation. Brain *60*, 389–443.

Pereira Luppi, M., Azcorra, M., Caronia-Brown, G., Poulin, J.-F., Gaertner, Z., Gatica, S., Moreno-Ramos, O.A., Nouri, N., Dubois, M., Ma, Y.C., et al. (2021). Sox6 expression distinguishes dorsally and ventrally biased dopamine neurons in the substantia nigra with distinctive properties and embryonic origins. Cell Rep. *37*, 109975.

Poulin, J.-F., Zou, J., Drouin-Ouellet, J., Kim, K.-Y.A., Cicchetti, F., and Awatramani, R.B. (2014). Defining Midbrain Dopaminergic Neuron Diversity by Single-Cell Gene Expression Profiling. Cell Rep. *9*, 930–943.

Poulin, J.-F., Caronia, G., Hofer, C., Cui, Q., Helm, B., Ramakrishnan, C., Chan, C.S., Dombeck, D.A., Deisseroth, K., and Awatramani, R. (2018). Mapping projections of molecularly defined dopamine neuron subtypes using intersectional genetic approaches. Nat. Neurosci. *21*, 1260–1271.

Prönneke, A., Scheuer, B., Wagener, R.J., Möck, M., Witte, M., and Staiger, J.F. (2015). Characterizing VIP Neurons in the Barrel Cortex of VIPcre/tdTomato Mice Reveals Layer-Specific Differences. Cereb. Cortex *25*, 4854–4868.

Puig, M.V., and Miller, E.K. (2015). Neural Substrates of Dopamine D2 Receptor Modulated Executive Functions in the Monkey Prefrontal Cortex. Cereb. Cortex *25*, 2980–2987.

Qi, J., Zhang, S., Wang, H.-L., Wang, H., de Jesus Aceves Buendia, J., Hoffman, A.F., Lupica, C.R., Seal, R.P., and Morales, M. (2014). A glutamatergic reward input from the dorsal raphe

to ventral tegmental area dopamine neurons. Nat. Commun. *5*, 5390.

Raghanti, M.A., Stimpson, C.D., Marcinkiewicz, J.L., Erwin, J.M., Hof, P.R., and Sherwood, C.C. (2008). Cortical dopaminergic innervation among humans, chimpanzees, and macaque monkeys: a comparative study. Neuroscience *155*, 203–220.

Rani, M., and Kanungo, M.S. (2006). Expression of D2 dopamine receptor in the mouse brain. Biochem. Biophys. Res. Commun. *344*, 981–986.

Rioult-Pedotti, M.-S., Pekanovic, A., Atiemo, C.O., Marshall, J., and Luft, A.R. (2015). Dopamine Promotes Motor Cortex Plasticity and Motor Skill Learning via PLC Activation. PLoS One *10*, e0124986.

Rosenbaum, D.M., Rasmussen, S.G.F., and Kobilka, B.K. (2009). The structure and function of G-protein-coupled receptors. Nature *459*, 356–363.

Rudy, B., and McBain, C.J. (2001). Kv3 channels: voltage-gated K+ channels designed for high-frequency repetitive firing. Trends Neurosci. *24*, 517–526.

Rudy, B., Fishell, G., Lee, S., and Hjerling-Leffler, J. (2011). Three groups of interneurons account for nearly 100% of neocortical GABAergic neurons. Dev. Neurobiol. *71*, 45–61.

Saucedo-Cardenas, O., Quintana-Hau, J.D., Le, W.-D., Smidt, M.P., Cox, J.J., De Mayo, F., Burbach, J.P.H., and Conneely, O.M. (1998). Nurr1 is essential for the induction of the dopaminergic phenotype and the survival of ventral mesencephalic late dopaminergic precursor neurons. Proc. Natl. Acad. Sci. *95*, 4013–4018.

Schuldiner, S., Shirvan, A., and Linial, M. (1995). Vesicular neurotransmitter transporters: from bacteria to humans. Physiol. Rev. *75*, 369–392.

Sheets, P.L., Suter, B.A., Kiritani, T., Chan, C.S., Surmeier, D.J., and Shepherd, G.M.G. (2011). Corticospinal-specific HCN expression in mouse motor cortex: I h -dependent synaptic integration as a candidate microcircuit mechanism involved in motor control. J. Neurophysiol. *106*, 2216–2231.

Shen, L.H., Liao, M.H., and Tseng, Y.C. (2012). Recent advances in imaging of dopaminergic neurons for evaluation of neuropsychiatric disorders. J. Biomed. Biotechnol. *2012*.

Shepherd, G.M.G. (2013). Corticostriatal connectivity and its role in disease. Nat. Rev. Neurosci. *14*, 278–291.

Shepherd, G.M.G., and Yamawaki, N. (2021). Untangling the cortico-thalamo-cortical loop: cellular pieces of a knotty circuit puzzle. Nat. Rev. Neurosci. *22*, 389–406.

Shipp, S. (2007). Structure and function of the cerebral cortex. Curr. Biol. *17*, R443–R449.

Sibley, D.R. (1999). New insights into dopaminergic receptor function using antisense and genetically altered animals. Annu. Rev. Pharmacol. Toxicol. *39*, 313–341.

Sidhu, A. (1998). Coupling of D1 and D5 dopamine receptors to multiple G proteins. Mol. Neurobiol. *16*, 125–134.

Sidhu, A., Sullivan, M., Kohout, T., Balen, P., and Fishman, P.H. (1991). D 1 Dopamine Receptors Can Interact with Both Stimulatory and Inhibitory Guanine Nucleotide Binding Proteins. J. Neurochem. *57*, 1445–1451.

Silberberg, G., and Markram, H. (2007). Disynaptic Inhibition between Neocortical Pyramidal

Cells Mediated by Martinotti Cells. Neuron *53*, 735–746.

Sirota, M.G. (2005). Three Channels of Corticothalamic Communication during Locomotion. J. Neurosci. *25*, 5915–5925.

Stoof, J.C., and Kebabian, J.W. (1981). Opposing roles for D-1 and D-2 dopamine receptors in efflux of cyclic AMP from rat neostriatum. Nature *294*, 366–368.

Stuber, G.D., Hnasko, T.S., Britt, J.P., Edwards, R.H., and Bonci, A. (2010). Dopaminergic Terminals in the Nucleus Accumbens But Not the Dorsal Striatum Corelease Glutamate. J. Neurosci. *30*, 8229–8233.

Subramaniam, M., and Roeper, J. (2016). Subtypes of Midbrain Dopamine Neurons. In Handbook of Behavioral Neuroscience, (Elsevier B.V.), pp. 317–334.

Sulzer, D., Joyce, M.P., Lin, L., Geldwert, D., Haber, S.N., Hattori, T., and Rayport, S. (1998). Dopamine Neurons Make Glutamatergic Synapses In Vitro. J. Neurosci. *18*, 4588–4602.

Sun, F., Zeng, J., Jing, M., Zhou, J., Feng, J., Owen, S.F., Luo, Y., Li, F., Wang, H., Yamaguchi, T., et al. (2018). A Genetically Encoded Fluorescent Sensor Enables Rapid and Specific Detection of Dopamine in Flies, Fish, and Mice. Cell *174*, 481-496.e19.

Sunahara, R.K., Niznik, H.B., Weiner, D.M., Stormann, T.M., Brann, M.R., Kennedy, J.L., Gelernter, J.E., Rozmahel, R., Yang, Y., Israel, Y., et al. (1990). Human dopamine D1 receptor encoded by an intronless gene on chromosome 5. Nature *347*, 80–83.

Sunahara, R.K., Guan, H.-C., O'Dowd, B.F., Seeman, P., Laurier, L.G., Ng, G., George, S.R., Torchia, J., Van Tol, H.H.M., and Niznik, H.B. (1991). Cloning of the gene for a human dopamine D5 receptor with higher affinity for dopamine than D1. Nature *350*, 614–619.

Sung, Y.K., Kyou, C.C., Min, S.C., Myoung, H.K., Sa, Y.K., Na, Y.S., Jong, E.L., Byung, K.J., Lee, B.H., and Baik, J.H. (2006). The dopamine D2 receptor regulates the development of dopaminergic neurons via extracellular signal-regulated kinase and Nurr1 activation. J. Neurosci. *26*, 4567–4576.

Surmeier, D.J. (2018). Determinants of dopaminergic neuron loss in Parkinson's disease. FEBS J. *285*, 3657–3668.

Svenningsson, P., and Le Moine, C. (2002). Dopamine D1/5 receptor stimulation induces c- fos expression in the subthalamic nucleus: possible involvement of local D5 receptors. Eur. J. Neurosci. *15*, 133–142.

Swanson, O.K., Semaan, R., and Maffei, A. (2020). Reduced dopamine signaling impacts pyramidal neuron excitability in mouse motor cortex. Eneuro ENEURO.0548-19.2021.

Swanson, O.K., Semaan, R., and Maffei, A. (2021). Reduced Dopamine Signaling Impacts Pyramidal Neuron Excitability in Mouse Motor Cortex. Eneuro *8*, ENEURO.0548-19.2021.

Taniguchi, H., Lu, J., and Huang, Z.J. (2013). The Spatial and Temporal Origin of Chandelier Cells in Mouse Neocortex. Science (80-.). *339*, 70–74.

Tarazi, F.I., Tomasini, E.C., and Baldessarini, R.J. (1998). Postnatal development of dopamine D4-like receptors in rat forebrain regions: comparison with D2-like receptors. Dev. Brain Res. *110*, 227–233.

Tarazi, F.I., Tomasini, E.C., and Baldessarini, R. (1999). Postnatal Development of Dopamine D_1-Like Receptors in Rat Cortical and Striatolimbic Brain Regions: An Autoradiographic

Study. Dev. Neurosci. *21*, 43–49.

Tecuapetla, F., Patel, J.C., Xenias, H., English, D., Tadros, I., Shah, F., Berlin, J., Deisseroth, K., Rice, M.E., Tepper, J.M., et al. (2010). Glutamatergic Signaling by Mesolimbic Dopamine Neurons in the Nucleus Accumbens. J. Neurosci. *30*, 7105–7110.

Tiberi, M., Jarvie, K.R., Silvia, C., Falardeau, P., Gingrich, J.A., Godinot, N., Bertrand, L., Yang-Feng, T.L., Fremeau, R.T., and Caron, M.G. (1991). Cloning, molecular characterization, and chromosomal assignment of a gene encoding a second D1 dopamine receptor subtype: differential expression pattern in rat brain compared with the D1A receptor. Proc. Natl. Acad. Sci. *88*, 7491–7495.

Van Tol, H.H.M., Bunzow, J.R., Guan, H.-C., Sunahara, R.K., Seeman, P., Niznik, H.B., and Civelli, O. (1991). Cloning of the gene for a human dopamine D4 receptor with high affinity for the antipsychotic clozapine. Nature *350*, 610–614.

Touvykine, B., Mansoori, B.K., Jean-Charles, L., Deffeyes, J., Quessy, S., and Dancause, N. (2016). The Effect of Lesion Size on the Organization of the Ipsilesional and Contralesional Motor Cortex. Neurorehabil. Neural Repair *30*, 280–292.

Tran, A.H., Tamura, R., Uwano, T., Kobayashi, T., Katsuki, M., and Ono, T. (2005). Dopamine D1 receptors involved in locomotor activity and accumbens neural responses to prediction of reward associated with place. Proc. Natl. Acad. Sci. *102*, 2117–2122.

Tritsch, N.X., Ding, J.B., and Sabatini, B.L. (2012). Dopaminergic neurons inhibit striatal output through non-canonical release of GABA. Nature *490*, 262–266.

Tritsch, N.X., Oh, W.-J., Gu, C., and Sabatini, B.L. (2014). Midbrain dopamine neurons sustain inhibitory transmission using plasma membrane uptake of GABA, not synthesis. Elife *3*, 1–20.

Tseng, K.-Y., and O'Donnell, P. (2006). Dopamine Modulation of Prefrontal Cortical Interneurons Changes during Adolescence. Cereb. Cortex *17*, 1235–1240.

Uhr, S.B., Pruitt, B., Berger, P.A., and Stahl, S.M. (1986). Improvement of Symptoms in Tourette Syndrome by Piquindone, A Novel Dopamine-2 Receptor Antagonist. Int. Clin. Psychopharmacol. *1*, 216–220.

Urs, N.M., Daigle, T.L., and Caron, M.G. (2011). A Dopamine D1 Receptor-Dependent β-Arrestin Signaling Complex Potentially Regulates Morphine-Induced Psychomotor Activation but not Reward in Mice. Neuropsychopharmacology *36*, 551–558.

Urs, N.M., Gee, S.M., Pack, T.F., McCorvy, J.D., Evron, T., Snyder, J.C., Yang, X., Rodriguiz, R.M., Borrelli, E., Wetsel, W.C., et al. (2016). Distinct cortical and striatal actions of a β-arrestin–biased dopamine D2 receptor ligand reveal unique antipsychotic-like properties. Proc. Natl. Acad. Sci. *113*, E8178–E8186.

Valjent, E., Corvol, J.-C., Trzaskos, J.M., Girault, J.-A., and Hervé, D. (2006). Role of the ERK pathway in psychostimulant-induced locomotor sensitization. BMC Neurosci. *7*, 20.

Vallone, D., Picetti, R., and Borrelli, E. (2000). Structure and function of dopamine receptors. Neurosci. Biobehav. Rev. *24*, 125–132.

Veenvliet, J. V., and Smidt, M.P. (2014). Molecular mechanisms of dopaminergic subset specification: fundamental aspects and clinical perspectives. Cell. Mol. Life Sci. *71*, 4703–4727.

Viosca, J., Lopez de Armentia, M., Jancic, D., and Barco, A. (2009). Enhanced CREB-

dependent gene expression increases the excitability of neurons in the basal amygdala and primes the consolidation of contextual and cued fear memory. Learn. Mem. *16*, 193–197.

Vitrac, C., Péron, S., Frappé, I., Fernagut, P.-O., Jaber, M., Gaillard, A., and Benoit-Marand, M. (2014). Dopamine control of pyramidal neuron activity in the primary motor cortex via D2 receptors. Front. Neural Circuits *8*, 1–8.

Wang, Y. (2002). Anatomical, Physiological, Molecular and Circuit Properties of Nest Basket Cells in the Developing Somatosensory Cortex. Cereb. Cortex *12*, 395–410.

Wang, H., and Pickel, V.M. (2002). Dopamine D2 receptors are present in prefrontal cortical afferents and their targets in patches of the rat caudate-putamen nucleus. J. Comp. Neurol. *442*, 392–404.

Wang, H.-L., Qi, J., Zhang, S., Wang, H., and Morales, M. (2015). Rewarding Effects of Optical Stimulation of Ventral Tegmental Area Glutamatergic Neurons. J. Neurosci. *35*, 15948–15954.

Wang, X., Liu, Y., Li, X., Zhang, Z., Yang, H., Zhang, Y., Williams, P.R., Alwahab, N.S.A., Kapur, K., Yu, B., et al. (2017). Deconstruction of Corticospinal Circuits for Goal-Directed Motor Skills. Cell *171*, 440-455.e14.

Wang, Y., Toledo-Rodriguez, M., Gupta, A., Wu, C., Silberberg, G., Luo, J., and Markram, H. (2004). Anatomical, physiological and molecular properties of Martinotti cells in the somatosensory cortex of the juvenile rat. J. Physiol. *561*, 65–90.

Watabe-Uchida, M., Zhu, L., Ogawa, S.K., Vamanrao, A., and Uchida, N. (2012). Whole-Brain Mapping of Direct Inputs to Midbrain Dopamine Neurons. Neuron *74*, 858–873.

Watanabe, Y., Kajiwara, R., and Takashima, I. (2009). Optical imaging of rat prefrontal neuronal activity evoked by stimulation of the ventral tegmental area. Neuroreport *20*, 875–880.

Weinshank, R.L., Adham, N., Macchi, M., Olsen, M.A., Branchek, T.A., and Hartig, P.R. (1991). Molecular cloning and characterization of a high affinity dopamine receptor (D1 beta) and its pseudogene. J. Biol. Chem. *266*, 22427–22435.

Weiss, F., Parsons, L.H., Schulteis, G., Hyytiä, P., Lorang, M.T., Bloom, F.E., and Koob, G.F. (1996). Ethanol Self-Administration Restores Withdrawal-Associated Deficiencies in Accumbal Dopamine and 5-Hydroxytryptamine Release in Dependent Rats. J. Neurosci. *16*, 3474–3485.

Westerink, R. (2006). Targeting Exocytosis: Ins and Outs of the Modulation of Quantal Dopamine Release. CNS Neurol. Disord. - Drug Targets *5*, 57–77.

Westlund, K.N., Krakower, T.J., Kwan, S.-W., and Abell, C.W. (1993). Intracellular distribution of monoamine oxidase A in selected regions of rat and monkey brain and spinal cord. Brain Res. *612*, 221–230.

Whishaw, I.Q. (2000). Loss of the innate cortical engram for action patterns used in skilled reaching and the development of behavioral compensation following motor cortex lesions in the rat. Neuropharmacology *39*, 788–805.

Whishaw, I.Q., O'Connor, Wi., and Dunnett, S.B. (1986). The contributions of motor cortex, nigrostriatal dopamine and caudate-putamen to skilled forelimb use in ratsT. Brain *109*, 805–843.

Williams, S. (1998). Widespread origin of the primate mesofrontal dopamine system. Cereb.

Cortex *8*, 321–345.

Wolf, M.E., and Roth, R.H. (1990). Autoreceptor Regulation of Dopamine Synthesis. Ann. N. Y. Acad. Sci. *604*, 323–343.

Wong, D.F., Singer, H.S., Brandt, J., Shaya, E., Chen, C., Brown, J., Kimball, A.W., Gjedde, A., Dannals, R.F., Ravert, H.T., et al. (1997). D2-like dopamine receptor density in Tourette syndrome measured by PET. J. Nucl. Med. *38*, 1243–1247.

Xia, Y., Driscoll, J.R., Wilbrecht, L., Margolis, E.B., Fields, H.L., and Hjelmstad, G.O. (2011). Nucleus Accumbens Medium Spiny Neurons Target Non-Dopaminergic Neurons in the Ventral Tegmental Area. J. Neurosci. *31*, 7811–7816.

Yaffe, D., Forrest, L.R., and Schuldiner, S. (2018). The ins and outs of vesicular monoamine transporters. J. Gen. Physiol. *150*, 671–682.

Yamaguchi, T., Sheen, W., and Morales, M. (2007). Glutamatergic neurons are present in the rat ventral tegmental area. Eur. J. Neurosci. *25*, 106–118.

Yamawaki, N., Borges, K., Suter, B.A., Harris, K.D., and Shepherd, G.M.G. (2014). A genuine layer 4 in motor cortex with prototypical synaptic circuit connectivity. Elife *3*, e05422.

Yao, Z., Liu, H., Xie, F., Fischer, S., Adkins, R.S., Aldridge, A.I., Ament, S.A., Bartlett, A., Behrens, M.M., Van den Berge, K., et al. (2021). A transcriptomic and epigenomic cell atlas of the mouse primary motor cortex. Nature *598*, 103–110.

Yoon, S., Choi, M., Chang, M.S., and Baik, J.-H. (2011). Wnt5a-Dopamine D2 Receptor Interactions Regulate Dopamine Neuron Development via Extracellular Signal-regulated Kinase (ERK) Activation. J. Biol. Chem. *286*, 15641–15651.

Zaaimi, B., Edgley, S.A., Soteropoulos, D.S., and Baker, S.N. (2012). Changes in descending motor pathway connectivity after corticospinal tract lesion in macaque monkey. Brain *135*, 2277–2289.

Zapata, A., and Shippenberg, T.S. (2002). D3 receptor ligands modulate extracellular dopamine clearance in the nucleus accumbens. J. Neurochem. *81*, 1035–1042.

van Zessen, R., Phillips, J.L., Budygin, E.A., and Stuber, G.D. (2012). Activation of VTA GABA Neurons Disrupts Reward Consumption. Neuron *73*, 1184–1194.

Zhang, S., Qi, J., Li, X., Wang, H.-L., Britt, J.P., Hoffman, A.F., Bonci, A., Lupica, C.R., and Morales, M. (2015). Dopaminergic and glutamatergic microdomains in a subset of rodent mesoaccumbens axons. Nat. Neurosci. *18*, 386–392.

Zhong, P., Qin, L., and Yan, Z. (2020). Dopamine Differentially Regulates Response Dynamics of Prefrontal Cortical Principal Neurons and Interneurons to Optogenetic Stimulation of Inputs from Ventral Tegmental Area. Cereb. Cortex *30*, 4402–4409.

Zhou, F.-W., Jin, Y., Matta, S.G., Xu, M., and Zhou, F.-M. (2009a). An Ultra-Short Dopamine Pathway Regulates Basal Ganglia Output. J. Neurosci. *29*, 10424–10435.

Zhou, Q.-Y., Grandy, D.K., Thambi, L., Kushner, J.A., Tol, H.H.M. Van, Cone, R., Pribnow, D., Salon, J., Bunzow, J.R., and Civelli, O. (1990). Cloning and expression of human and rat Dt dopamine receptors. Nature *347*, 76–80.

Zhou, Y., Won, J., Karlsson, M.G., Zhou, M., Rogerson, T., Balaji, J., Neve, R., Poirazi, P., and Silva, A.J. (2009b). CREB regulates excitability and the allocation of memory to subsets

of neurons in the amygdala. Nat. Neurosci. *12*, 1438–1443.

Zong, W., Obenhaus, H.A., Skytøen, E.R., Eneqvist, H., de Jong, N.L., Vale, R., Jorge, M.R., Moser, M.-B., and Moser, E.I. (2022). Large-scale two-photon calcium imaging in freely moving mice. Cell *185*, 1240-1256.e30.

Publications and communications

Publications:

- Plateau,V., Baufreton., J., and Le bon-Jego., M. Age-dependent modulation of layer V pyramidal neurons by dopamine D1 receptor in mouse primary motor cortex. *In prep*
- Cousineau, J., Plateau, V., Baufreton, J., and Le Bon-Jégo, M. (2022). Dopaminergic modulation of primary motor cortex: From cellular and synaptic mechanisms underlying motor learning to cognitive symptoms in Parkinson's disease. Neurobiol. Dis. *167*, 105674.

Posters:

- Plateau, V., and Le Bon-Jego, M. Characterization of the dopaminergic projections from the midbrain to M1 primary motor Cortex. NeuroFrance, Online event, 19-21 May 2021.
- Plateau, V., Georges, F., Baufreton, J., and Le Bon-Jego, M. Age-dependent modulation of layer V pyramidal neurons by dopamine D1 receptor in mouse primary motor cortex. Society for Neuroscience, San Diego, 12-16 November 2022.

Annexes

Neurobiology of Disease 167 (2022) 105674

Contents lists available at ScienceDirect

Neurobiology of Disease

journal homepage: www.elsevier.com/locate/ynbdi

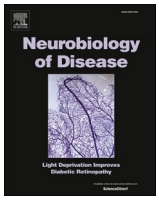

Review

Dopaminergic modulation of primary motor cortex: From cellular and synaptic mechanisms underlying motor learning to cognitive symptoms in Parkinson's disease

Jérémy Cousineau, Valentin Plateau, Jérôme Baufreton, Morgane Le Bon-Jégo *

Univ. Bordeaux, CNRS, IMN, UMR 5293, F-33000 Bordeaux, France

ARTICLE INFO

Keywords:
Primary motor cortex
Dopamine
M1 forelimb area
Motor learning
Intrinsic and synaptic plasticity
Parkinson's disease

ABSTRACT

The primary motor cortex (M1) is crucial for movement execution, especially dexterous ones, but also for cognitive functions like motor learning. The acquisition of motor skills to execute dexterous movements requires dopamine-dependent and -independent plasticity mechanisms within M1. In addition to the basal ganglia, M1 is disturbed in Parkinson's disease (PD). However, little is known about how the lack of dopamine (DA), characteristic of PD, directly or indirectly impacts M1 circuitry. Here we review data from studies of PD patients and the substantial research in non-human primate and rodent models of DA depletion. These models enable us to understand the importance of DA in M1 physiology at the behavioral, network, cellular, and synaptic levels. We first summarize M1 functions and neuronal populations in mammals. We then look at the origin of M1 DA and the cellular location of its receptors and explore the impact of DA loss on M1 physiology, motor, and executive functions. Finally, we discuss how PD treatments impact M1 functions.

1. Introduction

The primary motor cortex (M1) is one of the major brain areas responsible for planning and execution of motor commands (Ebbesen and Brecht, 2017; L. Guo et al., 2015a, 2015b; Whishaw et al., 1986). Coordinated movements necessitate constant adjustments to adapt to an ever-changing environment and require plasticity mechanisms within M1 that are crucial for the acquisition and maintenance of motor skills. Numerous alterations of cortical functions have been observed in neurodegenerative diseases and particularly in Parkinson's disease (PD; Swann et al., 2016). This disease, first described in 1817 by James Parkinson, is characterized by progressive degeneration of the dopaminergic (DAergic) neurons in the *substantia nigra pars compacta* (SNc), inducing dramatically reduced levels of dopamine (DA) in the brain of PD patients. The loss of DA results in dysfunction in neuronal circuits controlling motor execution, mainly in the basal ganglia, a brain region highly innervated by DAergic afferents and involved in motor function. This leads to the typical motor impairment observed in PD: resting tremor, akinesia, rigidity, and postural instability (Nambu et al., 2015). Interestingly, M1, which integrates information from the sensory and premotor cortices and transmits appropriate motor commands to the spinal cord and basal ganglia, also receives DAergic innervation. Disturbances in the function of M1 have also been identified in PD, leading to cognitive dysfunctions such as deficits in motor skill learning (Burciu and Vaillancourt, 2018; Marinelli et al., 2017). In this review, we will first describe M1 microcircuit organization and M1 function in motor execution and motor learning, based on studies in rodents and humans. Then, we will show the importance of M1 DA in physiological conditions and the consequences of its depletion in experimental models of PD and in PD patients. Finally, we will give a non-exhaustive review of the impact of current PD therapy on M1 functions and discuss the possibility of targeting M1 to treat cognitive symptoms in PD.

Abbreviations: 6-OHDA, 6-hydroxydopamine; CStr, cortico-striatal; CThNs, cortico-thalamic neurons; DA, dopamine; DAergic, dopaminergic; DBS, deep brain stimulation; EMCS, extradural motor cortex stimulation; GABA, γ-aminobutyric acid; ITNs, intratelencephalic neurons; LID, levodopa-induced dyskinesia; LIPUS, low-frequency low-intensity pulsed ultrasound; LTP, long-term plasticity; M1, primary motor cortex; MPTP, 1-méthyl-4-phényl-1,2,3,6-tétrahydropyridine; PD, Parkinson's disease; PKA, protein kinase A; PLC, phospholipase C; PNs, pyramidal neurons; PT, pyramidal tract; PV, parvalbumin; SNc, *substantia nigra pars compacta*; SST, somatostatin; STN, subthalamic nucleus; UPRDS, unified Parkinson's disease rating scale; VTA, ventral tegmental area..

* Corresponding author.
E-mail address: morgane.jego@u-bordeaux.fr (M. Le Bon-Jégo).

https://doi.org/10.1016/j.nbd.2022.105674
Received 21 October 2021; Received in revised form 23 February 2022; Accepted 25 February 2022
Available online 1 March 2022

2. Cellular organization of the M1 microcircuit

2.1. Organization of M1 into 6 layers

Like other cortices, M1 is organized into 6 layers of interconnected neurons. It is composed of two main neuronal populations: approximately 75% glutamatergic excitatory pyramidal neurons (PNs) and 25% GABAergic (GABA, γ-aminobutyric acid) inhibitory neurons (Shipp, 2007; Callaway et al., 2021). Interestingly, a species-specific adaptation in the proportion of GABAergic neurons is observed: they represent 16% of M1 neurons in mice, 23% in marmosets and 33% in humans (Bakken et al., 2021). It should be noted that the existence of layer 4 (L4) in M1 is debated (Barbas and García-Cabezas, 2015; Donoghue and Wise, 1982), though recent functional investigations suggest that M1 contains a circuit-level equivalent of L4 in the mouse, i.e., with the same synaptic organization as L4 neurons in the sensory cortex (Yamawaki et al., 2014; Yao et al., 2021).

2.2. Cell types in M1

2.2.1. PNs

The PNs are the main projection neurons of the structure and are divided into 3 different subtypes, depending on the location of the soma in the cortical layers and on their projection targets: the pyramidal tract neurons (PTNs), the intratelencephalic neurons (ITNs), and the corticothalamic neurons (CThNs; Hooks et al., 2013). PTNs are found in L5 and project to the brainstem and spinal cord and can also project to the thalamus and striatum (Cowan and Wilson, 1994; Donoghue and Kitai, 1981; Kita and Kita, 2012; Parent and Parent, 2006). They respond to somatosensory stimulation, mainly proprioceptive stimuli. Moreover, PTNs fire just before the onset (~200 ms before) and during flexion movements and stop firing during extension movements (Beloozerova et al., 2006; Economo et al., 2018; Li et al., 2016; Li et al., 2015; Turner and DeLong, 2000). These PTNs are topographically organized in M1 in a logical manner to coordinate multi-joint forelimb muscle contraction during performance of motor skills (Wang et al., 2017). ITNs can be found in L2 to L6. Those in L2/3 project to other cortices (ipsi- or contralaterally) and are called cortico-cortical ITNs (CC). ITNs in deeper layers project to the striatum and are therefore called cortico-striatal (CStr) ITNs. CStr ITNs are not as responsive to somatosensory stimuli compared to PTNs, and they are selectively activated depending on the direction of the movement to ensure the proper transmission of cortical states to specific spiny projection neurons of the striatum for subcortical processing (Turner and DeLong, 2000). Finally, M1 CThNs project mainly to the posterior and ventro-medial thalamic nuclei and these CT pathways are believed to re-enforce sensorimotor integration and motor control (Shepherd and Yamawaki, 2021).

2.2.2. GABAergic cortical neurons

The GABAergic cortical neurons can be classified into different classes depending on their morphology, intrinsic properties, and expression of specific transcription and molecular factors (Bouzas et al., 2008; Scala et al., 2021). Three major classes stand out regarding the latter criteria, which together account for nearly 100% of cortical GABAergic neurons: the parvalbumin-expressing (PV) neurons, the somatostatin-expressing (SST) neurons, and the $5HT_{3A}$ receptor-expressing neurons (Rudy et al., 2011). PV neurons, representing around 40% of the population, are the major group of cortical GABAergic and comprise basket cells and chandelier cells. They exhibit a unique electrical profile, clearly distinct from the other cortical neurons. Their short action potential duration and high spiking frequency has seen them classified as fast-spiking neurons. In the neocortex, PV neurons can massively project onto the somata and proximal dendrites of PN (for the basket cells) and onto the axon initial segment (for the chandelier cells), enabling the control of the output of these cells (Hu et al., 2014). Interestingly, PV neurons are the only neocortical GABAergic neurons making autapses. These synapses made on themselves enable a decrease of their firing frequency, but most importantly, facilitate precise spike timing (Bacci and Huguenard, 2006). PV neurons also have the particularity in the neocortex of being the major population surrounded by mesh-like structures composed of hierarchical assemblies of extracellular matrix molecules called perineuronal nets, which limit plasticity in adulthood (Sorg et al., 2016; Van't Spijker and Kwok, 2017 for reviews). SST neurons, also classified as low-threshold spiking or regular-spiking non-pyramidal neurons, are the neocortex's second main GABAergic population (Urban-Ciecko and Barth, 2016). They project mainly to the apical and distal dendrites of PNs, enabling the control of the excitatory inputs received. PV and SST neurons are often referred to as 'interneurons'. However, a non-negligible proportion of them are long-range neurons and can project to the contralateral homotypic cortex (Rock et al., 2016; Zurita et al., 2018) or to the striatum (Melzer et al., 2017). Up to a third of the direct pathway's spiny projection neurons respond to optogenetic stimulation of these long-range cortical GABAergic neurons (Melzer et al., 2017). While long-range PV neuron stimulation decreases locomotion, long-range SST neuron stimulation promotes locomotion. Finally, $5HT_{3A}R$ neurons represent the third-largest class of GABAergic cortical neurons. It is a very heterogeneous group that can be divided into two sub-classes: one expressing the neuropeptide VIP and the other non-VIP, also called the neurogliaform. Such VIP-positive neurons preferentially target other GABAergic neurons in the motor cortex (Bohannon and Hablitz, 2018), such as PV neurons (Donato et al., 2013), while neurogliaform cells preferentially target PNs (Schuman et al., 2019).

3. M1, a key structure in motor function and motor learning of dexterous movements

3.1. Role of M1 in movement execution

The involvement of M1 in motor function was first demonstrated in 1870 by Fritsch and Hitzig, when they showed that electrical stimulation of specific regions of the cerebral cortex of a non-anesthetized dog induces discrete movements (Fritsch and Hitzig, 2009; republished and translated to English, 2009). Later, Penfield and Boldrey described the motor homunculus in a locally anesthetized human by electrically stimulating various cortical regions (Penfield and Boldrey, 1937). This functional somatotopy consists of the representation of the different body parts along the M1 region. The size of the representation of the body part depends on the complexity of movements that can be achieved; the more complex the movements, the larger the region. Such M1 mapping has been described across many other animal species, like non-human primates, rodents, or cats (Woolsey et al., 1952; Brown and Teskey, 2014). However, defining M1 boundaries in some species is difficult as M1 may overlap with the somatosensory cortex (Hall and Lindholm, 1974). Interestingly, a complete overlap between those two cortices has been reported in a marsupial opossum considered to be a 'primitive' species (Frost et al., 2000). This tends to suggest that the segregation between M1 and the sensory cortex might be linked to the appearance of more dexterous movements and may underlie a specification of pure motor M1 areas that are highly involved in dexterous abilities.

Lesion approaches have also contributed to dissecting the role of M1 in movement execution and motor skill learning. Unilateral lesions of the M1 forelimb area in rodents induce deficits in contralateral forelimb movements, and the larger the lesion, the larger the impairments (Touvykine et al., 2016; Whishaw, 2000). Thus, the largest and longest-lasting effects of M1 lesions are seen in movements requiring dexterity and finer control of the digits. These lesion approaches primarily show differences among species in M1 rehabilitation. In humans, lesions of M1 or the pyramidal tract (PT) lead to paralysis that may be partially recovered if the lesion is superficial (Darling et al., 2011; Kwakkel et al., 2003).Furthermore, lesions in humans induce deficits in movements

and, more specifically, considerable deficits in dexterous movements. If the lesion is too large, it can lead to total paralysis with no possible recovery (Kwakkel et al., 2003). In non-human primates, M1 lesions especially affect dexterous movements, like grasping (Savidan et al., 2017). In other primates, M1 lesions can be recovered entirely, presumably through compensation by subcortical areas, including reticulospinal pathways (Darling et al., 2011; Lashley, 1924; Leyton and Sherrington, 1917; Zaaimi et al., 2012). After M1 lesions, non-primate mammals and rodents can recover rapidly and can still perform most of their behavioral repertoire, which is already learned and mainly non-dexterous (Kawai et al., 2015). Overall, lesion approaches support the hypothesis that M1 plays an essential role in dexterous movements, which take a prominent place in the human behavioral repertoire. More recently, using an optogenetic approach in rodents, Galiñanes et al. showed that the selective silencing of M1 is able to block movement initiation and to stop already-initiated movements in a forelimb reaching and grasping task (Galiñanes et al., 2018). This work emphasizes once again the prominent role of M1 in dexterous motor sequences. Interestingly, it has been shown in monkeys that a short electrical stimulation of the motor cortex is able to elicit muscle contraction, while an electrical stimulation lasting for a behaviorally-relevant duration (0.5 seconds) is sufficient to create complex and multi-joint movements (Graziano et al., 2002, 2005). These movements belong to the natural behavioral repertoire of the studied species and are arranged across the cortex, depending on the target location in space to which the movement is directed. Such arrangement of movement can be found at the cellular level in rodents: L2/3 PNs are activated for specific movement directions and target positions for reaching movements (Galiñanes et al., 2018).

3.2. Role of M1 in motor skill learning

Besides its prominent role in motor execution, M1 is also crucial for cognitive functions such as learning new motor skills (Bachtiar et al., 2018; Dupont-Hadwen et al., 2019; Kida et al., 2016; Smyth et al., 2010). Complex motor skills and habits are not innate; they must be learned through trial and error. Motor skill learning consists of improving the speed, accuracy, and consistency of a specific movement throughout training that lasts over time. Once learned, the stereotyped movement sequence is executed automatically in response to its specific cue. M1 is instrumental for both the acquisition (Hosp et al., 2011) and maintenance (Ohbayashi, 2020) of motor sequences. During motor training and learning, the M1 corticomotor map is reorganized with, for instance, an increase in the area corresponding to the body part involved in the trained task (Monfils et al., 2005). However, the role of M1 in the maintenance of motor sequences is not as clear across different species. Rodents that have learned a task in which they have to pull a lever are still able to do it after M1 lesion (Kawai et al., 2015). The blockade of protein synthesis is also not sufficient to impair a learned motor sequence in rodents, while it is sufficient to impair the learning of this same task (Hosp et al., 2011). However, protein synthesis blockade in M1 of primates is sufficient to alter learned motor sequences without altering motor execution (Ohbayashi, 2020). Those concordant data may underlie, once again, the fact that M1 may play a critical role for dexterous skill learning and that subcortical areas may not be able to compensate in species with a more dexterous behavioral repertoire.

The development of a forelimb prehensive task in rodents (Guo et al., 2015a; Guo et al., 2015b; Metz and Whishaw, 2000; Fig. 1A) combined with cell type-specific manipulations and monitoring (Guo et al., 2015a; Levy et al., 2020; Li et al., 2017b) have been instrumental for the in-depth dissection of the role played by different M1 neuronal subtypes in motor skill learning. The single pellet reaching task (Chen et al., 2014) is classically used in rodents, as this task is highly relevant to study motor dexterity. The movement is composed of different phases, which are very similar in rodents and humans (Klein et al., 2012), making results easily transposable from rodents to humans. Recordings of neurons in all layers of M1 during single pellet reaching task have revealed that L5 PNs and fast-spiking GABAergic interneurons are primarily recruited during movement execution (Huber et al., 2012; Isomura et al., 2009; Levy et al., 2020; Li et al., 2017b), while L2/3 neuronal activity is primarily outcome-related (Levy et al., 2020; Fig. 1B) in the murine forelimb area. This suggests there is a cell type- and layer-specific separation of monitoring and control of motor function during motor skill learning. Furthermore, reporting of motor outcome by L2/3 neurons seems to emerge from the learning process, as the number of indicative neurons increases during learning (Levy et al., 2020).

At the cellular level, several plasticity mechanisms take place during motor skill learning. It has been shown that following motor skill training, cortico-spinal neurons that control distal forelimb musculature express increased excitability (Biane et al., 2019) and that local L5 recurrent excitation between these neurons is also increased (Biane et al., 2019), as is that of thalamo-cortical projections (Biane et al., 2016). During the learning process, a substantial proportion of L5b

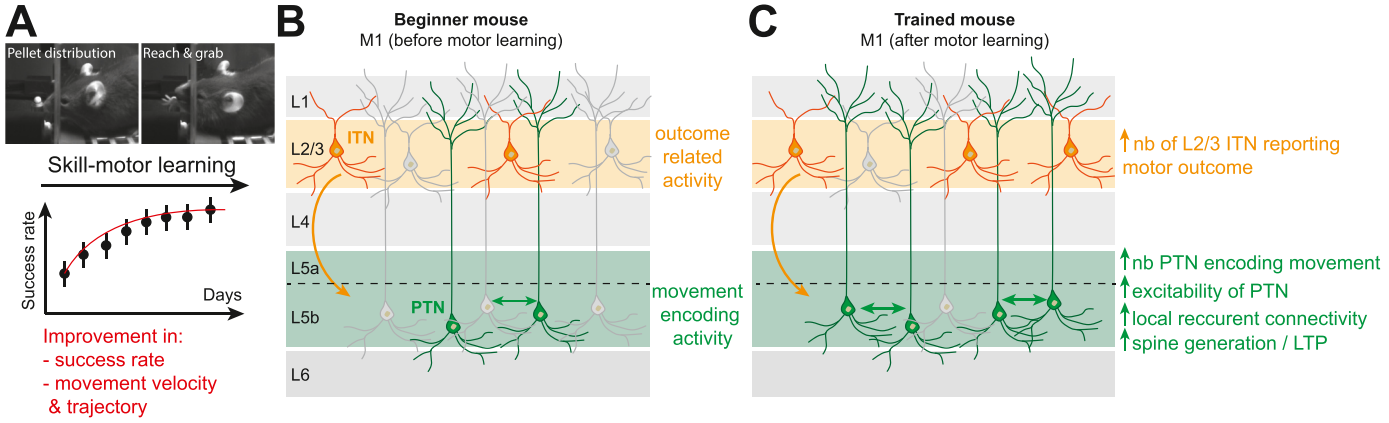

Fig. 1. Intrinsic and synaptic plasticity in M1 induced by motor skill learning.
A: A mouse performing pellet prehension in a reaching skill task. Over several days of training, the mouse improves its skills, which can be monitored by an increase in the success rate of prehension, an increase in movement velocity and the acquisition of stereotyped movements. B: Simplified diagram of M1 before training, in which L2/3 and L5b PN are represented. Only a subset of neurons (colored neurons) is involved in movement encoding (L5b neurons) and monitoring of motor performance (L2/3 neurons). C: After motor skill learning, the numbers of L2/3 neurons reporting motor outcomes and movement-encoding L5b neurons are increased. Intrinsic and synaptic plasticity is observed in L5b neurons. IT neurons, which are present in all layers, are shown only in L2/3. CThN, which are present in L6, are not represented for the sake of simplicity of the diagram.
CThN: cortico-thalamic neurons; IT-CC: intra-telencephalic cortico-cortical neurons; PTN: pyramidal track neurons.

neurons progressively change, from being non-informative about forelimb velocity and trajectory to possessing similar information about motor behavioral outputs to neurons that exhibit clear movement-encoding firing at the beginning of training (Li et al., 2017b). Several studies also report the induction of long-term plasticity (LTP) during motor skill learning (Guo et al., 2015b; Li et al., 2017b). These intrinsic and synaptic plasticities are thought to stabilize the activity patterns in M1 which accompany motor learning (Li et al., 2017b; Peters et al., 2014) and certainly contribute to the augmentation of movement-encoding L5 neurons in trained animals. It has also been shown that new spines in the dendrites of L5 PN are generated when motor skills are learned (Guo et al., 2015b; Harms et al., 2008; Xu et al., 2009; Fig. 1C). A recent study provides an insight about the mechanism underlying spinogenesis during motor skill learning (Albarran et al., 2021). Using mice lacking paired immunoglobulin receptor B ($PirB^{-/-}$), Albarran and colleagues demonstrate that NMDA-dependent LTP, whose expression is under the control of PirB, promotes M1 PN stabilization of newly-formed dendritic spines that are associated with enhanced acquisition and maintenance of motor skills (Albarran et al., 2021). These findings are consistent with previous studies showing that impairing intrinsic or/and synaptic plasticity in M1 is sufficient to impair motor skill learning (Biane et al., 2019; Hayashi-Takagi et al., 2015).

4. Dopaminergic innervation, dopamine receptor expression and function in M1

4.1. Origins of DA within M1

The first evidence of the presence of DA in the cortex, not as a precursor of norepinephrine, dates from the 1970s (Thierry et al., 1974). A decade later, DAergic terminals were clearly described in the frontal cortex, coming from the ventral tegmental area (VTA) and the substantia nigra *pars compacta* (SNc; Fallon, 1981; Swanson, 1982). These DAergic terminals were then identified in M1 with tyrosine hydroxylase (TH) immunocytochemistry after NE terminal depletion (Berger et al., 1985). In rodents, they are mainly located in the deepest layers of the motor cortex, while in primates, they are widespread in all layers (Berger et al., 1991; Descarries et al., 1987; Lewis et al., 1987). Labeling of the DA transporter in rats also reveals that DAergic terminals innervate deep layers of M1, especially those targeting the forelimb representation area (Hosp et al., 2015; Vitrac et al., 2014). Using retrograde tracing in rats, it has been shown that those DAergic projections in M1 come from the VTA and to a lesser extent, from the SNc (Hosp et al., 2011; Molina-Luna et al., 2009), in a similar fashion as in the frontal cortex (Ott and Nieder, 2019). This finding supports the conclusion that the meso-cortical pathway is preserved across species and thus is a functionally important pathway for M1 computations. In humans, it has also been shown that VTA DAergic neurons project to motor areas (Hosp et al., 2019). More importantly, both D1-like and D2-like DAergic receptors are expressed in M1 of many mammalian species (Camps et al., 1990; Gaspar et al., 1995; Huntley et al., 1992; Mansour et al., 1990). Notably, PTNs in rodents express D1, D2, and D5 DAergic receptors (Awenowicz and Porter, 2002; Fig. 2). In addition, taking advantage of the *Drd2-Cre: Ribotag* mouse line, it has also been shown that D2 receptor-expressing cells are distributed in all cortical layers and in a wide variety of M1 GABAergic neurons, in particular PV neurons (Cousineau et al., 2020).

Apart from the DA release from midbrain neurons, it has also been shown thanks to voltage sensitive dye imaging in rat M1 that glutamate can also be released by midbrain neurons, underlying a potential role of excitatory transmission from the midbrain to M1 in motor processes (Kunori et al., 2014). These findings are not surprising as similar mechanisms have already been observed in the PFC (Mercuri et al., 1985; Watanabe et al., 2009). Interestingly, the release of glutamate by midbrain neurons is thought to enable the fast transmission of reward information (Lapish et al., 2007; Lavin et al., 2005). The role of release of glutamate by midbrain neurons in M1 could be similar, as glutamate

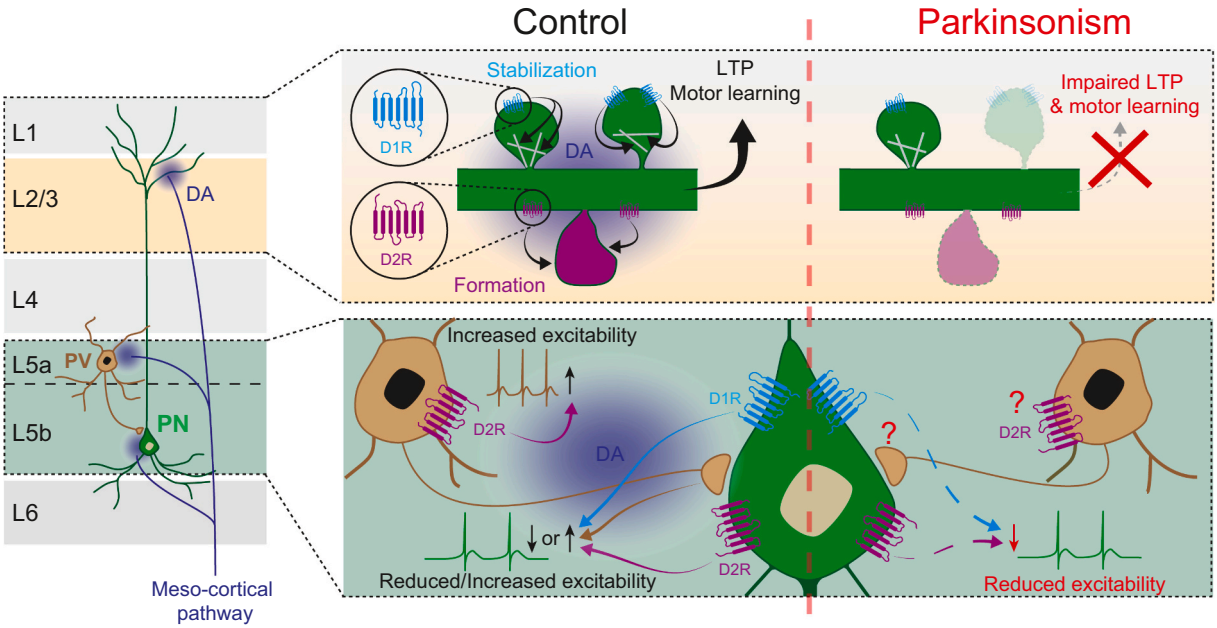

Fig. 2. DA-dependent plasticity in M1.
Schematic depicting an L5 PN and an L5 PV neuron and dopaminergic meso-cortical inputs.
The top dashed rectangle shows a dendritic branch of an L5 PN receiving DAergic innervation. On the left is the D2 receptor-dependent spine formation (in magenta) and the D1 receptor-dependent stabilization of spines (grey lines inside the spines). This form of DA-dependent structural plasticity underlies long term plasticity (LTP) at glutamatergic synapses and motor learning. In Parkinson's disease, the levels of DA progressively decrease in the brain (including M1) and DA-dependent plasticity is lost. Spine turnover is increased, leading to impaired LTP at glutamatergic synapses and impairment of motor performance.
The bottom dashed rectangle represents a magnification of the cell body of an L5b PN and PV neurons. On the left is the effect of DA (shown as the purple cloud) on D1- and D2-like receptors on the excitability of the neurons. On the right part of the rectangle, the reduced tone of DA in the brain (including M1) during the progression of PD leads to direct and indirect (circuit mediated) alterations of L5b PN excitability.

could signal the reward and DA could induce M1 plasticity in order to refine the movement to get the reward.

4.2. Effect of DA receptor stimulation on M1 neuron excitability

Intracellular cascades induced by DAergic receptor activation are complex and vary with the cell types and the brain region. In M1, little is known about the signaling pathways used by DA-receptors to modulate neuronal excitability. Traditionally, activation of D1-like or D2-like receptors have opposite physiological effects via different G proteins, stimulating or inhibiting, respectively, the protein kinase A (PKA) signaling cascade (Mishra et al., 2018). However, in M1, it has been shown that DAergic receptors may work differently. As a matter of fact, phospholipase C (PLC) inhibitors and PKA inhibitors impair LTP in M1 neurons (Rioult-Pedotti et al., 2015). Further, D1 or D2 blockade in M1 induces impaired motor skill learning and M1 LTP, but PLC agonist injection is sufficient to prevent this impairment. Therefore, these data suggest a similar effect of both types of receptors in M1. At the cellular level, the modulations exerted by DA on the excitability of the different M1 neuronal populations are multiple (Table 1). It is clear in the literature that a discrepancy of the effect of DA on PNs is observed. In this review, we tried to summarize what has been discovered so far, being careful to separate what has been done *in vivo* or *ex vivo*. An *ex vivo* study in mice showed changes in intrinsic properties (input resistance, action potential half width) and an increase in the excitability of PNs following D1R and/or D2R receptor blockade (Swanson et al., 2020). Another one, still *ex vivo* in mice, reported however no modulation of L5 PNs by bath application of a D2R agonist (Cousineau et al., 2020). In other species, *in vivo* recordings showed a decrease in excitability of PNs following DA local microinjection in rats (Awenowicz and Porter, 2002), as well as in cats (Huda et al., 1999). However, D2R agonist quinpirole local injections in rats induced an increase in the spike firing rate of PNs (Vitrac et al., 2014), and systemic injection of D2R antagonist haloperidol in rats induced the opposite effect, *i.e.* a reduced spike firing rate (Parr-Brownlie and Hyland, 2005). The divergence of these *in vivo* studies' results could be due to the drug used and its application method (local microinjection vs systemic injection); nevertheless, the impact of DA on PNs is still unclear. There is a need of studies using the same experimental design in order to decipher the impact of DA receptors activation or blockade on PNs. It is also crucial to take into account the diversity of PNs to better understand the action of DA on M1 PNs. Overall it seems that activation of D1 or D2 receptors globally decrease excitability of some PNs (Awenowicz and Porter, 2002; Huda et al., 2001, Huda et al., 1999; Fig. 2). It has also been shown that activation of D2-like receptors *ex vivo* induces an increase in PV neurons' excitability and their synaptic transmission onto L5 PNs in M1 (Cousineau et al., 2020; Fig. 2), corroborating the fact that D2-like receptor activation can have an excitatory effect on M1 neurons. Moreover, activation of D2 receptors via quinpirole infusion in M1 increases the firing frequency of PN in a dose-dependent manner *in vivo* (Vitrac et al., 2014), which is reminiscent of the quinpirole-mediated increased excitability of prefrontal cortex L5 PNs (Gee et al., 2012). This mono-directional effect of both types of DAergic receptors is not surprising in M1, as it is also found in the prefrontal cortex. Regarding synaptic transmission, numerous pieces of evidence highlight the effect of DA on both glutamatergic and GABAergic transmission and neuronal properties in the prefrontal cortex (Trantham-Davidson, 2004). The downstream β-arrestin2 signaling pathway (Urs et al., 2016) or the release of neurotensin via activation of D2 autoreceptors of M1 DAergic neuron terminals could explain the D2 excitatory effect (Petrie et al., 2005), as is the case in the prefrontal cortex. Nonetheless, it has been shown that *in vivo* DA infusion in the forepaw representation of the cat motor cortex decreases the activity of PTNs and their evoked response to callosal and thalamic inputs (Huda et al., 2001; Huda et al., 1999); those effects are rescued by the application of DAergic antagonists, for either D1 or D2 (Awenowicz and Porter, 2002; Huda et al., 2001). This decrease in PTN activity could be

Table 1
Effect of dopaminergic pharmacology and dopamine-depletion on M1 neuronal subtype activity.

Type of manipulation	Neuronal subtype		Recording conditions	References
	Pyramidal neurons	GABAergic interneurons		
DA	↓ in response of PN to callosal & thalamic excitatory inputs	N/D	*In vivo* anesthetized Local microinjections	Huda et al., 1999, 2001
	↓ in firing rate of PTN		*In vivo* anesthetized Local microinjections	Awenowicz and Porter, 2002
D1 agonist	N/D	N/D		
D2 agonist	No effect on L5 PN excitability	↑ in L5 PV-IN excitability	*Ex vivo*	Cousineau et al., 2020
		↑ in PV-IN to PN GABAergic transmission	*Ex vivo*	Cousineau et al., 2020
	↑ in firing rate of L5 PN		*In vivo* anesthetized Systemic i.p. injections	Vitrac et al., 2014
D1 antagonist	↑ in L5 PN excitability	N/D	*Ex vivo*	Swanson et al., 2020
D2 antagonist	↓ in firing rate of PN	N/D	*In vivo* freely-moving Systemic i.p. injections	Parr-Brownlie and Hyland, 2005
	↑ in L5 PN excitability		*Ex vivo*	Swanson et al., 2020
DA-depletion in the midbrain	↓ in excitability of L2/3 PN and ↑ in excitability in L5 PN		*Ex vivo*	Swanson et al., 2020
	↓ in excitability of L5 PTN / No effect on ITN		*Ex vivo*	Chen et al., 2021
	↓ in firing rate of PN	No effect on the firing activity of putative PV-IN	*In vivo* freely-moving Unilateral MFB 6-OHDA injection	Li et al., 2021
		↓ in firing rate of SST-IN	*In vivo* head-fixed Systemic i.p. MPTP injections, also local cortical MPTP injections	Chen et al., 2019
	↓ in firing rate of PTN during freezing and grasp ↓ in late phase firing rate of L2/3 ITN		*In vivo* head-fixed Striatal 6-OHDA injection	Aeed et al., 2021*

(*continued on next page*)

Table 1 (*continued*)

Type of manipulation	Neuronal subtype		Recording conditions	References
	Pyramidal neurons	GABAergic interneurons		
DA-depletion in M1	↓ in L2/3 PN excitability	N/D	*Ex vivo*	Swanson et al., 2020
	No effect on L5 PN excitability			

i.p.: intraperitoneal; ITN: intratelencephalic neurons; MFB: medial forebrain bundle; PN: pyramidal neurons; PTN: pyramidal track neurons; PV-IN: parvalbumin interneurons; SST-IN: somatostatin interneurons

* Unilateral striatal DA-depletion

due to the DA-mediated increased excitability of PV interneurons as neurons from the VTA, the main source of DA for M1, project directly to M1 GABAergic neurons (Duan et al., 2020). As PV interneurons are powerful regulators of cortical activity (Ferguson and Gao, 2018), they would be well-placed to select the inputs coming to the motor cortex to refine its outputs.

4.3. Role of DA in M1 plasticity

M1 undergoes learning-dependent plasticity during motor skill learning (Karni et al., 1995), and motor performance is correlated to DA metabolite levels in the cerebrospinal fluid (McEntee et al., 1987). Furthermore, the *in vivo* pharmacological blockade of D1 or D2 DAergic receptors in M1 both induces a decrease of LTP in L2/3 of rats and is sufficient to alter skill learning (Molina-Luna et al., 2009). In addition, the selective blockade of D2 receptors in M1 induces a decrease of M1 neurons' activity, leading to the increase in movement time, *i.e.* bradykinesia, during a skilled reaching task in rats (Parr-Brownlie and Hyland, 2005). Moreover, spine turnover in M1 L5 PNs is under the control of DA: while the stabilization/elimination of spines involves D1 receptors, spine formation involves D2 receptors (Guo et al., 2015a; Fig. 2). However, the selective blockade of DAergic receptors has no effect on skill performance once the skill is learned. These data emphasize the role of the meso-cortical pathway and hence cortical DA in the acquisition of motor skills, but not in their maintenance, by selecting and potentiating the newly-formed spines necessary for the execution of the movement in the learning process while depressing the unnecessary ones.

5. M1 disturbances in Parkinson's disease

5.1. M1 disturbances in animal models of PD

In addition to the cardinal motor symptoms (tremor, rigidity bradykinesia and postural instability), PD patients also experience significant disability in executing fine motor tasks (Dan et al., 2019; Proud and Morris, 2010; Vanbellingen et al., 2011), like tying shoelaces or handwriting (Pohar and Allyson Jones, 2009). These fine motor symptoms respond to DA replacement therapy (Gebhardt et al., 2008; Lee et al., 2018) suggesting that DA plays an important role in dexterous skills. Indeed, a substantial loss of DA innervation in M1 has been reported in PD patients (Gaspar et al., 1991). Although VTA DAergic neurons, the main source of DA for M1, are not as sensitive to oxidative stress occurring during PD as SNc DAergic neurons (Surmeier et al., 2011), they still degenerate (Alberico et al., 2015) and this degeneration takes place later than SNc DAergic neurons (Harrison et al., 2016).

To look further at the role of DA in the pathophysiology of M1 during PD, animal models are essential. Many neurotoxins have been used to model PD, especially 6-hydroxydopamine (6-OHDA) and MPTP, which selectively destroy DAergic neurons (Betarbet et al., 2002; Schober, 2004). These two neurotoxins mimic different aspects of the pathophysiology of PD. MPTP and 6-OHDA do not use the same cellular pathway to kill catecholaminergic neurons. Moreover as MPTP can cross the blood brain barrier but the 6-OHDA not, the administration mode and the effect are different. Classically, systemic injection of MPTP mimics well the early stages of PD as it induces less degeneration of DAergic neurons and less loss of cell body compared to unilateral 6-OHDA injection, which is a good model for a dramatic loss of DA as observed in late stages of PD (Schober, 2004; Ferro et al., 2005). Treatment with rotenone, another neurotoxin, also reproduces most features of PD (Radad et al., 2019), by entering in DAergic neurons thanks to its lipophilic properties and mediating cell death through oxidative stress, α-synuclein phosphorylation and aggregation. Recently, non-neurotoxin models based on injections of Lewy bodies extracted from the brain of PD patients or α-synuclein fibrils (Chu et al., 2019), which are closer to the pathophysiology of PD, have been developed. These different compounds reproduce more or less the features of PD at the behavioral, network, cellular, and molecular levels, but also the chronic and progressive aspects of PD (Chia et al., 2020; Gerlach and Riederer, 1996; Lorigados et al., 1996), as some of them are more relevant than others depending on the aspect of PD studied and their ability to induce PD symptoms in the animal model used (rats' resistance to MPTP toxicity for example). Among the studies done on M1, it is important to distinguish those in which DA-depletion has been achieved by toxin injections in the midbrain (in the medial forebrain bundle or the SNc) to dramatically reduce DA tone in the brain, as occurs in late stages of PD (Chen et al., 2019, 2021; Li et al., 2021) with those that directly manipulate M1 to investigate the role of cortical DA (Guo et al., 2015a, 2015b. Here, we give a non-exhaustive review of the pathophysiology of M1 in PD models.

The midbrain 6-OHDA model has been widely used to investigate the changes observed in M1 during PD, especially in rats (Campos et al., 2021; Hosp et al., 2011; Molina-Luna et al., 2009). Proteomic analysis of M1 in 6-OHDA rats showed alterations in the expression of proteins involved in autophagy, mRNA processing, ATP binding, and maintaining the balance of neurotransmitters (Li et al., 2017a). DA-depletion also induces a loss in excitability of L2/3 and L5 PNs in M1 *ex vivo* (Chen et al., 2021; Swanson et al., 2020; Table 1; Fig. 2). PET functional imaging of 6-OHDA rats also reveals significant glucose hypometabolism in M1 and the *substantia nigra*, suggesting an impairment of the cortico-subcortical network as observed in PD patients (Jang et al., 2012). Moreover, striatal DA depletion also disrupts the forelimb representation map in M1 (Plowman et al., 2011; Viaro et al., 2010). In 6-OHDA rats, it has been shown that M1 activity is disturbed during the grasping phase of the movement after DA depletion (Hyland et al., 2019), and PN firing frequency is decreased during a reaching movement compared to control rodents (Aeed et al., 2021; Li et al., 2021). Additionally, 6-OHDA rats display an abnormal local field potential power at beta frequencies in the cortex at rest (Mallet et al., 2008) and during a reaching movement (Li et al., 2021). Two recent studies also report that the excitation of M1 or M2 PNs with optogenetics can partially restore motor performance in mice (Aeed et al., 2021; Magno et al., 2019). This may underline that the dexterity disturbance observed in PD patients could be due to alteration of M1 activity following DA loss, highlighting the need for cortical treatment to target those fine motor issues. Moreover, projections from M1 to subcortical structures are also disturbed in 6-OHDA rats. In addition to cortico-striatal dysfunctions which have been extensively studied (Zhai et al., 2018), direct glutamatergic inputs from M1 to the subthalamic nucleus, known as the hyperdirect pathway, are highly reduced in 6-OHDA rats (Wang et al., 2018), mice (Chu et al., 2017) and MPTP-treated monkeys (Mathai et al., 2015). The activation of the hyperdirect pathway leads to an inhibition of movements, and together with the direct and indirect pathways, enables proper control of motor behaviors. In addition to their decreased number, inputs from M1 to STN are also weaker in 6-OHDA mice, as both amplitude and frequency of cortico-STN excitatory post-synaptic currents are diminished after DA depletion (Chu et al., 2017). This

weakening of synaptic transmission of cortico-STN axon terminals could be due to the decreased amount of vesicular glutamate transporter 1 in the subthalamic nucleus (Wang et al., 2018; Chu et al., 2017; Mathai et al., 2015), thus leading to the abnormal activity of this pathway observed in PD patients.

5.2. Comparison between animal models of PD and PD patient symptoms

In addition to motor deficits, PD patients also exhibit cognitive impairments such as impairments in long-term memory, visual information processing, motor learning and executive function (Watson and Leverenz, 2010). Electroencephalographic recordings in PD patients also revealed a reduced functional connectivity within the primary motor cortex (Formaggio et al., 2021). Moreover, functional MRI studies in PD patients have shown a decreased functional connectivity between parietal and motor cortical areas (Palomar et al., 2013), as well as the functional connectivity between sensory and motor cortex (Wang et al., 2021). The isolation of motor areas from these other areas certainly contributes to difficulties of PD patients to learn and perform day life movements. Furthermore, the functional connectivity between M1 and the rostral supplementary area is increased in PD patients (Wu et al., 2011), while the functional connectivity between the rostral supplementary area and structures involved in motor preparation and initiation (*i.e.* left putamen, right premotor cortex) are decreased (Wu et al., 2011). This suggests that cognitive processes necessary to learn, prepare and initiate the movement are at least as disturbed as processes needed for movement execution during PD. As for humans, motor skill learning is also altered and well-documented in animal models of DA loss (Molina-Luna et al., 2009; Hosp et al., 2011; L. Guo et al., 2015a, 2015b). Using the single pellet reaching task, it has been shown that selective depletion of DAergic fibers that project to the M1 and correspond to the trained limb alters the acquisition of this skill in rats (6-OHDA) and mice (MPTP; Molina-Luna et al., 2009; L. Guo et al., 2015a, 2015b). However, the same M1 DA depletion did not affect performance once the skill had been learned, indicating a role for M1 DA in skill acquisition but not in its maintenance. Furthermore, 6-OHDA injection directly in the VTA highlighted the importance of M1 DA coming from this region in motor learning. Indeed, the VTA is the main source of DA in M1, and the destruction of these DAergic neurons leads to a suppression of skill learning that can be partially re-established with levodopa infusion in M1 (Hosp et al., 2011). VTA DAergic neurons projecting onto M1 are specifically activated during successful food-rewarded skill acquisition and not by the reward alone (Leemburg et al., 2018). Interestingly, those VTA to M1 DAergic neurons are no longer recruited once the task is learned or in individuals unable to learn the motor sequence. This emphasizes that M1 DA is crucial for skill learning but no longer necessary for skills already learned. The structural and functional plasticity of dendritic spines is important for learning and memory. In mice, Guo and colleagues showed the impact of DA loss following MPTP treatment on M1 dendritic spines in the context of skill learning (Guo et al., 2015a). Throughout the training of a new motor skill, the survivability of these spines increases and is still increased 30 days after the last training session. This increased spine survivability is only present during the first training session in M1 MPTP-treated mice and is no longer present 8 days after the last training session. Furthermore, this increase in spine turnover is accompanied by impaired LTP (Fig. 2), suggesting that this phenomenon may contribute to the observed learning deficiency in these DA-depleted mice (Guo et al., 2015a). These different studies laid the foundations of the significance of M1 DA for the accurate learning of dexterous movements, and the potential implication of its depletion in PD.

GABAergic neurons play a crucial role in M1 network activity and the balance of excitation/inhibition is crucial for proper neocortex function. It is not surprising that GABAergic inhibition in M1 is disturbed in PD patients (Chu et al., 2009; Ni et al., 2013; Sailer et al., 2003). A decrease in the activity of SST interneurons has been observed after MPTP infusion in the rat cortex, which is associated with a destabilization of dendritic spines in PN as well as impairments in motor learning (Chen et al., 2019). Interestingly, re-establishing activity in SST neurons with a chemogenetic approach rescues dendritic spine loss and motor deficits. In addition, parvalbumin levels are increased in PD model rats (Capper-Loup et al., 2005), suggesting a putative dysfunction of this neuronal cell type in this model, since electrical properties of PV neurons are strongly linked to their parvalbumin levels (Chard et al., 1993; Donato et al., 2013). In monkeys, carotid artery injection of MPTP has been used to induce a Parkinson-like syndrome, leading to several effects relative to the different M1 neuronal populations (Pasquereau and Turner, 2011). M1 activity related to movement is decreased, mainly in PTN but not in CStr ITNs (Pasquereau and Turner, 2015). Timing of M1 activation is also disturbed in this model. Indeed, the movement-related activity of PTN is impaired, with earlier onset activation and a longer activation. PTN excitability has been shown to be decreased in M1 L5 of 6-OHDA mice, while ITNs remain unaffected (Chen et al., 2021), which may explain this timing alteration and also lead to lesser M1 outputs. Moreover, the firing pattern of M1 neurons is dramatically modified in MPTP-treated monkeys, with an increase in burst discharge and an abnormal level of synchrony at beta frequencies (Goldberg et al., 2002). This excessive level of M1 synchronization may be at the origin of the rigidity observed in PD, by causing the simultaneous contraction of antagonistic muscles (Goldberg et al., 2002).

6. M1 as a potential target for treatment of motor and cognitive impairments in PD

6.1. Impact of PD treatments on M1 activity and function

Levodopa medication has been the first-line treatment for PD since 1967, when it was discovered that high doses of this DA precursor were highly efficient against PD (Cotzias et al., 1967). Levodopa presents the advantage of crossing the blood-brain barrier, while DA cannot. It is then converted into DA by the action of the DOPA-decarboxylase enzyme, thus leading to a DA concentration increase (Fahn, 2008). Levodopa treatment is often combined with an inhibitor of the peripheral DOPA decarboxylase, like carbidopa, to specifically increase DA concentration within the central nervous system (Fahn, 2006). Besides the effects of this DA replacement therapy in the basal ganglia, levodopa also has an impact on M1. As previously mentioned, inhibition in M1 is disturbed in PD patients (Chu et al., 2009; Ni et al., 2013; Sailer et al., 2003). This inhibition shapes oscillatory activity within M1, since blocking GABA receptors or GABA transporter with specific antagonists abolish beta and gamma oscillations (Yamawaki et al., 2008). In addition, DA also plays a role in M1 oscillatory activity, given that both D1-like and D2-like receptor agonists promote both beta and gamma oscillations within M1 (Özkan et al., 2017), the same oscillations that are shaped by interneurons. Thus, it is not surprising that levodopa treatment increases the power of beta oscillations within M1 in PD patients (Cao et al., 2020), putting into question the contribution of these oscillations in M1 to causing PD symptoms.

Deep Brain Stimulation of the subthalamic nucleus (STN-DBS) is another symptomatic PD treatment, but due to inter-individual differences in the spectrum of symptoms of the patients and its surgical invasiveness, it only benefits a minority of PD patients. It is thus essential to determine the precise mechanism of how DBS suppresses PD symptoms, in order to make it accessible to a broader population. Several hypotheses have been proposed to explain the beneficial effects of STN-DBS (Deniau et al., 2010; Eusebio et al., 2011; Hammond et al., 2008), including a growing body of evidence on a cortical effect of STN-DBS in both experimental models of PD (Degos et al., 2013; Gradinaru et al., 2009; Li et al., 2007) and PD patients (Cunic et al., 2002; Fraix et al., 2008; Payoux et al., 2004). Further, an interesting study investigated the role of M1 neurons forming the hyperdirect pathway in STN-DBS in 6-OHDA rats (Li et al., 2012). STN-DBS antidromically activates

M1 passing fibers with several consequences for M1 microcircuit activity. Firstly, the STN-DBS restored the basal activity of M1 neurons in 6-OHDA rats. Secondly, the new M1 basal activity is correlated with the most beneficial DBS frequency, e.g. 125 Hz (Li et al., 2014; Li et al., 2012). Finally, the most beneficial stimulation frequency induces the biggest reduction of abnormal beta oscillations (de Hemptinne et al., 2015), M1 neuronal synchrony, and burst discharge occurrence (Li et al., 2014; Li et al., 2012). Together, these results indicate that STN-DBS directly influences M1 neuronal activity at the single-cell and network levels, thus contributing to the alleviation of PD symptoms. The mechanism underlying the regularization of M1 PN activity by STN-DBS has been investigated recently in hemiparkinsonian rodents (Valverde et al., 2020). In this study, the authors reported that the excitability of PNs was reduced following STN-DBS stimulation. Surprisingly, STN-DBS has opposite effects on cortical GABAergic neurons, as it decreases the firing rate of PV neurons while increasing that of SST neurons. In addition, specifically increasing SST neuronal activity *via* an optogenetics approach alleviates motor symptoms in PD model rodents (Valverde et al., 2020). The optogenetic activation of M1 PV neurons leads to motor improvement to a lesser extent. These data suggest that the disturbance of M1 circuitry may come from the integration and treatment of PN excitatory inputs, and not from their electrical properties. Indeed, SST neurons project to the apical dendrites of PNs, thus controlling the excitatory inputs they receive. Opto-activation of SST neurons in PD model rodents can then lead to improved processing of the information in M1. PV neurons are known to control the spiking activity of PNs; their opto-activation may only shut down PN activity, not helping the processing of disturbed excitatory inputs to M1. It may explain the lesser impact on motor symptoms when stimulating PVs rather than SSTs. Together, this evidence suggests that M1 GABAergic neurons could be a putative target for a more precise alternative to STN DBS.

Physical activity has been shown to improve motor symptoms in early PD patients (Emig et al., 2021; Gilat et al., 2021; Tiihonen et al., 2021) suggesting that exercise could partially balance the effects of DA loss within M1. As mentioned before, M1 activity impairments during PD are characterized by a decrease in PTN spontaneous firing rate, but also by exaggerated synchrony of these neurons at beta frequencies (Goldberg et al., 2002; Pasquereau and Turner, 2011). 6-OHDA rats that undergo treadmill exercise have a significantly increased firing rate of PTN and decreased power spectrum of β oscillations. These rats also made fewer foot faults during a ladder test (Shi et al., 2021), thereby exhibiting improved PD symptoms at the network and behavioral levels. Even if the beneficial effects of physical activity on PD symptoms are well-acknowledged, there is still a gap in our understanding of its mode of action. This is the case with M1, as the causal link between changes in M1 neurons' activity and improvement of PD symptoms has not yet been made. However, it could be possible that exercising increases M1 DA levels in PD patients, leading to improved motor and cognitive symptoms, since DA levels are increased during exercise in healthy people (Singh and Staines, 2015). Also, as serotonin, norepinephrine and brain derived neurotrophic factor levels are also increased in healthy people during physical activity (Singh and Staines, 2015) the levels of these compounds could be increased in PD patients during exercise and compensate for the DAergic depletion in M1 as well as in sub-cortical systems.

6.2. Targeting M1 to improve symptoms of PD

Apart from its beneficial effects on motor symptoms, levodopa is well-known to induce major side effects, the most frequent and debilitating being levodopa-induced dyskinesia (LID). Interestingly, it has recently been shown in 6-OHDA rats that LID is strongly correlated with an augmented GABA efflux in M1, leading to increased inhibition within M1. This phenomenon has been identified as a compensatory mechanism for LID, as exogenously increasing this already-increased inhibition within M1 with a $GABA_A$ receptor agonist reduces the severity of LID (Lindenbach et al., 2015). This is consistent with the fact that the emergence of LID in PD patients has been associated with abnormal synaptic plasticity within M1 (Morgante et al., 2006). Furthermore, levodopa administration in 6-OHDA rats induces an increase in c-Fos and activity-regulated cytoskeletal-associated protein expression in M1, which are early genes involved in plasticity phenomena. This suggests that hyperactivity of M1 occurs during dyskinesia (Lindenbach et al., 2015), explaining the need to increase inhibition within M1. Thus, restoring more physiological synaptic plasticity could potentiate inhibition within M1, and could consequently be a potential therapeutic target to reduce severity of LID.

It has been shown that high-frequency motor cortex stimulation in MPTP-treated baboons significantly reduced PD symptoms (Drouot et al., 2004). More recently, low-frequency low-intensity pulsed ultrasound (LIPUS) targeting M1 has also been found to have beneficial effects on PD models. In MPTP-treated mice, M1-targeted LIPUS increases rearing in the open field test after 4 days of treatment, and locomotor activity during a pole test after 5 days of treatment. Furthermore, LIPUS increases superoxide dismutase and glutathione peroxidase levels in MPTP-treated mice (Zhou et al., 2019); the levels of these two enzymes are diminished in PD patients, leading to oxidative stress (Nikam et al., 2009; Surendran and Rajasankar, 2010). Furthermore, overexpression of superoxide dismutase has been found to improve DAergic neuron survival over time (Botella et al., 2008). Even if the entire mechanism of action of M1-targeted LIPUS remains unclear, the re-establishment of more physiological levels of antioxidants could partially explain its effect, making M1-targeted LIPUS a good treatment for oxidative stress during PD.

In addition to motor impairments, persistent pain is another feature of PD, contributing to the decreased quality of life of people affected by the disease. M1 has been identified as a good target for chronic pain treatment (Canavero and Bonicalzi, 1995; Tsubokawa et al., 1991), and Canavero and Paolotti used it for the first time to treat chronic pain during PD. They showed improvements in pain symptoms, separate from the motor improvement (Canavero and Paolotti, 2000). Campos and colleagues showed evidence of how M1-targeted stimulation may alleviate these symptoms during PD (Campos et al., 2021). While DA depletion in rats induces pain hypersensitivity, M1 stimulation was able to reverse it. Furthermore, M1 stimulation was able to restore the descending serotonergic pathway to the spinal cord, crucial for analgesia control. For the spinal cord network, motor cortex stimulation also restores proper neuronal and astrocytic activity (Campos et al., 2021). Finally, M1 stimulation induces a release of endogenous opioids (Maarrawi et al., 2007), which could contribute to the alleviation of chronic pain during PD.

Extradural motor cortex stimulation (EMCS) was identified primarily as a treatment for chronic pain (Canavero and Bonicalzi, 1995; Tsubokawa et al., 1991). EMCS has been performed on PD patients, and a first case of motor symptom improvement was observed in the early 2000s (Canavero and Paolotti, 2000). Several similar cases of motor improvements with EMCS were reported a few years later (Canavero et al., 2002; Pagni et al., 2003; Pagni et al., 2005). PD patients treated with EMCS exhibit long-lasting improved scores on the unified PD rating scale (UPRDS) with no complications observed due to the surgical procedure after several years (Bentivoglio et al., 2012; De Rose et al., 2012; Piano et al., 2021). Notably, patients exhibit improvements in axial symptoms, *i.e.* decreased bradykinesia, rigidity, tremor and akinesia, and also decreased LID when off medication, thus increasing their quality of life. Furthermore, symptoms like postural instability, gait freezing, dysphonia, and dysphagia are improved, while STN-DBS has no effect on these symptoms and can have side effects, especially on dysphonia and dysphagia (Cioni, 2005; Lavano et al., 2016). These improvements are noticeable especially when off levodopa medication, but also when on medication, meaning that it is possible to decrease the drug treatment (Cioni, 2005). While the mechanism of action of EMCS is not fully

understood, it is now known that EMCS enhances the activity of M1-related cortical areas, such as the supplementary motor area, whose activity is decreased during PD (Fasano et al., 2008; Piano et al., 2021). A modeling study carried out in 2012 showed that EMCS activates the axons of either basket cells or PTN (Zwartjes et al., 2012). This is consistent with the fact that both PNs (Vitrac et al., 2014) and PV interneurons (hence basket cells; Cousineau et al., 2020) are excited by D2-like receptor activation, and therefore their activity may decrease during PD. Stimulating the axons of these two neuronal populations should restore more physiological levels of activity and information transmission, and so improve PD symptoms. To conclude, even if the motor improvements are smaller compared to STN-DBS, EMCS treatment offers an alternative choice to treat some symptoms that are not improved by DBS, especially for patients who are not eligible for DBS, notably older patients, thanks to the less invasive nature of EMCS.

6.3. *Levodopa-induced dyskinesia as drug-induced side effect on M1 function*

Apart from its beneficial effects on motor symptoms, levodopa is well-known to induce major side effects, the most frequent and debilitating being levodopa-induced dyskinesia (LID). Interestingly, it has recently been shown in 6-OHDA rats that LID is strongly correlated with an augmented GABA efflux in M1, leading to increased inhibition within M1. This phenomenon has been identified as a compensatory mechanism for LID, as exogenously increasing this already-increased inhibition within M1 with a $GABA_A$ receptor agonist reduces the severity of LID (Lindenbach et al., 2015). This is consistent with the fact that the emergence of LID in PD patients has been associated with abnormal synaptic plasticity within M1 (Morgante et al., 2006). Furthermore, levodopa administration in 6-OHDA rats induces an increase in c-Fos and activity-regulated cytoskeletal-associated protein expression in M1, which are early genes involved in plasticity phenomena. This suggests that hyperactivity of M1 occurs during dyskinesia (Lindenbach et al., 2015), explaining the need to increase inhibition within M1. Thus, restoring more physiological synaptic plasticity could potentiate inhibition within M1, and could consequently be a potential therapeutic target to reduce severity of LID.

7. Conclusion & perspectives

It is now well-established that M1 is instrumental both in motor execution and motor learning. By ensuring proper synaptic plasticity within M1, DA appears to be a key neuromodulator for motor learning and execution of dexterous movements. Hence, DA loss during PD dramatically affects M1 functions, as seen in the different animal models of PD, but especially in PD patients. Notably, DA manages the inhibitory network within M1, which plays an important role in shaping PN activity, ensuring both the execution and learning of dexterous movements. It is not surprising to find the excitation/inhibition balance is disturbed in PD, resulting in an overall decreased inhibition within M1, and that both DA replacement therapies and stimulation approaches enhance it, highlighting a potential target for more precise DBS. Therefore, the precise mechanism of action of DA on M1 GABAergic neurons should be explored more in detail. It would be significant to investigate whether their electrical properties or activity are affected in absence of DA. In addition, studying their activity with *in vivo* calcium imaging throughout the acquisition of a new motor sequence could unravel their precise role together with their dysfunction in physiological and pathophysiological conditions. Moreover, increasing research indicates that M1 is a good target to alleviate some symptoms of PD, motor and non-motor, making it a good alternative for people no longer responsive to first-line treatments, not eligible for DBS, or as a complementary treatment.

While our understanding of the role of M1 in motor learning has greatly progressed in recent years, several questions remain open. What is the contribution of the different types of GABAergic interneurons to motor learning? What is the net impact of DA on M1 L5 PNs? What is the dynamic of DA release during the acquisition of new motor skills? Which cell types and synapses are specifically modulated by DA during motor skill learning and thus preferentially affected after the loss of DA in PD? The field now has new tools and techniques at its disposal to address these questions. For instance, fluorescent DA sensors (Labouesse et al., 2020; Patriarchi et al., 2018; Sun et al., 2018 for review) coupled with a miniaturized microscope (Aharoni and Hoogland, 2019; de Groot et al., 2020; Gulati et al., 2017; Kondo et al., 2018; Rynes et al., 2021) could help us investigate how M1 DA is released *in vivo* in freely-moving rodents or non-human primates, enabling us to better understand i) the kinematics of DA release, especially throughout the different steps of motor skill acquisition, and ii) the M1 cognitive impairments displayed in PD patients. More generally, identifying key cellular and synaptic mechanisms including DA-dependent structural and functional plasticity involved in motor-related cognitive symptoms of PD would enable development of new treatment that could improve the quality of life of PD patients.

Acknowledgements

This work was supported by the University of Bordeaux, the CNRS (Centre National de la Recherche Scientifique), the French government in the framework of the University of Bordeaux's IdEx "Investments for the Future" program / GPR BRAIN_2030 (to J.B. and M. L. B.J.), and the Bordeaux Neurocampus Department (Seed project Damoco). J.C. is supported by a Ph.D. fellowship from the FRM (ECO201806006853 – Fondation Yolande Calvet) and V. P. is supported by a Ph.D. fellowship from the Bordeaux Neurocampus Ph.D. Program. We thank Dr. N. Mallet and F. Georges for helpful comments. We are also grateful to Dr. Patricia Gongal (Innovology, Canada) for language assistance on the manuscript.

References

Aeed, F., Cermak, N., Schiller, J., Schiller, Y., 2021. Intrinsic disruption of the M1 cortical network in a mouse model of Parkinson's Disease. Mov. Disord. 36, 1565–1577. https://doi.org/10.1002/mds.28538.

Aharoni, D., Hoogland, T.M., 2019. Circuit investigations with open-source miniaturized microscopes: past, present and future. Front. Cell. Neurosci. 13, 1–12. https://doi.org/10.3389/fncel.2019.00141.

Albarran, E., Raissi, A., Jáidar, O., Shatz, C.J., Ding, J.B., 2021. Enhancing motor learning by increasing stability of newly formed dendritic spines in motor cortex. SSRN Electron. J. https://doi.org/10.2139/ssrn.3775181.

Alberico, S.L., Cassell, M.D., Narayanan, N.S., 2015. The vulnerable ventral tegmental area in Parkinson's disease. Basal Ganglia 5, 51–55. https://doi.org/10.1016/j.baga.2015.06.001.

Awenowicz, P.W., Porter, L.L., 2002. Local application of dopamine inhibits pyramidal tract neuron activity in the rodent motor cortex. J. Neurophysiol. 88, 3439–3451. https://doi.org/10.1152/jn.00078.2002.

Bacci, A., Huguenard, J.R., 2006. Enhancement of spike-timing precision by autaptic transmission in neocortical inhibitory interneurons. Neuron 49, 119–130. https://doi.org/10.1016/j.neuron.2005.12.014.

Bachtiar, V., Johnstone, A., Berrington, A., Lemke, C., Johansen-Berg, H., Emir, U., Stagg, C.J., 2018. Modulating regional motor cortical excitability with noninvasive brain stimulation results in neurochemical changes in bilateral motor cortices. J. Neurosci. 38, 7327–7336. https://doi.org/10.1523/JNEUROSCI.2853-17.2018.

Bakken, T.E., van Velthoven, C.T., Menon, V., Hodge, R.D., Yao, Z., Nguyen, T.N., Graybuck, L.T., Horwitz, G.D., Bertagnolli, D., Goldy, J., Yanny, A.M., Garren, E., Parry, S., Casper, T., Shehata, S.I., Barkan, E.R., Szafer, A., Levi, B.P., Dee, N., Smith, K.A., Sunkin, S.M., Bernard, A., Phillips, J., Hawrylycz, M.J., Koch, C., Murphy, G.J., Lein, E., Zeng, H., Tasic, B., 2021. Single-cell and single-nucleus RNA-seq uncovers shared and distinct axes of variation in dorsal LGN neurons in mice, non-human primates, and humans. Elife 10, 1–20. https://doi.org/10.7554/eLife.64875.

Barbas, H., García-Cabezas, M., 2015. Motor cortex layer 4: Less is more. Trends Neurosci. 38, 259–261. https://doi.org/10.1016/j.tins.2015.03.005.

Beloozerova, I.N., Sirota, M.G., Orlovsky, G.N., Deliagina, T.G., 2006. Comparison of activity of individual pyramidal tract neurons during balancing, locomotion, and scratching. Behav. Brain Res. 169, 98–110. https://doi.org/10.1016/j.bbr.2005.12.009.

Bentivoglio, A.R., Fasano, A., Piano, C., Soleti, F., Daniele, A., Zinno, M., Piccininni, C., De Simone, C., Policicchio, D., Tufo, T., Meglio, M., Cioni, B., 2012. Unilateral extradural motor cortex stimulation is safe and improves Parkinson Disease at 1

Year. Neurosurgery 71, 815–825. https://doi.org/10.1227/NEU.0b013e318266e6a5.
Berger, B., Verney, C., Alvarez, C., Vigny, A., Helle, K.B., 1985. New dopaminergic terminal fields in the motor, visual (area 18b) and retrosplenial cortex in the young and adult rat. Immunocytochemical and catecholamine histochemical analyses. Neuroscience 15, 983–998. https://doi.org/10.1016/0306-4522(85)90248-9.
Berger, B., Gaspar, P., Verney, C., 1991. Dopaminergic innervation of the cerebral cortex: unexpected differences between rodents and primates. Trends Neurosci. 14, 21–27. https://doi.org/10.1016/0166-2236(91)90179-X.
Betarbet, R., Sherer, T.B., Timothy Greenamyre, J., 2002. Animal models of Parkinson's disease. BioEssays 24, 308–318. https://doi.org/10.1002/bies.10067.
Biane, J.S., Takashima, Y., Scanziani, M., Conner, J.M., Tuszynski, M.H., 2016. Thalamocortical projections onto behaviorally relevant neurons exhibit plasticity during adult motor learning. Neuron 89, 1173–1179. https://doi.org/10.1016/j.neuron.2016.02.001.
Biane, J.S., Takashima, Y., Scanziani, M., Conner, J.M., Tuszynski, M.H., 2019. Reorganization of recurrent Layer 5 corticospinal networks following adult motor training. J. Neurosci. 39, 4684–4693. https://doi.org/10.1523/JNEUROSCI.3442-17.2019.
Bohannon, A.S., Hablitz, J.J., 2018. Optogenetic dissection of roles of specific cortical interneuron subtypes in GABAergic network synchronization. J. Physiol. 596, 901–919. https://doi.org/10.1113/JP275317.
Botella, J.A., Bayersdorfer, F., Schneuwly, S., 2008. Superoxide dismutase overexpression protects dopaminergic neurons in a Drosophila model of Parkinson's disease. Neurobiol. Dis. 30, 65–73. https://doi.org/10.1016/j.nbd.2007.11.013.
Bouzas, E.A., Karadimas, P., Alexandrou, A., Panagopoulos, I., 2008. Petilla terminology: nomenclature of features of GABAergic interneurons of the cerebral cortex. Nat. Rev. Neurosci. 9, 557–568. https://doi.org/10.1038/nrn2402.
Brown, A.R., Teskey, G.C., 2014. Motor cortex is functionally organized as a set of spatially distinct representations for complex movements. J. Neurosci. 34, 13574–13585. https://doi.org/10.1523/JNEUROSCI.2500-14.2014.
Burciu, R.G., Vaillancourt, D.E., 2018. Imaging of motor cortex physiology in Parkinson's Disease. Mov. Disord. 33, 1688–1699. https://doi.org/10.1002/mds.102.
Callaway, EM, et al., 2021. A multimodal cell census and atlas of the mammalian primary motor cortex. Nature 598, 86–102. https://doi.org/10.1038/s41586-021-03950-0.
Campos, A.C.P., Berzuíno, M.B., Barbosa, G.R., Freire, H.M.R.C., Lopes, P.S., Assis, D.V., Fonoff, E.T., Pagano, R.L., 2021. Motor cortex stimulation reversed hypernociception, increased serotonin in raphe neurons, and caused inhibition of spinal astrocytes in a Parkinson's Disease Rat Model. Cells 10, 1158. https://doi.org/10.3390/cells10051158.
Camps, M., Kelly, P.H., Palacios, J.M., 1990. Autoradiographic localization of dopamine D1 and D2 receptors in the brain of several mammalian species. J. Neural Transm. 80, 105–127. https://doi.org/10.1007/BF01257077.
Canavero, S., Bonicalzi, V., 1995. Cortical stimulation for central pain. J. Neurosurg. 83, 1993. https://doi.org/10.3171/jns.1995.83.6.1117.
Canavero, S., Paolotti, R., 2000. Extradural motor cortex stimulation for advanced Parkinson's disease: Case report. Mov. Disord. 15, 169–171. https://doi.org/10.1002/1531-8257(200001)15:1<169::AID-MDS1030>3.0.CO;2-W.
Canavero, S., Paolotti, R., Bonicalzi, V., Castellano, G., Greco-Crasto, S., Rizzo, L., Davini, O., Zenga, F., Ragazzi, P., 2002. Extradural motor cortex stimulation for advanced Parkinson disease. J. Neurosurg. 97, 1208–1211. https://doi.org/10.3171/jns.2002.97.5.1208.
Cao, C., Li, D., Zhan, S., Zhang, C., Sun, B., Litvak, V., 2020. L-dopa treatment increases oscillatory power in the motor cortex of Parkinson's disease patients. NeuroImage Clin. 26, 102255 https://doi.org/10.1016/j.nicl.2020.102255.
Capper-Loup, C., Burgunder, J.-M., Kaelin-Lang, A., 2005. Modulation of parvalbumin expression in the motor cortex of parkinsonian rats. Exp. Neurol. 193, 234–237. https://doi.org/10.1016/j.expneurol.2004.12.007.
Chard, P.S., Bleakman, D., Christakos, S., Fullmer, C.S., Miller, R.J., 1993. Calcium buffering properties of calbindin D28k and parvalbumin in rat sensory neurones. J. Physiol. 472, 341–357. https://doi.org/10.1113/jphysiol.1993.sp019950.
Chen, C., Gilmore, A., Zuo, Y., 2014. Study motor skill learning by single-pellet reaching tasks in mice. J. Vis. Exp. 1–7 https://doi.org/10.3791/51238.
Chen, K., Yang, G., So, K.-F., Zhang, L., 2019. Activation of cortical somatostatin interneurons rescues synapse loss and motor deficits after acute MPTP Infusion. iScience 17, 230–241. https://doi.org/10.1016/j.isci.2019.06.040.
Chen, L., Daniels, S., Kim, Y., Chu, H.-Y., 2021. Cell type-specific decrease of the intrinsic excitability of motor cortical pyramidal neurons in Parkinsonism. J. Neurosci. 41, 5553–5565. https://doi.org/10.1523/JNEUROSCI.2694-20.2021.
Chia, S.J., Tan, E., Chao, Y., 2020. Historical perspective: models of Parkinson's Disease. Int. J. Mol. Sci. 21, 2464. https://doi.org/10.3390/ijms21072464.
Chu, J., Wagle-Shukla, A., Gunraj, C., Lang, A.E., Chen, R., 2009. Impaired presynaptic inhibition in the motor cortex in Parkinson disease. Neurology 72, 842–849. https://doi.org/10.1212/01.wnl.0000343881.27524.e8.
Chu, H.-Y., McIver, E.L., Kovaleski, R.F., Atherton, J.F., Bevan, M.D., 2017. Loss of hyperdirect pathway cortico-subthalamic inputs following degeneration of midbrain dopamine neurons. Neuron 95. https://doi.org/10.1016/j.neuron.2017.08.038, 1306-1318.e5.
Chu, Y., Muller, S., Tavares, A., Barret, O., Alagille, D., Seibyl, J., Tamagnan, G., Marek, K., Luk, K.C., Trojanowski, J.Q., Lee, V.M.Y., Kordower, J.H., 2019. Intrastriatal alpha-synuclein fibrils in monkeys: spreading, imaging and neuropathological changes. Brain 142, 3565–3579. https://doi.org/10.1093/brain/awz296.
Cioni, B., 2005. Motor cortex stimulation for Parkinson's disease? Neuroscientist 11, 105. https://doi.org/10.1016/b978-0-12-815950-7.00023-0.
Cotzias, G.C., Van Woert, M.H., Schiffer, L.M., 1967. Aromatic amino acids and modification of Parkinsonism. N. Engl. J. Med. 276, 374–379. https://doi.org/10.1056/NEJM196702162760703.
Cousineau, J., Lescouzères, L., Taupignon, A., Delgado-Zabalza, L., Valjent, E., Baufreton, J., Le Bon-Jégo, M., 2020. Dopamine D2-Like receptors modulate intrinsic properties and synaptic transmission of parvalbumin interneurons in the mouse primary motor cortex. eneuro 7. https://doi.org/10.1523/ENEURO.0081-20.2020. ENEURO.0081-20.2020.
Cowan, R.L., Wilson, C.J., 1994. Spontaneous firing patterns and axonal projections of single corticostriatal neurons in the rat medial agranular cortex. J. Neurophysiol. 71, 17–32. https://doi.org/10.1152/jn.1994.71.1.17.
Cunic, D., Roshan, L., Khan, F.I., Lozano, A.M., Lang, A.E., Chen, R., 2002. Effects of subthalamic nucleus stimulation on motor cortex excitability in Parkinson's disease. Neurology 58, 1665–1672. https://doi.org/10.1212/WNL.58.11.1665.
Dan, X., Liu, J., Doyon, J., Zhou, Y., Ma, J., Chan, P., 2019. Impaired fine motor function of the asymptomatic hand in unilateral Parkinson's Disease. Front. Aging Neurosci. 11, 1–9. https://doi.org/10.3389/fnagi.2019.00266.
Darling, W.G., Pizzimenti, M.A., Morecraft, R.J., 2011. Functional recovery following motor cortex lesions in non-human primates : experimental implications for human stroke patients. J. Integr. Neurosci. 10, 353–384. https://doi.org/10.1142/S0219635211002737.
de Groot, A., van den Boom, B.J.G., van Genderen, R.M., Coppens, J., van Veldhuijzen, J., Bos, J., Hoedemaker, H., Negrello, M., Willuhn, I., De Zeeuw, C.I., Hoogland, T.M., 2020. NINscope, a versatile miniscope for multi-region circuit investigations. Elife 9, 1–24. https://doi.org/10.7554/eLife.49987.
de Hemptinne, C., Swann, N.C., Ostrem, J.L., Ryapolova-Webb, E.S., San Luciano, M., Galifianakis, N.B., Starr, P.A., 2015. Therapeutic deep brain stimulation reduces cortical phase-amplitude coupling in Parkinson's disease. Nat. Neurosci. 18, 779–786. https://doi.org/10.1038/nn.3997.
De Rose, M., Guzzi, G., Bosco, D., Romano, M., Lavano, S.M., Plastino, M., Volpentesta, G., Marotta, R., Lavano, A., 2012. Motor cortex stimulation in Parkinson's Disease. Neurol. Res. Int. 2012, 1–7. https://doi.org/10.1155/2012/502096.
Degos, B., Deniau, J.-M., Chavez, M., Maurice, N., 2013. Subthalamic nucleus high-frequency stimulation restores altered electrophysiological properties of cortical neurons in Parkinsonian Rat. PLoS One 8, e83608. https://doi.org/10.1371/journal.pone.0083608.
Deniau, J.-M., Degos, B., Bosch, C., Maurice, N., 2010. Deep brain stimulation mechanisms: beyond the concept of local functional inhibition. Eur. J. Neurosci. 32, 1080–1091. https://doi.org/10.1111/j.1460-9568.2010.07413.x.
Descarries, L., Lemay, B., Doucet, G., Berger, B., 1987. Regional and laminar density of the dopamine innervation in adult rat cerebral cortex. Neuroscience 21, 807–824. https://doi.org/10.1016/0306-4522(87)90038-8.
Donato, F., Rompani, S.B., Caroni, P., 2013. Parvalbumin-expressing basket-cell network plasticity induced by experience regulates adult learning. Nature 504, 272–276. https://doi.org/10.1038/nature12866.
Donoghue, J.P., Kitai, S.T., 1981. A collateral pathway to the neostriatum from corticofugal neurons of the rat sensory-motor cortex: an intracellular HRP study. J. Comp. Neurol. 201, 1–13. https://doi.org/10.1002/cne.902010102.
Donoghue, J.P., Wise, S.P., 1982. The motor cortex of the rat: cytoarchitecture and microstimulation mapping. J. Comp. Neurol. 212, 76–88. https://doi.org/10.1002/cne.902120106.
Drouot, X., Oshino, S., Jarraya, B., Besret, L., Kishima, H., Remy, P., Dauguet, J., Lefaucheur, J.P., Dollé, F., Condé, F., Bottlaender, M., Peschanski, M., Kéravel, Y., Hantraye, P., Palfi, S., 2004. Functional recovery in a primate model of Parkinson's Disease following motor cortex stimulation. Neuron 44, 769–778. https://doi.org/10.1016/j.neuron.2004.11.023.
Duan, Z., Li, A., Gong, H., Li, X., 2020. A Whole-brain Map of Long-range Inputs to GABAergic Interneurons in the Mouse Caudal Forelimb Area. Neurosci. Bull. 36, 493–505. https://doi.org/10.1007/s12264-019-00458-6.
Dupont-Hadwen, J., Bestmann, S., Stagg, C.J., 2019. Motor training modulates intracortical inhibitory dynamics in motor cortex during movement preparation. Brain Stimul. 12, 300–308. https://doi.org/10.1016/j.brs.2018.11.002.
Ebbesen, C.L., Brecht, M., 2017. Motor cortex — to act or not to act? Nat. Rev. Neurosci. 18, 694–705. https://doi.org/10.1038/nrn.2017.119.
Economo, M.N., Viswanathan, S., Tasic, B., Bas, E., Winnubst, J., Menon, V., Graybuck, L. T., Nguyen, T.N., Smith, K.A., Yao, Z., Wang, L., Gerfen, C.R., Chandrashekar, J., Zeng, H., Looger, L.L., Svoboda, K., 2018. Distinct descending motor cortex pathways and their roles in movement. Nature 563, 79–84. https://doi.org/10.1038/s41586-018-0642-9.
Emig, M., George, T., Zhang, J.K., Soudagar-Turkey, M., 2021. The role of exercise in Parkinson's Disease. J. Geriatr. Psychiatry Neurol. 34, 321–330. https://doi.org/10.1177/08919887211018273.
Eusebio, A., Thevathasan, W., Doyle Gaynor, L., Pogosyan, A., Bye, E., Foltynie, T., Zrinzo, L., Ashkan, K., Aziz, T., Brown, P., 2011. Deep brain stimulation can suppress pathological synchronisation in parkinsonian patients. J. Neurol. Neurosurg. Psychiatry 82, 569–573. https://doi.org/10.1136/jnnp.2010.217489.
Fahn, S., 2006. Levodopa in the treatment of Parkinson's disease, in: Oxidative Stress and Neuroprotection. Springer Vienna, Vienna, pp. 1–15. https://doi.org/10.1007/978-3-211-33328-0_1.
Fahn, S., 2008. The history of dopamine and levodopa in the treatment of Parkinson's disease. Mov. Disord. 23, S497–S508. https://doi.org/10.1002/mds.22028.
Fallon, J., 1981. Collateralization of monoamine neurons: mesotelencephalic dopamine projections to caudate, septum, and frontal cortex. J. Neurosci. 1, 1361–1368. https://doi.org/10.1523/JNEUROSCI.01-12-01361.1981.

Fasano, A., Piano, C., De Simone, C., Cioni, B., Di Giuda, D., Zinno, M., Daniele, A., Meglio, M., Giordano, A., Bentivoglio, A.R., 2008. High frequency extradural motor cortex stimulation transiently improves axial symptoms in a patient with Parkinson's disease. Mov. Disord. 23, 1916–1919. https://doi.org/10.1002/mds.21977.

Ferguson, B.R., Gao, W.-J., 2018. PV Interneurons: critical regulators of E/I balance for prefrontal cortex-dependent behavior and psychiatric disorders. Front. Neural Circuits 12, 1–13. https://doi.org/10.3389/fncir.2018.00037.

Ferro, M.M., Bellissimo, M.I., Anselmo-Franci, J.A., Angellucci, M.E.M., Canteras, N.S., Da Cunha, C., 2005. Comparison of bilaterally 6-OHDA- and MPTP-lesioned rats as models of the early phase of Parkinson's disease: Histological, neurochemical, motor and memory alterations. J. Neurosci. Methods 148, 78–87. https://doi.org/10.1016/j.jneumeth.2005.04.005.

Formaggio, E., Rubega, M., Rupil, J., Antonini, A., Masiero, S., Toffolo, G.M., Del Felice, A., 2021. Reduced effective connectivity in the motor cortex in Parkinson's Disease. Brain Sci. 11, 1200. https://doi.org/10.3390/brainsci11091200.

Fraix, V., Pollak, P., Vercueil, L., Benabid, A.-L., Mauguière, F., 2008. Effects of subthalamic nucleus stimulation on motor cortex excitability in Parkinson's disease. Clin. Neurophysiol. 119, 2513–2518. https://doi.org/10.1016/j.clinph.2008.07.217.

Fritsch, G., Hitzig, E., 2009. Electric excitability of the cerebrum (Über die elektrische Erregbarkeit des Grosshirns). Epilepsy Behav. 15, 123–130. https://doi.org/10.1016/j.yebeh.2009.03.001.

Frost, S.B., Milliken, G.W., Plautz, E.J., Masterton, R.B., Nudo, R.J., 2000. Somatosensory and motor representations in cerebral cortex of a primitive mammal (Monodelphis domestica): A window into the early evolution of sensorimotor cortex. J. Comp. Neurol. 421, 29–51. https://doi.org/10.1002/(SICI)1096-9861(20000522)421:1<29::AID-CNE3>3.0.CO;2-9.

Galiñanes, G.L., Bonardi, C., Huber, D., 2018. Directional reaching for water as a cortex-dependent behavioral framework for mice. Cell Rep. 22, 2767–2783. https://doi.org/10.1016/j.celrep.2018.02.042.

Gaspar, P., Duyckaerts, C., Alvarez, C., Javoy-Agid, F., Berger, B., 1991. Alterations of dopaminergic and noradrenergic innervations in motor cortex in parkinson's disease. Ann. Neurol. 30, 365–374. https://doi.org/10.1002/ana.410300308.

Gaspar, P., Bloch, B., Moine, C., 1995. D1 and D2 receptor gene expression in the rat frontal cortex: cellular localization in different classes of efferent neurons. Eur. J. Neurosci. 7, 1050–1063. https://doi.org/10.1111/j.1460-9568.1995.tb01092.x.

Gebhardt, A., Vanbellingen, T., Baronti, F., Kersten, B., Bohlhalter, S., 2008. Poor dopaminergic response of impaired dexterity in Parkinson's disease: Bradykinesia or limb kinetic apraxia? Mov. Disord. 23, 1701–1706. https://doi.org/10.1002/mds.22199.

Gee, S., Ellwood, I., Patel, T., Luongo, F., Deisseroth, K., Sohal, V.S., 2012. Synaptic activity unmasks dopamine D2 receptor modulation of a specific class of layer V pyramidal neurons in prefrontal cortex. J. Neurosci. 32, 4959–4971. https://doi.org/10.1523/JNEUROSCI.5835-11.2012.

Gerlach, M., Riederer, P., 1996. Animal models of Parkinson's disease: An empirical comparison with the phenomenology of the disease in man. J. Neural Transm. 103, 987–1041. https://doi.org/10.1007/BF01291788.

Gilat, M., Ginis, P., Zoetewei, D., De Vleeschhauwer, J., Hulzinga, F., D'Cruz, N., Nieuwboer, A., 2021. A systematic review on exercise and training-based interventions for freezing of gait in Parkinson's disease. npj Park Dis. 7, 81. https://doi.org/10.1038/s41531-021-00224-4.

Goldberg, J.A., Boraud, T., Maraton, S., Haber, S.N., Vaadia, E., Bergman, H., 2002. Enhanced synchrony among primary motor cortex neurons in the 1-methyl-4-phenyl-1,2,3,6-tetrahydropyridine primate model of Parkinson's Disease. J. Neurosci. 22, 4639–4653. https://doi.org/10.1523/JNEUROSCI.22-11-04639.2002.

Gradinaru, V., Mogri, M., Thompson, K.R., Henderson, J.M., Deisseroth, K., 2009. Optical deconstruction of parkinsonian neural circuitry. Science (80-). 324, 354–359. https://doi.org/10.1126/science.1167093.

Graziano, M.S., Taylor, C.S., Moore, T., Cooke, D.F., 2002. The cortical control of movement revisited. Neuron 36, 349–362. https://doi.org/10.1016/S0896-6273(02)01003-6.

Graziano, M.S.A., Aflalo, T.N.S., Cooke, D.F., 2005. Arm movements evoked by electrical stimulation in the motor cortex of monkeys. J. Neurophysiol. 94, 4209–4223. https://doi.org/10.1152/jn.01303.2004.

Gulati, S., Cao, V.Y., Otte, S., 2017. Multi-layer cortical Ca^{2+} imaging in freely moving mice with prism probes and miniaturized fluorescence microscopy. J. Vis. Exp. 2017, 1–9. https://doi.org/10.3791/55579.

Guo, J.-Z., Graves, A.R., Guo, W.W., Zheng, J., Lee, A., Rodríguez-González, J., Li, N., Macklin, J.J., Phillips, J.W., Mensh, B.D., Branson, K., Hantman, A.W., 2015a. Cortex commands the performance of skilled movement. Elife 4, 1–18. https://doi.org/10.7554/eLife.10774.

Guo, L., Xiong, H., Kim, J.-I., Wu, Y.-W., Lalchandani, R.R., Cui, Y., Shu, Y., Xu, T., Ding, J.B., 2015b. Dynamic rewiring of neural circuits in the motor cortex in mouse models of Parkinson's disease. Nat. Neurosci. 18, 1299–1309. https://doi.org/10.1038/nn.4082.

Hall, R.D., Lindholm, E.P., 1974. Organization of motor and somatosensory neocortex in the albino rat. Brain Res. 66, 23–38. https://doi.org/10.1016/0006-8993(74)90076-6.

Hammond, C., Ammari, R., Bioulac, B., Garcia, L., 2008. Latest view on the mechanism of action of deep brain stimulation. Mov. Disord. 23, 2111–2121. https://doi.org/10.1002/mds.22120.

Harms, K.J., Rioult-Pedotti, M.S., Carter, D.R., Dunaevsky, A., 2008. Transient spine expansion and learning-induced plasticity in Layer 1 primary motor cortex. J. Neurosci. 28, 5686–5690. https://doi.org/10.1523/JNEUROSCI.0584-08.2008.

Harrison, I.F., Anis, H.K., Dexter, D.T., 2016. Associated degeneration of ventral tegmental area dopaminergic neurons in the rat nigrostriatal lactacystin model of parkinsonism and their neuroprotection by valproate. Neurosci. Lett. 614, 16–23. https://doi.org/10.1016/j.neulet.2015.12.052.

Hayashi-Takagi, A., Yagishita, S., Nakamura, M., Shirai, F., Wu, Y.I., Loshbaugh, A.L., Kuhlman, B., Hahn, K.M., Kasai, H., 2015. Labelling and optical erasure of synaptic memory traces in the motor cortex. Nature 525, 333–338. https://doi.org/10.1038/nature15257.

Hooks, B.M., Mao, T., Gutnisky, D.A., Yamawaki, N., Svoboda, K., Shepherd, G.M.G., 2013. Organization of cortical and thalamic input to pyramidal neurons in mouse motor cortex. J. Neurosci. 33, 748–760. https://doi.org/10.1523/JNEUROSCI.4338-12.2013.

Hosp, J.A., Pekanovic, A., Rioult-Pedotti, M.S., Luft, A.R., 2011. Dopaminergic projections from midbrain to primary motor cortex mediate motor skill learning. J. Neurosci. 31, 2481–2487. https://doi.org/10.1523/JNEUROSCI.5411-10.2011.

Hosp, J.A., Nolan, H.E., Luft, A.R., 2015. Topography and collateralization of dopaminergic projections to primary motor cortex in rats. Exp. Brain Res. 233, 1365–1375. https://doi.org/10.1007/s00221-015-4211-2.

Hosp, J.A., Coenen, V.A., Rijntjes, M., Egger, K., Urbach, H., Weiller, C., Reisert, M., 2019. Ventral tegmental area connections to motor and sensory cortical fields in humans. Brain Struct. Funct. 224, 2839–2855. https://doi.org/10.1007/s00429-019-01939-0.

Hu, H., Gan, J., Jonas, P., 2014. Fast-spiking, parvalbumin+ GABAergic interneurons: from cellular design to microcircuit function. Science 345 (6196), 1255263. https://doi.org/10.1126/science.1255263.

Huber, D., Gutnisky, D.A., Peron, S., O'Connor, D.H., Wiegert, J.S., Tian, L., Oertner, T.G., Looger, L.L., Svoboda, K., 2012. Multiple dynamic representations in the motor cortex during sensorimotor learning. Nature 484, 473–478. https://doi.org/10.1038/nature11039.

Huda, K., Salunga, T.L., Chowdhury, S.A., Kawashima, T., Matsunami, K., 1999. Dopaminergic modulation of transcallosal activity of cat motor cortical neurons. Neurosci. Res. 33, 33–40. https://doi.org/10.1016/S0168-0102(98)00108-4.

Huda, K., Salunga, T.L., Matsunami, K., 2001. Dopaminergic inhibition of excitatory inputs onto pyramidal tract neurons in cat motor cortex. Neurosci. Lett. 307, 175–178. https://doi.org/10.1016/S0304-3940(01)01960-7.

Huntley, G.W., Morrison, J.H., Prikhozhan, A., Sealfon, S.C., 1992. Localization of multiple dopamine receptor subtype mRNAs in human and monkey motor cortex and striatum. Mol. Brain Res. 15, 181–188. https://doi.org/10.1016/0169-328X(92)90107-M.

Hyland, B.I., Seeger-Armbruster, S., Smither, R.A., Parr-Brownlie, L.C., 2019. Altered recruitment of motor cortex neuronal activity during the grasping phase of skilled reaching in a chronic rat model of unilateral Parkinsonism. J. Neurosci. 39, 9660–9672. https://doi.org/10.1523/JNEUROSCI.0720-19.2019.

Isomura, Y., Harukuni, R., Takekawa, T., Aizawa, H., Fukai, T., 2009. Microcircuitry coordination of cortical motor information in self-initiation of voluntary movements. Nat. Neurosci. 12, 1586–1593. https://doi.org/10.1038/nn.2431.

Jang, D.P., Min, H.-K., Lee, S.-Y., Kim, I.Y., Park, H.W., Im, Y.H., Lee, S., Sim, J., Kim, Y.-B., Paek, S.H., Cho, Z.-H., 2012. Functional neuroimaging of the 6-OHDA lesion rat model of Parkinson's disease. Neurosci. Lett. 513, 187–192. https://doi.org/10.1016/j.neulet.2012.02.034.

Karni, A., Meyer, G., Jezzard, P., Adams, M.M., Turner, R., Ungerleider, L.G., 1995. Functional MRI evidence for adult motor cortex plasticity during motor skill learning. Nature 377, 155–158. https://doi.org/10.1038/377155a0.

Kawai, R., Markman, T., Poddar, R., Ko, R., Fantana, A.L., Dhawale, A.K., Kampff, A.R., Ölveczky, B.P., 2015. Motor cortex is required for learning but not for executing a motor skill. Neuron 86, 800–812. https://doi.org/10.1016/j.neuron.2015.03.024.

Kida, H., Tsuda, Y., Ito, N., Yamamoto, Y., Owada, Y., Kamiya, Y., Mitsushima, D., 2016. Motor training promotes both synaptic and intrinsic plasticity of layer II/III pyramidal neurons in the primary motor cortex. Cereb. Cortex 26, 3494–3507. https://doi.org/10.1093/cercor/bhw134.

Kita, T., Kita, H., 2012. The subthalamic nucleus is one of multiple innervation sites for long-range corticofugal axons: a single-axon tracing study in the rat. J. Neurosci. 32, 5990–5999. https://doi.org/10.1523/JNEUROSCI.5717-11.2012.

Klein, A., Sacrey, L.-A.R., Whishaw, I.Q., Dunnett, S.B., 2012. The use of rodent skilled reaching as a translational model for investigating brain damage and disease. Neurosci. Biobehav. Rev. 36, 1030–1042. https://doi.org/10.1016/j.neubiorev.2011.12.010.

Kondo, T., Saito, R., Otaka, M., Yoshino-Saito, K., Yamanaka, A., Yamamori, T., Watakabe, A., Mizukami, H., Schnitzer, M.J., Tanaka, K.F., Ushiba, J., Okano, H., 2018. Calcium transient dynamics of neural ensembles in the primary motor cortex of naturally behaving monkeys. Cell Rep. 24, 2191–2195.e4. https://doi.org/10.1016/j.celrep.2018.07.057.

Kunori, N., Kajiwara, R., Takashima, I., 2014. Voltage-sensitive dye imaging of primary motor cortex activity produced by ventral tegmental area stimulation. J. Neurosci. 34, 8894–8903. https://doi.org/10.1523/JNEUROSCI.5286-13.2014.

Kwakkel, G., Kollen, B.J., van der Grond, J., Prevo, A.J.H., 2003. Probability of regaining dexterity in the flaccid upper limb. Stroke 34, 2181–2186. https://doi.org/10.1161/01.STR.0000087172.16305.CD.

Labouesse, M.A., Cola, R.B., Patriarchi, T., 2020. GPCR-based dopamine sensors—a detailed guide to inform sensor choice for in vivo imaging. Int. J. Mol. Sci. 21, 8048. https://doi.org/10.3390/ijms21218048.

Lapish, C.C., Kroener, S., Durstewitz, D., Lavin, A., Seamans, J.K., 2007. The ability of the mesocortical dopamine system to operate in distinct temporal modes. Psychopharmacology 191, 609–625. https://doi.org/10.1007/s00213-006-0527-8.

Lashley, K.S., 1924. Studies of cerebral function in learning. Arch. Neurol. Psychiatr. 12, 249. https://doi.org/10.1001/archneurpsyc.1924.02200030002001.

Lavano, A., Guzzi, G., De Rose, M., Romano, M., Della Torre, A., Vescio, G., Deodato, F., Lavano, F., Volpentesta, G., 2016. Minimally invasive motor cortex stimulation for Parkinson's disease. J. Neurosurg. Sci. 61, 77–87. https://doi.org/10.23736/S0390-5616.16.03246-X.

Lavin, A., Nogueira, L., Lapish, C.C., Wightman, R.M., Phillips, P.E.M., Seamans, J.K., 2005. Mesocortical dopamine neurons operate in distinct temporal domains using multimodal signaling. J. Neurosci. 25, 5013–5023. https://doi.org/10.1523/JNEUROSCI.0557-05.2005.

Lee, D., Dallapiazza, R., De Vloo, P., Lozano, A., 2018. Current surgical treatments for Parkinson's disease and potential therapeutic targets. Neural Regen. Res. 13, 1342. https://doi.org/10.4103/1673-5374.235220.

Leemburg, S., Canonica, T., Luft, A., 2018. Motor skill learning and reward consumption differentially affect VTA activation. Sci. Rep. 8, 687. https://doi.org/10.1038/s41598-017-18716-w.

Levy, S., Lavzin, M., Benisty, H., Ghanayim, A., Dubin, U., Achvat, S., Brosh, Z., Aeed, F., Mensh, B.D., Schiller, Y., Meir, R., Barak, O., Talmon, R., Hantman, A.W., Schiller, J., 2020. Cell-type-specific outcome representation in the primary motor cortex. Neuron 107, 954–971.e9. https://doi.org/10.1016/j.neuron.2020.06.006.

Lewis, D., Campbell, M., Foote, S., Goldstein, M., Morrison, J., 1987. The distribution of tyrosine hydroxylase-immunoreactive fibers in primate neocortex is widespread but regionally specific. J. Neurosci. 7, 279–290. https://doi.org/10.1523/JNEUROSCI.07-01-00279.1987.

Leyton, A.S.F., Sherrington, C.S., 1917. Observations on the excitable cortex of the chimpanzee, orang-utan, and gorilla. Q. J. Exp. Physiol. 11, 135–222. https://doi.org/10.1113/expphysiol.1917.sp000240.

Li, S., Arbuthnott, G.W., Jutras, M.J., Goldberg, J.A., Jaeger, D., 2007. Resonant antidromic cortical circuit activation as a consequence of high-frequency subthalamic deep-brain stimulation. J. Neurophysiol. 98, 3525–3537. https://doi.org/10.1152/jn.00808.2007.

Li, Q., Ke, Y., Chan, D.C.W., Qian, Z.-M., Yung, K.K.L., Ko, H., Arbuthnott, G.W., Yung, W.-H., 2012. Therapeutic deep brain stimulation in parkinsonian rats directly influences motor cortex. Neuron 76, 1030–1041. https://doi.org/10.1016/j.neuron.2012.09.032.

Li, Q., Qian, Z.-M., Arbuthnott, G.W., Ke, Y., Yung, W.-H., 2014. Cortical effects of deep brain stimulation. JAMA Neurol. 71, 100. https://doi.org/10.1001/jamaneurol.2013.4221.

Li, N., Chen, T.-W., Guo, Z.V., Gerfen, C.R., Svoboda, K., 2015. A motor cortex circuit for motor planning and movement. Nature 519, 51–56. https://doi.org/10.1038/nature14178.

Li, N., Daie, K., Svoboda, K., Druckmann, S., 2016. Robust neuronal dynamics in premotor cortex during motor planning. Nature 532, 459–464. https://doi.org/10.1038/nature17643.

Li, M., Li, L., Wang, K., Su, W., Jia, J., Wang, X., 2017a. The effect of electroacupuncture on proteomic changes in the motor cortex of 6-OHDA Parkinsonian rats. Brain Res. 1673, 52–63. https://doi.org/10.1016/j.brainres.2017.07.027.

Li, Q., Ko, H., Qian, Z.-M., Yan, L.Y.C., Chan, D.C.W., Arbuthnott, G., Ke, Y., Yung, W.-H., 2017b. Refinement of learned skilled movement representation in motor cortex deep output layer. Nat. Commun. 8, 15834. https://doi.org/10.1038/ncomms15834.

Li, M., Wang, Xuenan, Yao, X., Wang, Xiaojun, Chen, F., Zhang, X., Sun, S., He, F., Jia, Q., Guo, M., Chen, D., Sun, Y., Li, Y., He, Q., Zhu, Z., Wang, M., 2021. Roles of motor cortex neuron classes in reach-related modulation for Hemiparkinsonian rats. Front. Neurosci. 15, 1–23. https://doi.org/10.3389/fnins.2021.645849.

Lindenbach, D., Conti, M.M., Ostock, C.Y., George, J.A., Goldenberg, A.A., Melikhov-Sosin, M., Nuss, E.E., Bishop, C., 2015. The role of primary motor cortex (M1) glutamate and GABA signaling in L-DOPA-induced dyskinesia in Parkinsonian Rats. J. Neurosci. 36, 9873–9887. https://doi.org/10.1523/JNEUROSCI.1318-16.2016.

Lorigados, L., Alvarez, P., Pavón, N., Serrano, T., Blanco, L., MacÍas, R., 1996. NGF in experimental models of Parkinson disease. Mol. Chem. Neuropathol. 28, 225–228. https://doi.org/10.1007/BF02815226.

Maarrawi, J., Peyron, R., Mertens, P., Costes, N., Magnin, M., Sindou, M., Laurent, B., Garcia-Larrea, L., 2007. Motor cortex stimulation for pain control induces changes in the endogenous opioid system. Neurology 69, 827–834. https://doi.org/10.1212/01.wnl.0000269783.86997.37.

Magno, L.A.V., Tenza-Ferrer, H., Collodetti, M., Aguiar, M.F.G., Rodrigues, A.P.C., da Silva, R.S., Do Silva, J.P., Nicolau, N.F., Rosa, D.V.F., Birbrair, A., Miranda, D.M., Romano-Silva, M.A., 2019. Optogenetic stimulation of the M2 cortex reverts motor dysfunction in a mouse model of Parkinson's Disease. J. Neurosci. 39, 3234–3248. https://doi.org/10.1523/JNEUROSCI.2277-18.2019.

Mallet, N., Pogosyan, A., Sharott, A., Csicsvari, J., Bolam, J.P., Brown, P., Magill, P.J., 2008. Disrupted dopamine transmission and the emergence of exaggerated beta oscillations in subthalamic nucleus and cerebral cortex. J. Neurosci. 28, 4795–4806. https://doi.org/10.1523/JNEUROSCI.0123-08.2008.

Mansour, A., Meador-Woodruff, J., Bunzow, J., Civelli, O., Akil, H., Watson, S., 1990. Localization of dopamine D2 receptor mRNA and D1 and D2 receptor binding in the rat brain and pituitary: an in situ hybridization- receptor autoradiographic analysis. J. Neurosci. 10, 2587–2600. https://doi.org/10.1523/JNEUROSCI.10-08-02587.1990.

Marinelli, L., Quartarone, A., Hallett, M., Frazzitta, G., Ghilardi, M.F., 2017. The many facets of motor learning and their relevance for Parkinson's disease. Clin. Neurophysiol. 128, 1127–1141. https://doi.org/10.1016/j.clinph.2017.03.042.

Mathai, A., Ma, Y., Paré, J.-F., Villalba, R.M., Wichmann, T., Smith, Y., 2015. Reduced cortical innervation of the subthalamic nucleus in MPTP-treated parkinsonian monkeys. Brain 138, 946–962. https://doi.org/10.1093/brain/awv018.

McEntee, W.J., Mair, R.G., Langlais, P.J., 1987. Neurochemical specificity of learning: dopamine and motor learning. Yale J. Biol. Med. 60, 187–193.

Melzer, S., Gil, M., Koser, D.E., Michael, M., Huang, K.W., Monyer, H., 2017. Distinct corticostriatal GABAergic neurons modulate striatal output neurons and motor activity. Cell Rep. 19, 1045–1055. https://doi.org/10.1016/j.celrep.2017.04.024.

Mercuri, N., Calabresi, P., Stanzione, P., Bernardi, G., 1985. Electrical stimulation of mesencephalic cell groups (A9-A10) produces monosynaptic excitatory potentials in rat frontal cortex. Brain Res. 338, 192–195. https://doi.org/10.1016/0006-8993(85)90267-7.

Metz, G.A.S., Whishaw, I.Q., 2000. Skilled reaching an action pattern: stability in rat (Rattus norvegicus) grasping movements as a function of changing food pellet size. Behav. Brain Res. 116, 111–122. https://doi.org/10.1016/S0166-4328(00)00245-X.

Mishra, A., Singh, S., Shukla, S., 2018. Physiological and functional basis of dopamine receptors and their role in neurogenesis: possible implication for Parkinson's disease. J. Exp. Neurosci. 12 https://doi.org/10.1177/1179069518779829, 117906951877982.

Molina-Luna, K., Pekanovic, A., Röhrich, S., Hertler, B., Schubring-Giese, M., Rioult-Pedotti, M.-S., Luft, A.R., 2009. Dopamine in motor cortex is necessary for skill learning and synaptic plasticity. PLoS One 4, e7082. https://doi.org/10.1371/journal.pone.0007082.

Monfils, M.H., Plautz, E.J., Kleim, J.A., 2005. In Search of the motor engram: motor map plasticity as a mechanism for encoding motor experience. Neurosci. 11, 471–483. https://doi.org/10.1177/1073858405278015.

Morgante, F., Espay, A.J., Gunraj, C., Lang, A.E., Chen, R., 2006. Motor cortex plasticity in Parkinson's disease and levodopa-induced dyskinesias. Brain 129, 1059–1069. https://doi.org/10.1093/brain/awl031.

Nambu, A., Tachibana, Y., Chiken, S., 2015. Cause of parkinsonian symptoms: Firing rate, firing pattern or dynamic activity changes? Basal Ganglia 5, 1–6. https://doi.org/10.1016/j.baga.2014.11.001.

Ni, Z., Bahl, N., Gunraj, C.A., Mazzella, F., Chen, R., 2013. Increased motor cortical facilitation and decreased inhibition in Parkinson disease. Neurology 80, 1746–1753. https://doi.org/10.1212/WNL.0b013e3182919029.

Nikam, S., Nikam, P., Ahaley, S.K., Sontakke, A.V., 2009. Oxidative stress in Parkinson's disease. Indian J. Clin. Biochem. 24, 98–101. https://doi.org/10.1007/s12291-009-0017-y.

Ohbayashi, M., 2020. Inhibition of protein synthesis in M1 of monkeys disrupts performance of sequential movements guided by memory. Elife 9, 1–20. https://doi.org/10.7554/eLife.53038.

Ott, T., Nieder, A., 2019. Dopamine and cognitive control in prefrontal cortex. Trends Cogn. Sci. 23, 213–234. https://doi.org/10.1016/j.tics.2018.12.006.

Özkan, M., Johnson, N.W., Sehirli, U.S., Woodhall, G.L., Stanford, I.M., 2017. Dopamine acting at D1-like, D2-like and α1-adrenergic receptors differentially modulates theta and gamma oscillatory activity in primary motor cortex. PLoS One 12, e0181633. https://doi.org/10.1371/journal.pone.0181633.

Pagni, C.A., Altibrandi, M.G., Bentivoglio, A., Caruso, G., Cioni, B., Fiorella, C., Insola, A., Lavano, A., Maina, R., Mazzone, P., Signorelli, C.D., Sturiale, C., Valzania, F., Zeme, S., Zenga, F., 2005. Extradural Motor Cortex Stimulation (EMCS) for Parkinson's disease. History and first results by the study group of the Italian neurosurgical society. Acta Neurochir. Suppl. 113–119. https://doi.org/10.1007/3-211-27577-0_19.

Pagni, CA, Zeme, S, Zenga, F, 2003. Further experience with extradural motor cortex stimulation for treatment of advanced Parkinson's disease. Report of 3 new cases. J. Neurosurg Sci. 47 (4), 189–193.

Palomar, F.J., Conde, V., Carrillo, F., Fernández-del-Olmo, M., Koch, G., Mir, P., 2013. Parieto-motor functional connectivity is impaired in Parkinson's disease. Brain Stimul. 6, 147–154. https://doi.org/10.1016/j.brs.2012.03.017.

Parent, M., Parent, A., 2006. Single-axon tracing study of corticostriatal projections arising from primary motor cortex in primates. J. Comp. Neurol. 496, 202–213. https://doi.org/10.1002/cne.20925.

Parr-Brownlie, LC, Hyland, BI, 2005. Bradykinesia induced by dopamine D2 receptor blockade is associated with reduced motor cortex activity in the rat. J. Neurosci. 25 (24), 5700—9. https://doi.org/10.1523/JNEUROSCI.0523-05.2005.

Pasquereau, B., Turner, R.S., 2011. Primary motor cortex of the Parkinsonian monkey: differential effects on the spontaneous activity of pyramidal tract-type neurons. Cereb. Cortex 21, 1362–1378. https://doi.org/10.1093/cercor/bhq217.

Pasquereau, B., Turner, R.S., 2015. Dopamine neurons encode errors in predicting movement trigger occurrence. J. Neurophysiol. 113, 1110–1123. https://doi.org/10.1152/jn.00401.2014.

Patriarchi, T., Cho, J.R., Merten, K., Howe, M.W., Marley, A., Xiong, W.-H., Folk, R.W., Broussard, G.J., Liang, R., Jang, M.J., Zhong, H., Dombeck, D., von Zastrow, M., Nimmerjahn, A., Gradinaru, V., Williams, J.T., Tian, L., 2018. Ultrafast neuronal imaging of dopamine dynamics with designed genetically encoded sensors. Science (80-.) 360, eaat4422. https://doi.org/10.1126/science.aat4422.

Payoux, P., Remy, P., Damier, P., Miloudi, M., Loubinoux, I., Pidoux, B., Gaura, V., Rascol, O., Samson, Y., Agid, Y., 2004. Subthalamic nucleus stimulation reduces abnormal motor cortical overactivity in Parkinson Disease. Arch. Neurol. 61, 1307–1313. https://doi.org/10.1001/archneur.61.8.1307.

Penfield, W., Boldrey, E., 1937. Somatic motor and sensory representation in the cerebral cortex of man as studied by electrical stimulation. Brain 60, 389–443. https://doi.org/10.1093/brain/60.4.389.

Peters, A.J., Chen, S.X., Komiyama, T., 2014. Emergence of reproducible spatiotemporal activity during motor learning. Nature 510, 263–267. https://doi.org/10.1038/nature13235.

Petrie, K.A., Schmidt, D., Bubser, M., Fadel, J., Carraway, R.E., Deutch, A.Y., 2005. Neurotensin activates GABAergic interneurons in the prefrontal cortex. J. Neurosci. 25, 1629–1636. https://doi.org/10.1523/JNEUROSCI.3579-04.2005.

Piano, C., Bove, F., Mulas, D., Di Stasio, E., Fasano, A., Bentivoglio, A.R., Daniele, A., Cioni, B., Calabresi, P., Tufo, T., 2021. Extradural motor cortex stimulation in

Parkinson's Disease: long-term clinical outcome. Brain Sci. 11, 416. https://doi.org/10.3390/brainsci11040416.
Plowman, E.K., Thomas, N.J., Kleim, J.A., 2011. Striatal dopamine depletion induces forelimb motor impairments and disrupts forelimb movement representations within the motor cortex. J. Parkinsons Dis. 1, 93–100. https://doi.org/10.3233/JPD-2011-11017.
Pohar, S.L., Allyson Jones, C., 2009. The burden of Parkinson disease (PD) and concomitant comorbidities. Arch. Gerontol. Geriatr. 49, 317–321. https://doi.org/10.1016/j.archger.2008.11.006.
Proud, E.L., Morris, M.E., 2010. Skilled hand dexterity in Parkinson's Disease: effects of adding a concurrent task. Arch. Phys. Med. Rehabil. 91, 794–799. https://doi.org/10.1016/j.apmr.2010.01.008.
Radad, K., Al-Shraim, M., Al-Emam, A., Wang, F., Kranner, B., Rausch, W.-D., Moldzio, R., 2019. Rotenone: from modelling to implication in Parkinson's disease. Folia Neuropathol. 57, 317–326. https://doi.org/10.5114/fn.2019.89857.
Rioult-Pedotti, M.-S., Pekanovic, A., Atiemo, C.O., Marshall, J., Luft, A.R., 2015. Dopamine promotes motor cortex plasticity and motor skill learning via PLC activation. PLoS One 10, e0124986. https://doi.org/10.1371/journal.pone.0124986.
Rock, C., Zurita, H., Wilson, C., Apicella, A.J., 2016. An inhibitory corticostriatal pathway. Elife 5, 1–17. https://doi.org/10.7554/eLife.15890.
Rudy, B., Fishell, G., Lee, S., Hjerling-Leffler, J., 2011. Three groups of interneurons account for nearly 100% of neocortical GABAergic neurons. Dev. Neurobiol. 71, 45–61. https://doi.org/10.1002/dneu.20853.
Rynes, M.L., Surinach, D.A., Linn, S., Laroque, M., Rajendran, V., Dominguez, J., Hadjistamoulou, O., Navabi, Z.S., Ghanbari, L., Johnson, G.W., Nazari, M., Mohajerani, M.H., Kodandaramaiah, S.B., 2021. Miniaturized head-mounted microscope for whole-cortex mesoscale imaging in freely behaving mice. Nat. Methods 18, 417–425. https://doi.org/10.1038/s41592-021-01104-8.
Sailer, A., Molnar, G.F., Paradisio, G., Gunraj, C., Lang, A.E., Chen, R., 2003. Short and long latency afferent inhibition in Parkinson's disease. Brain 126, 1883–1894. https://doi.org/10.1093/brain/awg183.
Savidan, J., Kaeser, M., Belhaj-Saïf, A., Schmidlin, E., Rouiller, E.M., 2017. Role of primary motor cortex in the control of manual dexterity assessed via sequential bilateral lesion in the adult macaque monkey: A case study. Neuroscience 357, 303–324. https://doi.org/10.1016/j.neuroscience.2017.06.018.
Scala, F., Kobak, D., Bernabucci, M., Bernaerts, Y., Cadwell, C.R., Castro, J.R., Hartmanis, L., Jiang, X., Laturnus, S., Miranda, E., Mulherkar, S., Tan, Z.H., Yao, Z., Zeng, H., Sandberg, R., Berens, P., Tolias, A.S., 2021. Phenotypic variation of transcriptomic cell types in mouse motor cortex. Nature 598, 144–150. https://doi.org/10.1038/s41586-020-2907-3.
Schober, A., 2004. Classic toxin-induced animal models of Parkinson's disease: 6-OHDA and MPTP. Cell Tissue Res. 318, 215–224. https://doi.org/10.1007/s00441-004-0938-y.
Schuman, B., Machold, R.P., Hashikawa, Y., Fuzik, J., Fishell, G.J., Rudy, B., 2019. Four unique interneuron populations reside in neocortical layer 1. J. Neurosci. 39, 125–139. https://doi.org/10.1523/JNEUROSCI.1613-18.2018.
Shepherd, G.M.G., Yamawaki, N., 2021. Untangling the cortico-thalamo-cortical loop: cellular pieces of a knotty circuit puzzle. Nat. Rev. Neurosci. 22, 389–406. https://doi.org/10.1038/s41583-021-00459-3.
Shi, K., Liu, X., Hou, L., Qiao, D., Peng, Y., 2021. Exercise Improves movement by regulating the plasticity of cortical function in Hemiparkinsonian rats. Front. Aging Neurosci. 13, 1–11. https://doi.org/10.3389/fnagi.2021.695108.
Shipp, S., 2007. Structure and function of the cerebral cortex. Curr. Biol. 17, R443–R449. https://doi.org/10.1016/j.cub.2007.03.044.
Singh, A.M., Staines, W.R., 2015. The effects of acute aerobic exercise on the primary motor cortex. J. Mot. Behav. 47, 328–339. https://doi.org/10.1080/00222895.2014.983450.
Smyth, C., Summers, J.J., Garry, M.I., 2010. Differences in motor learning success are associated with differences in M1 excitability. Hum. Mov. Sci. 29, 618–630. https://doi.org/10.1016/j.humov.2010.02.006.
Sorg, B.A., Berretta, S., Blacktop, J.M., Fawcett, J.W., Kitagawa, H., Kwok, J.C.F., Miquel, M., 2016. Casting a wide net: role of perineuronal nets in neural plasticity. J. Neurosci. 36, 11459–11468. https://doi.org/10.1523/JNEUROSCI.2351-16.2016.
Sun, F., Zeng, J., Jing, M., Zhou, J., Feng, J., Owen, S.F., Luo, Y., Li, F., Wang, H., Yamaguchi, T., Yong, Z., Gao, Y., Peng, W., Wang, L., Zhang, S., Du, J., Lin, D., Xu, M., Kreitzer, A.C., Cui, G., Li, Y., 2018. A genetically encoded fluorescent sensor enables rapid and specific detection of dopamine in flies, fish, and mice. Cell 174, 481–496.e19. https://doi.org/10.1016/j.cell.2018.06.042.
Surendran, S., Rajasankar, S., 2010. Parkinson's disease: oxidative stress and therapeutic approaches. Neurol. Sci. 31, 531–540. https://doi.org/10.1007/s10072-010-0245-1.
Surmeier, D.J., Guzman, J.N., Sanchez-Padilla, J., Schumacker, P.T., 2011. The role of calcium and mitochondrial oxidant stress in the loss of substantia nigra pars compacta dopaminergic neurons in Parkinson's disease. Neuroscience 198, 221–231. https://doi.org/10.1016/j.neuroscience.2011.08.045.
Swann, N.C., de Hemptinne, C., Miocinovic, S., Qasim, S., Wang, S.S., Ziman, N., Ostrem, J.L., San Luciano, M., Galifianakis, N.B., Starr, P.A., 2016. Gamma oscillations in the hyperkinetic state detected with chronic human brain recordings in Parkinson's Disease. J. Neurosci. 36, 6445–6458. https://doi.org/10.1523/JNEUROSCI.1128-16.2016.
Swanson, L.W., 1982. The projections of the ventral tegmental area and adjacent regions: a combined fluorescent retrograde tracer and immunofluorescence study in the rat. Brain Res. Bull. 9, 321–353. https://doi.org/10.1016/0361-9230(82)90145-9.
Swanson, O.K., Semaan, R., Maffei, A., 2020. Reduced dopamine signaling impacts pyramidal neuron excitability in mouse motor cortex. eneuro ENEURO. https://doi.org/10.1523/ENEURO.0548-19.2021, 0548-19.2021.
Thierry, A.M., Hirsch, J.C., Tassin, J.P., Blanc, G., Glowinski, J., 1974. Presence of dopaminergic terminals and absence of dopaminergic cell bodies in the cerebral cortex of the cat. Brain Res. 79, 77–88. https://doi.org/10.1016/0006-8993(74)90567-8.
Tiihonen, M., Westner, B.U., Butz, M., Dalal, S.S., 2021. Parkinson's disease patients benefit from bicycling - a systematic review and meta-analysis. npj Park Dis. 7, 86. https://doi.org/10.1038/s41531-021-00222-6.
Touvykine, B., Mansoori, B.K., Jean-Charles, L., Deffeyes, J., Quessy, S., Dancause, N., 2016. The effect of lesion size on the organization of the ipsilesional and contralesional motor cortex. Neurorehabil. Neural Repair 30, 280–292. https://doi.org/10.1177/1545968315585356.
Trantham-Davidson, H., 2004. Mechanisms Underlying Differential D1 versus D2 Dopamine Receptor Regulation of Inhibition in Prefrontal Cortex. J. Neurosci. 24, 10652–10659. https://doi.org/10.1523/JNEUROSCI.3179-04.2004.
Tsubokawa, T., Katayama, Y., Yamamoto, T., Hirayama, T., Koyama, S., 1991. Chronic motor cortex stimulation for the treatment of central pain. Acta Neurochir. Suppl. 137–139. https://doi.org/10.1007/978-3-7091-9160-6_37.
Turner, R.S., DeLong, M.R., 2000. Corticostriatal activity in primary motor cortex of the Macaque. J. Neurosci. 20, 7096–7108. https://doi.org/10.1523/JNEUROSCI.20-18-07096.2000.
Urban-Ciecko, J., Barth, A.L., 2016. Somatostatin-expressing neurons in cortical networks. Nat. Rev. Neurosci. 17, 401–409. https://doi.org/10.1038/nrn.2016.53.
Urs, N.M., Gee, S.M., Pack, T.F., McCorvy, J.D., Evron, T., Snyder, J.C., Yang, X., Rodriguiz, R.M., Borrelli, E., Wetsel, W.C., Jin, J., Roth, B.L., O'Donnell, P., Caron, M.G., 2016. Distinct cortical and striatal actions of a β-arrestin–biased dopamine D2 receptor ligand reveal unique antipsychotic-like properties. Proc. Natl. Acad. Sci. 113, E8178–E8186. https://doi.org/10.1073/pnas.1614347113.
Valverde, S., Vandecasteele, M., Piette, C., Derousseaux, W., Gangarossa, G., Aristieta Arbelaiz, A., Touboul, J., Degos, B., Venance, L., 2020. Deep brain stimulation-guided optogenetic rescue of parkinsonian symptoms. Nat. Commun. 11, 2388. https://doi.org/10.1038/s41467-020-16046-6.
Van't Spijker, H.M., Kwok, J.C.F., 2017. A sweet talk: the molecular systems of perineuronal nets in controlling neuronal communication. Front. Integr. Neurosci. 11, 1–10. https://doi.org/10.3389/fnint.2017.00033.
Vanbellingen, T., Kersten, B., Bellion, M., Temperli, P., Baronti, F., Müri, R., Bohlhalter, S., 2011. Impaired finger dexterity in Parkinson's disease is associated with praxis function. Brain Cogn. 77, 48–52. https://doi.org/10.1016/j.bandc.2011.06.003.
Viaro, R., Marti, M., Morari, M., 2010. Dual motor response to l-dopa and nociceptin/orphanin FQ receptor antagonists in 1-methyl-4-phenyl-1,2,5,6-tetrahydropyridine (MPTP) treated mice: Paradoxical inhibition is relieved by D(2)/D(3) receptor blockade. Exp. Neurol. 223, 473–484. https://doi.org/10.1016/j.expneurol.2010.01.014.
Vitrac, C., Péron, S., Frappé, I., Fernagut, P.-O., Jaber, M., Gaillard, A., Benoit-Marand, M., 2014. Dopamine control of pyramidal neuron activity in the primary motor cortex via D2 receptors. Front. Neural Circuits 8, 1–8. https://doi.org/10.3389/fncir.2014.00013.
Wang, X., Liu, Y., Li, X., Zhang, Z., Yang, H., Zhang, Yu, Williams, P.R., Alwahab, N.S.A., Kapur, K., Yu, B., Zhang, Yiming, Chen, M., Ding, H., Gerfen, C.R., Wang, K.H., He, Z., 2017. Deconstruction of corticospinal circuits for goal-directed motor skills. Cell 171, 440–455.e14. https://doi.org/10.1016/j.cell.2017.08.014.
Wang, Y.-Y., Wang, Y., Jiang, H.-F., Liu, J.-H., Jia, J., Wang, K., Zhao, F., Luo, M.-H., Luo, M.-M., Wang, X.-M., 2018. Impaired glutamatergic projection from the motor cortex to the subthalamic nucleus in 6-hydroxydopamine-lesioned hemi-parkinsonian rats. Exp. Neurol. 300, 135–148. https://doi.org/10.1016/j.expneurol.2017.11.006.
Wang, S., Zhang, Y., Lei, J., Guo, S., 2021. Investigation of sensorimotor dysfunction in Parkinson disease by resting-state fMRI. Neurosci. Lett. 742, 135512 https://doi.org/10.1016/j.neulet.2020.135512.
Watanabe, Y., Kajiwara, R., Takashima, I., 2009. Optical imaging of rat prefrontal neuronal activity evoked by stimulation of the ventral tegmental area. Neuroreport 20, 875–880. https://doi.org/10.1097/WNR.0b013e32832c5e98.
Watson, G.S., Leverenz, J.B., 2010. Profile of Cognitive Impairment in Parkinson's Disease. Brain Pathol. 20, 640–645. https://doi.org/10.1111/j.1750-3639.2010.00373.x.
Whishaw, I.Q., 2000. Loss of the innate cortical engram for action patterns used in skilled reaching and the development of behavioral compensation following motor cortex lesions in the rat. Neuropharmacology 39, 788–805. https://doi.org/10.1016/S0028-3908(99)00259-2.
Whishaw, I.Q., O'Connor, W.T., Dunnett, S.B., 1986. The contributions of motor cortex, nigrostriatal dopamine and caudate-putamen to skilled forelimb use in the rat. Brain 109 (Pt 5), 805–843. https://doi.org/10.1093/brain/109.5.805.
Woolsey, CN, Settlage, PH, Meyer, DR, Sencer, W, Pinto Hamuy, T, Travis, AM, 1952. Patterns of localization in precentral and "supplementary" motor areas and their relation to the concept of a premotor area. Res. Publ. Assoc. Res. Nerv. Ment. Dis. 30, 238–264.
Wu, T., Long, X., Wang, L., Hallett, M., Zang, Y., Li, K., Chan, P., 2011. Functional connectivity of cortical motor areas in the resting state in Parkinson's disease. Hum. Brain Mapp. 32, 1443–1457. https://doi.org/10.1002/hbm.21118.
Xu, T., Yu, X., Perlik, A.J., Tobin, W.F., Zweig, J.A., Tennant, K., Jones, T., Zuo, Y., 2009. Rapid formation and selective stabilization of synapses for enduring motor memories. Nature 462, 915–919. https://doi.org/10.1038/nature08389.
Yamawaki, N., Stanford, I.M., Hall, S.D., Woodhall, G.L., 2008. Pharmacologically induced and stimulus evoked rhythmic neuronal oscillatory activity in the primary motor cortex in vitro. Neuroscience 151, 386–395. https://doi.org/10.1016/j.neuroscience.2007.10.021.

Yamawaki, N., Borges, K., Suter, B.A., Harris, K.D., Shepherd, G.M.G., 2014. A genuine layer 4 in motor cortex with prototypical synaptic circuit connectivity. Elife 3, e05422. https://doi.org/10.7554/eLife.05422.

Yao, Z., Liu, H., Xie, F., Fischer, S., Adkins, R.S., Aldridge, A.I., Ament, S.A., Bartlett, A., Behrens, M.M., Van den Berge, K., Bertagnolli, D., de Bézieux, H.R., Biancalani, T., Booeshaghi, A.S., Bravo, H.C., Casper, T., Colantuoni, C., Crabtree, J., Creasy, H., Crichton, K., Crow, M., Dee, N., Dougherty, E.L., Doyle, W.I., Dudoit, S., Fang, R., Felix, V., Fong, O., Giglio, M., Goldy, J., Hawrylycz, M., Herb, B.R., Hertzano, R., Hou, X., Hu, Q., Kancherla, J., Kroll, M., Lathia, K., Li, Y.E., Lucero, J.D., Luo, C., Mahurkar, A., McMillen, D., Nadaf, N.M., Nery, J.R., Nguyen, T.N., Niu, S.-Y., Ntranos, V., Orvis, J., Osteen, J.K., Pham, T., Pinto-Duarte, A., Poirion, O., Preissl, S., Purdom, E., Rimorin, C., Risso, D., Rivkin, A.C., Smith, K., Street, K., Sulc, J., Svensson, V., Tieu, M., Torkelson, A., Tung, H., Vaishnav, E.D., Vanderburg, C.R., van Velthoven, C., Wang, X., White, O.R., Huang, Z.J., Kharchenko, P.V., Pachter, L., Ngai, J., Regev, A., Tasic, B., Welch, J.D., Gillis, J., Macosko, E.Z., Ren, B., Ecker, J. R., Zeng, H., Mukamel, E.A., 2021. A transcriptomic and epigenomic cell atlas of the mouse primary motor cortex. Nature 598, 103–110. https://doi.org/10.1038/s41586-021-03500-8.

Zaaimi, B., Edgley, S.A., Soteropoulos, D.S., Baker, S.N., 2012. Changes in descending motor pathway connectivity after corticospinal tract lesion in macaque monkey. Brain 135, 2277–2289. https://doi.org/10.1093/brain/aws115.

Zhai, S., Tanimura, A., Graves, S.M., Shen, W., Surmeier, D.J., 2018. Striatal synapses, circuits, and Parkinson's disease. Curr. Opin. Neurobiol. 48, 9–16. https://doi.org/10.1016/j.conb.2017.08.004.

Zhou, H, Niu, L, Xia, X, Lin, Z, Liu, X, Su, M, Guo, R, Meng, L, Zheng, H, 2019. Wearable Ultrasound Improves Motor Function in an MPTP Mouse Model of Parkinson's Disease. IEEE Trans Biomed Eng. 66 (11), 3006–3013. https://doi.org/10.1109/TBME.2019.2899631.

Zurita, H., Feyen, P.L.C., Apicella, A.J., 2018. Layer 5 callosal parvalbumin-expressing neurons: A distinct functional group of gabaergic neurons. Front. Cell. Neurosci. 12, 1–14. https://doi.org/10.3389/fncel.2018.00053.

Zwartjes, D.G.M., Heida, T., Feirabend, H.K.P., Janssen, M.L.F., Visser-Vandewalle, V., Martens, H.C.F., Veltink, P.H., 2012. Motor cortex stimulation for Parkinson's disease: a modelling study. J. Neural Eng. 9, 056005 https://doi.org/10.1088/1741-2560/9/5/056005.